EXPLORING MEMORY IMPAIRMENT AND POST-TRAUMATIC AMNESIA FOLLOWING TRAUMATIC BRAIN INJURY

EMMA-JANE MALLAS

Computational, Cognitive & Clinical Neuroimaging Laboratory (C^3NL)
Department of Brain Sciences
Imperial College London

A thesis submitted for the degree of
Doctor of Philosophy
Clinical Medicine Research

2021

ABSTRACT

Memory disturbances are among the most common and significant consequences of traumatic brain injury (TBI). The severity of these deficits can vary widely across the trajectory of recovery from TBI and can be highly heterogenous across individuals. In the acute stages memory disturbance can occur in the form of post-traumatic amnesia (PTA), but deficits are also present into the chronic stages of recovery. I present four studies that aim to understand the characteristics and underlying mechanisms of memory impairment following TBI.

I investigated the cognitive profile of acute TBI patients with and without PTA. I found PTA patients show a transient deficit in working memory binding. I then assessed electrophysiological abnormalities to test the hypothesis that the binding deficit is underpinned by pathological low frequency slow-wave activity. PTA patients showed a significantly higher delta to alpha power ratio that correlated with binding impairment. To understand how this disruption to cortical communication impacts upon large-scale networks I performed a dynamic functional connectivity analysis on the resting state fMRI of acute TBI patients. I found four independent brain states that showed striking anti-correlation between core cognitive control networks. Patients in a more profound period of PTA spent more time in fewer states than those with less cognitive impairment. These findings suggest that PTA is likely underpinned by disruption to communication required for integration of features in working memory.

Finally, I examined enduring memory failures in chronic TBI patients and found that patients with episodic memory impairment showed differential activation of key networks required for memory and attention. Memory impairment related to the white matter integrity directly underpinning the task-derived encoding networks. These findings suggest that in chronic TBI memory impairment may be associated with failed control of attentional resources.

ACKNOWLEDGEMENTS

First and foremost, I would like to thank my supervisors, Professor David Sharp, and Dr Nikos Gorgoraptis for their guidance, support, and insight. I am very grateful for the opportunities you have afforded me. It has been a privilege to learn from you and develop as a scientist under your mentorship.

Thank you to the C3NL team for being supportive and inspiring colleagues. I am thankful for the many discussions, memories, and friendships that I will take from my PhD years. I would especially like to thank Dr Sara De Simoni and Dr Greg Scott for their patience and generosity in all they have taught me.

None of this work would have been possible without the generous permission of the many patients and their relatives involved. Thank you for contributing your time and energy during what I hope will be the worst of your days.

I am eternally grateful to my closest friends, near and far, for your support over these years. Thank you for always cheering me on, lifting me up and being there to help 'forget about life for a while'.

Thank you to Kara and Alfred for proof-reading this work and being a constant source of support. More importantly, thank you for teaching me that neuroplasticity is possible.

I am fortunate to have my wonderful partner Combiz by my side in life, and throughout this journey. Thank you for your love, kindness, and support.

Finally, to my parents, Caroline and Denis for their unwavering love, support, and belief in my abilities. Thank you for all you have done for me.

STATEMENT OF PUBLICATIONS

The data presented in Chapter 6 have been published in Brain:

> Mallas, E.-J., De Simoni, S., Scott, G., Jolly, A.E., et al. (2021) Abnormal dorsal attention network activation in memory impairment after traumatic brain injury. *Brain*. 144 (1), 114–127.

The data presented in Chapter 3 and 4 are being prepared for submission to Brain.

A subset of the data presented in Chapter 5 have been used in a previous publication:

> De Simoni, S., Grover, P.J., Jenkins, P.O., Honeyfield, L., et al. (2016) Disconnection between the default mode network and medial temporal lobes in post-traumatic amnesia. *Brain*. 1–14.

STATEMENT OF ORIGINALITY

Collection of the data presented in Chapters 3, 4 and 5 referred to as the 'new acute cohort' was assisted by Dr Sophie Dautricourt. A subset of the behavioural data presented in Chapter 3 was collected with the assistance of Dr Rituja Kamble. Part of the data presented in Chapter 5, referred to as the 'historical acute cohort' was from a previously published study by Dr Sara De Simoni. The data presented in Chapter 6 was collected by Dr Amy Jolly, Dr Stuart Roberts, Dr Claire Feeney, Dr Greg Scott, Dr Lucia Li, Dr Nikos Gorgoraptis and myself as part of previous research projects within C^3NL.

The precision spatial working memory task presented in Chapter 3 was programmed by Dr Nikos Gorgoraptis.

The entropy ratio measure presented in Chapter 3 and the EEG analysis pipeline in Chapter 4 was devised with the help of Dr. Greg Scott. All statistical analysis with this data was conducted by myself.

The dynamic functional connectivity analysis pipeline in Chapter 5 was devised in collaboration with Dr Nádia Moreira da Silva at Newcastle University. All statistical analysis of this data was conducted by myself.

The subsequent memory task presented in Chapter 6 was provided by Dr Adam Hampshire.

Lesion masks presented in Chapter 6 were drawn by Dr Niall Bourke. Analysis of these was performed by myself.

All other work contained in this thesis is my own and conforms to the rules and guidelines set out for PhD theses by Imperial College London.

COPYRIGHT DECLARATION

The copyright of this thesis rests with the author. Unless otherwise indicated, its contents are licensed under a Creative Commons Attribution-NonCommercial 4.0 International Licence (CC BY-NC).

Under this licence, you may copy and redistribute the material in any medium or format. You may also create and distribute modified versions of the work. This is on the condition that: you credit the author and do not use it, or any derivative works, for a commercial purpose.

When reusing or sharing this work, ensure you make the licence terms clear to others by naming the licence and linking to the licence text. Where a work has been adapted, you should indicate that the work has been changed and describe those changes.

Please seek permission from the copyright holder for uses of this work that are not included in this licence or permitted under UK Copyright Law.

TABLE OF CONTENTS

LIST OF TABLES **11**

LIST OF FIGURES **12**

LIST OF ABBREVIATIONS **14**

1 CHAPTER ONE: GENERAL INTRODUCTION **18**

1.1 TRAUMATIC BRAIN INJURY 19

1.1.1 Definition *19*

1.1.2 Epidemiology *19*

1.1.3 Aetiology *19*

1.1.4 Clinical consequences of TBI *20*

1.1.5 Pathophysiology of TBI *20*

1.1.6 Network dysfunction in TBI *24*

1.2 MEMORY 26

1.2.1 Episodic memory *26*

1.2.2 Working memory *28*

1.2.3 Memory systems in the healthy brain *29*

1.2.4 Memory disturbances in TBI *31*

1.3 POST-TRAUMATIC AMNESIA 34

1.3.1 Definition *34*

1.3.2 Epidemiology and aetiology *34*

1.3.3 Clinical presentation *34*

1.3.4 Assessment and diagnosis *35*

1.3.5 Clinical and scientific relevance *36*

1.3.6 Cognitive profile *36*

1.3.7 Current mechanistic understanding *38*

1.4 SUMMARY 40

2 CHAPTER TWO: MATERIALS & METHODS **41**

2.1 OVERVIEW & EXPERIMENTAL DESIGN 42

2.2 PARTICIPANTS 43

2.2.1 Recruitment of acute TBI cohorts *43*

2.2.2 Recruitment of chronic TBI cohort *44*

2.2.3 Inclusion criteria *46*

2.2.4 Exclusion criteria *46*

2.3 CLINICAL AND COGNITIVE ASSESSMENTS 47

2.3.1 TBI severity *47*

2.3.2 PTA Assessment *47*
2.3.3 Neuropsychology *50*
2.4 ELECTROENCEPHALOGRAPHY 56
2.4.1 Principles of EEG *56*
2.4.2 EEG data acquisition *63*
2.4.3 EEG pre-processing *65*
2.5 MAGNETIC RESONANCE IMAGING 66
2.5.1 Principles of MRI *66*
2.5.2 MRI acquisition *72*
2.5.3 Pre-processing of MRI data *73*
3 CHAPTER THREE: VISUAL SHORT-TERM MEMORY BINDING IN PTA 75
3.1 INTRODUCTION 76
3.2 METHODS 78
3.2.1 Study design and participants *78*
3.2.2 Neuropsychology assessment *78*
3.2.3 Experimental task paradigm *78*
3.3 RESULTS 82
3.3.1 Neuropsychological performance at baseline *84*
3.3.2 Longitudinal changes in neuropsychological performance *87*
3.3.3 PTA patients show impaired object-location binding *90*
3.3.4 PTA patients show abnormal response distributions and a bias towards the non-target *92*
3.3.5 Impaired binding ability is transient and specific to a period of PTA *94*
3.4 DISCUSSION 96
3.4.1 Limitations *98*
3.4.2 Future Directions *99*
3.4.3 Conclusion *100*
4 CHAPTER FOUR: ELECTROPHYSIOLOGICAL ABNORMALITIES IN ACUTE TBI 101
4.1 INTRODUCTION 102
4.2 METHODS 105
4.2.1 Study design and participants *105*
4.2.2 Neuropsychological assessment *105*
4.2.3 EEG analysis *105*
4.3 RESULTS 109
4.3.1 Clinical demographics *109*
4.3.2 Neuropsychological performance *111*
4.3.3 Global normalised power in PTA *116*
4.3.4 Low frequency power abnormalities resolve at follow-up *119*

4.3.5 Individual case studies ... *121*
4.3.6 Increased slow-wave activity is associated with disruption to working memory binding ... *124*
4.3.7 Frontal-parietal theta phase synchronisation is increased following acute TBI ... *126*
4.3.8 Theta-gamma cross-frequency coupling is not altered in acute TBI ... *128*
4.4 DISCUSSION ... 130
4.4.1 Limitations ... *132*
4.4.2 Future Directions ... *133*
4.4.3 Conclusion ... *134*
5 CHAPTER FIVE: NETWORK DYNAMICS IN PTA ... 135
5.1 INTRODUCTION ... 136
5.2 METHODS ... 139
5.2.1 Participants ... *139*
5.2.2 Study protocol ... *139*
5.2.3 Neuropsychological Assessment ... *140*
5.2.4 Imaging analysis ... *140*
5.3 RESULTS ... 146
5.3.1 Demographics ... *146*
5.3.2 Neuropsychology ... *146*
5.3.3 Static functional connectivity ... *149*
5.3.4 Dynamic functional connectivity ... *151*
5.3.5 State transitions ... *153*
5.3.6 Motion analyses ... *153*
5.4 DISCUSSION ... 155
5.4.1 Limitations ... *158*
5.4.2 Future Directions ... *160*
5.4.3 Conclusion ... *161*
6 CHAPTER SIX: NETWORK DYSFUNCTION IN CHRONIC TBI ... 162
6.1 INTRODUCTION ... 163
6.2 METHODS ... 166
6.2.1 Patient group and clinical details ... *166*
6.2.2 Control group ... *166*
6.2.3 Neuropsychology assessment ... *166*
6.2.4 Subsequent memory task ... *166*
6.2.5 Imaging analysis ... *169*
6.2.6 Lesions ... *172*
6.3 RESULTS ... 173
6.3.1 Patient classification and demographics ... *173*

6.3.2 Neuropsychological performance ... *175*
6.3.3 Successful encoding is associated with activation changes in the dorsal attention network and default mode network *178*
6.3.4 TBI patients with memory impairment show differential activation during successful encoding ... *178*
6.3.5 Patients with impaired subsequent memory show reduced white matter integrity ... *181*
6.3.6 Quality control analyses ... *185*
6.4 DISCUSSION ... 187
6.4.1 Limitations ... *190*
6.4.2 Future Directions ... *191*
6.4.3 Conclusion ... *192*
7 CHAPTER SEVEN: GENERAL DISCUSSION ... 193
7.1 OVERVIEW OF EXPERIMENTAL CHAPTERS ... 194
7.1.1 Chapter Three ... *194*
7.1.2 Chapter Four ... *194*
7.1.3 Chapter Five ... *195*
7.1.4 Chapter Six ... *196*
7.2 NOVEL CONTRIBUTIONS ... 198
7.2.1 A novel acute cohort ... *198*
7.2.2 Cognitive heterogeneity in TBI ... *199*
7.3 INTERPRETATION ... 201
7.3.1 Are patients with more severe memory impairments more severely injured? ... *201*
7.3.2 What are the mechanisms of memory impairment in TBI? ... *202*
7.3.3 Is PTA an extension of a period of reduced consciousness? ... *204*
7.4 FUTURE DIRECTIONS ... 206
8 REFERENCES ... 208
9 APPENDIX ... 244

LIST OF TABLES

Table 2.1 The Mayo TBI classification system 48

Table 3.1 Clinical Demographics 83

Table 3.2 Neuropsychology in the acute cohort at baseline 86

Table 3.3 Neuropsychology in the acute cohort at follow-up 89

Table 4.1 Clinical demographics for EEG cohort 110

Table 4.2 Neuropsychology statistics for the EEG cohort at baseline 112

Table 4.3 Neuropsychology statistics for the EEG cohort at follow-up 114

Table 5.1 MNI co-ordinates for regions of interest used in the dynamic functional connectivity analysis 142

Table 6.1 Demographics in the chronic TBI cohort 174

Table 6.2 Neuropsychological performance in the chronic TBI cohort 177

Supplementary Table 9.1 Demographics and clinical characteristics of patients in the new acute cohort 245

Supplementary Table 9.2 Entropy ratio statistics across varying bin widths 247

Supplementary Table 9.3 Demographics and clinical characteristics of the TBI patients in Chapter 6 249

Supplementary Table 9.4 Permission to reuse figures 252

LIST OF FIGURES

Figure 1.1 Axonal injury and the consequences for large-scale network disruption 23

Figure 2.1 Flow of data across experimental chapters 45

Figure 2.2 The Westmead Post-Traumatic Amnesia Scale 49

Figure 2.3 Battery of computerised cognitive assessments 55

Figure 2.4 The neural basis of EEG signal 59

Figure 2.5 Defining oscillations with frequency, phase and power 61

Figure 2.6 Frequency bands in EEG 62

Figure 2.7 EEG channel layout 64

Figure 2.8 The haemodynamic response function 69

Figure 2.9 Fractional anisotropy in the axon membrane 71

Figure 3.1 Precision working memory experimental task paradigm 81

Figure 3.2 Neuropsychological performance in the acute cohort at baseline 85

Figure 3.3 Neuropsychological performance in the acute cohort at follow-up 88

Figure 3.4 Performance on the precision spatial working memory task 91

Figure 3.5 Spatial distribution of errors on the precision working-memory task at baseline 93

Figure 3.6 Spatial distribution of errors on the precision working memory task at follow-up 95

Figure 4.1 Neuropsychology results for the EEG cohort at baseline 113

Figure 4.2 Neuropsychology results for the EEG cohort at follow-up 115

Figure 4.3 Normalised power at baseline 118

Figure 4.4 Normalised power at follow-up 120

Figure 4.5 Individual patient case studies 123

Figure 4.6 Association between global delta to alpha ratio and working memory 125

Figure 4.7 Theta phase synchronisation in acute TBI patients and controls 127

Figure 4.8 Frontal theta phase to parietal and temporal gamma amplitude coupling in acute TBI patients and controls 129

Figure 5.1 Dynamic functional connectivity analysis 145

Figure 5.2 Cognitive performance in the acute and historical cohorts 148
Figure 5.3 Static functional DMN connectivity 150
Figure 5.4 Dynamic functional connectivity states 152
Figure 5.5 Temporal characteristics of dynamic functional connectivity states 154
Figure 6.1 The subsequent memory task paradigm 168
Figure 6.2 Defining the structural connectome underpinning task derived functional networks 171
Figure 6.3 Subsequent memory and neuropsychological performance in the chronic TBI cohort 176
Figure 6.4 Changes in BOLD activity associated with performance on the subsequent memory task 180
Figure 6.5 Fractional anisotropy across the whole brain in TBI patients with and without memory impairment 183
Figure 6.6 Fractional anisotropy in the structural connectome underpinning encoding networks 184
Figure 6.7 Lesion probability in TBI patients with and without memory impairment 186
Supplementary Figure 9.1 Entropy ratio at different bin widths 248
Supplementary Figure 9.2 Alterations in BOLD activity associated with performance on the memory encoding task for TBI patients alone. 251

LIST OF ABBREVIATIONS

AD	Alzheimer's disease
aINS	Anterior insula
ANOVA	Analysis of variance
aPFC	Anterior prefrontal cortex
BET	Brain extraction tool
BOLD	Blood oxygen level dependent
BVMT-R	Brief Visuospatial Memory Test Revised
CON	Healthy control
CSF	Cerebral Spinal Fluid
CT	Computerised tomography
dACC	Dorsal anterior cingulate cortex
DAI	Diffuse axonal injury
DAN	Dorsal attention network
DAR	Delta to alpha ratio
DBS	Deep brain stimulation
DF	Degrees of freedom
dFC	Dynamic functional connectivity
DMN	Default mode network
dPCC	Dorsal posterior cingulate cortex
dpss	Discrete prolate spheroidal sequences
DR	Delayed recall
DTI	Diffusion tensor imaging
dwPLI	debiased weighted phase lag index
EEG	Electroencephalography
EPI	Echo planar imaging
FA	fractional anisotropy
FDR	False-discovery rate
FEAT	fMRI expert analysis tool
FFT	Fast fourier transform

FLAIR	Fluid-attenuated inversion recovery
FLIRT	FMRIB's linear image registration tool
fMRI	Functional magnetic resonance imaging
FMRIB	Oxford Centre for Functional MRI of the Brain
FOp	Frontal operculum
FOV	Field of view
FPN	Fronto-parietal network
FSL	FMRIB software library
GCS	Glasgow Coma Scale
GIFT	Group ICA of fMRI Toolbox
GLM	General linear model
GOAT	Galveston orientation and amnesia test
HAPPE	Harvard Automated Processing Pipeline for EEG
Hb	Deoxygenated haemoglobin
HbO2	Oxygenated haemoglobin
HRF	Haemodynamic response function
HVLT-R	Hopkins Verbal Learning Test-Revised
ICA	Independent component analysis
IFG	Inferior frontal gyrus
IFIS-SA	Integrated functional imaging system standalone
IIT	Illinois Institute of Technology
IMSEG	Image segmentation
IPG	Inferior parietal gyrus
IPS	Intra-parietal sulcus
IR	Immediate recall
ISM	Impaired subsequent memory
JHU	John Hopkins University
KL	Kullback-Leibler
L	Left
LOC	Loss of consciousness
MARA	Multiple artifact rejection algorithm
MCFLIRT	Motion Correct using FLIRT

MI	Modulation index
MNI	Montreal Neurological Institute
MODREC	Ministry of Defence Research Ethics Committee
MRI	Magnetic resonance imaging
MTG	Middle temporal gyrus
MTL	Medial temporal lobe
MTW	Major trauma ward
NBS	Network based statistic
NHS	National Health Service
NIHR	National Institute for Health Research
NSM	Normal subsequent memory
PAC	Phase-amplitude coupling
PAL	Paired associates learning
PCC	Posterior cingulate cortex
PCG	Paracingulate gyrus
PFC	Prefrontal cortex
PHG	Parahippocampal gyrus
PLI	phase lag index
pSMG	Posterior supramarginal gyrus
PTA	Post-traumatic amnesia
PTA-	TBI patient not in PTA
PTA+	TBI patient in PTA
R	Right
ROI	Region of interest
ROIs	Regions of interest
SAH	Subarachnoid haemorrhage
SD	Standard deviation
SDH	Subdural haemorrhage
SEM	Standard error of the mean
SFG	Superior frontal gyrus
SM	Subsequent memory
SMA	Supplementary motor area

SN	Salience network
SPG	Superior parietal gyrus
TBI	Traumatic brain injury
TBSS	Tract-based spatial statistics
tDCS	Transcranial direct current stimulation
TDI	Track density imaging
TE	Echo time
TMS	Transcranial magnetic stimulation
TR	Repetition time
UK	United Kingdom
v1	Visit one (baseline)
v2	Visit two (follow-up)
vmPFC	Ventro-medial prefrontal cortex
vPCC	Ventral posterior cingulate cortex
WASI	Wechsler Abbreviated Scale of Adult Intelligence
WMS-III	Wechsler Memory Scale, Third Edition
WPTAS	Westmead post-traumatic amnesia scale
WTAR	Wechsler Test of Adult Reading

1

General Introduction

In this introductory chapter, I first give an overview of traumatic brain injury, outlining the epidemiology, clinical and pathological consequences. I explain the concept of network dysfunction and how it may contribute to cognitive disturbances in this population. I introduce episodic and working memory, the core cognitive domains of memory that will be the focus of this thesis in the context of theoretical models of memory function and the systems involved in healthy memory function. I consider how deficits in these domains relate to the pathophysiology of TBI in the context of structural and functional brain networks. Finally, I introduce post-traumatic amnesia, review the current literature, and discuss how studying this clinical population can advance our mechanistic understanding of memory function from both clinical and cognitive neuroscience perspectives.

1.1 TRAUMATIC BRAIN INJURY

1.1.1 Definition

Traumatic brain injury (TBI) refers to structural or functional damage to the brain caused by external forces. TBI can be formally defined as "an alteration in brain function, or other evidence of brain pathology, caused by an external force" (Menon *et al.*, 2010). Within this definition, an "alteration in brain function" can encompass loss of consciousness, memory loss for events immediately before or after the event, neurologic deficit, or alterations in mental state at the time of injury. "Other evidence of brain pathology" may include visual, radiological or laboratory findings. An "external force" in this context may include the head being struck by or striking an object, the brain undergoing an acceleration/deceleration movement, penetration of a foreign body into the brain or forces generated from a blast or explosion.

1.1.2 Epidemiology

TBI is a leading cause of death and disability in young adults worldwide (Fleminger & Ponsford, 2005). Global estimates suggest that over 27 million people are affected by TBI every year, with age-standardised incidence rates of 369 new cases per 100,000 (James *et al.*, 2019). In the UK, approximately 1.4 million patients attend hospital every year following a head injury (Lawrence *et al.*, 2016), and the prevalence of TBI in the population is over 382,000 (James *et al.*, 2019).

1.1.3 Aetiology

Risk of TBI is influenced by factors including geographic region, age, sex, and socioeconomic status. Central and eastern Europe, and central Asia have a higher incidence of TBI than the rest of the world (James *et al.*, 2019), and there are higher rates of TBI in urban compared to suburban or rural areas (Whitman, Coonley-Hoganson & Desai, 1984; Yates *et al.*, 2006). TBI is approximately three times more likely to affect men than women, and is associated with greater rates of complications and mortality in men (Berry *et al.*, 2009). This effect of sex is most marked in young adults between the ages of 15-29 years (Yates *et al.*, 2006). Factors associated with lower

socioeconomic status (e.g. income and education levels) are associated with higher risk of recurrent TBI (Lasry *et al.*, 2017).

Worldwide, the most common mechanisms of injury are road traffic accidents (including pedestrians, drivers, motorcyclists, cyclists, and other transport users) and falls (James *et al.*, 2019). TBI may also occur through sports injuries, interpersonal violence, explosive blasts, or other exposure to mechanical forces. In the UK, younger patients are more likely to sustain TBI as a result of road traffic collisions and assault, whereas there is higher likelihood of TBI from falls in older adults (Lawrence *et al.*, 2016).

1.1.4 Clinical consequences of TBI

Advances in acute management of TBI mean that survival rates are high (Bigler, 2013) though the outcome for many survivors is generally poor (Fleminger & Ponsford, 2005). TBI is associated with a wide range of disabling clinical consequences including neurological (e.g. epilepsy, neuroendocrine dysfunction, neurodegeneration), psychiatric (e.g. depression, apathy, anxiety) behavioural (e.g. disinhibition, impulsivity, personality changes) and cognitive changes (Bramlett & Dietrich, 2015; Azouvi *et al.*, 2017; Graham *et al.*, 2020).

Cognitive impairment is a common and disabling consequence of TBI and is a major cause of ongoing disability, long-term unemployment and reduced quality of life (Wood & Rutterford, 2006; Whitnall *et al.*, 2006; Gorgoraptis *et al.*, 2019). TBI patients show prominent deficits in information processing speed, sustained attention, executive function and memory impairment (Kinnunen *et al.*, 2011; Azouvi *et al.*, 2017; Pavlovic *et al.*, 2019). The most commonly and often severely affected cognitive domain is memory (Vakil, 2005) which is discussed in more detail in section 1.2.4.

1.1.5 Pathophysiology of TBI

TBI is a complex disease causing heterogenous damage to brain structure and function. The pathophysiology of TBI can be understood in the context of primary and secondary injuries, and how they impact upon grey and white matter.

1.1.5.1 Primary and secondary injuries

There are two distinct phases to TBI: acute, primary injury and delayed, secondary injury (Pearn *et al.*, 2017). Primary injury occurs during the initial insult. It is mechanical in nature and occurs as the result of an object directly striking the head, from the brain striking the inside of the skull or from acceleration-deceleration forces. Primary injury can be either focal or diffuse, and may include haemorrhage, contusion, axonal tearing and shearing, and necrotic cell death.

Secondary injury refers to delayed, non-mechanical damage that is initiated by the primary injury. This evolves over the following hours to months through a series of consecutive pathological processes (Pearn *et al.*, 2017). In the acute context, this can refer to increases in intracranial pressure, oedema, hypoxic and ischaemic injury, cerebral contusion, inflammation and blood-brain barrier disruption (Kunz, Dirnagl & Mergenthaler, 2010; Werner & Engelhard, 2007; Capizzi, Woo & Verduzco-Gutierrez, 2020). In the longer term, continued neuroinflammation can become an important contributor to neurodegeneration and cognitive deficit following TBI (Hosomi *et al.*, 2020).

1.1.5.2 Focal injury

Focal injury is caused by tissue strain and brain movement in response to mechanical forces resulting in contusions and haemorrhages in cortical grey matter (Graham *et al.*, 2000). Focal lesions most commonly occur in regions closest to a bony protrusion, and tend to occur in characteristic locations, most frequently the inferior aspect of the frontal lobes, the frontal poles and inferior aspect of the temporal lobes (Mckee & Daneshvar, 2015). Clinical convention tends to place emphasis on focal injuries such as contusions or haemorrhage as these are identifiable on standard clinical imaging and relevant to acute management. However within survivors, the spatial distribution of focal injuries is not as useful for predicting longer term clinical outcomes as markers of whole brain diffuse injury (Katz & Alexander, 1994; Bigler, 2007).

1.1.5.3 Diffuse injury

Diffuse brain injury refers to damage occurring throughout the brain and can consist of widespread axonal damage, microbleeds, oedema and hypoxic ischaemia. Diffuse axonal injury (DAI) is the most common pathological feature of TBI (Gentry, Godersky & Thompson, 1988) and results from rapid acceleration and deceleration forces to the head. Primary injury occurs due to mechanical shearing and compressive strains to axons under these forces which results in disruption to axonal transport (Figure 1.1; Sharp, Scott & Leech, 2014). Secondary effects involve disruption in axonal transport, disconnection and Wallerian degeneration which may persist for years after injury and contribute to neurodegenerative processes (Johnson, Stewart & Smith, 2013; Graham *et al.*, 2020).

The degree of damage to the axons forming the white matter microstructure can be quantified using diffusion tensor imaging (DTI) techniques which are described in Chapter 2. Neuroimaging studies demonstrate that the structural network disconnection produced by DAI is a significant factor in persistent cognitive impairments following TBI (Kinnunen *et al.*, 2011; Fagerholm *et al.*, 2015). This is likely due to the relationship between damage to structural connections and disruption to large-scale functional networks (Sharp, Scott & Leech, 2014).

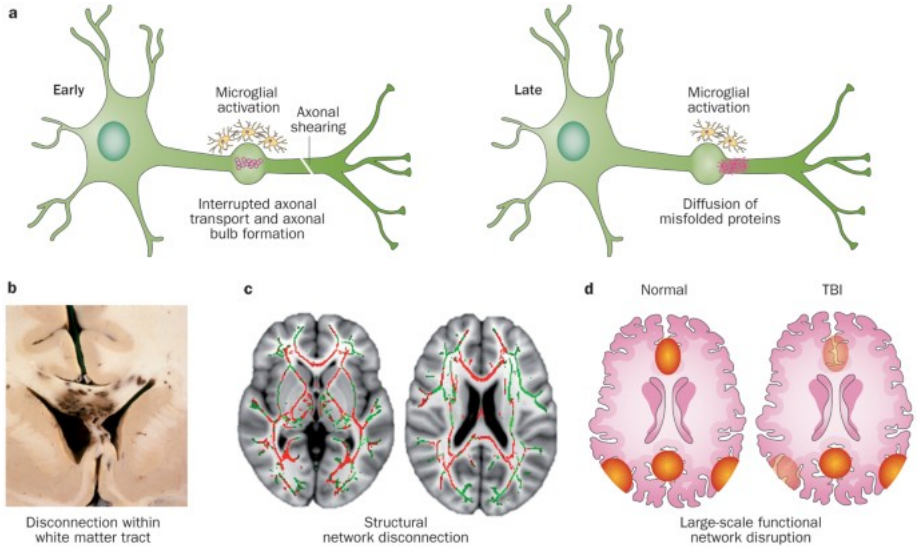

Figure 1.1 Axonal injury and the consequences for large-scale network disruption

A| Primary ('early') and secondary ('late') injury to axons at the microscopic scale. **B**| Injury to white matter tracts at the macroscopic scale illustrated in a postmortem specimen where regions of black show haemorrhage indicative of underlying damage to the white matter tract. **C**| Damage to white matter tracts at the whole-brain level disrupts long-range communication within structural networks: green represents the whole white matter skeleton with areas of damage shown in red. **D**| White matter damage can result in disruption to interactions between nodes of large-scale functional brain networks: red/yellow regions represent reduced interactions between nodes of the default mode network in traumatic brain injury (TBI). Figure reproduced with permission from Sharp, Scott & Leech *Nature Reviews Neurology*., 10(3),156-166 (2014).

1.1.6 Network dysfunction in TBI

Large-scale functional networks refer to spatially distributed brain regions exhibiting associated patterns of activation that reflect coupling between different neuronal populations (Friston, 2011; Cole, Smith & Beckmann, 2010). Resting-state functional magnetic resonance imaging (fMRI; Chapter 2) studies have consistently identified a characteristic set of functional networks in humans (Beckmann *et al.*, 2005; De Luca *et al.*, 2006; Damoiseaux *et al.*, 2006; Smith *et al.*, 2009). Communication within and between these large-scale functional resting state networks is integral to cognitive function. Four of the core neurocognitive networks discussed in this thesis include the dorsal attention network (DAN), default mode network (DMN), salience network (SN) and fronto-parietal network (FPN).

The DMN is disrupted following TBI. The DMN refers to a group of regions that show high metabolic activity and strong functional coupling at rest (Raichle *et al.*, 2001). The posterior cingulate cortex (PCC) and ventromedial prefrontal cortex (vmPFC) are considered the core nodes of the DMN (Sharp, Scott & Leech, 2014), but the network also includes inferior parietal lobes, superior frontal gyrus, anterior portions of the inferior temporal cortex, medial temporal cortex and medial cerebellum (Buckner, Andrews-Hanna & Schacter, 2008). TBI patients show abnormal patterns of activation, deactivation and functional connectivity within the DMN (Sharp *et al.*, 2011; Hillary *et al.*, 2011; Bonnelle *et al.*, 2011; Tang *et al.*, 2012; De Simoni *et al.*, 2016).

Damage to structural network connections following TBI, and abnormalities in activation of functional resting state networks are closely related. TBI patients show abnormal functional connectivity between subcortical and cortical regions in association with reduced structural integrity of the underlying white matter (De Simoni *et al.*, 2018). Damage to white matter integrity is also associated with reduced activation across a task-derived working memory network and the DMN (Palacios *et al.*, 2012) and abnormal DMN connectivity (Sharp *et al.*, 2011; Tang *et al.*, 2012). Disruption to white matter in the cingulum bundle, the structural connection between DMN and the medial temporal lobe, is associated with reduced functional connectivity between these regions (De Simoni *et al.*, 2016). This is also the case in between network connectivity: white matter damage within the tracts underlying the SN predicts abnormal

activation in the DMN (Bonnelle *et al.*, 2012). Widespread damage to white matter underpinning core functional networks required for higher order cognition as seen in DAI is a significant pathophysiological consequence of TBI contributing to enduring cognitive impairment.

Abnormal network function underpins cognitive impairment in TBI. Reduced functional connectivity of the caudate is associated with increases in executive dysfunction, information processing speed and memory impairment in TBI patients (De Simoni *et al.*, 2018) and abnormal communication between SN and DMN is associated with impaired cognitive control (Bonnelle *et al.*, 2012; Jilka *et al.*, 2014). Abnormal global functional connectivity is associated with impaired cognitive ability (Konstantinou *et al.*, 2018). There is also evidence for compensatory changes as seen in TBI patients with the greatest hyperactivation of DMN exhibiting the least cognitive impairment (Sharp *et al.*, 2011).

Disruption to large-scale functional networks and how this relates to memory impairment in TBI will be further discussed and examined in the context of both acute (Chapter 5) and chronic (Chapter 6) TBI cohorts.

1.2 MEMORY

Memory impairment is one of the most frequent and significant consequences of TBI (Vakil, 2005). It is the most frequently cited concern from patients and their caregivers (Jourdan *et al.*, 2018) and assistance with memory issues is a common need into the chronic stages of recovery (Corrigan, Whiteneck & Mellick, 2004). Memory deficits are therefore an important clinical consequence of TBI.

Memory is not a unitary construct and can be conceptualised as a number of different systems. TBI patients show deficits across a range of different memory systems (Vakil, 2005). This thesis focuses specifically on deficits related to episodic memory following traumatic brain injury and how it is supported by the integration of features in working memory processes.

1.2.1 Episodic memory

At the heart of what we think of as a personal experience of 'remembering' is episodic memory. Episodic memory is a form of long-term memory for events that are personally experienced, as opposed to semantic memory, which is memory for general facts (Tulving, 2002). It is the only memory system that affords autonoetic awareness, that is it allows for mental time travel, or the ability to consciously access and re-experience past experiences (Tulving, 2002). Episodic memory consists of three core processes: encoding, storage and retrieval.

1.2.1.1 Encoding

The encoding phase involves the initial perceiving and learning of information. Encoding can be intentional (consciously trying to learn and later remember information) or incidental (unintended learning of information without intending to encode it). Most experimental paradigms study intentional encoding (i.e. the participant is instructed that they will later be tested on this information), though many real world episodic memories are formed through incidental encoding (Kontaxopoulou *et al.*, 2017).

1.2.1.2 Storage

Storage refers to the maintenance of this encoded information over time, and how this is converted into long term memory. There are two key models of episodic memory storage: consolidation and contextual binding theory. The consolidation account proposes that newly acquired information will be quickly forgotten in the absence of a process to commit memories to long-term storage (Müller & Pilzecker, 1900; Dudai, 2004; Hebb, 2005). Consolidation processes take place at both synaptic (stabilisation of cellular changes invoked through encoding) and systems (neocortical representation independent from hippocampus) levels (Dudai, 2004; Yonelinas *et al.*, 2019). In contrast, the more recently proposed contextual binding theory proposes that episodic memory is dependent upon the hippocampus binding together item and context information required for later retrieval (Yonelinas *et al.*, 2019). This theory supports a role of feature binding in episodic memory which will be introduced below in the context of integrative working memory processes.

1.2.1.3 Retrieval

Retrieval, or recollection, of episodic memories is what enables one to relive the episode or memory. The retrieval process is often considered in the context of available cues. Free recall requires one to produce previously encoded stimuli in the absence of any prompts, whereas cued recall involves contextual hints to assist remembering. In contrast, recognition involves deciding whether a stimulus is novel or familiar.

1.2.1.4 Context

Much of the research into episodic memory has focused on studying memory for single items, for example word lists. While this approach allows examination of different stages of memory (e.g., brain activity during encoding) this approach lacks the ecological validity of the richer context that true episodic memories of our personal experiences contain. Episodic memories of real world, personally experienced events are contextual, that is they contain information of what happened, when it happened and where it happened. It is therefore comprised of collections of different features (e.g. time, space, colours, objects) which must be combined to form a complete

representation of an event (Quinette *et al.*, 2006). Episodic memory can therefore be considered reliant on a working memory processes that enable integration of different features.

1.2.2 Working memory

How different features of episodic memory are integrated in working memory is central to the understanding of the human memory system. Working memory refers to a limited capacity system dedicated to the temporary storage and manipulation of information required for higher order cognition (Baddeley & Hitch, 1974; Baddeley, 2000b; Cowan, 2005; D'Esposito & Postle, 2015). The most prominent and influential model of working memory (Chai, Abd Hamid & Abdullah, 2018) is the multicomponent working memory model proposed by Baddeley and Hitch (1974). The multicomponent working memory model was initially comprised of three subcomponents: the phonological loop, the visuospatial sketchpad, and the central executive. The former two components are considered subsidiary systems under control of the central executive. A fourth component, the episodic buffer was later introduced (Baddeley, 2000a), which was proposed as a temporary storage system that modulates and integrates different sensory information.

1.2.2.1 Object-location binding in visual working memory

The individual features that contribute to a coherent representation of an event must be integrated, or bound together (Schneegans & Bays, 2018). In the case of visual working memory this might include objects and scenes that are comprised of different visual features e.g., colour, shape, location, orientation. There is some debate in the literature regarding both the stage of memory and the contextual framework that support feature integration.

Two of the most influential models that have been used to conceptualise binding in visual working memory are feature integration theory and the multicomponent working memory model. Feature integration theory proposed that features such as colour and shape were processed independently in parallel streams during early visual processing, and later bound together at an attended location (Treisman & Gelade, 1980; Treisman, 1986). This theory highlighted the importance of focused attention being serially directed across features during the

encoding phase in successful binding. In the context of the multicomponent working memory model, the episodic buffer was initially proposed to provide a binding role, in which working memory processes were thought to consolidate and integrate individual features of episodic memories (Baddeley, 2000a). This view was later updated to suggest that visual features were initially bound together within the visuospatial sketchpad, and then stored as integrated features in the episodic buffer (Karlsen *et al.*, 2010; Baddeley, Allen & Hitch, 2011). Both models suggest that binding is taking place during the encoding stage of memory and stored as an integrated object for later retrieval.

On the contrary, there is also evidence to suggest that object features and object location information are stored separately and the two representations are then associated through a separate binding process (Darling *et al.*, 2006; Schneegans & Bays, 2018). This view is supported by a series of experiments examining the effect of the retention period on binding failures demonstrating that performance, and thus the association between object and location, declined across time. It was concluded that when objects were forgotten they were not absent from memory, rather the associations to their locations were gradually broken (Pertzov *et al.*, 2012). As well as supporting the idea of two separate memory stores, this would also suggest that binding failures may occur within the maintenance period rather than the encoding stage of memory.

Newer perspectives on binding in visual working memory argue that the traditional distinction of storing individual features versus storing integrated objects is too simplistic. It has been suggested that future research should consider how specific conjunctions between features are formed and maintained rather than taking the traditional binary view of whether a bound conjunction or individual feature memories are stored (Schneegans & Bays, 2018). Consideration of the point at which binding occurs in terms of stages of memory processes may be useful in the context of understanding the relationship between working memory and episodic memory deficits in impaired populations such as TBI.

1.2.3 Memory systems in the healthy brain

Human memory depends on a series of connected brain regions that communicate within and between networks to achieve higher order cognition. In healthy adults, successful episodic

memory formation is associated with increased activation of regions in the DAN, including inferior frontal junction, medial intraparietal sulcus, medial temporal and inferior temporal areas during the encoding period (Kim, 2011, 2015). When memory formation is not successful, the encoding period is associated with activation of the default mode network (DMN) and regions including superior-frontal cortex, frontal pole, temporo-parietal junction, posterior cingulate cortex/precuneus, and anterior cingulate cortex/ventromedial prefrontal cortex (Kim, 2011; De Chastelaine *et al.*, 2015; Daselaar *et al.*, 2009). Dynamic integration of networks, including DMN and SN with other sub-networks can create a state of optimal co-ordination between sets of regions for encoding to take place (Keerativittayayut *et al.*, 2018). Episodic memory encoding is therefore reliant on appropriate recruitment of large-scale functional brain networks.

Within these networks are regions considered integral to facilitating contextual binding required for episodic memory formation. The processing of contextual elements of episodic memory rely on distinct cortical pathways converging in the hippocampus. Information from the prefrontal cortex (PFC) is sent via a "what" stream to perirhinal cortex, and a "where" stream to parahippocampal cortex and integrated in the hippocampus to form complete representations (Ranganath, 2010; Preston & Eichenbaum, 2013). Functional imaging of object-location tasks in healthy cognition support the view that the hippocampus has a role in feature binding (Davachi & Wagner, 2002; Libby, Hannula & Ranganath, 2014; Zanto *et al.*, 2016) and the hippocampus is considered crucial in associative binding of episodic memories (Davachi, 2006; Yonelinas *et al.*, 2019; Cooper & Ritchey, 2020). The PFC and hippocampus therefore support complementary functions in the memory system. Indeed, the PFC is part of a wider cognitive control system required for eliciting top-down attentional control and selection of goal-relevant relevant information in memory processes (Miller, 2000; Lara & Wallis, 2015). Connections between the prefrontal cortex and hippocampus are therefore especially important for episodic memory.

Long range communication between key network hubs is supported by phase synchronisation of neural oscillations. Neural oscillations, as measured through electroencephalography (EEG; see Chapter 2) are a key process in memory formation (Luo & Guan, 2018). Phase synchronization, a measure of functional connectivity, refers to the relationship between the phase of oscillations

in two regions (Chapter 2). Long-range phase synchronisation in the theta band supports communication between prefrontal cortex and temporal lobe during encoding, retrieval and working memory maintenance (Sarnthein *et al.*, 1998; Sauseng *et al.*, 2005; Fell & Axmacher, 2011). Theta phase in frontal regions also modulates the amplitude of gamma in temporal and parietal regions in a process known as phase-amplitude coupling (see also Chapters 2 and 4). Theta-gamma phase amplitude coupling is important in encoding, working memory processes and associative binding (Alekseichuk *et al.*, 2016; Axmacher *et al.*, 2010; Friese *et al.*, 2013; Lega *et al.*, 2016; Daume *et al.*, 2017; Köster *et al.*, 2018) and this process is mechanistically supported by long range theta synchronisation (Daume *et al.*, 2017; von Nicolai *et al.*, 2014; Fell & Axmacher, 2011). Theta rhythms, and their interaction with other frequency bands, therefore have a primary role in associative memory that likely underpins memory processes at the large-scale network level (Jann *et al.*, 2010; Yuan *et al.*, 2012; Hacker *et al.*, 2017).

1.2.4 Memory disturbances in TBI

Memory deficits can vary in severity throughout the recovery of TBI: in the acute stages soon after injury memory disturbance can occur in the form of post-traumatic amnesia (PTA; see section 1.3), but deficits are also present in the chronic stages of recovery and can be slower to recover than other cognitive domains (Lezak, 1979).

Episodic memory is significantly impaired following TBI. Meta-analysis by Vakil *et al.* (2019) of 73 episodic memory studies in TBI patients show significant impairments in verbal, visuospatial, recall, recognition, immediate, delayed, word list and story memory compared to healthy controls. Recall, especially in tasks with a verbal component, is more significantly affected than recognition memory which may reflect a more effortful retrieval process than when cues are present (Vakil *et al.*, 2019).

TBI patients also show slower rates of learning and less efficient learning strategies, accelerated forgetting and impaired consolidation mechanisms (Vanderploeg *et al.*, 2014; Azouvi *et al.*, 2017). Learning ability after TBI can be predicted by individual working memory capacity (Chiou, Sandry & Chiaravalloti, 2015) suggesting that pervasive memory deficits in TBI may be underpinned by deficits in working memory (Azouvi *et al.*, 2016). Episodic memory function

relies on executive and working memory processes to appropriately direct attention and bind contextual features and indeed, deficits in executive functioning and working memory are considered a core cognitive deficit in studies of acute and chronic TBI patients (Mcdowell, Whyte & D'Esposito, 1997; Christodoulou *et al.*, 2001; Sanchez-Carrion *et al.*, 2008).

TBI patients show widespread abnormalities in white matter integrity, and damage to white matter microstructure in specific regions has been related to memory deficits. Abnormal white matter integrity across a range of different tracts including the superior-longitudinal fasciculus, inferior fronto-occipital fasciculus and thalamic radiation have been associated with learning and memory performances in TBI patients (Chiou, Genova & Chiaravalloti, 2016; Kim *et al.*, 2019) but the fornix and cingulum seem especially sensitive to memory deficits in TBI (Kinnunen *et al.*, 2011; Zhang *et al.*, 2019). These tracts form important and long-ranging connections within the limbic system, including hippocampal and parahippocampal projections and is thus consistent with disruption of memory circuitry.

White matter damage is widespread and heterogenous across the TBI population. It is therefore likely that cognitive disturbances are due to widespread damage disrupting communication between grey matter regions that serve as key hubs in functional networks required for memory processes. During episodic memory encoding tasks, TBI patients show hyperactivation compared to healthy controls in lateral temporal lobes bilaterally, left MTL, and left parietal lobe (Gillis & Hampstead, 2015), frontoparietal network (Arenth *et al.*, 2012) and subcortical regions (Russell *et al.*, 2011), though others have found no differences (Strangman *et al.*, 2008). These findings have been interpreted as compensatory activation drawing more heavily on other cognitive systems that support memory function (Russell *et al.*, 2011; Arenth *et al.*, 2012). Working memory impairment in TBI correlates with functional activation patterns and the degree of damage to the associated white matter (Palacios *et al.*, 2012) and graph theory analyses in TBI cohorts have demonstrated that damage to the structural connections between network hubs significantly disrupts the cognitive processes associated with those networks (Fagerholm *et al.*, 2015; Jolly *et al.*, 2020). Abnormal activation of brain regions contributing to large-scale functional networks during memory encoding in TBI is likely due to structural disconnection of key functional network hubs. In Chapter 6 I use task-based functional magnetic resonance fMRI

with DTI to explore how brain function and structure differs between chronic TBI patients with and without enduring episodic mnemonic deficits.

Communication across brain regions and the associated disruption to memory processes is also evident at the level of neuronal oscillations. Disruptions to synchronisation, a measure of functional connectivity between regions, has been observed in TBI patients across multiple brain regions and frequency bands: gamma connectivity is decreased across frontal-central and central-parietal electrode pairs (Wang *et al.*, 2017), alpha band demonstrates long range hypoconnectivity and short range hyperconnectivity (Cao & Slobounov, 2010) and synchronisation between frontal regions is disrupted in multiple frequency bands (Sponheim *et al.*, 2011; Thatcher *et al.*, 1989, 2001). These abnormalities are associated with memory deficits. Reductions in low-frequency connectivity are associated with improved neuropsychological performance (Castellanos *et al.*, 2010) and patients with visuospatial working memory impairment show reduced coherence across theta, alpha and beta bands (Kumar *et al.*, 2009). During memory retention, TBI patients show abnormal increases in gamma connectivity between long range interhemispheric frontal-temporal to parietal-occipital regions (Bailey *et al.*, 2017), suggesting compensatory mechanisms may be involved. In Chapter 4 I test whether abnormalities in oscillatory activity and connectivity underlie memory impairment in acute TBI.

There are clearly marked abnormalities in memory function and the underlying processes in TBI patients that endure for many years after injury. The majority of the research focuses on patients in the sub-acute and chronic stages of injury, but memory deficits following TBI in the acute stage should also be considered. Many patients will experience a period of PTA that involves more extreme memory deficits and may be associated with dissociable underlying mechanisms.

1.3 POST-TRAUMATIC AMNESIA

1.3.1 Definition

The concept of PTA was formally introduced by Russell in 1935 who noted that following head injuries, profound memory disturbances were often present. During this period of reduced consciousness, patients may be able to answer simple questions but are disoriented to time and place. Notably, when full consciousness was regained there was little or no recollection of events from this period (Russell, 1935). It was also observed that once the patient emerges from the confused state they may return to a further period of amnesia a concept referred to as 'islands of memory' (Symonds & Ritchie Russell, 1943). There is therefore an emphasis on the return of continuous memory for events, rather than the first memory, in considering the endpoint of PTA. PTA can therefore be formally defined as "the interval of time between injury and the return of continuous memory for everyday events" (McMillan, 2015).

1.3.2 Epidemiology and aetiology

PTA duration can vary from a few seconds through to days, weeks, or months. Despite the highly heterogenous injuries observed some duration of PTA occurs in almost all moderate-severe TBI patients (Ponsford, Sloan & Snow, 2012) and will continue into the rehabilitation stages in around 70% of patients (Marshman *et al.*, 2013). Risk factors for a longer PTA duration include older age, lower initial GCS, slower pupillary responses and longer periods of loss of consciousness (Ellenberg, Levin & Saydjari, 1996; Katz & Alexander, 1994; Sherer *et al.*, 2008).

1.3.3 Clinical presentation

Consistent with the definition provided above, PTA presents primarily as a state of confusion, disorientation and anterograde amnesia (McMillan, 2015) with other marked behavioural abnormalities. Changes in attention and concentration are one of the more common behavioural features of PTA (Nott, Chapparo & Heard, 2008; Hennessy, Delle Baite & Marshman, 2021). Lack of insight into injury severity or inability to understand or engage with

the environment can result in patients being highly irritable, agitated and aggressive (Hennessy, Delle Baite & Marshman, 2021; McMillan, 2015; Spiteri *et al.*, 2021). Patients may also exhibit impulsivity, distractibility, restlessness, repetitive behaviours, emotional lability and less commonly sexually inappropriate or self-abusive behaviours (Corrigan *et al.*, 1992; McKay *et al.*, 2020; Spiteri *et al.*, 2021). The presence of disorientation to self, time and place is also common (Levin, O'Donnell & Grossman, 1979; Shores *et al.*, 1986) and can be reflected in confabulation as patients attempt to interpret surroundings in terms of past experiences (Marshman *et al.*, 2013). Speech can vary in levels of coherence during emergence from PTA but tends to be perseverative around certain ideas (Symonds, 1937). Many patients in the later emergent stages of PTA will appear coherent but conversation depending upon memory for recent events will contain confabulation and perseverance.

1.3.4 Assessment and diagnosis

Tools used to clinically assess PTA in the acute setting focus on measures of orientation and memory. In the UK these are usually delivered on a daily basis by occupational therapists. The most commonly used assessment tools are the Galveston Orientation and Amnesia Test (GOAT; Levin, O'Donnell & Grossman, 1979) and the Westmead PTA Scale (WPTAS; Shores *et al.*, 1986; Marosszeky *et al.*, 2009). The GOAT comprises 10 items that assess orientation and recall of events both before and after injury, thus including assessment of both anterograde and retrograde amnesia. The WPTAS (also see Chapter 2) contains 12 items that incorporate orientation questions with a formal anterograde memory test. Concerningly, there is a substantial discrepancy in estimation of PTA duration depending on the tool used which can lead to under or over-estimation (Marshman *et al.*, 2013; Tate *et al.*, 2006; Hennessy *et al.*, 2020; Tate & Pfaff, 2000). While it is acknowledged that there is a need for brevity in acute clinical assessment, neither tool captures the cognitive complexity in PTA patients. Taken together with the lack of reliability across the two most commonly used tools, there is poor clarity regarding the true construct of PTA. Current assessment tools are restricted and problematic in their criterion (Hennessy, Delle Baite & Marshman, 2021; Marshman *et al.*, 2013; Tate & Pfaff, 2000) and there is a need for more sensitive cognitive measures of PTA as well as better tracking of the emergence from this period.

1.3.5 Clinical and scientific relevance

From a clinical perspective, diagnosing PTA and tracking the duration a patient remains in PTA for is important for several reasons. Firstly, considering their clinical profile, patients in PTA may require additional care provisions and tracking emergence from PTA is therefore useful for allocation of resources and discharge planning. PTA is also a marker of TBI severity (Russell & Nathan, 1946; Bishara *et al.*, 1992; Walker *et al.*, 2010; Friedland & Swash, 2016) and is used as part of the Mayo Classification of TBI severity criteria (Malec *et al.*, 2007; Chapter 2). PTA duration is associated with functional outcomes and therefore has important prognostic value (Ponsford, Spitz & McKenzie, 2015; Nakase-Richardson *et al.*, 2011; Eastvold *et al.*, 2013; Gurin, Rabinowitz & Blum, 2016). PTA duration also predicts impairments in general intelligence (Königs, De Kieviet & Oosterlaan, 2012) and cerebral atrophy (Wilde *et al.*, 2006) suggesting that patients with a longer duration are likely more cognitively impaired in the long term.

From a scientific perspective PTA offers a rare opportunity to study the memory system when it is transiently broken. While many other clinical groups show impaired memory function these tend to be irreversible or degenerative. This limits the ability to be specific about the neurophysiological changes that are associated with impairments in cognition as these cannot be separated from other aspects of the disease. Recovery of cognitive abilities that are most profoundly impaired during PTA allows for within-subject comparison and more precise inferences regarding the relationship between memory deficits and changes in brain function and structure to be made. This not only furthers understanding of PTA as a clinical construct but also serves as a well-controlled model to enhance understanding of memory processes.

1.3.6 Cognitive profile

Patients in PTA were initially thought to be globally more impaired than TBI patients without PTA and have a wider range of cognitive deficits than patients with chronic memory impairment or amnesic syndrome (Mandleberg, 1975; Wilson *et al.*, 1992). Cognitive disturbances are common in PTA, but there is growing evidence that these patients exhibit a more specific cognitive profile (Keelan *et al.*, 2019; Hennessy, Delle Baite & Marshman, 2021).

Memory deficits are among the most pronounced abnormalities in PTA. Working memory capacity is reduced in PTA patients for verbal and spatial information (Wilson *et al.*, 1999; De Simoni *et al.*, 2016). Cued and free recall memory is impaired (Baird *et al.*, 2005; Gasquoine, 1991; Ewert *et al.*, 1989; Andriessen *et al.*, 2009; Keelan *et al.*, 2019; Kalmar *et al.*, 2008) and less information is acquired during learning (Gasquoine, 1991; Kalmar *et al.*, 2008; Keelan *et al.*, 2019; Wilson *et al.*, 1999). Information that is acquired is more readily forgotten, especially with longer maintenance periods (Andriessen *et al.*, 2009; Levin, High & Eisenberg, 1988). Recognition memory and procedural memory generally remain intact (Ewert *et al.*, 1989; Glisky & Delaney, 1996; Wilson *et al.*, 1992), supporting the idea that some information can be encoded in PTA.

PTA patients also demonstrate impairments in information processing and attention. Simple and choice reaction time measures are sensitive to PTA (Baird *et al.*, 2005; De Monte *et al.*, 2006; Kalmar *et al.*, 2008; Keelan *et al.*, 2019; De Simoni *et al.*, 2016; Wilson *et al.*, 1999) and attentional impairments prominent (Ahmed *et al.*, 2000; Stuss *et al.*, 1999; Hennessy, Delle Baite & Marshman, 2021). Deficits in attention may account for some of the behavioural features of PTA such as disorientation and agitation (Stuss *et al.*, 1999; Corrigan *et al.*, 1992; Tittle & Burgess, 2011) but may also be related to disturbances in encoding abilities.

Discrepancies in the degree of cognitive impairment across different cohorts could be due to the degree of emergence from PTA. Recognition memory recovers prior to free recall (Tate, Pfaff & Jurjevic, 2000; Geffen, Encel & Forrester, 1991; Leach *et al.*, 2006; Stuss *et al.*, 1999) and reorientation to person occurs prior to place or time (High, Levin & Gary, 1990; Geffen, Encel & Forrester, 1991; McFarland, Jackson & Geffe, 2001; Tate, Pfaff & Jurjevic, 2000). More complex cognitive processes requiring goal-directed attention take longer to recover than simpler, automatic functions (Roberts, Spitz & Ponsford, 2015; Spiteri *et al.*, 2021) suggesting that PTA may be better conceptualized as a spectrum of deficits rather than a dichotomously defined period of amnesia.

1.3.7 Current mechanistic understanding

While the clinical and behavioural deficits apparent in PTA have been extensively studied, the mechanistic underpinnings of PTA are not well understood. There is no clear consensus on aetiology, though it is likely that a disruption in systems-level brain dynamics, rather than focal damage to individual regions, underpins the clinical presentation.

The hippocampus, a structure within the medial temporal lobe (MTL) has a well-established role in memory (Turner, 1969; Bird & Burgess, 2008) and hippocampal involvement in PTA might therefore be expected. Patients with a longer PTA duration are reported to exhibit more prominent hippocampal atrophy than those with a shorter duration, though some patients with PTA exhibit no hippocampal atrophy (Brezova *et al.*, 2014). This would suggest that PTA pathology is unlikely to be due to MTL damage alone, and is more likely due to whole brain network disturbances (Bigler, 2016).

Consistent with the network disruption hypothesis is evidence that damage to white matter microstructure is associated with PTA duration. Preferential damage to white matter connecting deep brain structures and diffuse whole brain microstructural damage have both been associated with duration of PTA in severe TBI (Andreasen *et al.*, 2020; Cho & Jang, 2021; Mazwi *et al.*, 2019; De Simoni *et al.*, 2016). White matter connections support communication between functional brain networks and it is therefore likely that the disruption to white matter integrity is reflected in functional disturbances important for cognition (Sharp, Scott & Leech, 2014). Indeed, associative learning and memory disturbances in PTA are associated with reduced functional connectivity between the PCC, a key hub of the DMN, and the parahippocampus (De Simoni *et al.*, 2016). Functional connectivity between these key brain regions important for within and between network communication was transient and specific to the period of PTA. This suggests that disruption to cognitive control networks is involved in PTA.

Disruption to white matter integrity is also present in chronic TBI and endures long after the transient period of PTA has resolved (Kinnunen *et al.*, 2011). The relationship between PTA duration and reductions in white matter might therefore be reflective of injury severity rather than reduced white matter reflecting a mechanism of PTA. Mechanisms underpinning memory

impairment in the acute and chronic stages are likely separable. The functional disturbances in PTA may reflect large scale disruption to cortical communication which is explored in the context of EEG measures of oscillatory power and coherence in Chapter 4 and functional resting state network dynamics in Chapter 5.

Updating our understanding of the concept of PTA from behavioural and mechanistic perspectives will aid in improvement of clinical understanding and rehabilitation needs in this patient group. It will also provide further insight into how memory systems in the brain interact to produce the transient but profound disruption to cognitive processes.

1.4 SUMMARY

Memory deficits following TBI are prominent throughout all stages of recovery. PTA is currently considered a dichotomy from a diagnostic perspective. Memory deficits are present for many years following TBI. However, there are remaining questions regarding how specific abnormalities, both cognitive and physiological, are to a period of PTA rather than being part of a spectrum of impairment that endures into the chronic stages of recovery.

In this thesis I combine in-depth cognitive assessments with multi-modal imaging techniques. I describe the neurocognitive profile of acute TBI patients and explore how abnormal brain function in this population may contribute to PTA. I examine enduring memory deficits in a chronic TBI population and assess how these are underpinned by abnormal functional and structural brain changes.

2

Materials & Methods

In this chapter I give an overview of the study designs, participants and materials and methods used within the experimental chapters of this thesis. I detail the clinical and cognitive assessments used to define and evaluate the participants. I introduce the main concepts behind the imaging techniques and outline the acquisition and pre-processing parameters used in the data presented in this thesis.

2.1 OVERVIEW & EXPERIMENTAL DESIGN

Many of the methodological approaches and experimental tools used in this thesis are relevant to multiple chapters and will therefore be described here with reference to which chapters of the thesis they pertain to. I will give a background to the core methods used and detail acquisition and pre-processing parameters where relevant, but details of individual analyses will be described in the relevant chapters.

This thesis consists of four key experimental chapters. The data presented in Chapters 3 and 4 are from longitudinal experiments and contain baseline and follow-up data in TBI patients compared to a single time-point in healthy controls. The data presented in Chapters 5 and 6 are from cross-sectional experiments and contain only a single timepoint.

All study procedures for data presented in Chapters 3, 4 and 5 were carried out in the Major Trauma Centre, St Mary's Hospital, Imperial College Healthcare NHS Trust (London, UK). Study procedures for data presented in Chapter 6 were carried out at the Clinical Imaging Facility, Hammersmith Hospital, Imperial College London (London, UK).

2.2 PARTICIPANTS

There are three cohorts of participants that have contributed to the data presented in this thesis. Figure 2.1 gives an overview of these cohorts and the subject data flow across chapters. Each row demonstrates a single subject and the chapters that their data contributed to. Characteristics of subjects included in each analysis are given within the relevant experimental chapters.

2.2.1 Recruitment of acute TBI cohorts

There are two cohorts of acute traumatic brain injury (TBI) patients recruited within the first two weeks of injury: the new acute cohort (Chapters 3, 4 and 5) is data that I collected during my PhD. Where possible, participants were invited to take part in all aspects of the study (Chapters 3, 4 and 5). However, due to the nature of recruitment within an acute clinical setting this was not always possible or appropriate. The historical acute cohort is previously published imaging data from De Simoni *et al.* (2016) that aligns with the study protocol presented in Chapter 5. Both acute cohorts also contain healthy control subjects. Healthy controls were recruited alongside the acute patient cohorts through friends and family of patients and gave written informed consent.

Patients in both the new and historical acute cohorts were recruited from the Major Trauma Ward (MTW) at St Mary's Hospital, Imperial College Healthcare Trust, London, UK within the first two weeks of injury (see sections 2.2.3 & 2.2.4 for inclusion and exclusion criteria). Written informed consent was obtained for patients judged to have capacity according to the Declaration of Helsinki. Patients currently in a period of post-traumatic amnesia (PTA) who were judged not to have capacity were deemed unable to give informed consent for participation in the study (see 2.3.2 for details of PTA assessment). In this case, written assent was obtained from these patients as well as informed written assent by a caregiver on behalf of the patient. Informed consent was gained retrospectively for these patients once they emerged from PTA. No patients withdrew their consent once they emerged from PTA.

All experiments presented in Chapter 3, 4 and 5 were conducted under approval by the West London Research Ethics Committee (09/HO707/82).

2.2.2 Recruitment of chronic TBI cohort

Chapter 6 contains data from a cohort consisting of TBI patients in the chronic stage of recovery and two separate cohorts of healthy controls. Details of the control groups are given in Chapter 6, section 6.2.2. Healthy controls were recruited through the National Institute for Health Research (NIHR) Imperial Clinical Research Facility, London, UK, and family members of patients.

Patients in the chronic TBI cohort that contributed data to Chapter 6 were recruited from specialist TBI clinics and military rehabilitation units. All TBI patients were in the post-acute/chronic stage of recovery from injury (see Chapter 6 section 6.2.1).

The study presented in Chapter 6 was approved by the Hammersmith and Queen Charlotte's and Chelsea Research Ethics Committee, and the Ministry of Defence Research Ethics Committee (MODREC). All participants gave written informed consent in accordance with the Declaration of Helsinki.

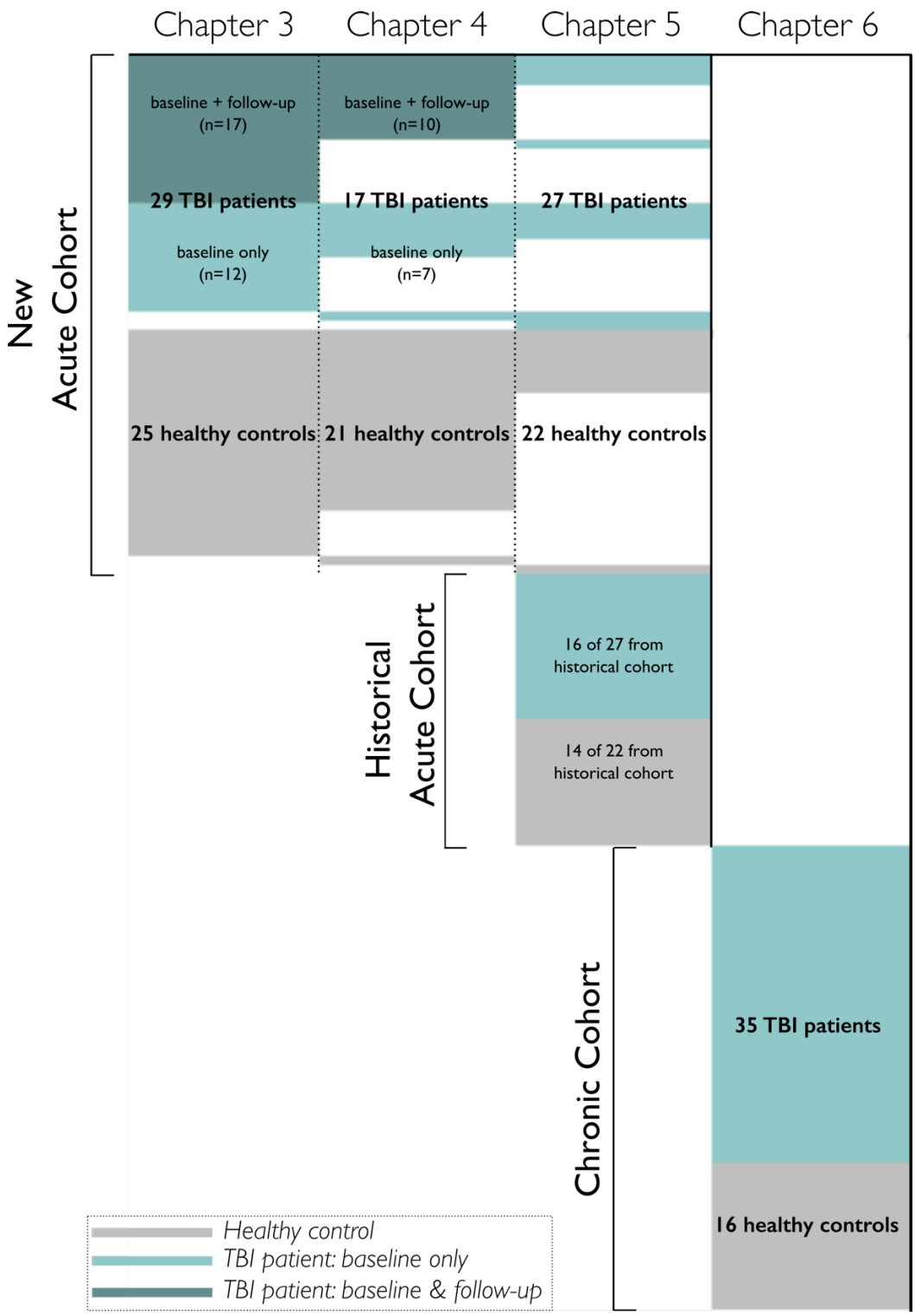

Figure 2.1 Flow of data across experimental chapters

The different cohorts included in the thesis and which chapters their data contributes to. One row represents a single subject to illustrate that some subjects contributed data to multiple chapters.

2.2.3 Inclusion criteria

The inclusion criteria for patients and controls across all experimental chapters and all study cohorts was as follows:

i) Aged 16 – 80 years
ii) Able to follow study procedures

In addition, inclusion criteria for patients:

iii) Diagnosis of a moderate-severe TBI as defined by the Mayo TBI Classification system (Malec *et al.*, 2007; see 1.4 Classification of TBI Severity).

2.2.4 Exclusion criteria

Exclusion criteria applied to all patients and controls across all experimental chapters was as follows:

i) Significant psychiatric or neurological illness (premorbid to current brain injury in patients)
ii) Previous brain injury
iii) Current or previous substance or alcohol abuse
iv) Current pregnancy or breastfeeding
v) Contraindication to MRI assessed using MRI safety questionnaire (Chapters 5 and 6 only)
vi) Recent neurosurgical intervention or other contraindication to scalp EEG (Chapter 4 only)

2.3 CLINICAL AND COGNITIVE ASSESSMENTS

2.3.1 TBI severity

TBI severity was assessed according to the Mayo TBI Classification system (Table 1.1; Malec *et al.*, 2007), which uses a combination of measures to grade injury severity as *Symptomatic (Possible)*, *Mild (Probable)* or *Moderate-Severe (Definite)*. Measures used to determine severity include duration of any loss of consciousness (LOC), PTA duration, lowest-recorded Glasgow Coma Scale (GCS) and imaging findings

2.3.2 PTA Assessment

PTA was assessed using the Westmead Post-Traumatic Amnesia Scale (WPTAS; Figure 2.2; Shores *et al.*, 1986; Marosszeky *et al.*, 2009) in accordance with standard clinical practice on the MTW at St Mary's Hospital. The WPTAS is a standardised tool designed to assess PTA and measure the duration of this period. It contains 7 orientation questions and 5 memory items. The WPTAS is administered daily. On the first day of testing the maximum score is 7/7. On subsequent days the memory items are tested (24 hr delay) and the maximum score is therefore 12/12. A person scoring < 12 is deemed to be in PTA. A person is deemed to be out of PTA from the first day of scoring 12/12 for three consecutive days.

Table 2.1 The Mayo TBI classification system

A.	Classify as ***Moderate-Severe (Definite)*** if one or more of the following apply	i)	Death secondary to this TBI
		ii)	LOC of 30 minutes or more
		iii)	PTA duration of 24 hours or more
		iv)	*Worst GCS in first 24 hours <13
		v)	One or more of the following present on imaging: • Intracerebral haematoma • Subdural haematoma • Epidural haematoma • Cerebral contusion • Haemorrhagic contusion • Penetrating TBI (dura penetrated) • Subarachnoid haemorrhage • Brain stem injury
B.	If none of Criteria apply, classify as ***Mild (Probable)*** if one or more of the following criteria apply:	i)	LOC of momentary to less than 30 minutes
		ii)	PTA of momentary to less than 24 hours
		iii)	Depressed, basilar, or linear skull fracture (dura intact)
C.	If none of Criteria A or B apply, classify as ***Symptomatic (Possible***) if one or more of the following symptoms are present:	i)	Blurred vision
		ii)	Confusion (mental state change)
		iii)	Dazed
		iv)	Dizziness
		v)	Focal neurologic symptoms
		vi)	Headache
		vii)	Nausea

TBI = traumatic brain injury; LOC = loss of consciousness; PTA= post traumatic amnesia; GCS = Glasgow Coma Scale; * unless invalidated upon review e.g. attributable to intoxication, sedation, systemic shock

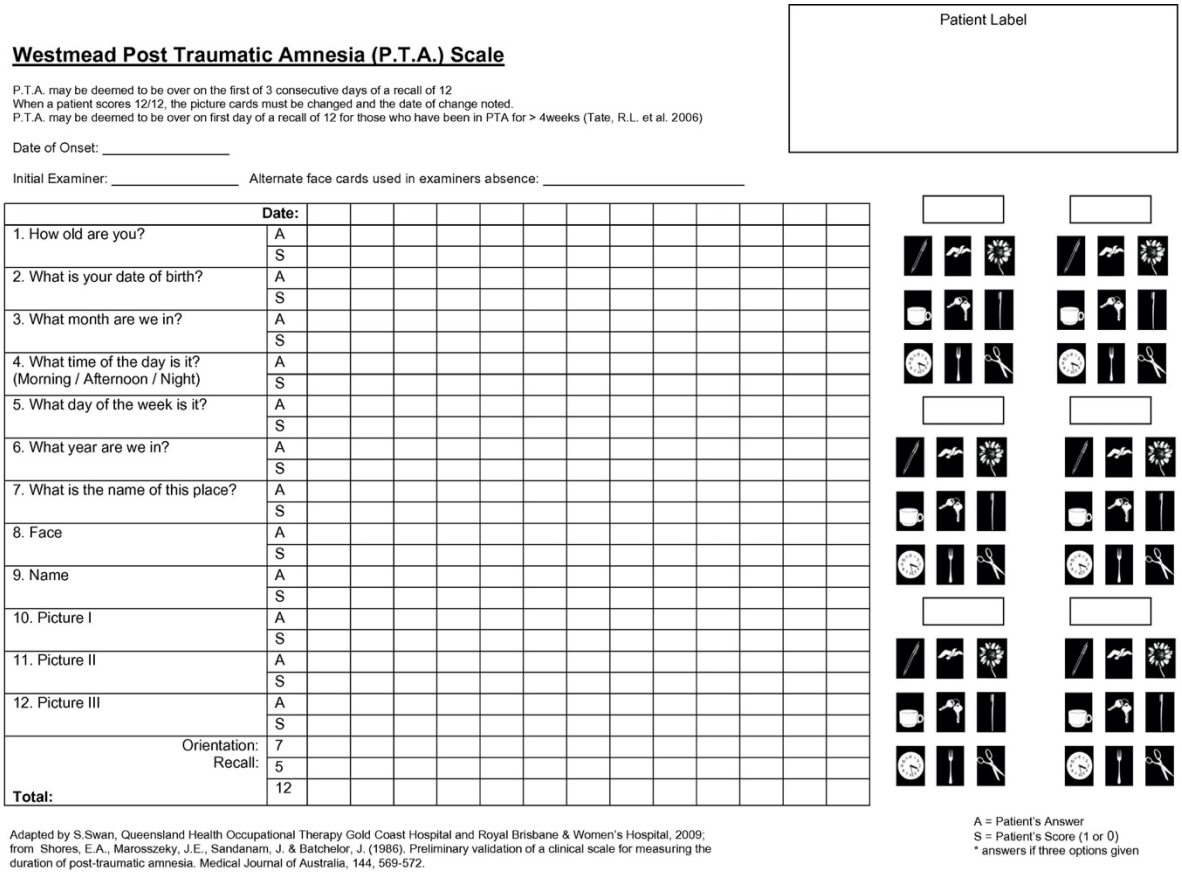

Westmead Post Traumatic Amnesia (P.T.A.) Scale

Patient Label

P.T.A. may be deemed to be over on the first of 3 consecutive days of a recall of 12
When a patient scores 12/12, the picture cards must be changed and the date of change noted.
P.T.A. may be deemed to be over on first day of a recall of 12 for those who have been in PTA for > 4weeks (Tate, R.L. et al. 2006)

Date of Onset: _____

Initial Examiner: _____ Alternate face cards used in examiners absence: _____

		Date:													
1. How old are you?	A														
	S														
2. What is your date of birth?	A														
	S														
3. What month are we in?	A														
	S														
4. What time of the day is it? (Morning / Afternoon / Night)	A														
	S														
5. What day of the week is it?	A														
	S														
6. What year are we in?	A														
	S														
7. What is the name of this place?	A														
	S														
8. Face	A														
	S														
9. Name	A														
	S														
10. Picture I	A														
	S														
11. Picture II	A														
	S														
12. Picture III	A														
	S														
Orientation:	7														
Recall:	5														
Total:	12														

A = Patient's Answer
S = Patient's Score (1 or 0)
* answers if three options given

Adapted by S.Swan, Queensland Health Occupational Therapy Gold Coast Hospital and Royal Brisbane & Women's Hospital, 2009; from Shores, E.A., Marosszeky, J.E., Sandanam, J. & Batchelor, J. (1986). Preliminary validation of a clinical scale for measuring the duration of post-traumatic amnesia. Medical Journal of Australia, 144, 569-572.

Figure 2.2 The Westmead Post-Traumatic Amnesia Scale

The Westmead Post-Traumatic Amnesia Scale (WPTAS) used to assess the presence and duration of PTA in acute TBI patients. The scale consists of 7 orientation questions and 5 memory questions. Questions 10, 11 and 12 use picture cards in rotation as displayed on the right of the image.

2.3.3 Neuropsychology

Detailed neuropsychological assessments in the form of standardised pen-and-paper assessments and a computerised battery based on classical test paradigms were used to assess cognitive function.

2.3.3.1 Standardised neuropsychological assessments

In the new acute cohort, measures of verbal recall and visuospatial memory were obtained using standard pen and paper neuropsychological tests including:

i) The Logical Memory I and II sub-tests of the Wechsler Memory Scale, third edition (Wechsler, 1997)

ii) The Brief Visuospatial Memory Test-Revised (Benedict *et al.*, 1996)

In the chronic cohort (Chapter 6), the standard pen and paper neuropsychology battery was more extensive and additionally included:

iii) The People Test from the Doors and People Test (Baddeley, Emslie & Nimmo-Smith, 1994)

iv) The Wechsler Test of Adult Reading (Wechsler, 2001)

v) The Matrix Reasoning subtest of the Wechsler Abbreviated Scale of Adult Intelligence (Corporation, 1999)

vi) The Colour-Word Interference (Stroop) tests from the Delis-Kaplan Executive Function System (Delis, Kaplan & Kramer, 2001)

vii) The Trail Making Test (forms A and B; (Reitan, 1958)

2.3.3.1.1 Logical Memory

The Logical Memory sub-test of the WMS-III measures immediate and delayed verbal memory recall (Wechsler, 1997). Participants are read a short story and immediately asked to repeat back in as much detail as possible what they remember of it. Following a twenty-minute delay they are once again asked to recall as much of the story as they remember. Points are awarded for specific

phrases recalled. A recognition memory test is also delivered in which participants are asked questions pertaining to the story to which they must answer yes or no. The task consists of two separate stories. A higher score represents a greater performance.

2.3.3.1.2 Brief Visuospatial Memory Test-Revised

The Brief Visuospatial Memory Test-Revised (BVMT-R; Benedict *et al.*, 1996) measures immediate and delayed visuospatial memory. In the three learning trials participants are shown a stimulus page consisting of 6 independent geometric figures printed in a 2x3 array for a duration of 10 seconds. They are then immediately asked to reproduce the stimulus page from memory. A delayed recall trial 25 minutes later requires them to reproduce the stimulus page without being shown it again. Marks are given for correct geometric features and spatial orientation. Scores on each of the trials are out of 12. Following the free-recall trials, a recognition test involves showing the participants 12 geometric shapes (6 novel) and asking them to state whether the shape was in the initial array.

2.3.3.1.3 The People Test

The People Test from the Doors and People Test (Baddeley, Emslie & Nimmo-Smith, 1994) measures verbal recall and forgetting. In the three learning trials, participants are shown photographs of four people and told their profession and name. After a short delay, participants are asked to verbally recall the name of the people as prompted by their profession (e.g. "What was the name of the doctor?"). Following a 20-minute delay, participants are once again asked to recall the name of the people using the same prompting.

2.3.3.1.4 Wechsler Test of Adult Reading

The Wechsler Test of Adult Reading (WTAR; Wechsler, 2001) provides a measure of premorbid intelligence. Participants are presented with a list of 50 words of increasing complexity and asked simply to read them. They receive a point for each correct pronunciation. Scores are then scaled according to population norms for the participants age group.

2.3.3.1.5 Matrix Reasoning

The matrix reasoning subtest of the Wechsler Abbreviated Scale of Adult Intelligence (WASI; Corporation, 1999) provides a measure of abstract reasoning and problem solving reflecting

intellectual ability. The test consists of 26 trials each involving a 2x2 grid. Three of the four grid squares contain a shape. Participants must select from a choice of five shapes, which would most appropriately fit in the grid based on a rule inferred from the other three shapes. One point is awarded for each correct trial thus a higher score represents a greater reasoning ability.

2.3.3.1.6 Colour-Word Interference Stroop Test

The Colour-Word Interference Test from the Delis-Kaplan Executive Function System provides a measure of executive function (Delis, Kaplan & Kramer, 2001). The test comprises of four trials of increasing difficulty. In the first trial participants name blocks of basic colour (red, green, blue). In the second trial participants read the names of colour in word form. In the third trial an inhibition element is introduced, and participants must name the colour of the ink based on words written in opposing colours (e.g., the word blue written in red ink). In the final trial, the task from trial three is repeated (naming the colour of the ink) except for a switching element is introduced whereby when a word is in a box it must be read (e.g., read the word, ignore the ink colour). Each trial is timed based on total completion without errors and contrasts between trials provide the time cost of inhibition and switching trials. A longer duration represents a greater impairment in processing speed and executive functioning.

2.3.3.1.7 The Trail Making Test

The Trail Making Test (forms A and B) measures executive function and processing speed (Reitan, 1958). This task comprises of two trials. The first trial involves a series of circles containing numbers ranging from 1-25. The participant must draw a continuous line between the circles in ascending order (e.g., 1-2-3). The second trial contains some circles with numbers and some with letters. The participant must connect the circles in ascending and alphabetical order, alternating between the two (e.g., 1-A-2-B-3-C). If an individual makes an error, they must return to the last correct point and continue from there. The outcome measure is the total duration of each trial. A switching cost is calculated based on the contrast between the trials.

2.3.3.2 Computerised neuropsychological assessments

A computerised battery of neuropsychological tests was used to supplement standardised neuropsychological testing in patients and controls included in Chapters 3, 4 and 5. The battery, comprised of 5 computerised tests (Figure 2.3) based on classical paradigms from the cognitive psychology literature, was delivered on a touchscreen tablet device using a custom-programmed application. The tasks used here are a subset of a longer, previously studied battery (Hampshire *et al.*, 2012).

2.3.3.2.1 Paired Associates

The paired associates learning (PAL) task is based on a paradigm commonly used to assess memory impairments in aging clinical populations (Gould *et al.*, 2005). The PAL was used to assess object-location association memory. Boxes are displayed at random locations across the screen within a 5x5 grid. One at a time the image hidden under each box will be revealed and disappear again. The participant is then shown an image in the centre of the screen and must decide which box it was previously hidden under. The task initially involves two squares and this increases for every correct trial. In the event of an incorrect trial the additional box is removed. The task ends after three errors. The main outcome measure is the maximum number of squares achieved. Population mean = 5.28, standard deviation (SD) = 1.13.

2.3.3.2.2 Monkey Ladder

Monkey Ladder, based on a task from the non-human primate literature (Inoue & Matsuzawa, 2007), was used to assess visuospatial working memory. Squares containing numbers are displayed on the screen at random locations within a 5x5 grid. Once the squares disappear the participant is required to tap each square in ascending numerical order. The task begins with just 2 squares and this increases by one extra square with each correct answer. An incorrect answer results in one less square. The task ends after three errors. The main outcome measure is the maximum number of squares achieved. Population mean = 7.85, SD =1.15.

2.3.3.2.3 Feature Match

Feature Match, based on the classical feature search task (Treisman & Gelade, 1980), was used to measure attentional processing. Two grids are presented side by side each containing a series

of shapes. The shapes presented in each grid are identical for half of all trials and differ by one shape in the other half of trials. The participant must state whether they match or mismatch. The first trial contains one shape in each grid and this increases with each correct response. One less shape in each grid is present following each incorrect response. The task lasts for 90 seconds during which the participant must solve as many trials as possible. The main outcome measure is the total score. Population mean = 131.35, SD = 32.79.

2.3.3.2.4 Self-ordered Search

Self-Ordered Search was used to measure strategy during search behaviour, based on an existing task (Collins *et al.*, 1998). Boxes are displayed on the screen in random locations within an invisible 5x5 grid. Participants are required to search through the boxes to collect hidden tokens. Within a trial, a token will appear in every box once, but never in the same box twice. If the participant searches in a box that has either already produced a token or that they have already searched in then they incur an error. The task begins with four boxes and increases by one box for each correct trial. If a trial results in an error the next trial contains one less box. The task ends after three errors are made. The main outcome measure is the maximum number of boxes achieved. Population mean = 8.23, SD = 2.10.

2.3.3.2.5 Spatial span

Spatial span, based on the Corsi Block Tapping Task (Corsi, 1973), was used to assess spatial short term memory capacity. Sixteen squares are displayed in a 4x4 grid and one at a time a series of the squares will flash. The participant is then required to tap the squares in the order that they flashed. The test starts with four squares flashing and increases by one square for every correct trial. If an error is made there is one less square in the subsequent trial. The task ends after three errors. The main outcome measure is the maximum number of squares achieved. Population mean = 6.15, SD = 1.07.

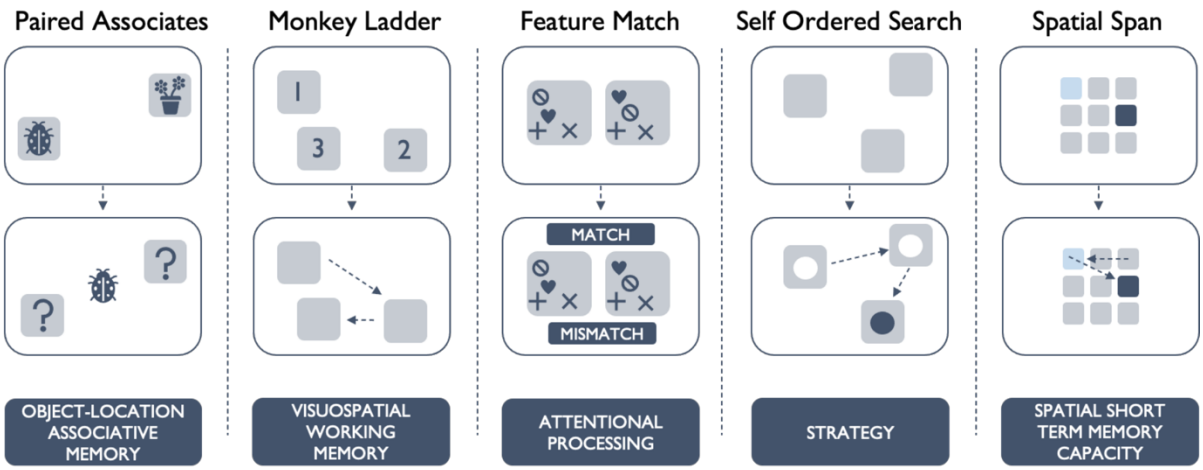

Figure 2.3 Battery of computerised cognitive assessments

The computerised cognitive assessments delivered on a touchscreen tablet device used to assess the cognitive domains of associative memory, visuospatial working memory, attentional processing, search strategy and spatial short-term memory capacity.

2.4 ELECTROENCEPHALOGRAPHY

Electroencephalography (EEG) is a non-invasive technique used to record the electrical activity arising from the human brain. It was first used in humans as early as 1924 by Hans Berger who observed rhythmic activity in the brain (Jung & Berger, 1979). EEG directly measures neural activity with high temporal precision and is therefore a popular technique for understanding the neural basis of cognitive processes.

2.4.1 Principles of EEG

EEG works on the principles of detecting synchronous neural activity from cortical regions using scalp electrodes.

2.4.1.1 Neural source of EEG

Neurons communicate via synaptic connections. Pre-synaptic action potentials travel down the length of the axon to release neurotransmitters into the synaptic cleft which bind to receptors of the postsynaptic neuron. Transmitter-gated ion channels in the postsynaptic neuron release a flow of ions that cause a voltage change across the membrane producing the post-synaptic potential. The electrical signal recorded by EEG is generated by these ionic currents in the dendritic membrane. The direction of this current flow depends on whether the synapse is excitatory or inhibitory. Inhibitory inputs are received near the cell body, while excitatory inputs are mainly into the distal regions of the dendrite creating an anatomical separation between positive and negative charge. The spatial separation of opposite charges allows for the dipole, a field with positive and negative poles, to exist (Beniczky & Schomer, 2020). In isolation, the dipole produced by the post-synaptic potential of a single neuron is too small to be measured from the scalp. The sum of many neurons synchronously firing in neuronal assemblies is necessary to produce a signal detectable at the scalp level (Figure 2.4).

An EEG scalp electrode measures the sum of positive and negative dipoles arising from post-synaptic potentials from multiple neurons (Jackson & Bolger, 2014). Pyramidal cells in cortical

layers IV and V are oriented perpendicular to the brain's surface in a manner such that the cell bodies are parallel to one another and the dendrites extend to superficial cortical layers (Beniczky & Schomer, 2020). This unique arrangement is necessary for EEG signal to be detected so individual dipoles' signals do not cancel each other out (Jackson & Bolger, 2014).

The EEG signal is therefore dependent on two necessary conditions being met: aligned neurons and synchronous activity. The signal detected at the electrode level is the summed dipoles that are formed between cell body and dendrites arising from post-synaptic potentials in cortical pyramidal cells (Figure 2.4).

2.4.1.2 Measuring EEG signals

In order to be measured non-invasively the EEG signal produced from neural firing in cortical layers must travel through dura layers, skull layers, the scalp and to the electrode (Louis *et al.*, 2016). Within the brain, the signal is carried via volume conduction, the process through which ions repel those of a like charge allowing for a wave of charge to travel through the extracellular space (Jackson & Bolger, 2014). Ions cannot pass through the skull, therefore once the signal reaches the skull it can travel no further, and conductive gel that can saturate the layers of poor conductors (e.g., dead skin cells, hair) is required to bridge the gap between scalp and electrode (Figure 2.4).

The strength of the EEG signal is measured in microvolts. Factors that can influence microvolt values detected at each electrode include individual differences such as skull shape and thickness, the scalp preparation, cortical folding, and the quality of the electrode and amplifier used (Cohen, 2014). To gain an EEG measure at one electrode, the voltage must be compared to another. A reference site is often used to achieve this, and the microvolt recorded from each electrode therefore represents the change in electrical potential between that electrode and the reference electrode. These values are magnified by an amplifier which multiplies the input voltage by some constant and measures the potential difference between pairs of electrodes (Ebner *et al.*, 1999).

Electrodes are placed at various locations across the scalp, and a standardised system such as the international 10-20 system (Jasper, 1958) can be used to describe their location. The 10-20 system describes each electrode with a letter to denote the cortical lobe they refer to (e.g., P = parietal, O = occipital), and the hemisphere (odd numbers = left hemisphere, even numbers = right hemisphere, z = midline). See section 2.4.2 for the montage used in the data collected for this thesis.

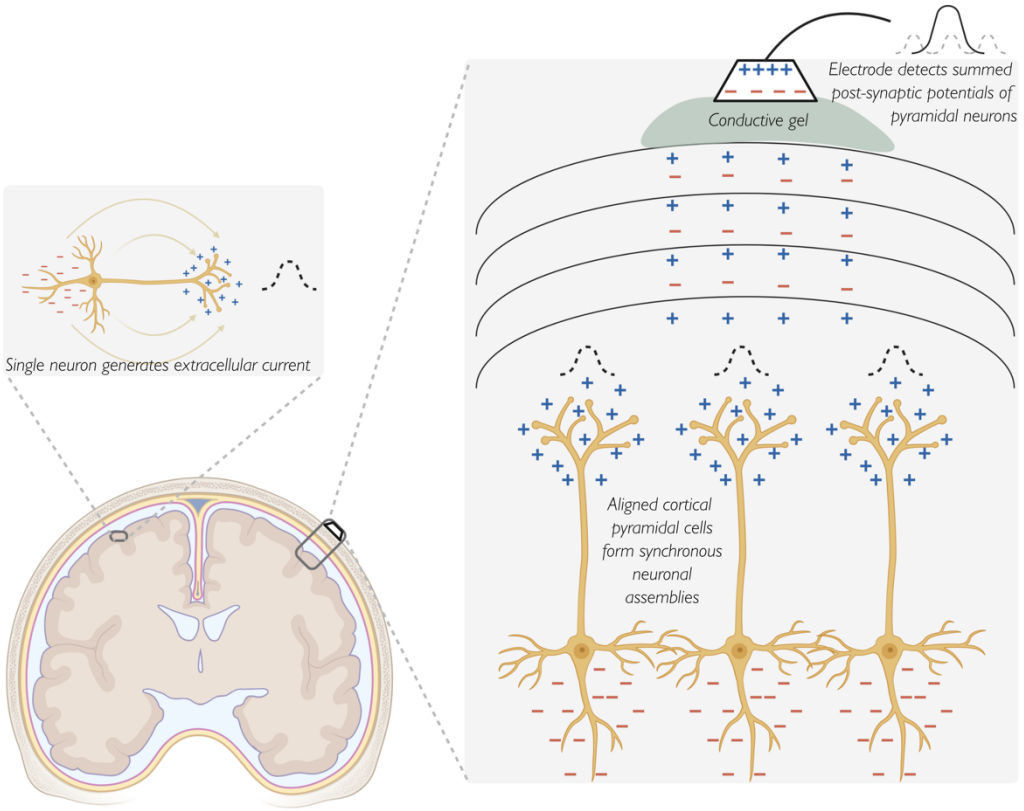

Figure 2.4 The neural basis of EEG signal

Single neurons generate extracellular current that in isolation cannot be detected by EEG. Aligned neurons in the cortical layers form synchronous neuronal assemblies that travel via volume conduction and are detected at the scalp level. Figure based in part on Jackson & Bolger, *Psychophysiology*, 2014

2.4.1.3 EEQ Time-Frequency

It is unusual to interpret EEG data in the context of absolute microvolt values, the signal intensity, but rather to consider the signal in terms of neural oscillations using time-frequency analysis techniques. Oscillations in the context of EEG refer to the rhythmic activity produced by the brain and are generally described using three pieces of information: frequency, power and phase (Cohen, 2014; Figure 2.5). The frequency, measured in Hertz is the speed of oscillations, or the number of oscillations per second. Power refers to the amount of energy that is in a frequency band, or how strong it is, and is typically expressed as squared amplitude. Phase is the amount of synchronisation present across neurons and refers to the position along the wave at any given point, expressed as a value between 0 and 360 degrees. Time-frequency analyses give additional information such as which frequencies are most dominant at specific points in space and time, and how their phase angles come in and out of synchrony (Roach & Mathalon, 2008). Transformation to the time-frequency domain is typically achieved using Fourier transformation (the mathematical decomposition of signal into the sine wave to represent the frequency domain) on windows of data that represent the time domain. Transformations of data presented in this thesis are described in the relevant EEG analysis sections in Chapter 4.

The frequency of neural oscillations can be separated out into different bands (Chatterjee, Datta, & Sanyal, 2019; Figure 2.6). The boundaries of these frequency bands can vary slightly across studies but are generally considered to be delta (0-4Hz), theta (4-8Hz), alpha (8-13Hz), beta (13-30Hz) and gamma (> 30Hz). The EEG analyses undertaken on the data presented in this thesis are detailed in Chapter 4.

Figure 2.5 Defining oscillations with frequency, phase, and power

Oscillations derived from EEG can be described using three dimensions. Frequency is how fast the oscillations are. Phase is the position along the wave. Power is how strong the oscillation is. Figure based on Analyzing Neural Time Series Data, Cohen, 2014.

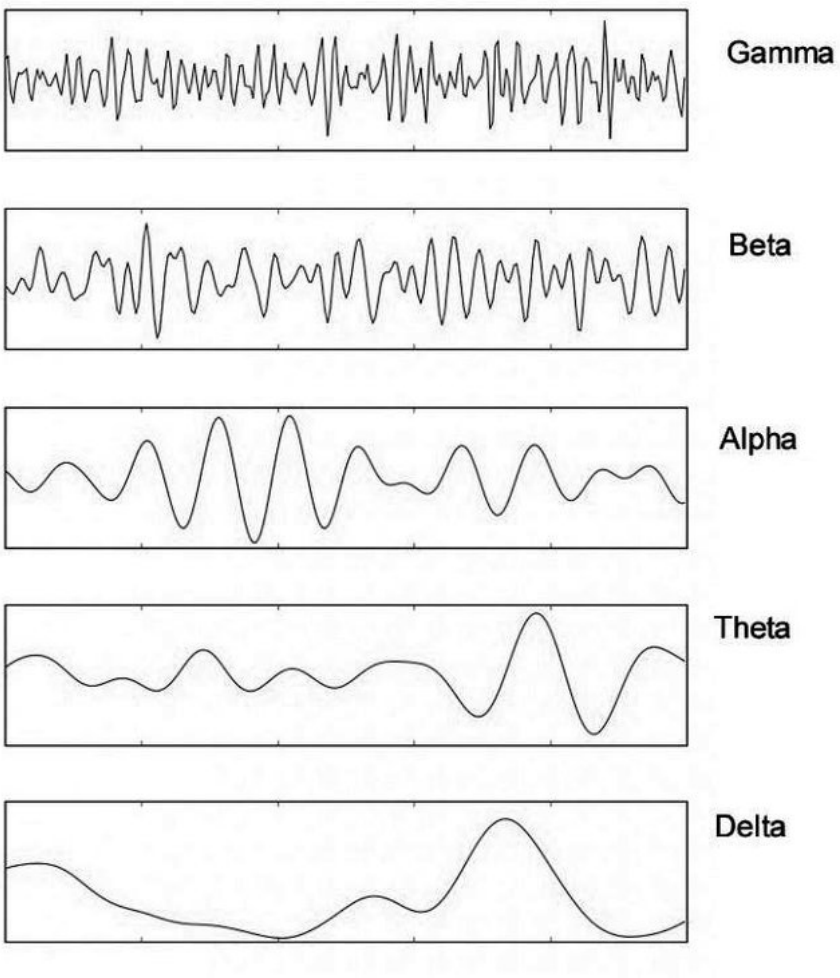

Figure 2.6 Frequency bands in EEG

Commonly used frequency bands in EEG. High (fast) frequencies are shown at the top descending down to low (slow) wave frequencies at the bottom. In descending order: Gamma (>30Hz); Beta (13-30Hz); Alpha (8-12 Hz); Theta (4-8Hz); Delta (0-4Hz). Figure from Chatterjee, Datta & Sanyal, 2019, Machine Learning in Bio-Signal Analysis and Diagnostic Imaging.

2.4.2 EEG data acquisition

Participants were seated facing a screen in dimly lit room and all unnecessary electrical equipment was switched off to minimise electrical noise. The scalp was prepared using clinical alcohol swabs to clean and disinfect the site and remove any excess oils. Participants were educated regarding the effect of eye blinks and muscle movement in generating artefacts and were encouraged to remain as still as possible throughout the acquisition.

A 32-channel active electrode standard actiCAP (Easycap) was used to acquire EEG data (Figure 2.7). Measurements were taken from nasion to inion and from left to right tragus to position the cap in accordance with the international 10-20 system with the vertex electrode (Cz) in the centre. The cap was secured with a chin strap to maintain positioning. A small amount of conductive electrode gel was applied to each electrode using a blunt needle. Impedances for ground (Fpz) and reference (Fz) electrodes were maintained at <5kΩ and aimed to be kept under 50kΩ across all other electrodes.

Electrodes were grounded to FPz and referenced to Fz during recording (Figure 2.7). Signals from the electrodes were amplified using the actiCHamp system and data were recorded using the BrainVision Recorder software (Brain Products GmbH; Gilching, Germany) at a sampling rate of 1000 Hz. Event triggers were marked in the data using a LabJack (LabJack Cooperation; Lakewood, CA, USA) system.

Resting state EEG was acquired for a duration of 5 minutes. Participants were requested to view a fixation cross on the screen in front of them with their eyes open for an initial 30 seconds after which a tone sounded and the fixation cross faded, indicating that participants should close their eyes. Event markers indicated the start and end of the eyes closed period, as well as any periods of non-compliance (e.g., opening eyes, significant movement, or speech) added manually according to my observations during the recording.

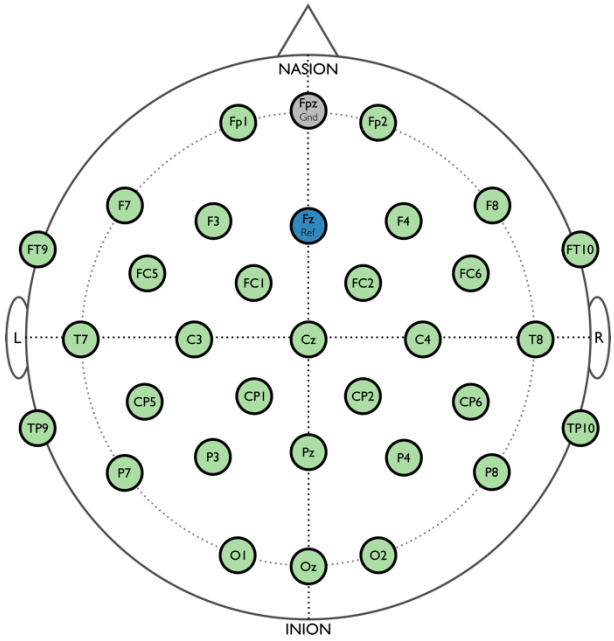

Figure 2.7 EEG channel layout

Schematic of actiCAP 32 channel EEG cap layout used to acquire the resting state EEG data presented in Chapter 4. Ground electrode, Fpz is shown in grey. Reference electrode Fz is shown in blue. All other active electrodes are shown in green.

2.4.3 EEG pre-processing

Raw EEG data were exported from BrainVision format into MATLAB format via EEGLAB. Data were pre-processed, cleaned and quality assessed using the Harvard Automated Processing Pipeline for EEG (HAPPE; Gabard-Durnam *et al.*, 2018), an automated pre-processing pipeline specifically developed for high artefact data as would be expected in acute TBI patients. HAPPE has been shown to be superior in optimising signal to noise ratio compared to manual editing in clinical data (Gabard-Durnam *et al.*, 2018). The following pre-processing steps were taken using the HAPPE pipeline: Data were high-pass filtered at 1Hz, low-pass filtered at 100Hz and band-pass filtered at 1- 249 Hz as recommended for HAPPE processing. Electrical line noise at 50Hz was removed using the CleanLine multi-taper approach (Mullen T, 2012). Bad channels (i.e., those with poor signal quality) were rejected using joint probability evaluation and those exceeding 3 standard deviations from the mean were excluded from further analyses (to be later interpolated). Wavelet-enhanced independent component analysis (ICA) was performed to correct for EEG artefact while retaining the whole dataset to improve ICA decomposition. ICA was then performed on the corrected data and components were rejected using the multiple artifact rejection algorithm (MARA; Winkler *et al.*, 2011). HAPPE rejects components with artifact probabilities > 0.5. Data were segmented into 5-second segments and all epochs were subjected to amplitude-based (+/- 40 uV) and joint-probability (< 3 SDs relative to the activity of other segments) rejection to remove segments with remaining artefact. Previously rejected bad channels were repopulated using spherical interpolation. Data were re-referenced to a common average to minimise bias of reference site activity.

2.5 MAGNETIC RESONANCE IMAGING

Magnetic resonance imaging (MRI) is a non-invasive technique that generates anatomical images. MRI has high spatial resolution for soft tissue and has thus become a widely used tool to glean structural and functional information about the brain in both clinical practice and research.

2.5.1 Principles of MRI

MRI works on the principles of detecting the magnetic field properties of different tissue types. Hydrogen atoms are abundant in the human body. Hydrogen nuclei contain one positively charged proton. Hydrogen protons create a magnetic dipole moment around them as they rotate on their own axis. This is referred to as their 'spin'. When no external magnetic field is present the dipoles are randomly oriented. An MRI scanner generates a static strong magnetic field. This external magnetic field causes a second spinning motion as the hydrogen nuclei align to the direction of the field, resulting in a gyroscopic precession around the axis of the magnetic field. The frequency at which the hydrogen nuclei precess is directly proportional to the strength of the applied magnetic field. This property is termed the Larmour frequency.

Intermittent radio frequency pulses that oscillate at the Larmour frequency can be used to perturb the hydrogen nuclei from their alignment. When nuclei are exposed to a frequency of oscillation that matches their own, they 'resonate' or gain energy. As the radio frequency is removed the nuclei begin to 'relax' and lose energy as they realign. This relaxation process emits a detectable radio frequency signal. Hydrogen atoms in different tissue types relax at different rates which influences the response signal. This can be described as constants T1 (longitudinal relaxation) and T2 (transverse relaxation). Variation of the pulse parameters in acquisition sequences will affect whether the resulting signal intensity is primarily due to T1, T2 or T2* relaxation. The interval between successive pulses is known as the repetition time (TR) and the time interval between excitation and relaxation is known as echo time (TE).

2.5.1.1 Functional MRI

Functional magnetic resonance imaging is an imaging technique used to quantify the metabolic demands of the brain across time. It relies on the principles of the haemodynamic response which corresponds to changes in cerebral blood flow, blood volume and blood oxygenation to provide active neurons with oxygen.

During neuronal firing oxygen consumption and cerebral blood flow increase thus neuronal activity is paralleled by an increased requirement for oxygenated blood. The oxygen required to support neuronal function is carried by haemoglobin. Haemoglobin has unique magnetic properties that change dependent on whether it is oxygenated or not. Oxygen-bound haemoglobin (HbO2) is diamagnetic and magnetically indistinguishable from brain tissue. Deoxygenated haemoglobin (Hb) is highly paramagnetic and shows different magnetic properties to brain tissue.

Due to their differences in magnetic susceptibility, the change in proportion of HbO2 to Hb during neural activity can be detected using fMRI. fMRI is commonly acquired using a T2* weighted sequence that sends one radio frequency pulse from a transmitter coil and then introduces rapidly changing magnetic field gradients. The differences in magnetic susceptibility induce small magnetic field distortions that lead to interference from signal within the tissue. This is reflected in the signal decay process by shortening the T2* relaxation time which is sensitive to these field inhomogeneities. Enhanced local blood flow due to greater neuronal activity thus have increased signal intensity relative to the baseline state.

This signal intensity is referred to as the blood oxygenation level dependent (BOLD) response. The BOLD signal is thus measuring local increases in blood oxygenation and is an indirect measure of neuronal activity. The BOLD response is represented as the haemodynamic response function (HRF; Figure 2.8). The increase in cerebral blood flow to the area takes around 5 seconds, peaks, and then is followed by an under-shoot. The time course of this change in the local ratio of HbO2 to Hb is what is represented as the HRF. The BOLD response thus reflects the deoxyhaemoglobin fluctuations over time and the signal should be weaker in areas with a

higher concentration of deoxygenated blood. It is proportional to underlying neural activity and thus represents a signal change.

The principles of resting state fMRI as I use in Chapter 5, and task-based fMRI as I use in Chapter 6 are the same except for the presence of stimulus. In resting-state fMRI the participant is not required to do anything and is not presented with any stimulus. The signal here thus represents spontaneous brain activity. Functional connectivity measures are derived based on correlations in brain activity between regions. In task-based fMRI the participant is presented with a series of stimuli and the corresponding brain activity in response to the stimulus is of interest. Statistical analysis of changes between task conditions can be used to derive which brain regions are involved in response to specific tasks.

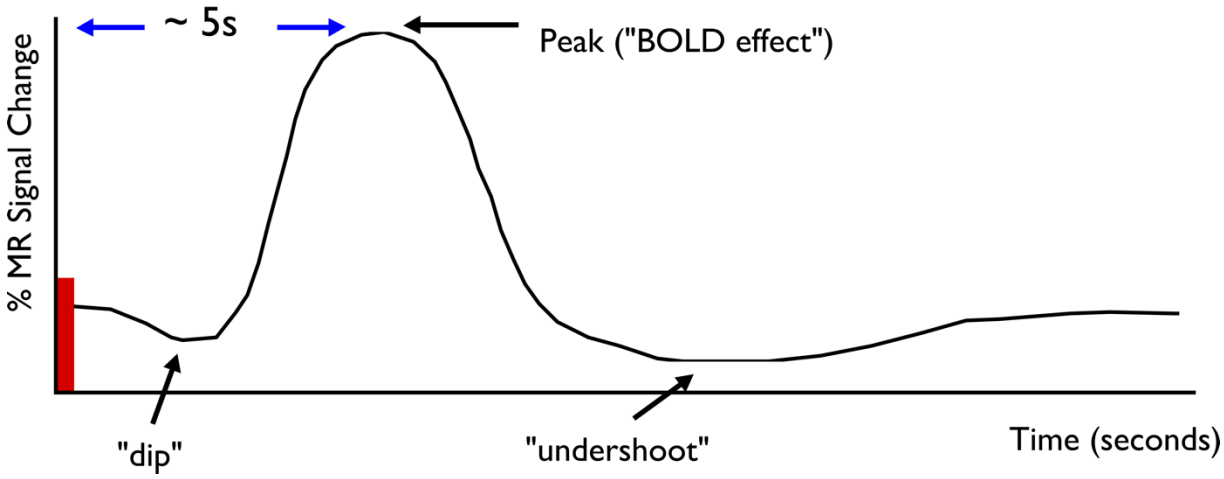

Figure 2.8 The haemodynamic response function

Neuronal activity triggers a change in the BOLD response which is represented as the haemodynamic response function. Figure reproduced with permission from Amaro & Barker, *Brain and Cognition*., 60 220-232 (2006).

2.5.1.2 Diffusion MRI

Diffusion tensor imaging (DTI) is an advanced MRI technique designed to quantify white matter microstructure. Diffusion imaging works based on characterising the diffusion properties of water molecules. In an unrestricted space, water molecules diffuse in a random manner according to Brownian motion principles. This is isotropic diffusion and represents that there is an equal probability that each molecule can move in any given direction. Anisotropic diffusion on the other hand refers to directional movement where movement of water molecules is restricted by various tissue components.

The application of magnetic gradient pulses allows for the diffusion of water molecules in three-dimensional space to be quantified. Diffusion weighted MRI is only sensitive to water diffusion occurring along the axis of the applied magnetic gradient. To detect the diffusion of water in different directions, the gradients must be applied along multiple axes and is thus repeated in a series of non-colinear directions. The diffusion tensor represents the diffusion across the combination of these directions.

A range of measures can be derived from the diffusion tensor (e.g., radial, axial, and mean diffusivity), but the most commonly used is fractional anisotropy (FA). FA values range from 0, representing isotropic diffusion, to 1 representing anisotropic diffusion. In intact white matter fibres, water molecules are constrained by axonal myelin sheath meaning diffusion will take place in the direction of the tract and FA will be high (anisotropic; Figure 2.9). When axonal damage or deterioration occurs, the diffusion is less constrained and therefore FA will be lower. Reduced FA thus reflects breaches in the integrity of white matter and can be taken as a proxy measure of damage to the white matter microstructure following TBI.

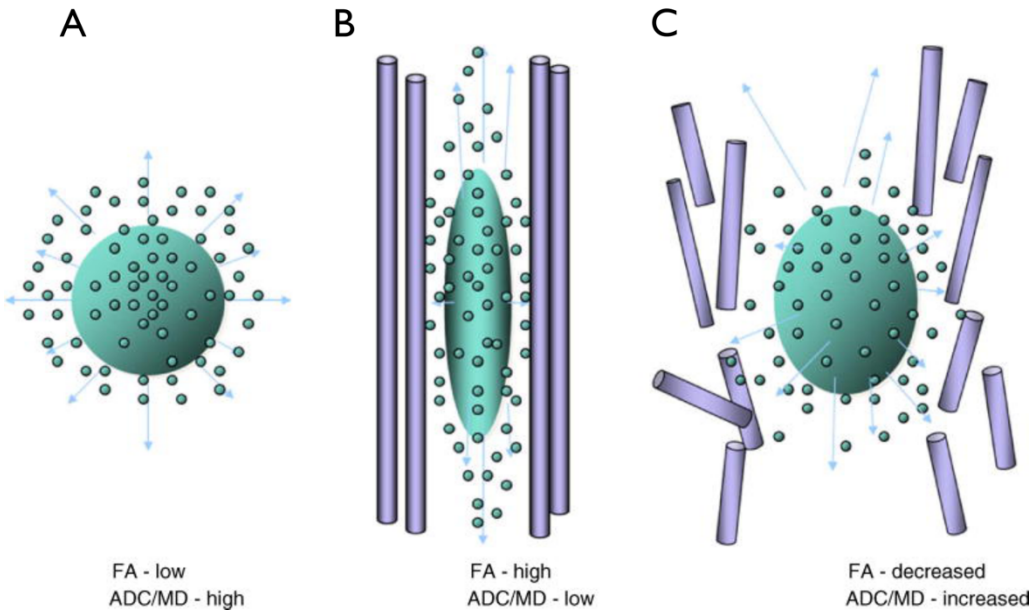

Figure 2.9 Fractional anisotropy in the axon membrane

Diagram depicting diffusion of water molecules **A|** in an unconstrained space water molecules can diffuse in any given direction. Diffusion is isotropic and FA is low. **B|** Within an axon with a membrane wall the movement of intracellular water molecules is constrained, and it moves in the same direction as the constraining membrane. Diffusion is anisotropic and FA is high. **C|** When damage occurs to the axonal membrane, water molecules are less constrained and thus disperse in a manner similar to the unconstrained space reflected in decreased FA values. Figure was created by Geri R. Hanten, Ph.D., Baylor College of Medicine and reproduced with permission from Hayes, Bigler and Verfaellie, *Journal of the International Neuropsychological Society*., 22 120-137 (2016).

2.5.2 MRI acquisition

MRI data presented in this thesis were acquired at two different sites and thus used different scanners and acquisition sequences. The data presented in Chapter 5 was at St Mary's Hospital, Imperial College Healthcare Trust, London. The data presented in Chapter 6 was acquired at the Clinical Imaging Facility, Hammersmith Hospital, Imperial College London. Data from across the sites was not combined for any analysis to avoid biases arising from between-scanner differences. Scanner details and acquisition parameters for each site are outlined below:

2.5.2.1 Imaging data acquisition for data presented in Chapter 5

MRI was performed on a GE Medical Systems 3.0 Tesla scanner with an 8-channel head coil. A high resolution T1-weighted FSPGR scan was acquired (156 1-mm-thick axial slices, repetition time (TR) = 8.516s, echo time (TE) = 3.336ms, flip angle = 12°, in-plane resolution = 1x1mm, matrix size = 256x256, field of view (FOV) = 25.6x25.6 cm).

fMRI images were obtained using a T2*-weighted gradient-echo echoplanar imaging (EPI) sequence with whole-brain coverage (TE =30ms, repetition time TR = 3000ms, 36 ascending slices with thickness 3.6mm, no interslice gap, in-plane resolution 3.75x3.75, flip angle 90°, field of view (FOV) 24 x 24cm, matrix 64 x 64). Participants were asked to keep their eyes open during the resting state scan.

2.5.2.2 Imaging data acquisition for data presented in Chapter 6

MRI was performed on a Siemens Verio 3.0 Tesla scanner with a 32-channel head coil. A high resolution structural T1-weighed MPRAGE scan was acquired (106 1-mm-thick transverse slices, TR=2300ms, TE=2.98ms, flip angle=9°, in-plane resolution=1x1mm, matrix size= 256x256, FOV=25.6x25.6cm).

fMRI images were obtained using a T2*-weighted gradient-echo EPI sequence with whole-brain coverage (TE = 30ms, TR = 2000ms; 31 ascending slices with thickness 3.25mm, gap 0.75mm,

voxel size 2.5x2.5x5mm, flip angle 90°, FOV 280x220x123mm, matrix 112x87). Participants undertook a subsequent memory task during the fMRI scan.

Diffusion-weighted volumes with gradients applied in 64 non-collinear directions were collected using the following parameters: 73 contiguous slices, slice thickness=2mm, FOV 224mm, matrix 128x128 (voxel size=1.75x1.75x2mm^3), b value=1000, and four images with no diffusion weighting (b=0s/mm^2).

2.5.3 Pre-processing of MRI data

Functional imaging analysis was performed using fMRI Expert Analysis Tool (FEAT), in FSL (Smith *et al.*, 2004). Image pre-processing involved realignment of EPI images, spatial smoothing using a 6mm full-width at half-maximum Gaussian kernel and temporal high-pass filtering using a cut-off frequency of 1/50 Hz. Estimates of motion were determined to 6 degrees of freedom using MCFLIRT within FSL (Jenkinson *et al.*, 2002). EPI functional datasets were registered into standard-space using individual high-resolution T1 images with FMRIB's Linear Image Registration Tool (Jenkinson *et al.*, 2002). Cerebrospinal fluid (CSF) and white matter signal was extracted using FMRIB's Automated Segmentation Tool (FAST; Zhang *et al.*, 2001) and regressed out of the data in order to remove any artefactual noise from these sources. The 6 motion estimates and their 24 temporal derivates were also applied as nuisance regressors to derive motion-corrected images. Framewise displacement (FD), a measure of how much the head position changes from one frame to the next (Power *et al.*, 2012) was obtained for each volume using the FSL motion outliers tool. Pre-processed fMRI data were subjected to ICA decomposition, and motion related components were removed using ICA-AROMA (Pruim *et al.*, 2015) by a semi-automated method. All components were visually inspected using spatial maps, time series, and power spectra, and those considered to be noise as per published guidance (Griffanti *et al.*, 2017) were removed.

Diffusion weighted images were corrected for motion artefacts and eddy currents, and skull-stripped using the brain-extraction tool (BET; Smith, 2002) part of the FSL image processing toolbox (Smith *et al.*, 2004). A tensor model was then fitted to the data using FMRIB's Diffusion Toolbox (FDT) and voxel-wise FA maps were generated. These maps were transformed into

standard 1mm space using tensor based registration in DTI-TK (Zhang *et al.*, 2006) and tract-based spatial statistics (TBSS; Smith *et al.*, 2006). Concatenated standard space FA maps of all participants were skeletonised at a threshold of 0.2 to sample from the centre of the white matter tracts and thus avoid partial volume effects.

3

Visual short-term memory binding in PTA

In this chapter I aim to quantify the specific cognitive impairments associated with PTA. I assess performance across a broad range of classic and novel neuropsychological tasks. I use a precision spatial working memory task to assess integrative failures in object-location binding. Using a novel analysis technique to quantify the distribution of spatial errors, I show that PTA patients demonstrate a profound binding impairment that is transient and specific to the amnestic period.

3.1 INTRODUCTION

Post-traumatic amnesia (PTA) is a transient state of profound cognitive impairment following traumatic brain injury (TBI; Marshman *et al.*, 2013; see Chapter 1). PTA is characterised by disorientation, confusion, and the inability to encode new memories. At the core of PTA is thought to be a failure of episodic memory (Leach *et al.*, 2006) though this may be underpinned by failures in integrative working memory function.

Episodic memories of real world, personally experienced events are contextual: they contain information of what happened, when it happened and where it happened. Different features (e.g. time, space, colours, objects) must therefore be combined in order to form a complete representation of an event (Quinette *et al.*, 2006; see also Chapter 1). Episodic memory can therefore be considered reliant on working memory processes that enable integration of, and association between, different features. In the case of visual associative working memory, two distinct processes can be identified: one underlying the location and one assigning an object to that location (Postma & De Haan, 1996). Object-location association memory can thus be considered a mnemonic process that integrates, or binds, contextual information in order for successful retrieval of 'what was where' to take place (Pertzov *et al.*, 2012). Failure on an object-location association test can thus be due to a failure to remember the identity, the location, or a binding failure.

In classic object-location association span tasks, object location is probed based on recognition memory limited to a finite number of predefined locations. While these tasks can be useful in showing deficits in associative working memory, they do not provide the granularity to discern what type of failures were made. Pertzov *et al.* (2012) introduced a precision recall spatial working memory task that requires participants to freely recall object location and thus enables analysis of the distribution of errors over space. This is important in discerning whether spatial errors are occurring randomly, and thus suggests a spatial location has not been remembered, or whether spatial errors are clustered around locations of other objects, suggesting a misbinding error has taken place. The precision recall approach can thus enable quantification of the types of failures being made with more precision than classic span tasks (Zokaei *et al.*, 2015).

There is evidence of episodic memory failure being underpinned by integrative working memory failures in disease groups. Amnesia patients demonstrate associative working memory impairments in addition to their episodic memory deficit (Olson *et al.*, 2006; Piekema *et al.*, 2007; Van Asselen *et al.*, 2005; Van Geldorp *et al.*, 2012) and binding deficits in Alzheimer's disease (AD) have been proposed as a sensitive cognitive biomarker to distinguish AD from other dementias (Pertzov *et al.*, 2015; Della Sala *et al.*, 2012; Cecchini *et al.*, 2017). These clinical conditions are all associated with medial temporal lobe pathology. Previous work in an acute TBI cohort has demonstrated that patients in PTA show reduced functional and structural connectivity between medial temporal lobes (MTL) and the rest of the default mode network (De Simoni *et al.*, 2016). Furthermore, this was associated with impaired associative memory function suggesting that PTA patients might be expected to show similar misbinding errors to other disease groups associated with MTL disruption. Failure to encode events into episodic memory as seen in PTA may therefore be associated with a failure in integrative working memory.

Quantification of binding ability in PTA could provide insight into whether an integration failure is part the clinical manifestation, and may provide a sensitive cognitive biomarker for PTA. In this chapter I investigate performance on a precision recall visual working memory task in acute moderate-severe TBI patients with and without PTA. I hypothesise that 1) patients in PTA will make more misbinding errors and be significantly more influenced by the non-target location than healthy and TBI controls, and 2) this will be transient and specific to a period of PTA.

3.2 METHODS

3.2.1 Study design and participants

30 acute TBI patients and 26 healthy controls were included in this longitudinal study. Recruitment information is detailed in Chapter 2.

At baseline, all participants underwent neuropsychological assessment and the experimental task paradigm. In addition, patients underwent a clinical PTA assessment according to the Westmead PTA Scale (Shores *et al.*, 1986; see Chapter 2). Patients were invited to attend a follow-up assessment within the first year post-injury at which the baseline protocol was repeated with some additional neuropsychology testing. Controls were assessed at one time-point only.

3.2.2 Neuropsychology assessment

All participants completed a detailed neuropsychology assessment with a focus on episodic and working memory. This assessment consisted of classic pen and paper neuropsychology tests and a battery of computerised assessments. Details of all cognitive assessments are given in Chapter 2.

3.2.3 Experimental task paradigm

3.2.3.1 Stimuli

The stimuli consisted of 60 fractal images (Sprott's Fractal Gallery; Sprott, 1996), chosen as complex visual objects that cannot be readily verbalised, with a maximum width and height of 120 pixels. Stimuli were presented on an interactive touch-sensitive screen with a 1920 x 1080 pixel matrix. The experiment consisted of 80 trials, including 20 trials with 1 fractal and 60 trials with 2 fractals. Object location was determined by a MATLAB script in a random manner at any possible location on the screen with exceptions: objects were never located within 600 pixels of each other within a single trial. They were positioned within a minimum distance of 200 pixels

from the screen edge. The threshold for the distance at which the response matched the target (or non-target) was 200 pixels.

3.2.3.2 Task Procedure

Each trial began with a central fixation point followed by the memory array consisting of 1 or 2 fractals presented for 2 seconds. A blank screen was then displayed for 2 seconds (maintenance period) after which an object identification task was introduced in which two fractals were displayed to the right and left of a central fixation. One of these fractals had been present in the memory array of that trial, the other was a foil item that was not present in the memory array. The foil item was part of the task stimuli and therefore was not unfamiliar but appeared in other trials throughout the experiment. Participants were required to touch the item that they remembered from the memory array and drag it to the remembered location. Localisation performance was only analysed in trials which the object identity was correctly remembered. The design of this paradigm thus allowed us to measure the distinct processes of object-location associative memory independently in order to quantify the types of error made (failure to remember the location or failure to bind).

3.2.3.3 Data Normalisation

Data from the precision working memory task were analysed using a) a thresholded approach in which a correct localisation was considered to be within 200 pixels of the original object (or a misbinding error within 200 pixels of the non-target object) to calculate a proportion of misbinding errors and b) a novel, threshold-free approach to study the distribution of responses across a transformed space, defined by the relative locations of target versus non-target items (Figure 3.1B). In this transformed space the target position is located at the origin and the non-target at 1,0 (x, y). Therefore, responses deviating from the origin along the x-axis indicate a spatial bias by the non-target item location, as happens when the target identity is misbound with the non-target location. In contrast, responses deviating along the y-axis do not indicate a spatial bias by the non-target location, but they are in keeping with imprecision in remembering the correct location, or with random error. The responses in this transformed co-ordinate space are

binned across ten uniformly spaced bins. A measure of entropy of the distribution of responses across each axis in the transformed space is then obtained.

Entropy is measure of disorder and predictability in a system. It quantifies the amount of information that is contained within an event. The entropy of a variable can be considered as the amount of surprise or uncertainty contained within the possible outcomes of the variable. If an outcome of a variable is certain, a probability of 1, then there is no information in the occurrence of an event and entropy is therefore low. The lower the entropy, the more ordered and less random the system is. Rare events on the other hand are more surprising and therefore need more information to represent them than common events. If an outcome of a variable is unlikely, or has a low probability of occurring, then the entropy will be high as it contains more information. In this context the entropy across the x-axis will be low if all responses are clustered around the origin and higher if the distribution of responses is more spread out. The distribution across the y axis is important to account for random responses that don't cluster near the target or the non-target. Thus a ratio of the entropy across the x and y axis was taken.

This entropy ratio serves as a quantitative measure of response bias by the location of non-target items, and the direction of the effect (bias toward vs. bias away from the non-target item) becomes apparent by plotting the responses in the transformed space. In this context a higher entropy ratio represents a greater response bias towards the non-target. This approach allows the influence of the non-target on the remembered location to be precisely examined without dichotomising responses based on arbitrarily defined thresholds. The number of bins chosen did not impact the difference in entropy ratio between groups (Supplementary Figure 9.1 and Supplementary Table 9.2). The design of this paradigm thus allowed us to measure the distinct processes of object-location associative memory independently to quantify the types of error made i.e., failure to remember the location or failure to bind.

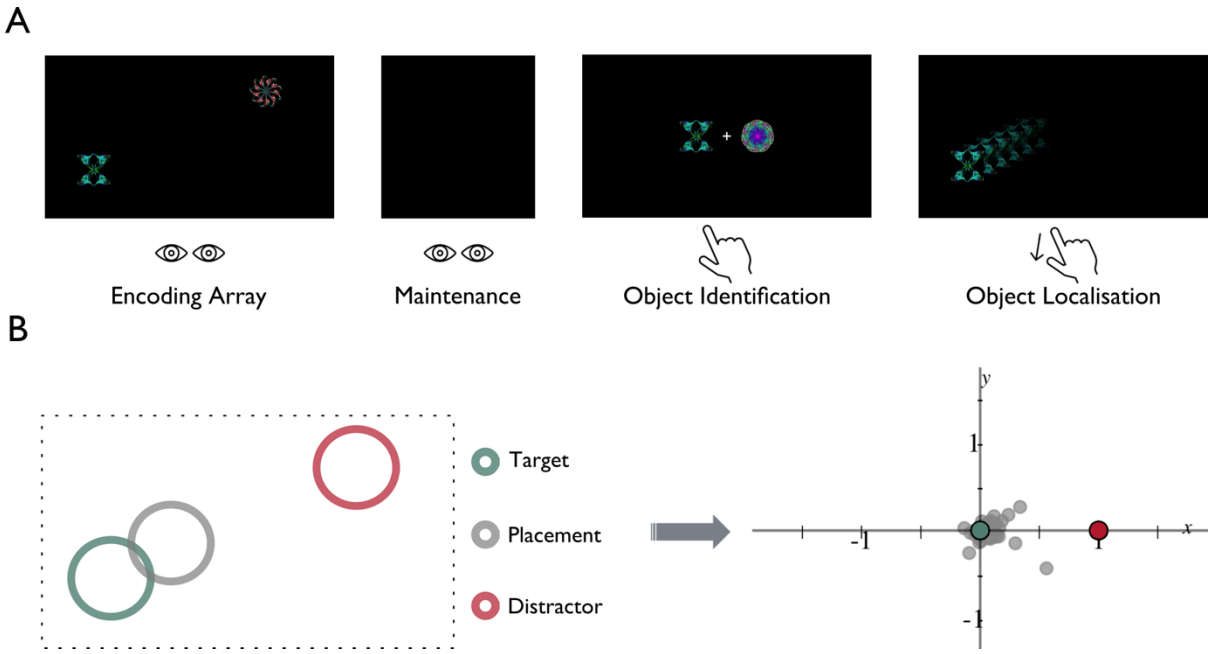

Figure 3.1 Precision working memory experimental task paradigm.

A| Object-location association task paradigm. One or two fractals were shown prior to a delay of 2 seconds after which one of the objects was displayed together with a foil (distractor which had not appeared in the memory array). Participants were required to select the item they recalled (object identification) and move it to its remembered location (object localisation). **B**| Data normalisation. Locations of the target, foil and guesses were translated into a normalised space in which the target lies at the origin, the foil at 1,0(x,y).

3.3 RESULTS

Table 3.1 shows clinical and demographic information for all participants. Following PTA assessment, 17 patients were deemed to be currently in a period of PTA, and 11 were deemed to have recovered from, or never had, a period of PTA. The mean WPTAS score in the PTA+ patients on the day of testing was 9.18 (SD = 1.38). All PTA- TBI patients scored 12 on the day of testing. As would be expected, the PTA+ group showed a significantly ($t(26.97)=2.87$, $p=0.00786$) longer duration (mean = 14.94 days, SD = 11.28) of PTA than the PTA- group that were not in PTA at the time of testing (mean = 4.58 days, SD = 8.14), and thus a significantly longer ($t(27.76)=2.42$, $p=0.0219$) hospital admission (PTA+ mean =16.76 days, SD = 11.39; PTA- mean = 8.23 days, SD = 7.83). The groups did not differ in time since injury (Table 3.1).

The PTA+ group had significantly fewer years of education (PTA+ mean 13.12 years, SD=1.90) than controls (mean 16.42 years, SD = 2.58, $p=0.0002$) and PTA- (mean = 16.38 years, SD = 2.69, $p=0.0009$). There was an effect of age across the groups ($F=4.92$, $df=2$, $p=0.0109$) driven by controls being significantly younger than both PTA+ ($p=0.026$) and PTA- ($p=0.0280$) patients. PTA+ and PTA- patients were well matched for age ($p=0.947$). There were no group differences in sex (Table 3.1).

Table 3.1 Clinical Demographics

	Controls (n=26) Mean (±SD)	**PTA+ (n=17)** Mean (±SD)	**PTA- (n=13)** Mean (±SD)	**Statistic**	***p***	**Post-hoc differences**
Days since Injury		11.00 (8.87)	8.69 (8.07)	t=-0.74	0.464	
PTA Duration		14.94 (11.28)	4.58 (8.14)	t=2.87	0.008**	
Admission Duration		16.76 (11.39)	8.23 (7.83)	t=2.43	0.021*	
Age	28.96 (11.85)	40.88 (15.18)	40.54 (16.31)	F=4.92	0.011*	PTA+>CON *p=0.026** PTA->CON *p=0.028**
Years of Education	16.42 (2.58)	13.12 (1.90)	16.38 (2.69)	F=10.93	0.0001***	CON>PTA+ *p=0.0002**** PTA->PTA+ *p= 0.0009****
Sex (M:F)	20:6	15:2	10:3	Fisher's Exact	0.681	

3.3.1 Neuropsychological performance at baseline

Neuropsychological assessment identified cognitive deficits in both acute TBI groups relative to healthy controls (Figure 3.2 ;Table 3.2). Some assessments identified impairments unique to the PTA+ group: PTA+ patients demonstrated significant impairment compared to PTA- patients (and healthy controls) in immediate verbal recall (PTA+ < PTA-: $t(34)=-2.66$, $p=0.018$; PTA+ < CON: $t(34)=-4.69$, $p<0.001$), delayed visuospatial memory recall (PTA+ < PTA-: $t(36)=2.26$, $p=0.045$; PTA+ < CON: $t(36)=-3.59$, $p=0.003$) associative working memory (PTA+ < PTA-: $t(45)=2.94$, $p=0.008$; PTA+ < CON: $t(45)=-4.43$, $p<0.001$) and search strategy (PTA+ < PTA-: $t(45)=4.11$, $p<0.001$; PTA+ < CON: $t(45)=-5.28$, $p<0.001$).

Other assessments were sensitive to an effect of injury, but not specifically to PTA: compared to controls, but not to PTA- patients, PTA+ patients showed impairments in delayed verbal memory recall (PTA+ < CON: $t(34)=-4.34$, $p<0.001$), immediate visuospatial memory recall (PTA+ < CON: $t(37)=-3.89$, $p=0.001$), visuospatial working memory (PTA+ < CON: $t(45)=-3.11$, $p=0.010$) , short term spatial memory (PTA+ <CON: $t(44)=-3.04$, $p=0.012$) and attentional processing (PTA+ < CON: $t(45)=-6.10$, $p<0.001$; PTA- < CON: $t(45)=-3.72$, $p<0.001$).

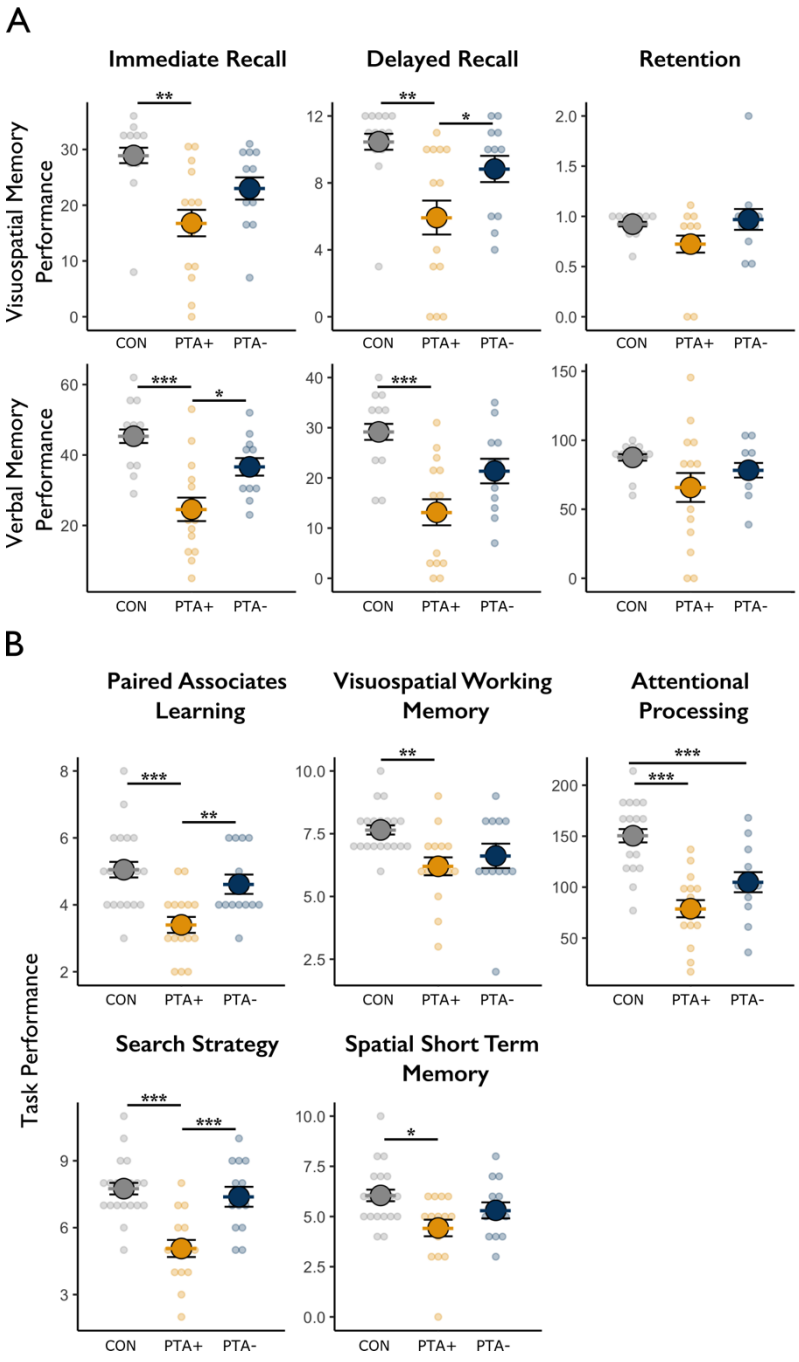

Figure 3.2 Neuropsychological performance in the acute cohort at baseline

Neuropsychological performance of PTA+ patients, PTA- patients and healthy controls at baseline. **A|** BVMT (top row) and Logical Memory (bottom row) performance for immediate recall, delayed recall, and retention. **B|** Performance on the computerised battery of tests. *** p<0.001; ** p<-0.01; * p<0.05. Error bars represent the standard error of the mean (SEM). CON = healthy controls.

Table 3.2 Neuropsychology in the acute cohort at baseline

Cognitive Domain	Assessment	CON Mean (±SD)	PTA+ Mean (±SD)	PTA- Mean (±SD)	ANOVA Group Effect F	ANOVA Group Effect p	Post-hoc group differences (FDR corrected)
Verbal Memory	Logical Memory Immediate Recall	45.33 (9.76)	24.57 (13.74)	36.64 (8.94)	11.20	0.0002	PTA+ < CON *p=0.0001**** PTA+ < PTA- *p=0.0176**
	Logical Memory Delayed Recall	29.17 (8.12)	13.14 (10.69)	21.36 (8.82)	9.46	0.0005	PTA+ < CON *p=0.0004****
	Logical Memory Retention	87.57 (11.93)	65.79 (43.34)	78.27 (19.06)	1.786	0.183	
Visuospatial Memory	BVMT Immediate Recall	28.92 (7.05)	16.80 (9.81)	23.00 (7.16)	7.572	0.002	PTA+ < CON *p=0.0012***
	BVMT Delayed Recall	10.46 (2.44)	5.93 (4.18)	8.83 (2.82)	6.66	0.003	PTA+ < CON *p=0.0029*** PTA+ < PTA- *p=0.0454**
	BVMT Retention	0.92 (0.12)	0.72 (0.35)	0.97 (0.37)	2.40	0.1058	
	Visuospatial Working Memory	7.65 (0.93)	6.20 (1.47)	6.62 (1.76)	5.26	0.0089	PTA+ < CON *p=0.0098***
Associative Working Memory	Paired Associates Learning	5.05 (1.19)	3.40 (0.99)	4.62 (1.04)	10.09	0.0002	PTA+ < CON *p=0.00018**** PTA+ < PTA- *p=0.00779***
Spatial Short Term Memory	Spatial span	6.05 (1.47)	4.43 (1.70)	5.31 (1.44)	4.63	0.0150	PTA+ < CON *p=0.0120**
Search Strategy	Self-ordered search	7.75 (1.33)	5.07 (1.58)	7.38 (1.61)	15.24	<0.0001	PTA+ < CON *p<0.0001**** PTA+ < PTA- *p=0.00025****
Attentional Processing	Feature Match	150.45 (33.41)	78.87 (33.68)	104.85 (35.51)	19.48	<0.0001	PTA+ < CON *p<0.0001**** PTA- < CON *p=0.00082****

3.3.2 Longitudinal changes in neuropsychological performance

A total of 18 patients returned for follow-up at 6 months. The average time between baseline and follow-up was 182 days (range 145 – 233 days). As expected, patients showed a general improvement in cognitive function at follow-up (Figure 3.3; Table 3.3). The PTA+ group showed significant improvement at follow-up compared to baseline in immediate visuospatial recall ($F(1,12)=5.16$, $p=0.04$; PTA+v2 > PTA+v1: $t(5)=-3.80$, $p=0.013$) and search strategy ($F(1,13)=6.55$, $p=0.02$; PTA+v2 > PTA+v1: $t(6)=-2.50$, $p=0.047$). The PTA- group showed improvement in attentional processing ($F(1,13)=5.40$, $p=0.037$; PTA-v2 > PTA-v1: $t(7)=-4.51$, $p=0.003$) and verbal memory (immediate recall: $F(1,11)=5.32$, $p=0.042$; PTA-v2 > PTA-v1: $t(5)=-7.07$, $p=0.001$; delayed recall ($F(1,11)=23.52$, $p<0.001$: PTA-v2 > PTA-v1: $t(5)=-5.97$, $p=0.002$), retention ($F(1,11)=5.14$, $p=0.045$; PTA-v2 > PTA-v1: ($t(5)=-3.69$, $p=0.014$)). There were no group by visit interaction effects for any of the neuropsychological assessments.

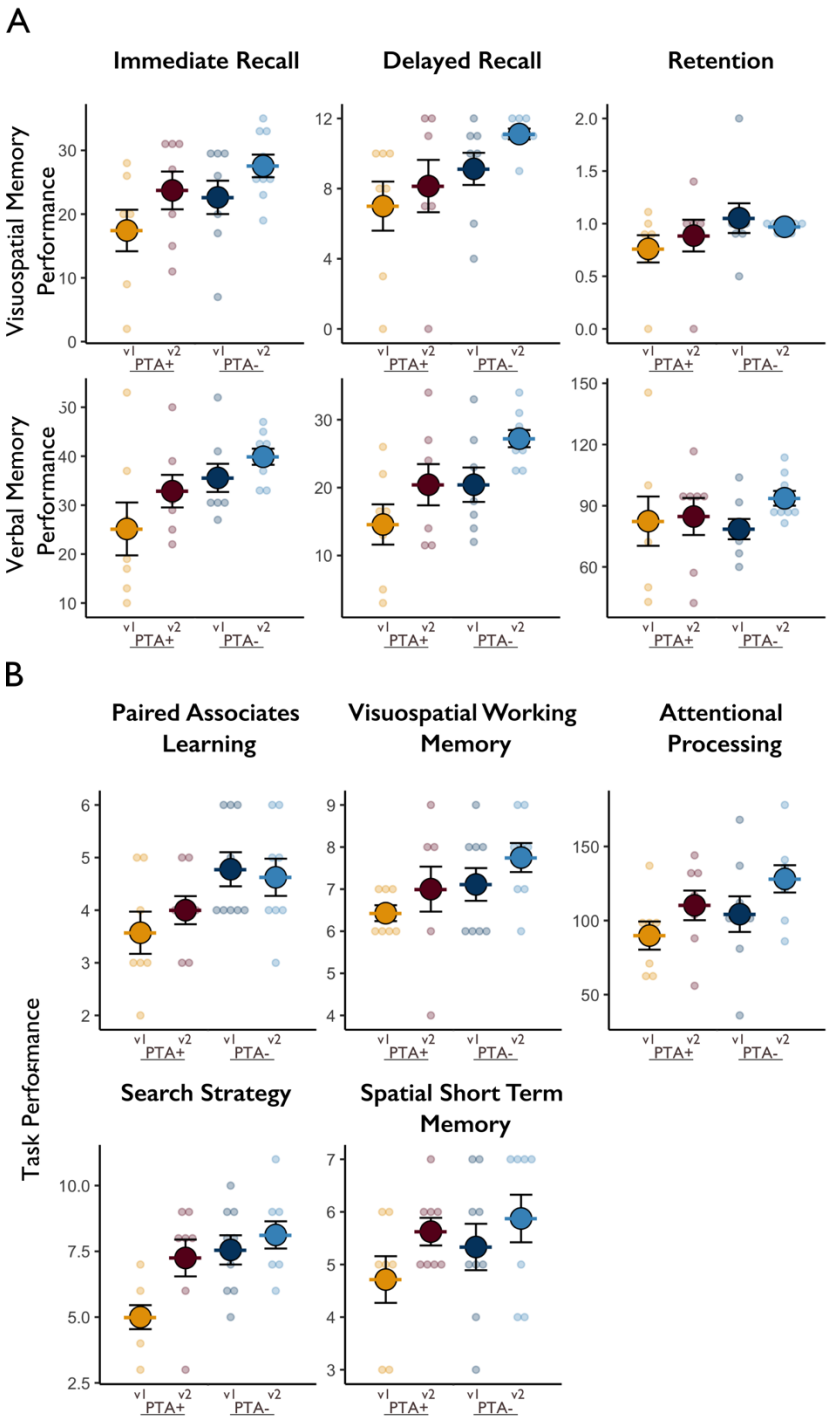

Figure 3.3 Neuropsychological performance in the acute cohort at follow-up

Neuropsychological performance. **A.** BVMT (top row) and Logical Memory (bottom row) performance for immediate recall, delayed recall, and retention. **B.** Performance on the computerised battery of tests. *** p<0.001; ** p<0.01; * p<0.05. Error bars represent the standard error of the mean (SEM). CON = healthy controls.

Table 3.3 Neuropsychology in the acute cohort at follow-up

Cognitive Domain	Assessment	PTA+ Mean (± SD)	PTA- Mean (± SD)	Group		Timepoint		Group x Timepoint	
				F	p	F	p	F	p
Verbal Memory	Logical Memory Immediate Recall	32.86 (9.41)	39.89 (4.94)	3.65	0.0785	5.32	0.0415*	0.08	0.7786
	Logical Memory Delayed Recall	20.43 (8.58)	27.22 (3.80)	3.79	0.0734	23.52	0.0005***	0.39	0.5474
	Logical Memory Retention	84.71 (25.65)	93.65 (10.81)	0.11	0.7510	5.14	0.0445*	1.88	0.1975
Visuospatial Memory	BVMT Immediate Recall	23.71 (8.38)	27.56 (5.32)	2.13	0.168	5.16	0.0424*	0.11	0.7487
	BVMT Delayed Recall	8.14 (4.22)	11.11 (0.93)	5.30	0.0385*	1.729	0.2130	0.05	0.8340
	BVMT Retention	0.89 (0.43)	0.97 (0.04)	2.04	0.1770	0.011	0.9190	0.75	0.4020
	Visuospatial Working Memory	7.00 (1.51)	7.75 (1.04)	2.42	0.144	1.53	0.2380	0.01	0.9380
Associative Working Memory	Paired Associates Learning	4.00 (0.76)	4.62 (1.06)	8.02	0.0142*	0.126	0.7280	0.14	0.710
Spatial Short Term Memory Capacity	Spatial span	5.62 (0.74)	5.88 (1.36)	0.70	0.4190	2.49	0.1390	0.18	0.6800
Search Strategy	Self-ordered search	7.25 (1.98)	8.12 (1.55)	6.15	0.0277*	6.54	0.0238*	1.61	0.2263
Attentional Processing	Feature Match	110.25 (28.31)	128.12 (27.66)	1.57	0.2330	5.40	0.0370*	0.29	0.601

3.3.3 PTA patients show impaired object-location binding

PTA patients demonstrated significant impairment in object-location binding that was not the result of overall task impairment (Figure 3.4).

All participants were able to understand and complete the basic requirements of the precision working memory task, as reflected by the high accuracy in object identification (Figure 3.4A). As expected, across all subjects, identification of the target item was less accurate in two item compared to one item trials ($F(1,51)=55.32$, $p<0.001$). There was also a significant effect of group ($F(2,51)=9.98$, $p<0.001$). This was the result of PTA+ making more identification errors than the other groups (PTA+ > PTA- ($t(105)=3.49$, $p=0.001$); PTA+ > CON ($t(105)=-5.46$, $p<0.001$)). There was no group by load interaction effect ($F(2,51)=2.89$, $p=0.065$).

PTA+ patients showed more impairment when attempting to freely recall location. Location was considered 'correct' if it was within 200 pixels of the target and 'incorrect' if it was outside of that. There was a significant group by load interaction effect on localisation accuracy (Figure 3.4B; $F(2,51)=7.32$, $p=0.002$). PTA+ patients showed significant impairment in remembering the target location compared to both other groups (PTA+ > PTA- ($t(105)=4.10$, $p<0.001$); PTA+ > CON $t(105)=-6.31$, $p<0.001$)).

These localisation errors were not random, but rather were placed nearer to the non-target item location. A trial was considered to include a misbinding error if the correct item was placed within 200 pixels of the non-target location. There was a significant effect of group on misbinding errors (Figure 3.4C; $F(2,51)=25.62$, $p<0.001$). This was the result of a significantly higher proportion of misbinding errors being made by the PTA+ group compared to the other groups (PTA+ > PTA- ($t(51)=-5.60$, $p<0.001$); PTA+ > CON ($t(51)=6.65$, $p<0.001$)).

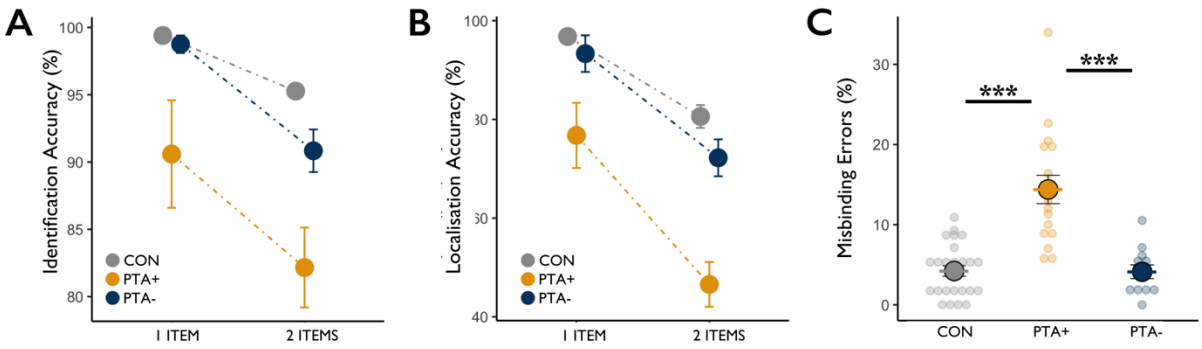

Figure 3.4 Performance on the precision spatial working memory task

Performance in healthy controls, PTA+ and PTA- TBI patients at baseline. **A|** Object identification accuracy at baseline for 1 and 2 item trials **B|** Percentage of correctly identified trials that were moved to the correct location in 1 and 2 item trials. **C|** Proportion of correctly identified trials that resulted in a misbinding error. *** p<0.001; ** p<0.01; * p<0.05. Error bars represent the standard error of the mean (SEM). CON = healthy controls.

3.3.4 PTA patients show abnormal response distributions and a bias towards the non-target

Next, I examined the distribution of individual responses on a trial-by-trial basis across a transformed space based on the relative locations of the target versus non-target items (Figure 3.5). Distributions visualised at both the individual level (Figure 3.5A) and the group level (Figure 3.5B) suggest that PTA+ show a greater bias towards the non-target item than healthy controls and PTA- patients. This was quantified using the entropy ratio. The entropy of the distribution of responses across the x-axis (defined by the relative locations of the target and non-target items) and y-axis were calculated separately, and a ratio of these values taken to reflect the influence of the non-target while accounting for random responses. PTA+ patients demonstrated a greater influence of the non-target, reflected in a significantly higher entropy ratio (Figure 3.5C; $F(2,51)=9.33$, $p<0.001$) than PTA- ($t(51)=-2.26$, $p=0.042$) and healthy controls ($t(51)=4.31$, $p<0.001$).

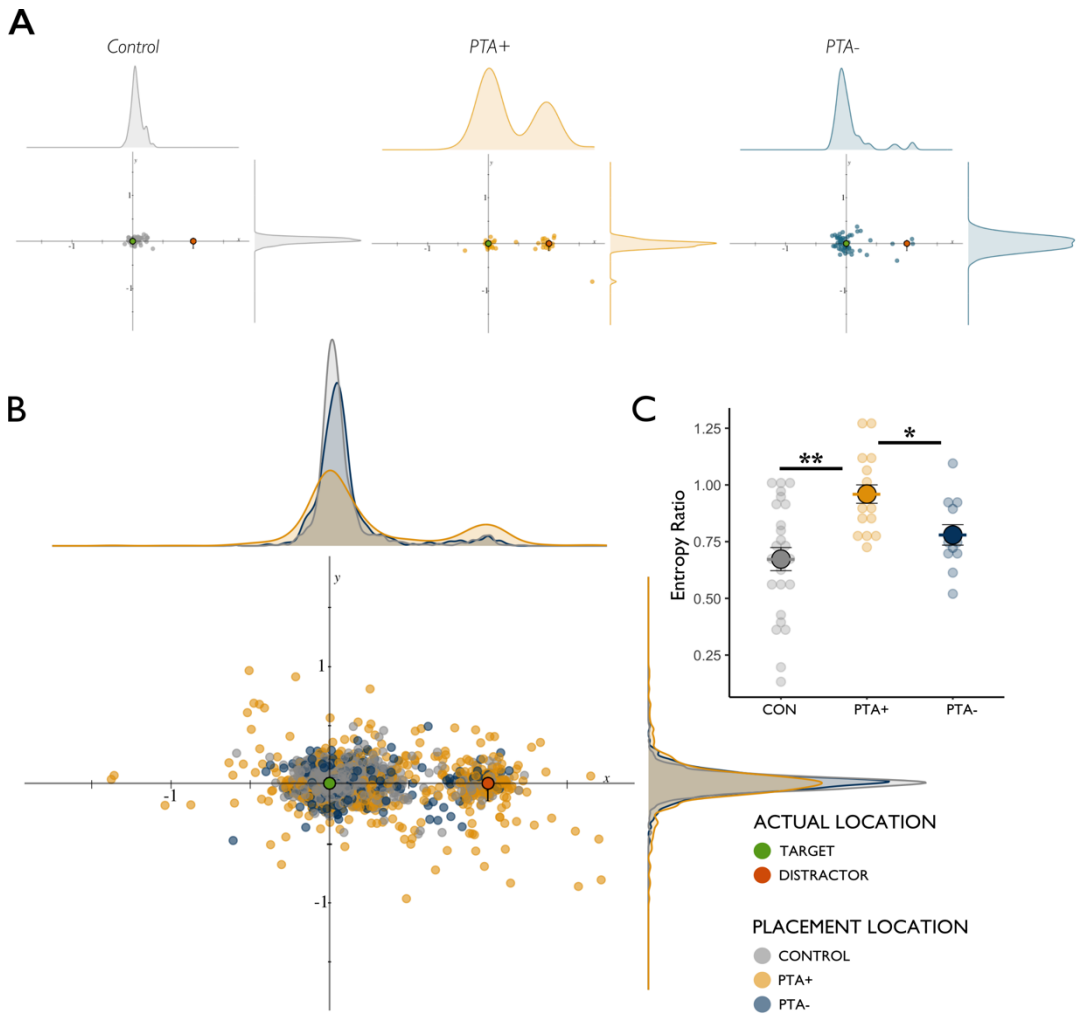

Figure 3.5 Spatial distribution of errors on the precision working-memory task at baseline

A| Examples of the distribution of responses in the normalized space shown at the single-subject level, in a healthy control, a PTA+ patient and a PTA- patient (left to right). **B|** The distribution of responses in the normalised at the group-level, for controls, PTA+ and PTA-. **C|** Entropy ratio in controls, PTA+ and PTA- groups. ** significant at $p<0.01$; * significant at $p<0.05$. Error bars represent the standard error of the mean (SEM). CON = healthy controls.

3.3.5 Impaired binding ability is transient and specific to a period of PTA

To assess whether the binding failures observed in the acute TBI patients were specific to a transient period of PTA, patients were assessed again at a 6-month follow-up. At follow-up, binding ability in PTA+ patients normalized (Figure 3.6). There was a significant group by visit interaction (Figure 3.6B; $F=20.99(1,15)$, $p<0.001$). This was driven by a significant reduction in misbinding errors in PTA+ patients between visits, but no longitudinal change in PTA- patients (PTA+ v1 > PTA+ v2 ($t(7)=4.60$, $p=0.002498$); PTA- v1 > PTA- v2 ($t(8)=-0.180$, $p=0.8621$)). There was no significant longitudinal changes in entropy ratio, but PTA+ patients were no longer abnormal compared to PTA- patients (Figure 3.6C; $t(8.76)=-0.25$, $p=0.807$).

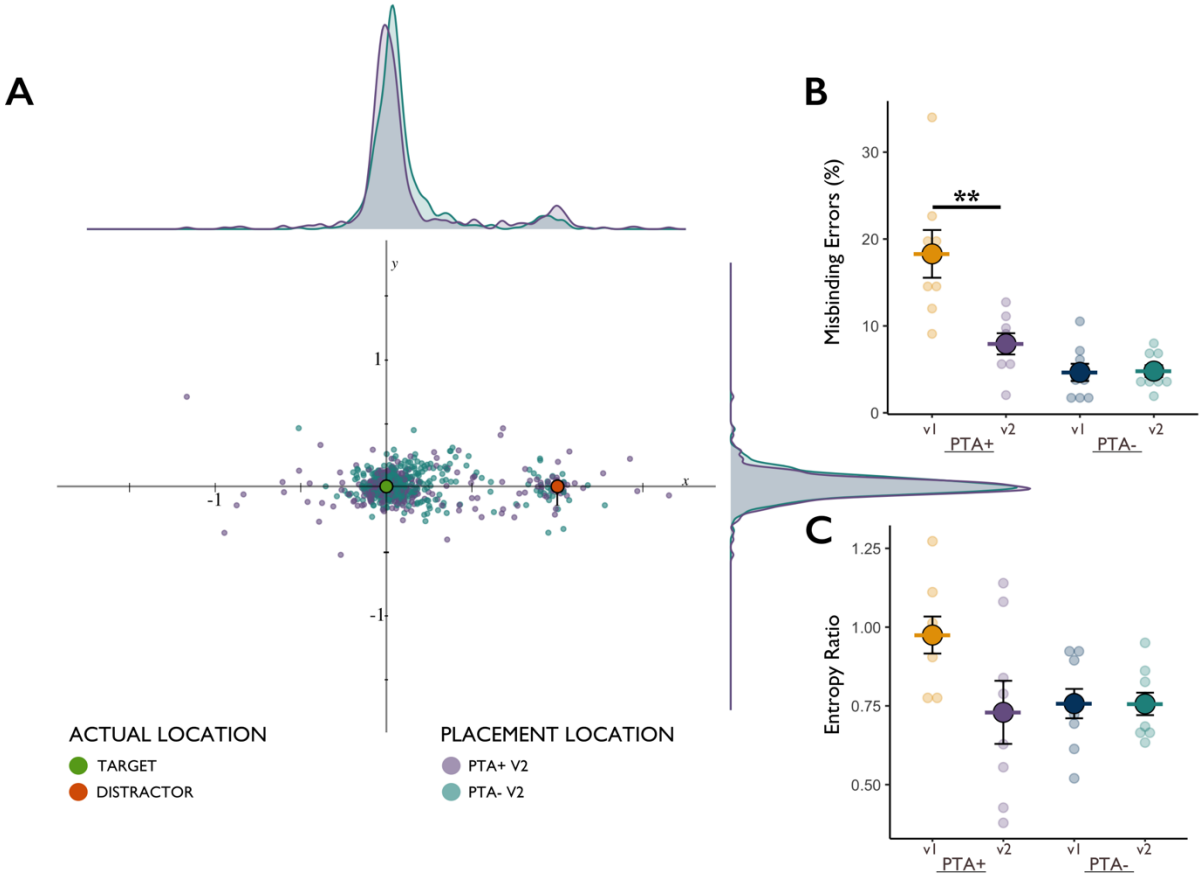

Figure 3.6 Spatial distribution of errors on the precision working memory task at follow-up

A| The distribution of responses at the group level for PTA+ and PTA- patients at follow-up **B|** The proportion of misbinding errors that were made in correctly identified trials for PTA+ and PTA- patients at baseline and follow-up. **C|** Entropy ratio in PTA+ and PTA- groups at baseline and follow-up. ** significant at $p<0.01$. Error bars represent the standard error of the mean (SEM). CON = healthy controls.

3.4 DISCUSSION

PTA is a common consequence of TBI with profound but transient cognitive disturbances. Despite being of high clinical relevance, the specificity of cognitive deficits and their neural underpinnings are poorly understood, limiting our understanding of memory processes early after TBI. Here, for the first time, I show that TBI patients experiencing a period of PTA demonstrate a binding impairment that is transient and specific to the amnestic period.

PTA patients demonstrated a significant impairment in object-location binding. By assessing localization during correctly identified trials, I show that there is intact memory for object identity and independently for object location. The misbinding errors cannot be simply due to a failure to remember the object because memory for object identity was very good and all groups performed well above chance. Furthermore, only trials in which the object identity was correctly recalled were included in the analysis so the number of misbinding errors was substantially higher than any object identification errors. These errors can also not be due to a failure to remember object location. Classic object-location association tasks require the participant to make a binary judgement regarding the feature they are being asked to recall e.g., "was this in the left or right box?". In this precision spatial recall task, the participant is being asked to reproduce the feature (in this case location) from memory rather than through a forced choice. The advantage of using a precision spatial working memory task as I have done here is therefore the ability to assess the type of error being made (Pertzov *et al.*, 2012). If there was no memory for object location, then the errors would be expected to be in random locations. Responses were rather clustered around the target or non-target location suggesting that a 'swap' error had occurred. The failure most prominent in PTA patients is therefore one of integration of these features rather than retrieval of object or location independently.

Quantifying misbinding errors has previously used simple measures of the distance between responses and the target or non-target locations (Pertzov *et al.*, 2012). This approach relies on an arbitrary threshold to be defined to decide whether a response constitutes as a 'hit' for a specific location and does not carry the possibility of examining the distribution of responses across trials. In this chapter I have presented a novel way to quantify the distribution across trials at the

individual subject level. The entropy ratio quantifies the relationship between the distribution of responses across the x and y axes in a normalized space where the target (x=0, y=0) and non-target (x=1, y=0) are in a consistent location relative to one another. It is the distribution of responses along the x axis that are of interest to see how responses cluster around the target and non-target but considering their position along the y axis is important for ensuring that random responses are not contributing to this distribution. A similar approach has recently been released as a mixture modelling toolbox designed for distinguishing the sources of spatial memory error (Grogan *et al.*, 2020) suggesting that this is a valuable approach to apply to this type of data. This approach is particularly valuable when studying individual clinical cases as the distribution of responses for each induvial can be readily visualized and quantified. In Chapter 4 I expand on the results presented here and consider the distribution of responses at the individual level alongside EEG measures of oscillatory power.

The finding that PTA+ patients make significantly more misbinding failures suggests that rather than a failure to encode, PTA+ patients are showing a deficit in the maintenance of working memory representations. There is some debate in the literature regarding the point at which binding occurs, and subsequently how features are stored (see Chapter 1). Some models such as feature integration theory (Treisman & Gelade, 1980; Treisman, 1986) and the multicomponent working memory model (Baddeley, Allen & Hitch, 2011; Karlsen *et al.*, 2010) propose that binding takes place during the encoding stage and a representation of integrated object is stored for retrieval. Other work supports the idea that object and location are encoded as independent representations and binding occurs separately (Darling *et al.*, 2006; Schneegans & Bays, 2018; Pertzov *et al.*, 2012). The data I present in this chapter shows that individual items are still accessible, but it is the representation of the integration between them that is broken. This work therefore offers support for the latter view that binding occurs as a process separate to the encoding of independent features.

This interpretation that PTA is a disorder of working memory integration, rather than purely of encoding ability has implications for updating the understanding of PTA as a concept as well as in clinical practice. The neuropsychological data presented in this chapter shows that patients in PTA showed widespread cognitive deficits compared to healthy controls, but only some of these effects could differentiate between acute TBI patients with and without PTA. Tasks requiring

working memory integration, such as paired associates learning and object search strategy, demonstrated sensitivity between the patient groups but those without the binding component (e.g., spatial span) were less discriminatory. It is not therefore the case that PTA patients are globally more impaired than TBI patients but rather there are transient and specific deficits associated with the period of PTA. This is largely consistent with recent work exploring the cognitive and behavioural profile of PTA and showed that PTA showed significant deficits across some, but not all, cognitive assessments (Hennessy, Delle Baite & Marshman, 2021). Taken together with the precision working memory task paradigm that shows that memory for individual features was largely intact, these results would not offer support for the concept of PTA as a disorder of encoding. This has significance in clinical practice in terms of neuro-rehabilitation strategies as it would suggest that patients in PTA can encode information if it is presented in a form that doesn't require integration of different features.

3.4.1 Limitations

The healthy control group was significantly younger than both the PTA+ and PTA- patient groups. It is unlikely that age is confounding the results shown here since there was no correlation in any of the groups between age and the entropy ratio (Controls: R=0.21, p=0.38; PTA+ R=0.22, p=0.54; PTA- R=0.14, p=0.79). Furthermore, there was no difference in age between the two patient groups and this variable cannot therefore explain the significant deficit in binding ability between acute TBI patients with PTA compared to those without.

Patients in PTA were less educated than healthy controls and acute TBI patients not in PTA. There is evidence that higher educational level is associated with improved visuospatial recall and better recovery following TBI (Vakil *et al.*, 2019). However, there was no relationship between the entropy ratio measure and the years of education for any of the groups (Controls: R=-0.3, p=0.18; PTA+: R=0.17, p=0.52; PTA-: -0.16, p=0.63) so this should not change the interpretation of the key results presented in this chapter.

In terms of the task design, the object identity recall was based on forced recognition and participants had the choice of one of two objects. It is therefore possible that in some trials these were not 'remembered' but chosen through chance. In these cases, the interpretation of that trial

as a misbinding trial, or a failure of the integration of two intact features, would be misleading as the object had not in fact been remembered. All participants did however perform well above chance level in object identification, so it is unlikely that these occurrences were prevalent. A key strength of this experiment is the precision spatial recall element that ensures no such ambiguity can be claimed with regards to the remembered location. Furthermore, by examining the distribution of results across a continuous space the few trials in which location was completely random (i.e., not close to the target or non-target) are readily apparent and accounted for when considering whether a trial was a misbinding error. The group differences in misbinding and entropy ratio can therefore be considered a true reflection of a failure to integrate features in working memory, rather than a failure to remember object or location.

3.4.2 Future Directions

Future work should develop a battery of cognitive tests to track emergence from PTA and sensitively define cognitive deficits unique to this population. PTA is classically assessed using measures primarily of recall and orientation (see Chapter 1, section 1.3.4). Although in clinical practice, memory impairment is clearly a significant component of PTA, these results suggest that it is integration of memory for different features that is impaired rather than memory for individual items or locations. Measures of visuospatial binding should therefore be incorporated into an assessment battery for PTA. A key advantage of the precision working memory task used here is that it can be used for repeated assessments without concern of significant learning effects and may therefore be useful to incorporate into a cognitive battery designed to track emergence from PTA. Considering the clinical importance of PTA duration for discharge planning and prognostic indications, developing a cognitive battery more sensitive to emergence from PTA would be fruitful from perspectives of both cognitive neuroscience and clinical practice.

Developing this work further should include experimentation with the optimum maintenance period and load to be sensitive to this clinical population. In this experiment these factors were

kept constant,[1] but in healthy controls more objects in memory and longer retention periods promote more errors (Pertzov *et al.*, 2012). It is therefore possible that PTA- TBI patients will also show a greater proportion of misbinding errors when the task is made more complex which may be useful in detecting more subtle cognitive impairments in patients who have emerged from PTA.

The binding deficit observed here in PTA+ patients, provides opportunity for learning how the integration processes of object and location information is supported by brain function. In the next chapter I examine a variety of features in the resting state EEG of a subset of the participants that took part in this experiment and test how these relate to binding failures.

3.4.3 Conclusion

Patients in PTA demonstrate a distinct cognitive profile from acute TBI patients no longer in PTA. The clustering around target and non-target items with very few random responses, as shown here in PTA+ patients, demonstrates that it is not a failure in remembering the identity of the object or its location but rather the integration (binding) of this information that fails. The results offer support for the view that the integration of information, rather than encoding ability, is a sensitive cognitive biomarker for identifying PTA patients in an acute TBI population.

[1] Maintenance period was the same across all trials. Item load was either 1 or 2 items, but since 1 item trials cannot yield a misbinding error only 2 item trials were included in the response distribution array.

4

Electrophysiological abnormalities in acute TBI

In this chapter I investigate the electrophysiological abnormalities associated with acute TBI and how these change at 6-month follow-up. I extend the work of the previous chapter by using electroencephalography to explore the neural basis of misbinding deficits in PTA.

4.1 INTRODUCTION

The mechanism by which information is bound together in working memory is a central question for cognitive neuroscience (see Chapter 1, section 1.2). This binding is key to normal memory function. In the previous chapter, I showed that binding is transiently disrupted following significant head injuries during periods of post-traumatic amnesia (PTA). The reason for this impairment is unclear, but it may be caused by electrophysiological changes produced by head impacts that disrupt cortical communication.

Electrophysiological abnormalities are often seen after traumatic brain injury (TBI). TBI patients demonstrate increases in low-frequency amplitude and oscillatory slowing (Gloor, Ball & Schaul, 1977; Huang *et al.*, 2009; Gosselin *et al.*, 2009; Dunkley *et al.*, 2015; Modarres *et al.*, 2017). Identifying pathological delta frequency waves has clinical utility: abnormal delta following head-injury is sensitive to detecting TBI on an individual level (Huang *et al.*, 2014) and increases in delta power are associated with poor functional outcomes (Leon-Carrion *et al.*, 2009). Slow-wave activity is also associated with personality change, depressive symptoms and cognitive impairment following TBI (Huang *et al.*, 2014; Robb Swan *et al.*, 2015).

Oscillatory slowing can be described using frequency specific power measures to quantify the relative contribution of slow compared to faster wave power. The delta-alpha ratio (DAR) is an effective index of cerebral pathophysiology and is sensitive to clinical outcomes and cognitive function in acquired brain injury (Claassen *et al.*, 2004; Schleiger *et al.*, 2014; Finnigan, Wong & Read, 2016). A higher DAR represents increases in power in the delta frequency band in conjunction with reduced alpha band power and thus a greater degree of slowing. Higher delta-alpha ratio (DAR), has been observed in TBI patients and associated with neurological outcome (Lewine *et al.*, 2007; Haveman *et al.*, 2019). Furthermore, ameliorating high DAR through transcranial direct current stimulation (tDCS) during subacute neurorehabilitation in TBI patients improved neuropsychological performance across the whole group but more so in those patients demonstrating excess slow wave activity at baseline (Ulam *et al.*, 2015). Taken together, this suggests that presence of pathological low-frequency power is not only indicative of injury presence and functional outcome, but also mechanistically important for neuropsychological function.

Oscillatory activity is hierarchically organised and abnormal slow-wave activity is likely to disrupt activity across other frequency bands (Lakatos *et al.*, 2005). Theta oscillations are integral to associative binding in episodic memory (Herweg, Solomon & Kahana, 2020) and the phase synchronisation of theta oscillations in different brain regions, a marker of functional connectivity, is associated with successful encoding and working memory processes (Fell & Axmacher, 2011; Burke *et al.*, 2013; Solomon *et al.*, 2017, 2019).

Theta phase also influences oscillations in the gamma frequency. This cross-frequency coupling, in which the phase of theta oscillations modulates the amplitude of gamma oscillations, supports the formatting and integration of multi-item information required for contextual binding in the hippocampus (Lisman & Jensen, 2013) and is important in learning and memory (Tort *et al.*, 2009; Heusser *et al.*, 2016; Jones, Johnson & Berryhill, 2020). Spatial working memory is reliant on theta-gamma phase-amplitude coupling (PAC; Alekseichuk *et al.*, 2016), and the degree of coupling increases with working memory load (Axmacher *et al.*, 2010). Increased PAC between frontal theta and temporal-parietal gamma has been associated with successful memory encoding (Friese *et al.*, 2013; Lega *et al.*, 2016), working memory maintenance (Axmacher *et al.*, 2010; Daume *et al.*, 2017) and associative binding (Köster *et al.*, 2018). Theta-gamma PAC between frontal and temporal-parietal regions is mechanistically supported through long-range theta phase synchronization (Daume *et al.*, 2017; von Nicolai *et al.*, 2014; Fell & Axmacher, 2011) to form a theta-gamma working memory system. Indeed, evidence of this can be seen in working memory deficits emerging from local and long-range hypo-connectivity marked by reductions in both temporal PAC and fronto-temporal phase synchronisation (Reinhart & Nguyen, 2019).

There is currently no direct evidence of disruptions to this theta-gamma working memory system underpinning cognitive impairment in TBI, but disruptions to frontal synchronisation are present following TBI across a range of frequency bands (Sponheim *et al.*, 2011; Thatcher *et al.*, 1989, 2001; Cao & Slobounov, 2010) including decreased gamma connectivity (Wang *et al.*, 2017). TBI patients can be reliably distinguished from healthy controls using PAC measures across multiple frequency bands (Antonakakis *et al.*, 2016) suggesting that cross-frequency coupling is also disrupted. These abnormalities likely underpin cognitive impairments. During working memory, TBI patients with visuospatial working memory impairment demonstrated

reduced coherence across theta, alpha and beta bands (Kumar *et al.*, 2009) and gamma connectivity is increased between long range interhemispheric frontal-temporal to parietal-occipital regions (Bailey *et al.*, 2017) during retention in mild-moderate TBI. Furthermore neuropsychological improvement correlated with reductions in low-frequency connectivity (Castellanos *et al.*, 2010). It is therefore possible that the increases in slow wave activity described in TBI are disrupting activity in other frequency bands that underpin working memory processes. In this chapter I aim to understand the neural underpinnings of the binding failures in acute TBI. I investigate how neural oscillatory activity in acute TBI is associated with a period of PTA and explore a potential mechanistic explanation. I expect that a shift towards dominant slow-wave power in patients will disrupt theta and gamma oscillations underpinning normal function of the working memory system resulting in associative working memory failures. Specifically, I test the following hypotheses:

i) There will be a shift towards dominant slow wave power reflected in an increase delta to alpha ratio in TBI patients: within patients this will correlate positively with clinical and behavioural measures of PTA.

ii) TBI patients will show disruption to the theta-gamma working memory system, and the extent of this disruption will correlate with behavioural markers of PTA. Specifically, I expect to see:

a) Altered long range theta synchronization, between frontal and parietal-temporal channels

b) Altered frontal theta-phase to parietal-temporal gamma amplitude coupling.

4.2 METHODS

4.2.1 Study design and participants

A subset of the participants from the previous chapter were included in the analysis presented here. Seventeen acute TBI patients (14 males, 3 females, mean age 41.12, range 19-73 years) and 21 healthy controls (18 males, 3 females; mean age 29.29, range 18-70 years) were included.

4.2.2 Neuropsychological assessment

A battery of computerised tests delivered on an iPad using a custom-programmed application was used to assess attentional processing, self-ordered strategy searching, spatial short-term memory capacity, visuospatial working memory, and paired-associates learning (PAL). The task designs are detailed in Chapter 2. In addition, participants completed a free-recall computerised visuospatial working memory task using fractal images used to assess spatial precision in object-location binding, a measure which was presented in Chapter 3.

4.2.3 EEG analysis

The acquisition and pre-processing of the 32-channel resting state EEG data presented in this chapter is described in detail in Chapter 2.

Pre-processed single subject data was imported into FieldTrip for time-frequency analysis in the channel domain. Channels were grouped into four regions of interest: frontal ('Fp1', 'Fp2', 'F3', 'F4', 'F7', 'F8'), temporal ('T7', 'T8', 'TP9', 'TP10', 'FT9', 'FT10'), parietal ('Pz', 'P3', 'P4', 'P7', 'P8'), occipital ('O1', 'O2', 'Oz'). Frequency bands were defined as follows: delta (0-4Hz); theta (4-8Hz); alpha (8-13Hz); beta (13-30Hz) and gamma (30-40Hz).

4.2.3.1 Normalised power

Power in each channel was calculated for each frequency band, normalised to total power across all five bands. Global power was calculated by averaging across all channels. Power estimates were performed within the FieldTrip function ft_freqanalysis using the 'mtmfft' method to give the average frequency content of each epoch. First, the data is windowed using a hanning taper to extract the temporal evolution of raw power values. The data is then transformed to the frequency domain using the multi-taper Fast Fourier Transform (FFT) and power values estimated.

Statistical comparison of global normalised power was conducted using one-way independent measures ANOVA followed by post-hoc t-tests. All p-values were corrected using false-discovery rate method for multiple comparisons. Group-level statistical analysis of normalised power was also performed using a cluster-based permutation approach (Maris & Oostenveld, 2007) in the frequency/channel domain on the whole montage. Power was compared between groups at each channel using two-sided independent samples t-tests and results clustered according to spatial adjacency at $p < 0.05$ using the maximum size criterion. Permutation distributions were then generated using the Monte-Carlo method and 5000 random iterations, and corrected p-values were then obtained through comparison of observed data to the random distributions. Follow-up data was assessed as detailed above. No cluster-based permutation analysis was performed on follow-up data.

4.2.3.2 Phase synchronisation

Phase synchronization is a measure of the coupling of oscillatory activity and reflects functional connectivity between brain regions. Phase lag index (PLI) calculates to what extent the phase of one signal is consistently lagging or leading relative to another signal, irrespective of the magnitude of the phase leads and lags (Stam, Nolte & Daffertshofer, 2007). To calculate the PLI, data was windowed using a discrete prolate spheroidal sequences (dpss) taper and transformed into the frequency domain using the 'mtmfft' multi-taper method in FieldTrip. Matrices containing the cross-spectral density were produced and the weighted PLI was calculated between

each channel using the ft_connectivity_wpli function in FieldTrip (Oostenveld *et al.*, 2011) to give a measure of phase based functional connectivity. The weighted PLI is weighted by the imaginary component of the cross-spectrum to overcome issues with spuriously related connectivity which can arise due to volume conduction (Vinck *et al.*, 2011). In addition, a further debiasing term (to give the dwPLI) to correct for inflation due to small sample size was implemented. dwPLI was calculated across all frequencies within the theta band (4-8Hz) for each channel pair.

Statistical comparison of connectivity at the group level was performed in two ways. Firstly I constructed 31x31 whole brain channel-wise theta connectivity matrices for each subject by averaging across dwPLI values for each channel pair across the theta band and the network-based statistic (NBS; Zalesky *et al.*, 2010), implemented in MATLAB, was used to compare connectivity across groups using an independent samples t-test design. The NBS is a non-parametric statistical method in which values at every node are tested against the null-hypothesis and those surviving the primary threshold are entered for Monte-Carlo simulation permutation testing at every channel pair. The primary threshold was set to $z=3.1$ (based on detecting a medium effect size (Cohen's d = 0.5)) and 10,000 random permutations were conducted with a threshold of $p<0.05$. Secondly, the average of dwPLI values across 1) frontal and parietal and 2) frontal and temporal channel groups were taken for each participant. These were compared using independent samples t-tests to compare connectivity across fronto-parietal channels and fronto-temporal channels between patients and controls. In patients who returned for follow-up, within-subjects t-tests were used to assess differences in the dwPLI across time.

4.2.3.3 Phase amplitude coupling

To quantify the intensity of phase-amplitude coupling between the phase of theta and the amplitude of gamma the modulation index (MI; Tort *et al.*, 2010) was calculated. Individual epochs were bandpass filtered at phase (4-8 Hz) and amplitude (30-40Hz) frequencies using a third order Butterworth filter. Using the Hilbert transformation, the instantaneous phase of frequencies between 4 and 8 Hz (in steps of 1 Hz) in the frontal channel group and the amplitudes of frequencies between 30 and 40 Hz (in steps of 2 Hz) in parietal and temporal channel groups individually were estimated. Theta phases were binned into 18 bins at 20-degree

intervals (from 0 to 360 degrees) and the mean amplitude of the gamma oscillation in each phase bin was derived to produce a probability-like distribution function. If no PAC is present, the amplitude distribution across the bins will be uniform. The Kullback-Leibler (KL) distance, a measure widely used to calculate the distance between two distributions, was used to measure how much the phase-amplitude distribution differed from the uniform distribution. The MI was obtained by dividing the KL distance by the logarithm of the number of phase bins (i.e., log (18)), thus resulting in a value between 0 and 1. An MI value of 0 represents no PAC, i.e., the distribution is equal to the uniform and the mean amplitude is the same for all phase bins. A higher MI value represents a distribution further away from the uniform i.e. a greater degree of PAC and the mean amplitude changes across phase bins (Tort *et al.*, 2009).

This process was repeated for all combinations of phase-amplitude frequencies. MI values were calculated i) between the theta phase of frontal electrodes and the gamma amplitude of parietal electrodes and ii) between the theta phase of frontal electrodes and the gamma amplitude of temporal electrodes, for each electrode within the respective channel groups.

To test for group differences in PAC, the average MI values across frontal and parietal, and separately, frontal, and temporal channel groups were taken for each participant and compared using independent samples t-tests. In patients who returned for follow-up, within-subjects t-tests were used to assess differences in the MI across time.

4.3 RESULTS

4.3.1 Clinical demographics

Table 4.1 shows the clinical demographics for the patients with EEG included in this Chapter. Following PTA assessment, 10 patients were deemed to be currently in a period of PTA, and 7 were deemed to have recovered from, or never had, a period of PTA. The mean WPTAS score in PTA patients on the day of testing was 9 (SD = 1.41). All PTA- TBI patients scored 12 on the day of testing. As would be expected, the PTA+ group showed a significantly longer duration of PTA than the PTA- at the time of testing ($t(10.8)=3.25$, $p=0.008$). The groups did not differ in time since injury or total hospital length of stay. Detailed clinical characteristics of patients can be found in Supplementary Table 9.1.

There was a significant group effect on years of education ($F(2)=5.88$, $p=0.006$). This was the result of the PTA+ group having had significantly fewer years of education than both PTA- and healthy controls (PTA+ > PTA- ($t(35)=-2.53$, $p=0.02$); PTA+ > CON ($t(35)=-3.30$, $p=0.007$)). There was also an effect of age across the groups ($F=3.34$, $df=2$, $p=0.046$). This was the result of a trend towards PTA+ patients being slightly older than controls (PTA+ > CON ($t(35)=2.48$, $p=0.055$)).

The number of patients who returned for follow-up assessment was 58%, a rate in keeping with this type of clinical study in which patients are recruited in the acute setting. The average time between baseline and follow-up was 177.8 days (range 145 – 233 days).

Table 4.1 Clinical demographics for EEG cohort

	Controls *n=21* Mean (± SD)	**PTA+** *n=10* Mean (± SD)	**PTA-** *n=7* Mean (± SD)	**Statistic**	***p***	**Post-hoc differences**
Days since Injury		9.4 (7.92)	9.43 (7.28)	t=-0.01	0.994	
PTA Duration		14.9 (11.81)	2.14 (3.18)	t=3.25	0.008**	
Admission Duration		16.1 (12.27)	8.43 (6.90)	t=1.64	0.122	
Age	29.29 (12.21)	43.1 (16.67)	38.29 (17.75)	F=3.35	0.047*	PTA+ > CON p=0.055
Years of Education	16.33 (2.87)	13.2 (1.93)	16.29 (1.60)	F=5.88	0.006**	CON > PTA+ p = 0.007** PTA- > PTA+ p= 0.024*
Sex (M:F)	18:3	9:1	5:2	Fisher's Exact	0.697	

4.3.2 Neuropsychological performance

The PTA+ group showed evidence of significant cognitive impairment across all neuropsychological tasks (Figure 4.1). There was a significant effect of group across all cognitive domains tested (Table 4.2). In associative working memory and search strategy the group effects were the result of differences between PTA+ and PTA-, as well as PTA+ and healthy controls (misbinding entropy ratio: PTA+ > PTA- ($t(33)= 2.34$, $p=0.039$); PTA+ > CON ($t(33)=4.22$, $p<0.001$); paired associates learning: PTA+ > PTA- ($t(29)=-3.34$, $p=0.003$); PTA+ > CON ($t(29)=-4.71$, $p<0.001$); self-ordered search: PTA+ > PTA- ($t(29)=-2.47$, $p=0.028$); PTA+ > CON $t(29)=3.98$, $p=0.001$)). In visuospatial working memory and spatial short term memory group differences were a result of PTA+ impairment relative to healthy controls only (monkey ladder: PTA+ > CON ($t(29)=-2.75$, $p=0.030$); spatial span: PTA+ > CON ($t(29)=-3.04$, $p=0.015$)). Attentional processing speed was impaired in both patient groups compared to healthy controls (feature match: PTA+ > CON ($t(29)=-5.41$, $p<0.001$); PTA- > CON ($t(29)=-4.29$, $p<0.001$)).

As expected, the PTA group showed a general improvement in cognitive function at follow with test scores within the normal range (Figure 4.2). There was a significant effect of group in the PAL ($F(1)=22.53$, $p=0.002$) which was driven by PTA+ showing impairment compared to PTA- patients across both visits ($t(16.10)=3.49$, $p=0.003$). There was a trend towards an improvement in performance from baseline to follow-up across all patients in search strategy and attentional processing speed (self-ordered search ($F(1)=4.90$, $p=0.058$); feature match ($F(1)=4.88$, $p=0.058$)).

Table 4.2 Neuropsychology statistics for the EEG cohort at baseline

Cognitive Domain	Assessment	CON Mean (± SD)	PTA + Mean (± SD)	PTA - Mean (± SD)	ANOVA Group Effect F	ANOVA Group Effect p	Post-hoc group differences (FDR corrected)
Associative Working Memory	Precision working memory misbinding (entropy ratio)	0.65 (0.27)	1.02 (0.17)	0.75 (0.10)	8.94	0.0008	PTA+ > CON p=0.00054*** PTA+ > PTA- p=0.03866*
	Paired Associates Learning	5.00 (1.2)	3.00 (0.82)	4.71 (0.95)	11.74	0.0002	PTA+ < CON p=0.00017*** PTA+ < PTA- p=0.00346**
Visuospatial Working Memory	Monkey Ladder	7.27 (0.59)	5.80 (1.48)	6.14 (2.04)	4.25	0.0240	PTA+ < CON p=0.03000*
Spatial Short Term Memory Capacity	Spatial span	6.13 (1.46)	4.2 (1.93)	5.14 (1.07)	4.69	0.0172	PTA+ < CON p=0.01500*
Search Strategy	Self-ordered search	7.47 (1.19)	5.00 (1.89)	6.86 (1.57)	8.11	0.0016	PTA+ < CON p=0.01200* PTA+ < PTA- p=0.02830*
Attentional Processing	Feature Match	145.60 (35.13)	73.30 (33.40)	81.43 (24.72)	17.86	<0.0001	PTA+ < CON p=0.00002*** PTA- < CON p=0.00027***

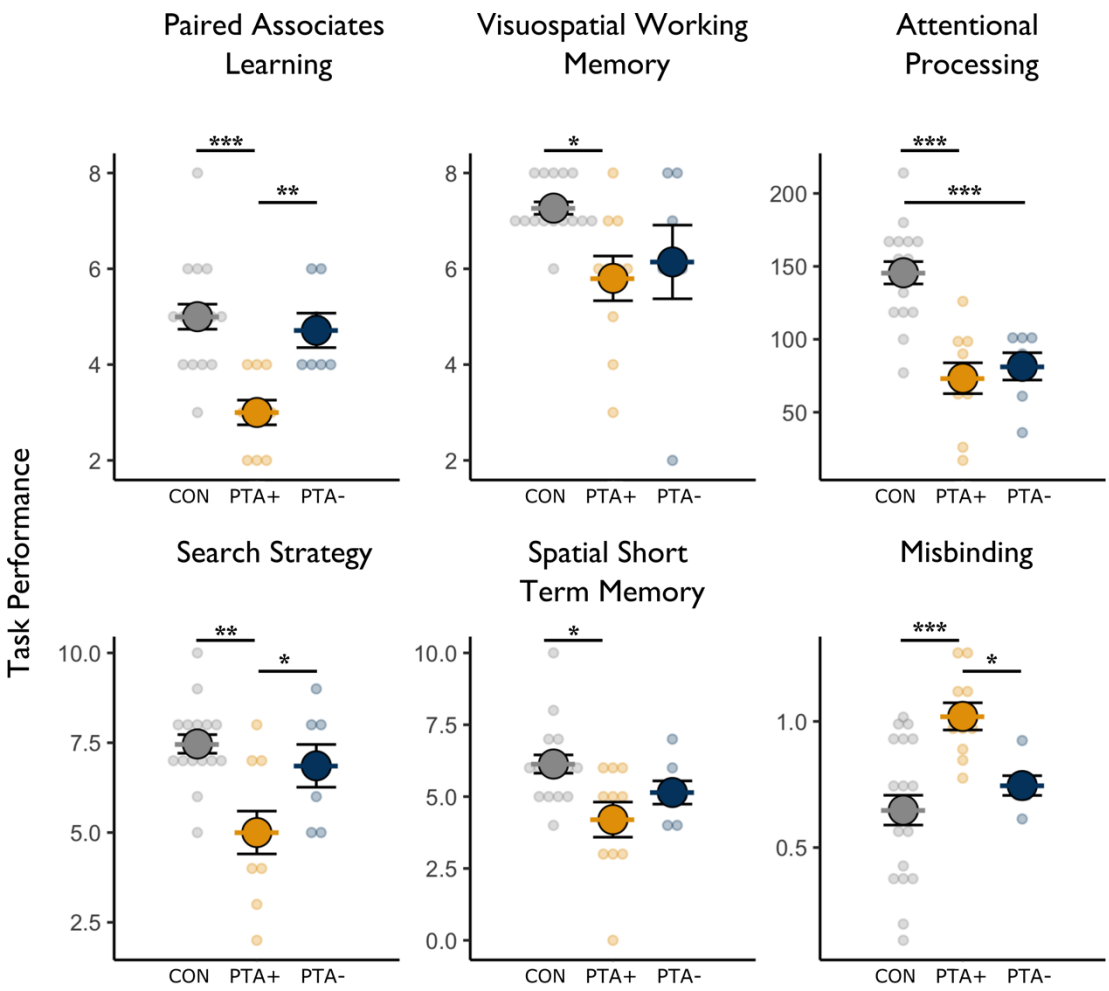

Figure 4.1 Neuropsychology results for the EEG cohort at baseline

Neuropsychological results in PTA+ patients, PTA- patients and healthy controls at baseline. *** Significant at p<0001; ** p<0.01; * p<0.05. Error bars represent the standard error of the mean (SEM). CON=healthy controls.

Table 4.3 Neuropsychology statistics for the EEG cohort at follow-up

Cognitive Domain	Assessment	PTA+ Mean (± SD)	PTA- Mean (± SD)	Group		Timepoint		Group x Timepoint	
				F	p	F	p	F	p
Associative Working Memory	Precision working memory misbinding (entropy ratio)	0.67 (0.32)	0.74 (0.13)	2.01	0.19400	2.86	0.13000	2.620	0.14400
	Paired Associates Learning	3.60 (0.55)	4.20 (0.84)	22.53	0.00145	0.057	0.81700	2.800	0.13300
Visuospatial Working Memory	Monkey Ladder	6.80 (1.92)	7.40 (0.89)	1.44	0.26400	0.485	0.50600	0.000	1.00000
Spatial Short Term Memory Capacity	Spatial span	5.60 (0.89)	5.60 (1.52)	0.909	0.36800	1.420	0.26800	0.725	0.41900
Search Strategy	Self-ordered search	7.20 (2.49)	7.80 (1.30)	2.864	0.12900	4.898	0.05780	0.831	0.38880
Attentional Processing	Feature Match	97.80 (28.18)	116.00 (22.70)	1.259	0.294	4.879	0.05820	0.312	0.59170

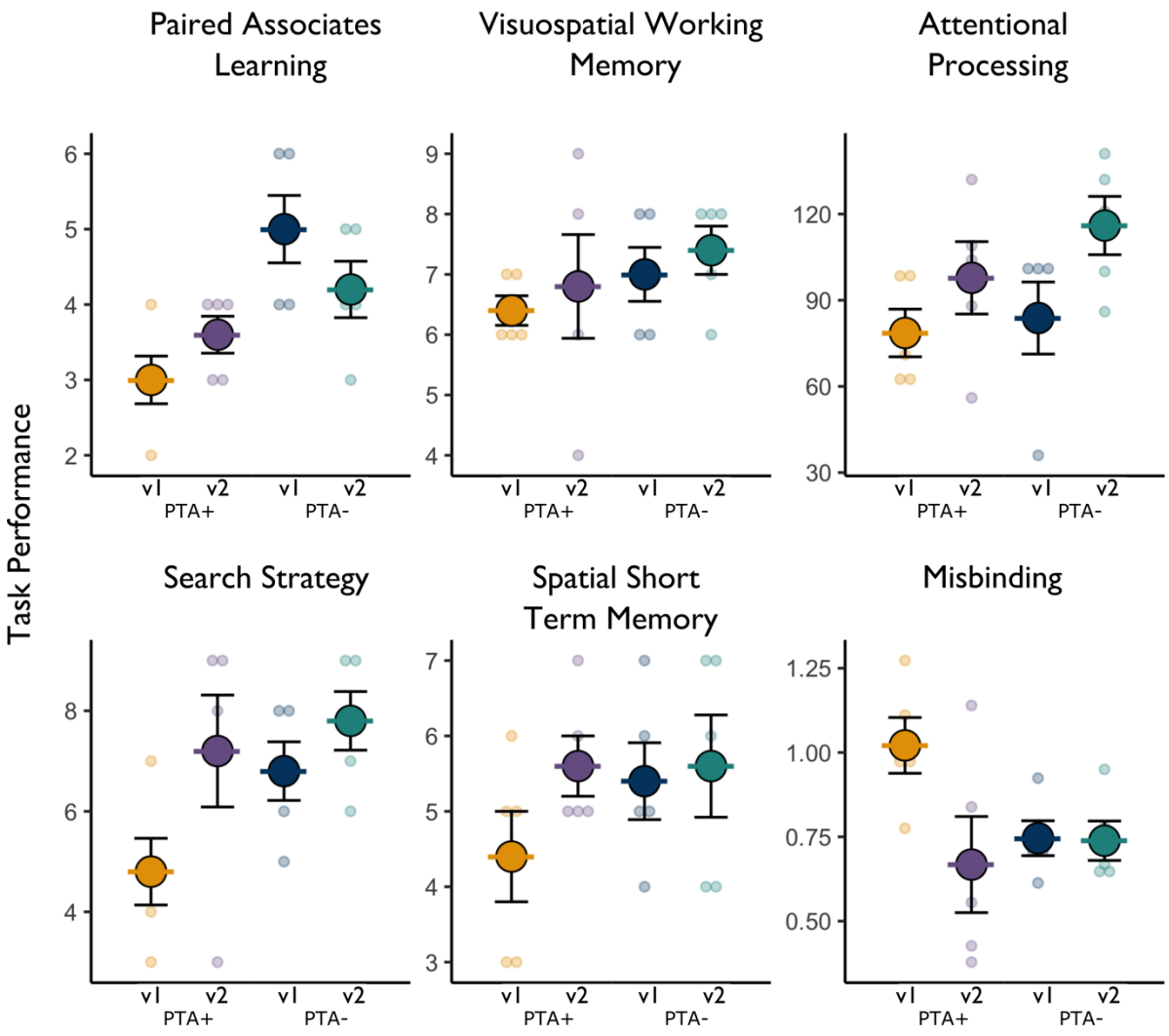

Figure 4.2 Neuropsychology results for the EEG cohort at follow-up

Neuropsychological results in PTA+ patients, PTA- patients and healthy controls at baseline. *** p<0001; ** p<0.01; * p<0.05. Error bars represent the standard error of the mean (SEM). CON=healthy controls.

4.3.3 Global normalised power in PTA

At the group level, TBI patients showed significant abnormalities in global normalised power in a range of frequency bands (delta $F(2,35)=5.97$, $p=0.006$), alpha ($F(2,35)=9.05$, $p<0.001$), beta ($F(2,35)=6.31$, $p=0.005$) and gamma ($F(2,35)=5.08$, $p=0.012$; Figure 4.3A)). In the delta band, these effects were driven by PTA+ patients exhibiting increased power compared to controls and a trend towards an increase compared to PTA- (PTA+ > CON: $t(35)=3.43$, $p=0.005$; PTA+ > PTA-: $t(35)=-2.16$, uncorrected $p=0.038$, $p=0.057$). In the alpha band, PTA+ showed reduced power compared to healthy controls and a trend towards a decrease compared to PTA- (PTA+ < CON: $t(35)=-4.25$, $p<0.001$; PTA+ < PTA-: $t(35)=2.09$, uncorrected $p=0.044$, $p=0.065$). PTA+ patients also showed reduced power in the beta band (PTA+ < CON: $t(35)=-3.01$, $p=0.014$; PTA- < CON: $t(35)=-2.66$, $p=0.018$). PTA+ patients did not demonstrate abnormalities in the gamma band: the group effect was driven by reduced power in PTA- compared to healthy controls (PTA- < CON: $t(35)=-2.97$, $p=0.016$).

There was a significant group difference in the global delta to alpha power ratio (DAR; $F(2,35)=9.12$, $p<0.001$; Figure 4.3B). This was the result of a significantly higher DAR in PTA+ patients compared to PTA- and healthy controls (PTA+ > PTA- ($t(35)=2.51$, $p=0.025$); PTA+ > CON ($t(35)=4.26$, $p<0.001$)).

Visual inspection of topoplots (Figure 4.3C) demonstrated abnormal patterns of power across multiple frequency bands in both patient groups. These were tested using cluster-based permutation statistics (Figure 4.3D). In the delta band, both PTA+ and PTA- patients showed a single significant cluster of increased power compared to controls: in both patient groups this encompassed frontal, parietal, and temporal channels and in PTA+ the more widespread cluster additionally encompassed occipital channels. Conversely in the alpha band patients showed reductions in power: compared to controls PTA+ patients showed significantly reduced occipital and right parietal alpha power across a single cluster, and widespread alpha reductions compared to PTA- patients in frontal, temporal, and parietal channels across a single cluster. Patients showed the opposite direction of effects in the theta band, with PTA- showing an increase in theta power across all channel groups in one widespread cluster compared to controls, while PTA+ did not differ significantly from controls but showed reduced power compared to PTA-

patients in a small right parietal-occipital cluster. Changes in the beta band were also observed in a similar pattern to theta; PTA- showed a cluster of increased temporal-parietal beta power compared to controls and PTA+ showed a cluster of decreased parietal power compared to PTA- but no difference from controls. There were no significant clusters found between any of the groups in the gamma frequency band.

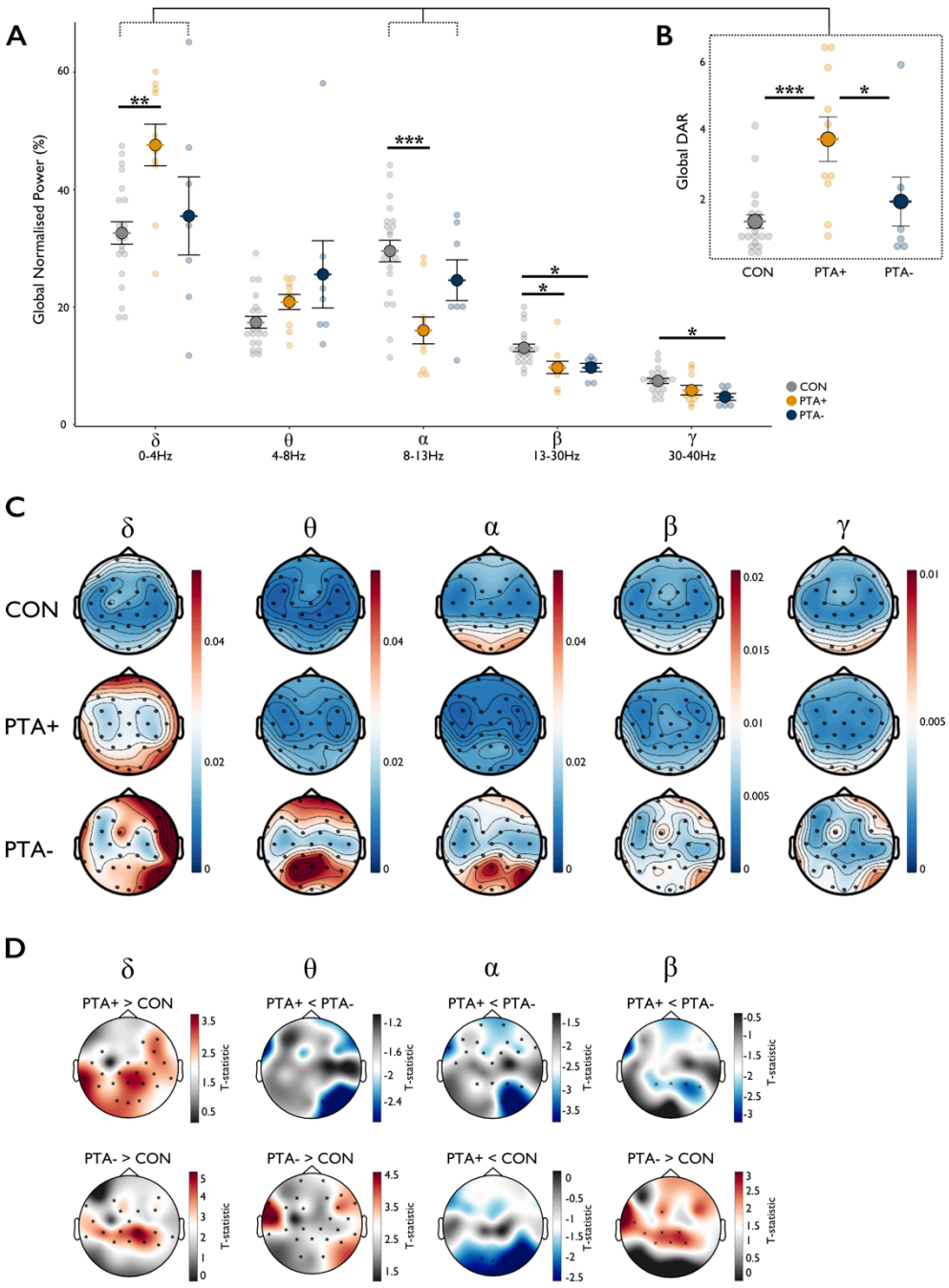

Figure 4.3 Normalised power at baseline

A| Mean global normalised power for all groups across all frequency bands. **B|** Global delta to alpha ratio across all groups. **C|** Topoplots depicting mean distribution of power for each group in each frequency band. Blue denotes low power; red denotes higher power. **D|** Cluster based statistical comparisons of power in (left to right) delta, theta, alpha, and beta frequency bands between PTA+, PTA- and healthy controls. Channels marked are those included in the significant cluster: * p>0.01; ˣ p>0.05.

4.3.4 Low frequency power abnormalities resolve at follow-up

By 6-month follow-up, the PTA+ group no longer showed abnormalities compared to the PTA- group (Figure 4.4). In individual frequency bands there was a significant effect of visit in delta and alpha (delta ($F(1,8)=13.65$, $p=0.006$); alpha ($F(1,8)=8.37$, $p=0.020$; Figure 4.4A)). In the delta band these were driven by decreases between baseline and follow-up in the PTA+ group ($t(4)=4.1234$, $p=0.029$). In the alpha band this was the result of an increase between baseline and follow-up in the PTA+ group ($t(4)=-4.0726$, $p=0.030$). There was also a significant group by time interaction in beta ($F(1,8)=13.23$, $p=0.007$) and gamma ($F(1,8)=6.30$, $p=0.0362$) bands but no longitudinal effects were observed in the theta band. At follow-up the marked baseline abnormality in DAR had resolved (Figure 5B). There was a significant group by time interaction ($F(1,8)=5.48$, $p=0.047$) which was driven by a significant reduction in DAR in the PTA+ group ($t(4)=3.008$, $p=0.0396$) while the PTA- group showed no change ($t(4)=0.521$, $p=0.6298$) between timepoints. Figure 4.4C depicts the spatial distribution in channel space of the change across time (follow-up minus baseline) for each frequency band for PTA+ (top row) and PTA- (bottom row) patients.

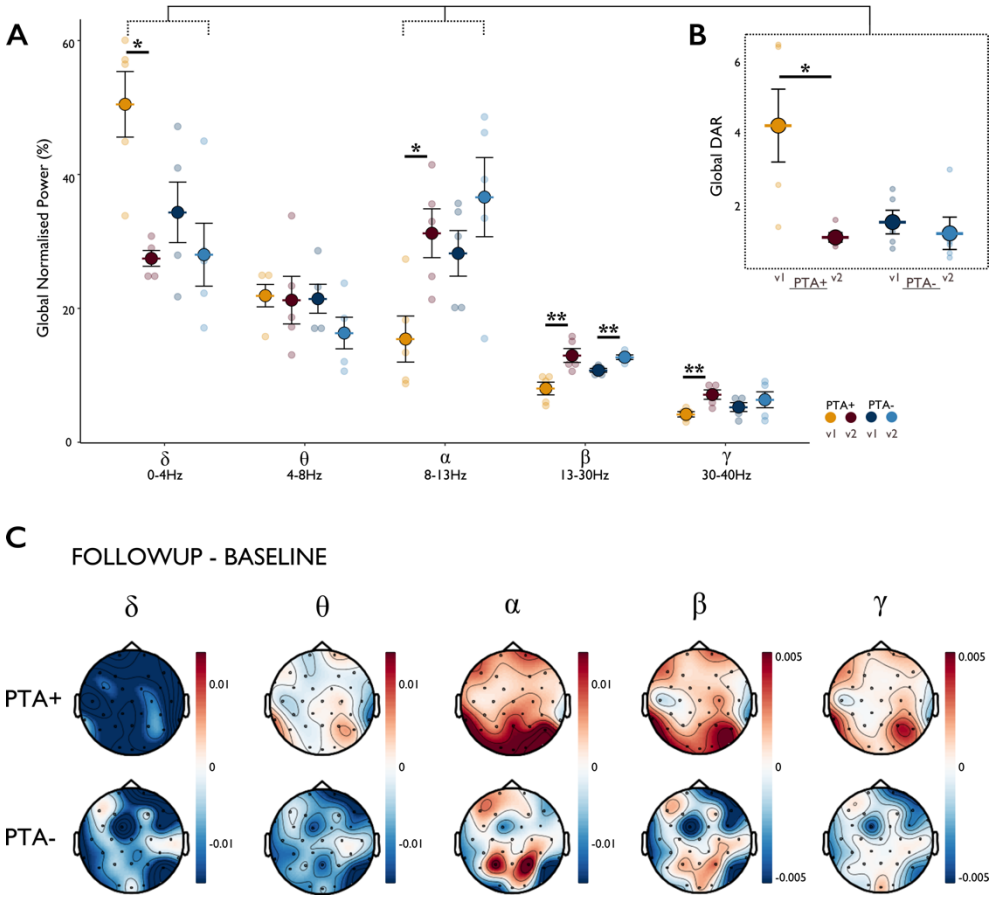

Figure 4.4 Normalised power at follow-up

A| Mean global normalised power for all patients with baseline and follow-up across all frequency bands. **B|** Global delta to alpha ratio. **C|** Topoplots showing change between baseline and follow-up (follow-up minus baseline) in PTA+ and PTA- TBI patients in power across all frequency bands. Blue denotes absolute reduction in power at follow-up from baseline, white denotes no change, red denotes absolute increase in power at follow-up from baseline.

4.3.5 Individual case studies

To better describe the transient binding impairment observed in Chapter 3 and how this might relate to the transient shift towards slow wave power observed in these results, I considered these changes at the single patient level. Figure 4.5 illustrates four individual case studies to highlight that the EEG changes I report here are more sensitive to abnormalities occurring during a period of PTA than conventional routine clinical imaging. Case studies one to three show TBI patients during a period of PTA at baseline and at follow-up once they were no longer in PTA. Case study four shows a TBI patient who was not in PTA.

Case study one is a 45-year-old male with a moderate-severe TBI acquired through a fall from standing. Clinical imaging reported presence of subdural haemorrhage (SDH), subarachnoid haemorrhage (SAH), bi-frontal contusions and midline shift. On the day of assessment, day eight post-injury, he was clinically deemed to be in PTA, scoring 8 on the WPTAS, and had a total PTA duration of 12 days. At baseline his distribution of responses on the precision spatial working memory task showed a bias towards the non-target with an entropy ratio of 1.27. He showed a dramatic improvement at follow-up to an entropy ratio of 0.56. At baseline he had a global DAR of 6.46 which reduced to 0.99 at follow-up.

Case study two is a 26-year-old male with a moderate-severe TBI acquired through a road traffic collision as a cyclist. There was no acute intracranial haemorrhage or space-occupying lesions on the initial clinical imaging, which was reported as normal. Further imaging with MRI revealed evidence of diffuse axonal injury. He was assessed on day 24 post-injury, scoring 7 on the WPTAS and thus still in a period of PTA. He had a total PTA duration of 38 days. Working memory binding performance at baseline was poor with an entropy ratio of 1.11 which reduced to 0.38 at follow-up. At baseline his global DAR was 6.52 and reduced to 0.82 at follow-up.

Case study three, a 67-year-old male, also acquired a moderate-severe TBI acquired through a road traffic collision as a cyclist. He had a total PTA duration of 28 days. Clinical imaging showed a left SDH, left temporal contusions, (probable) right extradural hemorrhage (EDH), skull base fractures and pneumocephalus. He was clinically deemed to be in PTA, scoring 8 on the WPTAS on the day of assessment which was day 5 post-injury. At baseline he had an entropy ratio of

0.98 which improved to 0.43 at follow-up. His global DAR was 4.21 at baseline and reduced to 0.75 at follow-up.

Case study four is a 33-year-old male with a moderate-severe TBI acquired through a road traffic collision as a pedestrian. Clinical imaging reported presence of left-sided extra-axial haematoma with associated comminuted fracture involving the left frontal bone. Evidence of diffuse axonal injury was present on MRI. On the day of assessment, day 5 post-injury, he was clinically deemed to not be in PTA, scoring 12 on the WPTAS, and had a PTA duration of 0 days. At baseline he did not demonstrate any binding deficit, with an entropy ratio of 0.72 which actually increased slightly at follow-up to 0.95. At baseline he had a global DAR of 2.04 which decreased to 0.48 at follow-up.

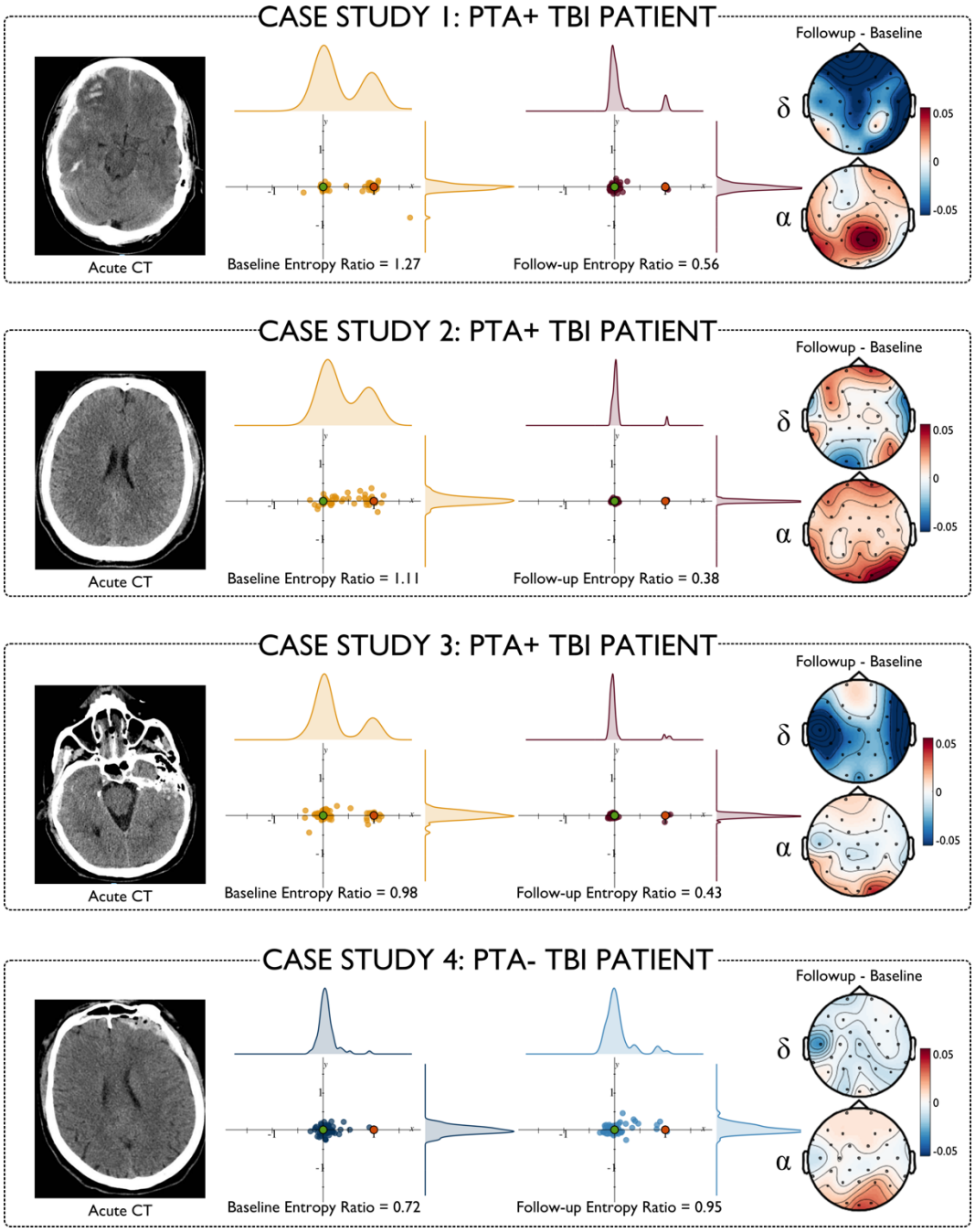

Figure 4.5 Individual patient case studies

A series of four acute TBI patient case studies. Case studies 1-3 are PTA+ patients. Case study 4 is a PTA- patient. In each case (from left to right) routine clinical CT scans on admission; spatial distribution of responses in the precision spatial working memory task for baseline and follow-up; topoplots showing changes in delta (top) and alpha (bottom) power changes between baseline and follow-up.

4.3.6 Increased slow-wave activity is associated with disruption to working memory binding

In order to understand how the abnormalities seen on EEG relate to the cognitive deficits observed without forcing patients into categories based on an arbitrarily defined threshold, I grouped PTA+ and PTA- patients together. When grouped together, TBI patients showed significantly higher DAR than healthy controls ($t(33.82)=3.43$, $p=0.002$; Figure 4.6A).

I then examined the effects of global DAR on continuous measures of working memory performance. In patients, but not controls, I found significant correlations between global DAR and performance on measures of associative working memory including the entropy ratio of distribution of responses in the precision working memory task, thresholded misbinding errors from the same task (Chapter 3), and score on the paired associates learning task (entropy ratio (TBI: $R=0.51$, $p=0.04$; controls: $R=-0.29$, $p=0.22$; Figure 4.6B); thresholded misbinding errors (TBI: $R=0.34$, $p=0.02$;controls=-0.23, $p=0.33$; Figure 4.6C); paired associates learning (TBI : $R=-0.6$, $p=0.01$; controls: $R=0.44$, $p=0.10$; Figure 4.6D)). The total duration of PTA, a proxy of injury severity, was not associated with the DAR in patients (Figure 6E; $R=0.34$, $p=0.18$).

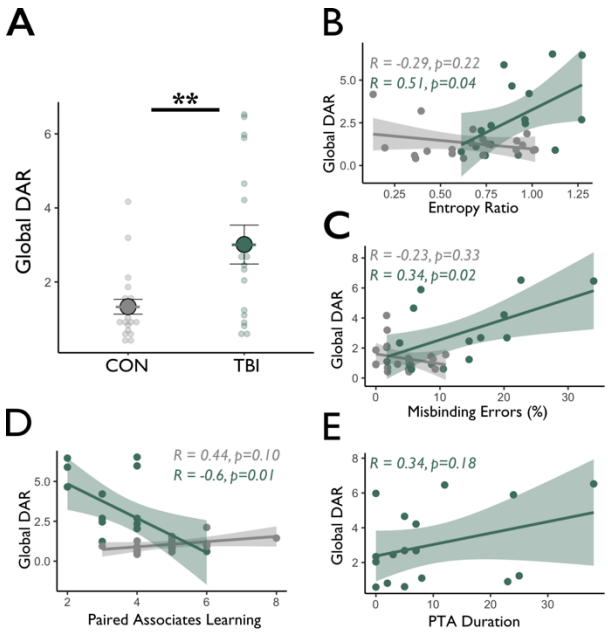

Figure 4.6 Association between global delta to alpha ratio and working memory

A| Global delta to alpha power ratio (DAR) between all TBI patients (PTA+ and PTA- combined) and healthy controls. Correlations between DAR and **B|** Entropy ratio of the distribution of location placements and **C|** Misbinding errors on the object-location association precision working memory task, **D|** Performance on the paired associates learning task and **E|** Total duration of PTA irrespective of PTA+/- status at the time of assessment.

4.3.7 Frontal-parietal theta phase synchronisation is increased following acute TBI

Phase synchronisation was quantified using the dwPLI. Whole brain connectivity matrices were constructed on a channel-wise basis for controls (Figure 4.7A) and patients (Figure 4.7B) in the theta band.

TBI patients showed increased mean dwPLI across the whole brain compared to healthy controls ($t(21.52)=-2.09$, $p=0.04869$). Network based statistics revealed that patients show theta hyperconnectivity compared to controls across one robust network consisting of 19 edges, including frontal-parietal connections (Figure 4.7C). The mean dwPLI across this network did not correlate with any behavioral measures that had distinguished PTA from TBI patients (PAL, misbinding, self-ordered search). There was a relationship between the mean dwPLI across this network and duration of PTA however this did not survive corrections for multiple comparisons ($R=0.57$, uncorrected $p=0.016$; fdr corrected $p=0.064$). When averaging values across frontal and parietal channel groups, patients showed significantly higher connectivity than controls ($t(18.59)=-2.268$, $p=0.02892$; Figure 4.7D). There was no difference in connectivity between patients and controls in frontal-temporal channels ($t(27.74)=-1.53$, $p=0.1376$).

At follow-up, there was a general reduction compared to baseline in mean whole brain dwPLI in patients (Figure 4.7E) at but no significant longitudinal changes in dwPLI in either frontal-parietal or frontal-temporal channel connectivity (Figure 4.7F).

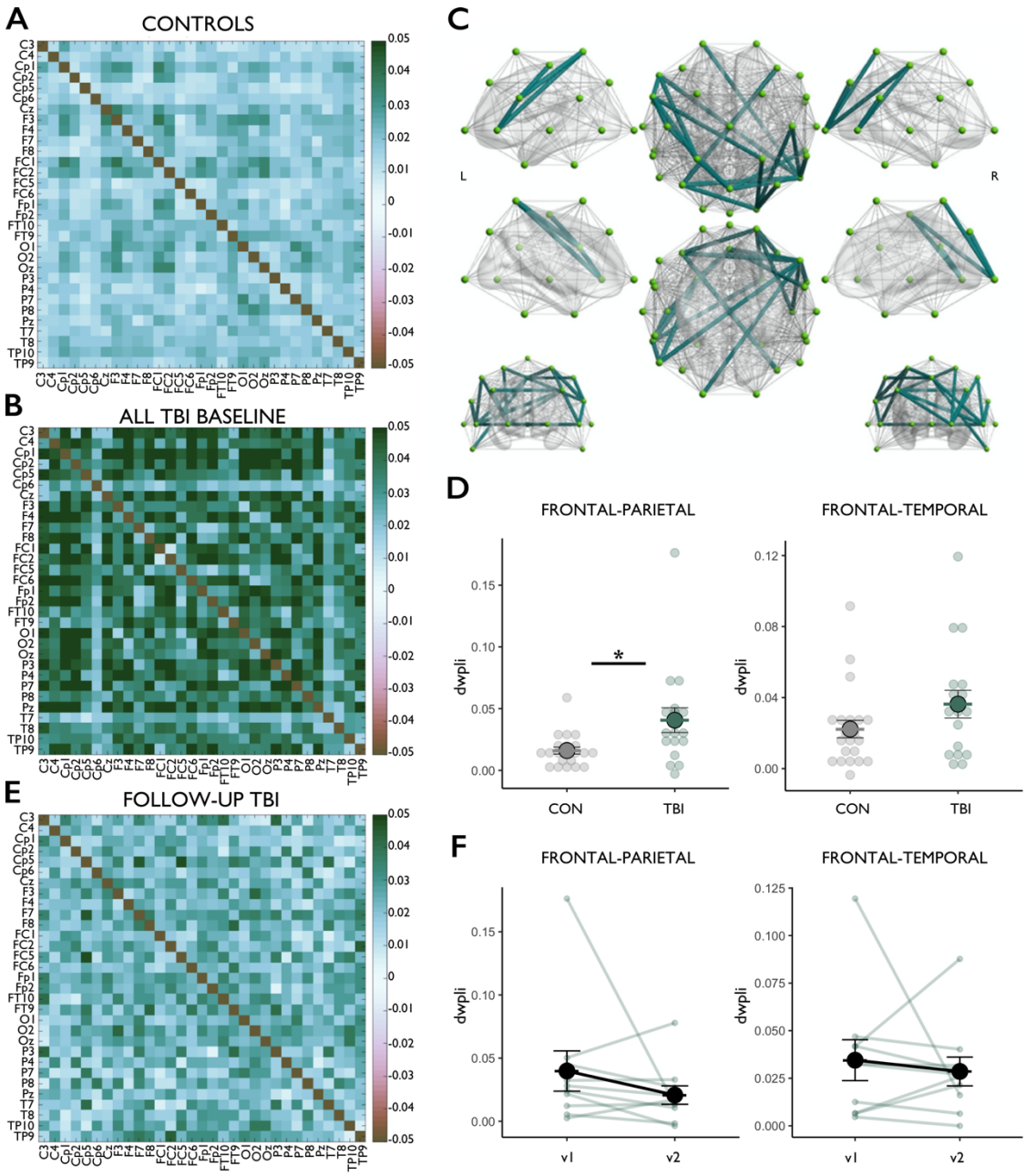

Figure 4.7 Theta phase synchronisation in acute TBI patients and controls.

A| Whole brain dwPLI connectivity matrices for controls (top) and patients (bottom) at baseline. **B|** Network based statistics revealed one robust network of hyperconnectivity in patients compared to controls. **C|** Mean dwPLI between frontal-parietal (left) and frontal-temporal (right) channels in patients and controls. **D|** Whole brain dwPLI connectivity matrix for patients at follow-up. **E|** Longitudinal change in mean dwPLI between frontal-parietal (left) and frontal-temporal (right) channels in patients. v1 = baseline; v2 = follow-up. Error bars represent standard error of the mean.

4.3.8 Theta-gamma cross-frequency coupling is not altered in acute TBI

Phase-amplitude coupling, specifically frontal theta phase to parietal and temporal gamma amplitude, was quantified using the modulation index. Contrary to our hypothesis, patients did not show increased phase-amplitude coupling for either frontal to parietal ($t(35.97)=-1.413$, $p=0.1662$) or frontal-temporal ($t(34.42)=-0.634$, $p=0.5303$) modulation. There were no significant longitudinal changes in patients returning for follow-up (Figure 4.8B) in the mean modulation index for either frontal-parietal ($t(9) = 1.567$, $p= 0.1516$) or frontal-temporal ($t(9) = 0.276$, $p = 0.7891$) channels.

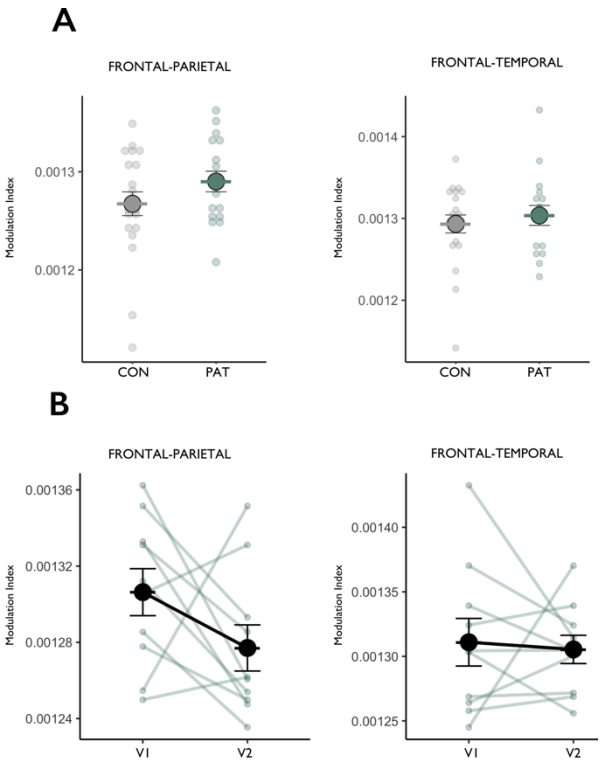

Figure 4.8 Frontal theta phase to parietal and temporal gamma amplitude coupling in acute TBI patients and controls

A| Average modulation index between frontal and parietal channels (left) and frontal and temporal channels (right) in patients and controls at baseline. **B|** Longitudinal changes in phase-amplitude coupling between frontal-parietal (left) and frontal-temporal (right) channels in patients at follow-up. Error bars represent standard error of the mean.

4.4 DISCUSSION

Electrophysiological abnormalities are commonly reported following TBI. In this chapter I show that TBI patients experiencing a period of PTA show a shift towards pathological slow wave oscillatory power. Furthermore, this is associated with the profound binding deficit evident in this patient group. I show that frontal-parietal connectivity in the theta band is abnormally high following acute TBI, but this is not specific to a period of PTA. The results provide novel insights into the cognitive profile of PTA and the neural underpinnings of object-location association memory in this clinical population.

Resting state EEG measures were used to identify abnormalities associated with a period of PTA in a subset of TBI patients. PTA+ patients showed a significantly higher DAR than PTA- and healthy controls which normalised at follow-up. This would suggest that increased DAR may be a sensitive electrophysiological marker of a period of PTA. Slow wave activity has previously been considered to be more sensitive than standard CT (Haveman *et al.*, 2019) in predicting neurological outcome in moderate-severe TBI and versus diffusion tensor imaging (DTI) in diagnosing mild TBI (Huang *et al.*, 2009). The results I present here suggest that DAR may be sensitive to detecting a period of profound cortical disruption. Indeed, in the series of clinical case studies I presented, acute abnormalities in slow wave power were more informative than acute imaging in distinguishing between PTA+ and PTA- patients.

EEG slowing is often viewed as a nonspecific sign of cerebral dysfunction. Pathological oscillatory slowing is well documented in the clinical literature. Global delta synchronization and alpha desynchronization are both associated with depression of the central nervous system and reduced levels of consciousness (Howells *et al.*, 2018). The increased DAR could therefore be interpreted as PTA being an extension of a period of reduced consciousness, with PTA being conceptualised as an 'emergent' state. From a cognitive perspective this isn't entirely consistent with the clinical presentation of PTA. PTA+ patients do show impaired attentional processing compared to healthy controls and TBI patients not in PTA, which could be interpreted to suggest PTA+ are somewhat less alert than PTA- patients. However, given the ability of these patients to engage with and perform well on tasks not requiring associative binding, this interpretation is not

satisfactory. Instead, these results may suggest that a shift from fast to slow oscillations may not only mediate alertness (in fully alert individuals) but is also important in feature integration within working memory.

The DAR was significantly associated with associative working memory measures in acute TBI patients but not controls. The results here demonstrate for the first time that impaired binding ability is associated with a higher global DAR. In TBI, a shift towards slower wave power has previously been associated with long-term neuropsychological outcome (Robb Swan *et al.*, 2015) functional outcome (Leon-Carrion *et al.*, 2009) and clinical symptoms of TBI (Lewine *et al.*, 2007). The results I present here, that DAR is also tightly associated with binding ability, suggest that this shift towards slow wave power is disrupting the memory process through which individual item memory is integrated with spatial location. This is consistent with other clinical populations. Patients with AD show profound binding impairments (Liang *et al.*, 2016; Parra *et al.*, 2010), and one of the most prominent EEG findings in the AD population is a shift towards lower frequency oscillations through delta synchronization and alpha de-synchronisation (Benwell *et al.*, 2020). Power decreases in the delta band are also associated with better working memory performance (Jaiswal *et al.*, 2019). Taken with the results I present here that show DAR normalizes when the binding impairments normalise, these findings would suggest that abnormal DAR is disrupting part of the process required for successful integration of object and location memory.

In order to understand how abnormal DAR was disrupting the memory system, I measured long range theta synchrony in frontal-parietal and frontal-temporal channels. I found that acute TBI patients show frontal-parietal theta hyperconnectivity, but this was irrespective of whether they were experiencing a period of PTA. In healthy controls, scalp EEG studies have shown that increases in theta coherence between frontal and temporal-parietal regions are associated with increases in working memory load and recruitment of executive control functions (Fell & Axmacher, 2011). I would therefore have expected to see a relationship between binding ability on the precision working memory task and theta connectivity, but this was not present. Instead, I found that a longer PTA duration, often taken as a proxy for injury severity (McMillan, 2015), is associated with higher connectivity across a singular robust network (at borderline statistical significance following multiple comparisons corrections). In the absence of any apparent

behavioral advantage to this hyperconnectivity, it is unlikely that it is serving a compensatory purpose but given the trend towards an association with PTA duration, it could be related to a restorative process reflecting neuroplastic recovery following TBI.

Evidence from the working memory literature in healthy populations suggested we would expect to find that associative binding was underpinned by an intricate theta-gamma phase-amplitude coupling relationship in which frontal theta phase modulated the gamma amplitude in temporal and parietal regions (Daume *et al.*, 2017; Köster *et al.*, 2018). Unexpectedly, I found no difference between TBI patients and controls in the modulation index for either frontal-temporal or frontal-parietal channel combinations. It is therefore possible that this specific system is not compromised following TBI and the degree to which frontal theta phase modulates temporal or parietal gamma amplitude is intact, but that this is relative to the overall power in these frequencies. A shift towards lower frequency oscillations may mean that the interactions between frequency bands remain the same but the overall influence they have over working memory processes is reduced.

4.4.1 Limitations

There are some limitations that should be considered. I have inferred that misbinding in PTA patients is underpinned by an abnormally high delta alpha ratio through an association observed in resting state EEG data. While this method allows us to draw conclusions about the general neural oscillatory abnormalities in this patient group, it does not offer precise task relevant changes. It is likely that by averaging over resting state data that valuable nuances in different memory process stages (encoding, maintenance, retrieval) are ignored. The association between DAR and misbinding should therefore be further explored to provide greater mechanistic insight.

There is great heterogeneity in the injury patterns present in TBI patients. Some patients in the cohort had acute bleeds while others had diffuse axonal injury. Subcutaneous blood could affect conductivity and thus different patterns of injury may differentially alter the EEG signal. Further work should explore whether different patterns of injury are associated with more specific alterations on EEG. Nevertheless, the DAR results were derived from a whole brain average and

reductions in DAR were observed in patients with a variety of injury patterns. Heterogeneity of injury patterns should therefore not alter the interpretation of the present results.

There was a trend towards the PTA+ group being slightly older than healthy controls. During healthy ageing there is a linear decrease of slow frequency resting-state activity (Vlahou *et al.*, 2014). This would suggest that if age alone were influencing the results, then the PTA+ group would be expected to show lower delta power than controls. In fact, the opposite was the case, and PTA+ showed significantly greater delta power than controls. The trend towards a difference in age between the groups should therefore not alter the interpretation of a significant shift towards lower frequency oscillations during PTA.

4.4.2 Future Directions

The results presented in this chapter suggest that increases in DAR may provide a sensitive electrophysiological marker of PTA. Close temporal monitoring of EEG in an acute TBI cohort would provide data to elucidate if this metric could inform the tracking of emergence from PTA. If combined with a rich battery of cognitive assessments, it would also provide the opportunity to better understand the direct relationship between DAR and recovery of brain function following TBI.

To directly expand on the result presented in this chapter, future work should consider EEG changes during the precision spatial working memory task in this clinical cohort to study with greater accuracy the neural changes associated with binding failures in these patients. EEG changes in Alzheimer's patients during an object-location association task show different abnormalities during encoding and retrieval (Han *et al.*, 2017). The ability to measure power and connectivity during specific stages of memory processes would provide valuable insight into whether there is e.g., failed compensatory mechanisms or inadequate maintenance activity underpinning binding impairments.

4.4.3 Conclusion

In this chapter I have shown that a shift towards low frequency power, as indexed by the DAR, is sensitive to a period of PTA and the associated integrative working memory impairments. DAR provides the potential to monitor recovery of brain function following TBI. Fronto-parietal hyperconnectivity in the theta band is present in acute TBI but is not sensitive to presence of PTA.

5

Network dynamics in PTA

In this chapter I investigate the impact of PTA on the temporal dynamics of core resting state networks involved in cognition. I use dynamic functional connectivity to define brain states and explore how the transitions between them is affected following TBI.

5.1 INTRODUCTION

Post-traumatic amnesia (PTA) is likely to result from a temporary disruption to the interactions within and between brain networks involved in memory processing (see Chapter 1, section 1.3.7). The brain is a dynamic system which constantly changes in response to ongoing internal or external demands (Du, Fu & Calhoun, 2018). The ability to flexibly transition between different patterns of connectivity within and between large-scale brain networks to achieve different configurations is therefore required.

The default mode network (DMN) is a functional resting state network central to memory processing (Andrews-Hanna, Smallwood & Spreng, 2014; Staffaroni *et al.*, 2018) and is frequently disrupted following traumatic brain injury (TBI; Bonnelle *et al.*, 2011; Palacios *et al.*, 2013; Sharp *et al.*, 2011; see also Chapter 1, section 1.1.6). Connectivity *within* the DMN, and between the subsystems it is comprised of (Andrews-Hanna *et al.*, 2010), is important for successful memory formation. The posterior cingulate cortex (PCC) and the ventromedial prefrontal cortex (vmPFC) are core nodes within the DMN and interactions between these regions are important for associative and working memory function (Hampson *et al.*, 2006; Andrews-Hanna *et al.*, 2007). The medial temporal lobe (MTL) subsystem of the DMN incorporates hippocampal and parahippocampal regions, retrosplenial cortex, posterior inferior parietal lobe and ventromedial prefrontal cortex (Andrews-Hanna, Smallwood & Spreng, 2014). Disruption to these connections are found in neurological conditions where memory is impaired, including amnestic mild cognitive impairment (Dunn *et al.*, 2014), Alzheimer's disease (Wang *et al.*, 2006; Zhou *et al.*, 2008) and MTL amnesia (Hayes, Salat & Verfaellie, 2012). Connectivity between nodes within the MTL subsystem and the PCC are primarily mediated by parahippocampal connections (Ward *et al.*, 2014). Previous research into network dysfunction in PTA has shown that both functional and structural connectivity between the PCC and parahippocampus is temporarily disrupted during the period that acute TBI patients are in PTA (De Simoni *et al.*, 2016).

Communication *between* networks is considered critical in integrating resources from different systems to support higher level function (Di & Biswal, 2014). The interaction between the DMN and other resting state functional networks are especially important in cognition. Resting state

functional connectivity studies show a tight inverse coupling between the DMN and "task-positive" networks such as the salience network and fronto-parietal networks (FPNs; Fox *et al.*, 2005). It is thought that this anti-correlation between DMN and cognitive control networks may serve as a mechanism for modulating goal-directed cognition (Kelly *et al.*, 2008; Spreng *et al.*, 2010; Anticevic *et al.*, 2012). Greater degrees of anti-correlation between DMN and cognitive control networks have been associated with improved executive functioning and working memory in healthy adults (Spreng *et al.*, 2010; Kim & Kang, 2018; Xin & Lei, 2014), and attenuations to this pattern are associated with psychiatric and neurological disease (Hur *et al.*, 2021; Boord *et al.*, 2017; Anticevic *et al.*, 2012; Weiler *et al.*, 2017).

The switching between DMN and FPN activity is thought to be modulated by the salience network (SN). The anterior insula (aINS) has been identified as a key functional hub in the SN facilitating communication and adaptive switching between DMN and cognitive control networks (Sridharan, Levitin & Menon, 2008; Goulden *et al.*, 2014). Functional connectivity analyses suggest projections between dorsal posterior cingulate cortex (dPCC), a key node within the DMN, and the right aINS form a system that regulates attentional focus and facilitates regulation of network activation appropriate for current cognitive demands (Leech & Sharp, 2014). Furthermore, disruption to connectivity of the aINS during anaesthesia has been shown to disable brain network transitions (Huang *et al.*, 2021) suggesting that appropriate communication between dPCC and aINS are crucial for facilitating between network connectivity required for higher order cognition.

Traditional resting state connectivity studies typically average mean values across the whole time series, and the connectivity results are therefore reflective of an average over the period of the scan. This is also referred to as static functional connectivity. While this approach is useful in understanding which regions interact to form functional networks and are required for different task demands, it is limited in its ability to inform how changing between these different patterns of connectivity over time facilitates cognition. Dynamic functional connectivity (dFC) allows for the study of network configurations and how they change across time. Differences in a wide range of behavioural and cognitive measures in healthy controls have been associated with markers of resting state dFC (Liégeois *et al.*, 2017; Vidaurre, Smith & Woolrich, 2017) and the ability to transition between different functional networks is relevant to cognition in the context

of psychiatric and neurological disorders (Liang *et al.*, 2020; Douw *et al.*, 2015; Nguyen *et al.*, 2017; Díez-Cirarda *et al.*, 2018). The temporal fluctuations in connectivity between different regions reflect non-stationary switching of discrete brain states in which different within and between network configurations may emerge. Studying network configurations and their time-related connectivity may therefore provide further insights into network abnormalities seen in TBI.

Previous studies that have employed dFC methods in TBI have demonstrated that patients with less favourable outcomes showed altered temporal dynamics and less movement between functional connectivity states compared to healthy controls (van der Horn *et al.*, 2020; Hou *et al.*, 2019). Gilbert *et al.* (2018) demonstrated moderate-severe TBI patients made fewer state transitions compared to healthy controls at 1-year post injury. These findings would suggest that dynamic estimates of functional connectivity may be sensitive to injury effects and cognitive recovery following TBI. It is possible that disruption to communication between networks, and the temporal dynamics of functional connectivity between them, is involved in the profound mnemonic deficits present in PTA following TBI.

Here I test the hypotheses that i) the expected anti-correlation between DMN and FPN will be less apparent in PTA patients compared to healthy controls and acute TBI patients not in PTA and they will spend less time in a state associated with this network configuration, ii) disruption to network dynamics is mediated by abnormal functional connectivity between key nodes of the DMN and the MTL subsystem (ventral PCC and parahippocampal gyrus) and between key nodes of DMN and SN (dorsal PCC and aINS), and iii) the ability to flexibly transition between network configurations will be associated with the mnemonic deficits present in PTA.

5.2 METHODS

5.2.1 Participants

5.2.1.1 Patients

Twenty-seven patients (21 males, 6 females, mean age 42.59, range 19-67 years) admitted with a recent history of TBI were recruited from the Major Trauma Ward, St. Mary's Hospital, London, UK. Sixteen of these patients were from the historical acute cohort previously published in De Simoni *et al.* (2016). I additionally recruited a further 11 patients into the new acute cohort (see Chapter 2, section 2.2 for an overview of subjects and recruitment details). All patients had moderate-severe injuries according to the Mayo Classification system for TBI severity (Malec *et al.*, 2007; Chapter 2 section 2.3.1). Injuries were secondary to road traffic accidents (44.4%), falls (33.3%), cycling accidents (11.1%), assault (7.4%) and sports injury (3.7%). Inclusion and exclusion criteria, and consent procedures are detailed in Chapter 2.

5.2.1.2 Controls

Twenty-two healthy controls (17 males, 5 females, mean age 30.45, range 19-49 years) were also recruited. Fourteen of these controls were from the historical acute cohort and I additionally recruited a further eight.

5.2.2 Study protocol

All patients were recruited within 2 weeks of injury and underwent PTA assessment using the Westmead PTA Scale (WPTAS; Shores *et al.*, 1986) on the day of recruitment. In the morning, patients underwent neuropsychological assessment and were scanned in the afternoon. The imaging protocol was identical for all patients and controls irrespective of which cohort they were recruited into. Details of PTA assessment, neuropsychological tasks and imaging protocols are outlined in Chapter 2.

5.2.3 Neuropsychological Assessment

The neuropsychological assessments were not aligned between cohorts. There was some overlap in the cognitive domains that were assessed and the results from those tasks will be presented in this chapter (separately for each cohort) to give an overview of the degree of cognitive impairment in each group.

Participants recruited into the new acute cohort underwent full neuropsychological assessment as detailed in Chapter 2 and reported in the context of the whole cohort in Chapter 3. Participants recruited in the historical acute cohort underwent neuropsychological assessment using the CANTAB battery (De Simoni *et al.*, 2016). The results of these cognitive assessments in the historical acute cohort are presented in De Simoni *et al.* (2016). Although there was no overlap in the exact versions of the neuropsychological assessments used, two of the tasks are very similar in design: the paired associates learning task and the spatial working memory task (referred to as 'self-ordered search task' in the new acute cohort).

5.2.4 Imaging analysis

Structural T1 scans and functional MRI data were acquired using a 3.0T GE Medical Systems Scanner with an 8-channel head coil according to the protocols and acquisition parameters described in Chapter 2. Imaging data were pre-processed and denoised according to protocols described in Chapter 2.

5.2.4.1 Resting-state dynamic functional connectivity analysis

dFC analysis was performed to identify large-scale patterns of connectivity across regions of interest chosen for their role in cognitive functions. Figure 5.1 depicts the methods utilised to perform this analysis. First a series of regions were selected to give representation across key brain networks. Secondly, a sliding window connectivity approach was taken to identify patterns of large-scale functional connectivity. Finally, the properties of those patterns, such as dwell time and transitional probabilities, were analysed.

Regions of interest (ROIs) were selected to represent large scale resting state networks involved in cognition. These were the DMN, SN, and right and left FPNs. ROIs in the DMN and SN were selected based on results from previous work (De Simoni *et al.*, 2016; Li *et al.*, 2019a, 2019b; Leech *et al.*, 2011). ROIs in the right and left FPN were selected based on the independent component (IC) networks derived in Smith et al., 2009. The peaks of spatially independent clusters within the IC spatial maps were extracted using the cluster tool in FSL using a threshold of 3.1. Peaks that fell within the cerebellum or outside of the imaging protocol field of view (FOV) were discarded. The taxonomy of these peaks was derived based on the most likely region of the co-ordinates using the Harvard-Oxford cortical structural atlas implemented in FSL.

For each ROI, a 5mm sphere was constructed around the centre of the MNI co-ordinates (Table 5.1). BOLD timeseries data from each ROI was extracted using the first stage of dual regression (Nickerson *et al.*, 2017) in FSL and variance normalised to limit the analysis to temporal modulation rather than magnitude. Timeseries for each ROI were detrended using the Group ICA of fMRI toolbox (GIFT) implemented in MATLAB to remove linear, quadratic, and cubic trends and low pass filtered at 0.15Hz.

Table 5.1 MNI co-ordinates for regions of interest used in the dynamic functional connectivity analysis

Network	Region	MNI		
		x	*y*	*z*
DMN	Left ventromedial prefrontal cortex (L vmPFC)	-8	46	-8
	Right ventromedial prefrontal cortex (R vmPFC)	6	52	-6
	Dorsal posterior cingulate cortex (dPCC)	2	-34	40
	Ventral posterior cingulate cortex (vPCC)	2	-58	28
	Left inferior parietal gyrus (IPG)	-48	-58	30
	Right inferior parietal gyrus (R IPG)	54	-52	30
	Left parahippocampal gyrus (L PHG)	-26	-22	-22
	Right parahippocampal gyrus (R PHG)	26	-22	-22
L FPN	Left inferior frontal gyrus (L IFG)	-48	18	24
	Left middle temporal gyrus (L MTG)	-54	-52	-6
	Left superior parietal (L SPG)	-34	-54	48
	Left superior frontal gyrus (SFG)	-4	28	48
	Right inferior frontal gyrus (R IFG)	44	30	14
R FPN	Right paracingulate gyrus (R PCG)	4	10	44
	Left frontal operculum (L FOp)	-34	18	6
	Right posterior supramarginal gyrus (R pSMG)	54	-36	30
	Right frontal operculum (R FOp)	42	14	8
SN	Dorsal anterior cingulate cortex (dACC) / supplementary motor area (SMA)	8	14	52
	Right anterior insula (R aINS)	40	20	0
	Right inferior frontal gyrus (R IFG)	56	30	-2

5.2.4.1.1 Sliding-window functional connectivity estimation

dFC was estimated using a sliding window approach whereby covariance matrices were generated at every window. A tapered window was used and created by convolving a rectangle (width = 15; TRs = 45s) with a Gaussian (σ = 3 TRs) and then slid in steps of 1 repetition time (TR=3s). Very similar parameter settings have been used previously (Bonkhoff *et al.*, 2020; Allen *et al.*, 2014; van der Horn *et al.*, 2020). This resulted in 195 windowed functional connectivity matrices per patient.

Due to each segment of signal being relatively short, it is possible that they may not carry enough information to characterise the full covariance matrix. In order to account for this, the GIFT toolbox computes an L1-regularised precision matrix from the connectivity matrices to promote sparsity (Allen *et al.*, 2014). Final dynamic FC estimates for each window were concatenated to form an array representing the changes in covariance between ROIs as a function of time. Dynamic functional connectivity matrices were Fisher transformed to stabilise variance for further analysis.

5.2.4.1.2 Clustering

To assess the frequency and structure of reoccurring patterns of functional connectivity, a k-means clustering algorithm (Lloyd, 1982) was applied to the windowed covariance matrices across all subjects. The Manhattan distance was used as it has been shown to be more suitable for high-dimensional data than the Euclidean distance (Aggarwal, Hinneburg & Keim, 2001). The optimal number of clusters in the data was determined using the elbow criterion of the cluster validity index, computed as the ratio between within cluster distance to between-cluster distance. All functional connectivity matrices were assigned to a cluster. Each cluster represents a distinct connectivity pattern across the ROIs that reoccurred across all subjects.

5.2.4.1.3 State properties

In addition to describing the differences in connectivity between ROIs as states, the temporal properties of these states can also be quantified and compared between groups. Fraction time,

the total time spent in a state, and dwell time, the time spent in a state before making a transition to a different state were calculated for each subject. The ability to transition between states was quantified by calculating the entropy of the stationary distribution of the Markov chain. This is a probability distribution that remains unchanged as time progresses and thus describes the distribution of state transitions over an infinite time so that the distribution does not change any longer. To calculate this, first transition matrices, the likelihood of transition between states, for each subject were obtained. Transition behaviour was then characterised by computing the fraction time over an infinite time as given by the stationary distribution of a Markov chain. Stationary distribution was computed by the left eigenvector of the transition matrices when eigenvalue equals to 1. The entropy rate of a stationary Markov chain represents the weighted average of the entropies at each state. Low values of entropy reflect a tendency to spend more time in fewer states, while higher entropy reflects a more even distribution of time spent in all states.

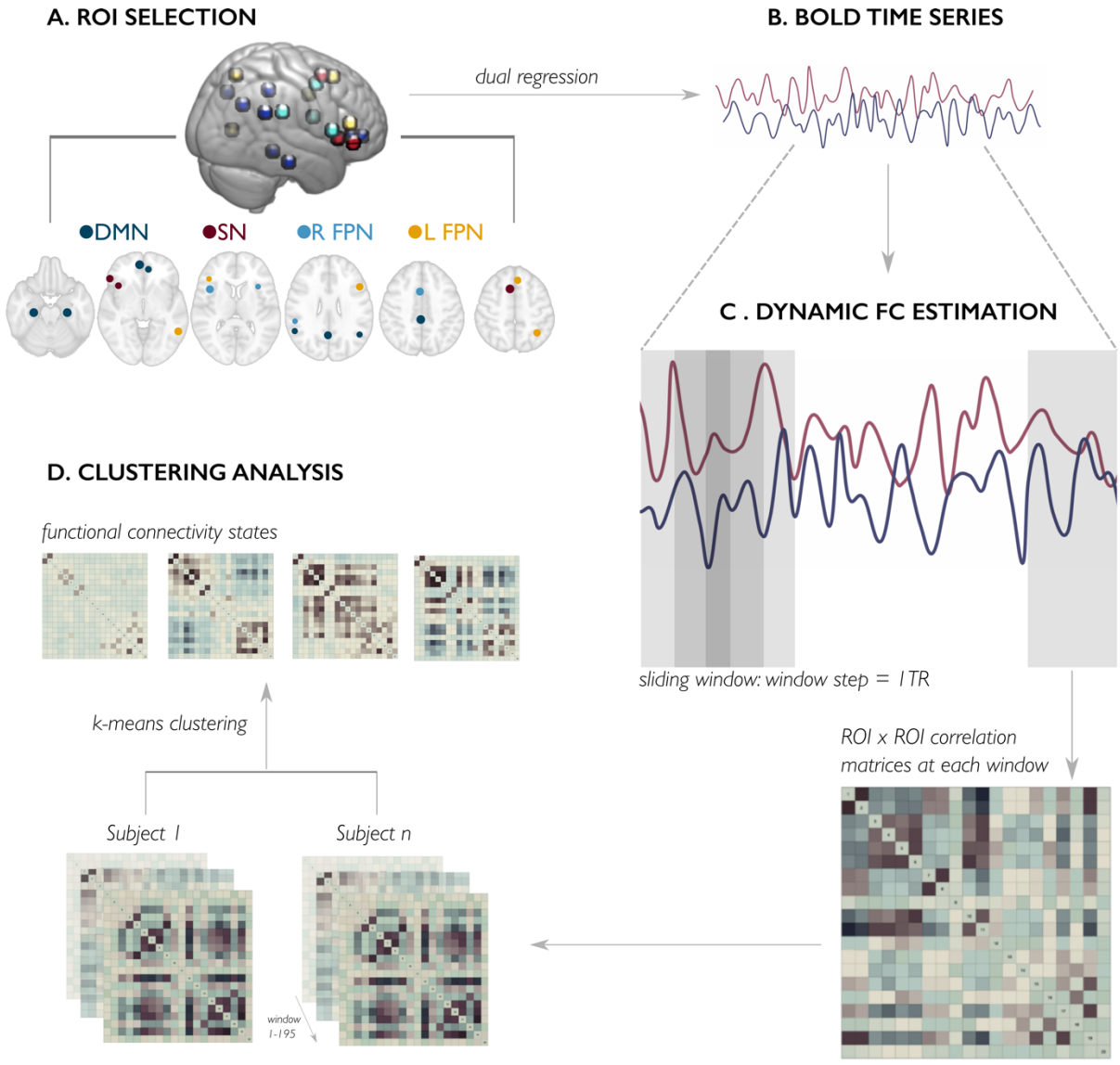

Figure 5.1 Dynamic functional connectivity analysis

A| Regions of interest (ROIs) were selected to represent coverage across large scale resting state networks: default mode network (DMN), salience network (SN), and right and left frontoparietal networks (R/L FPN). **B|** The BOLD signal timeseries was extracted from each ROI using dual regression. **C|** A dynamic sliding window approach was used to estimate connectivity between every pair of ROIs at every window. This was done for every subject. **D|** Correlation matrices for all subjects were concatenated and underwent k-means clustering to reveal functional connectivity states.

5.3 RESULTS

5.3.1 Demographics

Following PTA assessment, 14 patients were deemed to be currently in a period of PTA, and 13 were deemed to have recovered, or never had, a period of PTA. The mean WPTAS score in PTA patients on the day of testing was 9.43 (SD = 2.21). All non-PTA TBI patients scored 12 on the day of testing. There was an effect of age across the groups ($F=6.95$, $df=2$, $p=0.002$) driven by PTA patients (mean age 43.64 years, SD = 14.93) being older than controls (mean age 30.45, SD = 8.18; $t=3.37$, $df = 46$, $p=0.0046$). PTA- patients (mean age 41.45, SD=11.6) did not differ from either PTA+ or controls. There was no significant difference in sex distribution between the groups (Controls 17 males, 5 females; PTA+ 12 males, 2 females; PTA- 9 males, 4 females; Fisher's exact test = 0.56).

5.3.2 Neuropsychology

The neuropsychological profile of the new acute cohort is characterised in detail in the context of the whole cohort in Chapter 3. To provide a brief overview of the degree of cognitive impairment in the participants that were included in the imaging analysis in this chapter a subset of the tasks that have similar designs to the tasks used in the historical cohort are shown in Figure 5.2. Patients performed worse than controls on the paired associates learning (PAL) task in both cohorts. In the historical cohort (Figure 5.2A) there was a significant effect of group on the PAL ($F(2)=4.837$, $p=0.016$) which was driven by a significantly greater number of errors in the PTA+ group compared to healthy controls ($t(26)=3.00$, $p=0.018$). In the new acute cohort (Figure 5.2B) there was a significant effect of group on the maximum score achieved ($F(2)=15.01$, $p<0.001$) which was driven by both PTA+ ($t(11)=5.46$, $p<0.001$) and PTA- ($t(11)=-2.49$, $p=0.045$) showing reduced performance compared to healthy controls.

In the historical cohort there was a significant group effect on strategy search in visual working memory ($F(2)=6.48$, $p=0.006$; Figure 5.2C) which was driven by both PTA+ ($t(23)=2.38$, $p=0.038$) and PTA- ($t(23)=3.28$, $p=0.010$) patients making significantly more errors compared to healthy

control. There was no significant group effect in the new acute cohort on the performance on the self-ordered search task, but the PTA group did show a trend towards a reduced score in line with results from the larger cohort (Figure 5.2D).

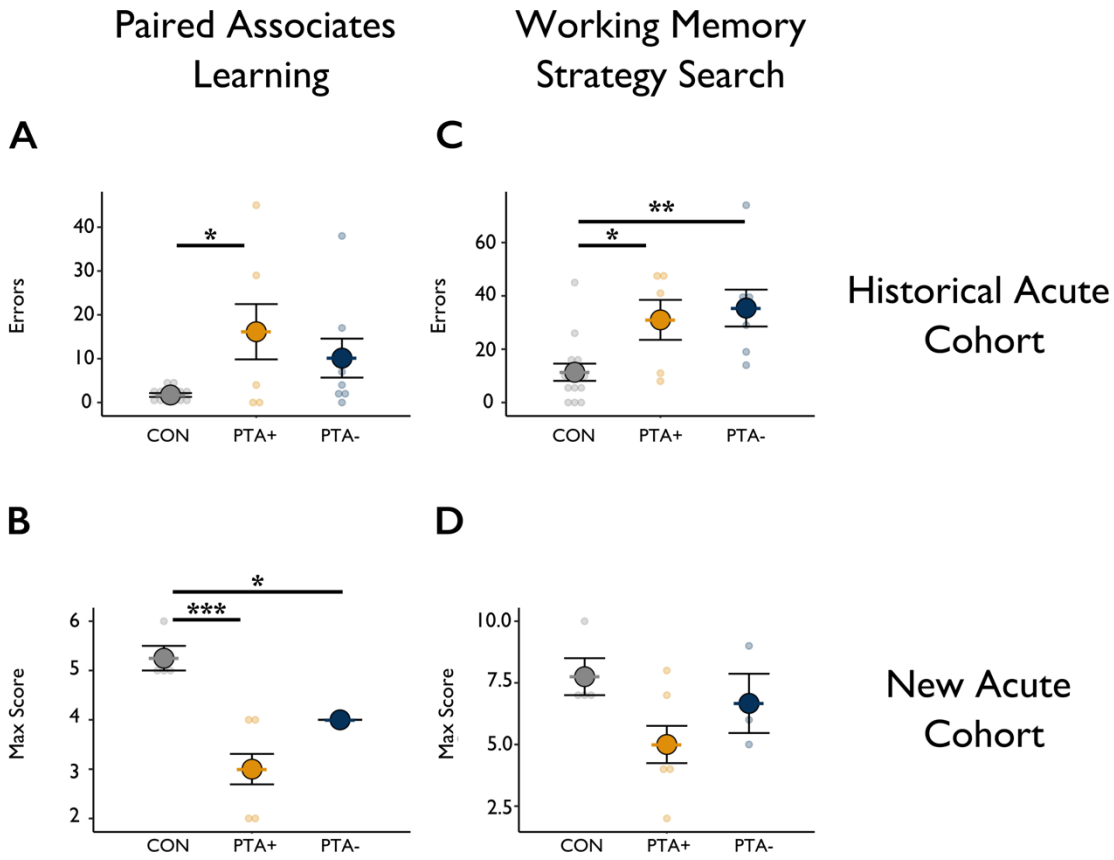

Figure 5.2 Cognitive performance in the acute and historical cohorts

Paired associates learning task from **A|** the CANTAB battery in the historical acute cohort and **B|** the computerised battery in the new acute cohort. **C|** Working memory strategy search measured by the spatial working memory task from the CANTAB battery in the historical acute cohort and **D|** from the self-ordered search task in the new acute cohort.

5.3.3 Static functional connectivity

Functional connectivity between core nodes of the DMN and MTL subsystem (Figure 5.3A) did not differ across groups ($F(2)=1.62$, $p=0.208$). To assess connectivity between DMN and SN, functional connectivity between the dorsal PCC and right aINS were extracted (Figure 5.3B), which revealed a trend towards an effect of group ($F(2)=3.05$, $p=0.057$) in the direction of reduced connectivity in patients compared to controls.

To assess the degree of anti-correlation between the DMN and FPN at the whole network level, time courses from the networks were compared and a single correlation-coefficient for each subject derived. There were no statistically significant group differences in the average correlation-coefficient between groups, however this was a negative value for controls and PTA-ve patients, thus showing an anticorrelation between DMN and FPN, whereas the PTA+ group showed a positive correlation (Figure 5.3C).

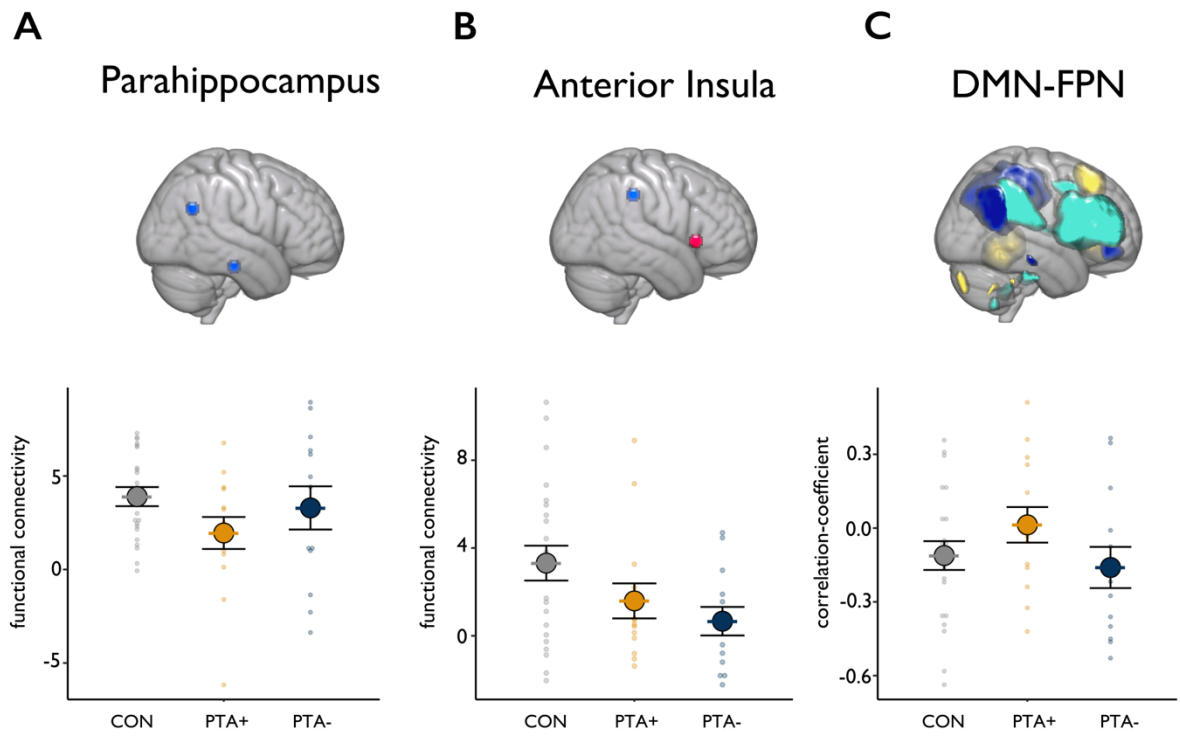

Figure 5.3 Static functional DMN connectivity

Functional connectivity **A|** within the DMN, between the vPCC and PHG **B|** between DMN and SN, using the dPCC and aINS as seed regions and **C|** whole network anti-correlation between DMN and FPN

5.3.4 Dynamic functional connectivity

To assess the temporal properties of functional connectivity across the baseline scans BOLD signal from ROIs representative of core cognitive resting state networks was derived. A sliding window approach to estimate connectivity between those ROIs at different timepoints resulted in 195 matrices per subject. These matrices were subjected to a k-means clustering approach which grouped them into a series of states. Using the elbow method, I identified four separate states, which are arranged in order of emergence in accordance with the k-means algorithm (Figure 5.4).

The first state accounted for 52% of the functional connectivity windows and appears to be an undifferentiated state. State 2 and State 4, accounting for 17% and 16% of windows respectively, are anticorrelation states. This is most pronounced in State 2 which represents the anticorrelation between DMN and cognitive control areas in SN, and bilateral FPNs. In State 4, the anticorrelation between DMN and right FPN and to a lesser degree SN is present but accompanies a positive correlation between DMN and left FPN. Correlations within right and left parahippocampal gyri (PHG) are notably weaker in this state. State 3, accounts for 15% of windows, shows strong correlation between right and left FPNs, SN and parts of the DMN excluding PHG and vmPFC bilaterally that show a weak negative correlation.

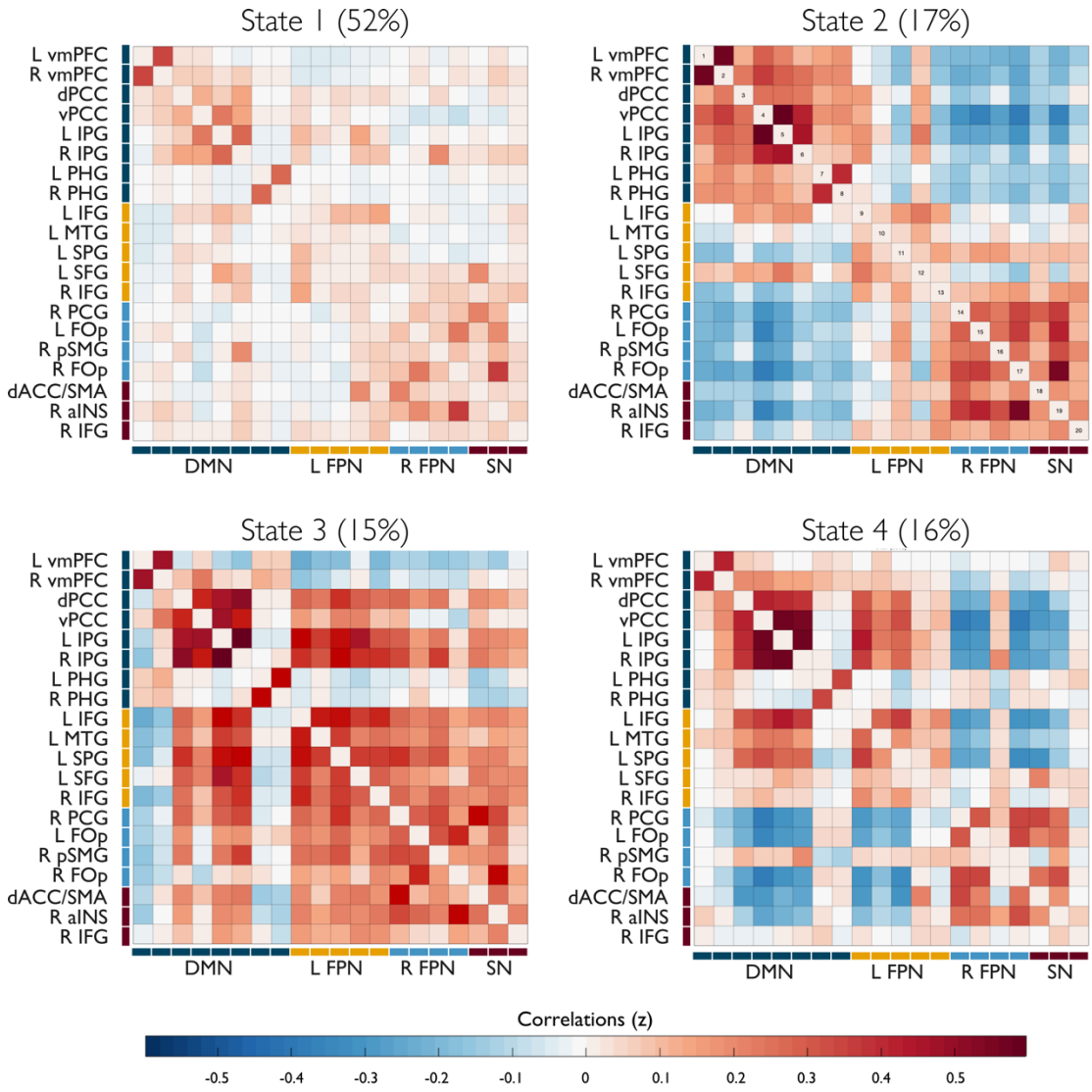

Figure 5.4 Dynamic functional connectivity states

The four dynamic functional connectivity states presented in their order of emergence from the k-means clustering. Blue represents a negative correlation and red represents a positive correlation between regions of interest.

5.3.5 State transitions

To assess how long was spent in each state in total and how long subjects spent in each state I calculated the fraction time and dwell time for every subject. There were no significant differences between groups in measures of fraction time for any of the states (Figure 5.5A). State 1 ($F(2)=0.08$, $p=0.923$) and State 3 ($F(2)=0.26$, $p=0.769$) showed very little variability between groups. Visual observation of the plots does suggest that TBI patients (both PTA+ and PTA-) spend less time in State 2 and more time in State 4 than controls but there was no effect of group for either state (State 2: $F(2)=2.20$, $p=0.123$; State 4: $F(2)=1.43$, $p=0.249$). There was also no effect of group on dwell time in any of the states (Figure 5.5B; State 1: $F(2)=0.06$,$p=0.946$; State 2: $F(2)=2.10$, $p=0.134$; State 3: $F(2)=0.67$, $p=0.517$; State 4: $F(2)=1.52$, $p=0.231$).

The number of transitions between states also did not differ between groups (Figure 5.5C; $F(2)=0.22$, $p=0.801$). This was quantified by calculating the entropy of the stationary distribution, a measure that describes the probability distribution (of transitions) over time (Figure 5.5D). There were no significant differences in entropy between groups ($F(2)=0.98$, $p=0.364$). However, there was a significant positive correlation within the PTA+ group between the entropy of the stationary distribution and WPTAS score ($R=0.58$, $p=0.03$) suggesting that the more profound a patients' amnesia, the less able they are to transition between states (Figure 5.5F).

5.3.6 Motion analyses

Motion analysis of the raw data revealed that TBI patients moved more than healthy controls during the scan ($F(2)=5.50$, $p=0.007$) which was driven by a greater mean framewise displacement in both PTA+ ($t(46)=2.83$, $p=0.016$) and PTA- ($t(46)=2.67$, $p=0.016$) compared to controls. In order to account for this, data were thoroughly 'denoised' (see Chapter 2, section 2.5.3) including using ICA-AROMA to guide removal of noise components. The proportion of components removed did not differ between groups ($F(2, 46)=2.12$, $p=0131$), with 60% of components being removed on average across all subjects (PTA+= 63%, PTA- =64%, Controls = 57%).

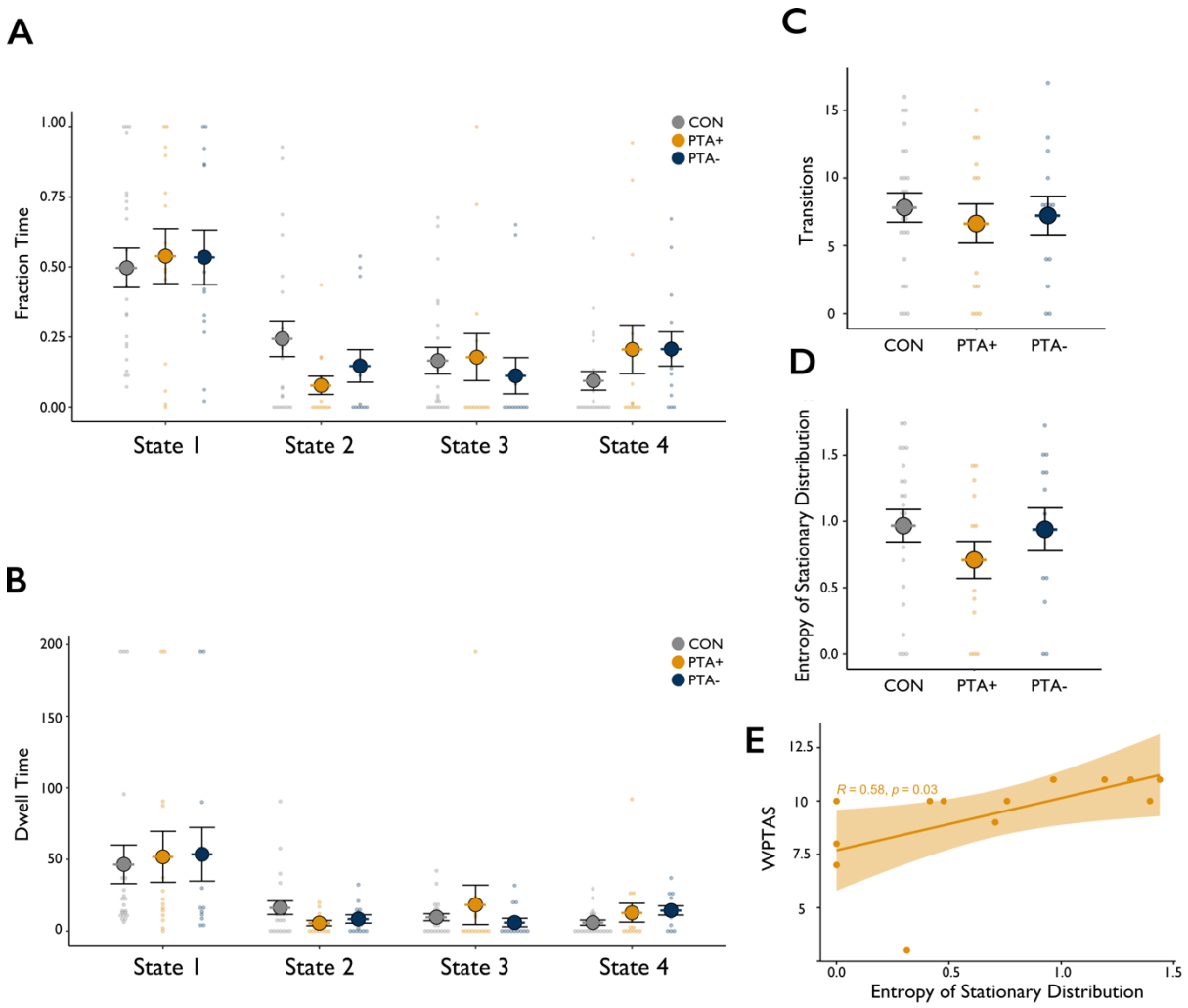

Figure 5.5 Temporal characteristics of dynamic functional connectivity states

The temporal characteristics of the four dynamic functional connectivity states. **A|** Fraction time, the total proportion of the scan time that was spent in each of the four states presented for controls, PTA+ and PTA- patients. **B|** Dwell time, the time spent in each state before transitioning to another state. **C|** Number of transitions made from any state to any state **D|** the entropy of the stationary distribution of the Markov chain representing the likelihood of transitions across states. **E|** the relationship between entropy of the stationary distribution and the WPTAS in PTA+ patients.

5.4 DISCUSSION

Network dysfunction affecting communication within and between the DMN and core cognitive control networks is a common consequence of TBI which produces persistent cognitive deficits (Jilka *et al.*, 2014; Sharp *et al.*, 2011; Bonnelle *et al.*, 2012; Hillary *et al.*, 2011; Hayes, Bigler & Verfaellie, 2016). In this chapter I show for the first time that acute TBI patients experiencing a period of PTA spend more time in fewer states of functional connectivity between large-scale brain networks when they have more profound amnestic deficits. The data suggest that an acute period of PTA may be associated with abnormal communication within and between brain networks.

Dynamic functional connectivity analysis produced four independent brain states. The amount of movement between these states was associated with the degree of cognitive impairment in PTA+ patients, as reflected by the WPTAS. This finding would suggest that the less transitions made between brain states, the more profound the amnestic state. This is highly consistent with previous literature in psychiatric and neurological disease groups (Douw *et al.*, 2015; Liang *et al.*, 2020; Nguyen *et al.*, 2017) supporting the relationship between impaired cognition and less flexible brain dynamics.

The reasons for spending more time in fewer different brain states is likely due to disrupted communication between core nodes of the DMN and cognitive control networks. Though the specific region of interest hypotheses tested here were inconclusive at the group level, these results show a trend towards decreased functional connectivity between the dorsal PCC and the aINS in patients compared to controls. Connections between the dorsal PCC and the aINS are important for communication between and appropriate activation of the DMN and SN (Sridharan, Levitin & Menon, 2008; Goulden *et al.*, 2014; Leech & Sharp, 2014). The aINS is important in the regulation of transitions between different brain networks (Huang *et al.*, 2021) so altered connectivity here is likely to impair cross-network communications required for higher order cognition.

The four states demonstrate that striking anti-correlation between large-scale brain networks is present for transient periods at rest. State 2 represents the anti-correlation between the DMN and cognitive control networks. In this state the right and left FPNs and the SN show strong correlations, and strong anti-correlations with nodes of the DMN. Although no significant differences were found between groups, visual observation of the plots of fraction time demonstrate that PTA+ show a trend towards spending less time in the anti-correlation state than PTA- and healthy controls. Previous work has shown that moderate-severe acute TBI patients with reduced consciousness fail to show the anti-correlation between DMN and cognitive control networks, but these do re-emerge in those patients that go on to regain consciousness (Threlkeld *et al.*, 2018). The time spent in an anti-correlated state during the acute stages of recovery may therefore serve as a useful prognostic marker of emergence from PTA and cognitive recovery.

In health, the DMN and FPN show a strong anti-correlation that is important in the modulation of goal-directed cognition (Kelly *et al.*, 2008; Spreng *et al.*, 2010; Anticevic *et al.*, 2012). The present results, even in healthy controls contain a lot of variability both in the time spent in an anti-correlated state and in the strength of anti-correlation in the static functional connectivity analysis. This is consistent with other literature that shows the strength of the negative relationship between the DMN, and cognitive control networks varies a lot between individuals. Within an individual, the strength of connectivity as well as the direction (positive vs negative) is extremely variable over time (Chang & Glover, 2010; Kiviniemi *et al.*, 2011). Individual differences in the strength of the negative correlation are also associated with intra-individual variability in goal-directed behaviour (Kelly *et al.*, 2008). It is therefore possible that the degree of anti-correlation seen here is reflective of individual differences in cognition that we are not able to test for within the current data set.

Another possible reason for the large individual variability, even amongst healthy subjects, in the degree to which the DMN and cognitive control networks are anti-correlated, is the participants state of mind during the scan. During the scan participants were instructed to relax and keep their eyes open, though no verification of this was employed. There is evidence that functional connectivity between networks is significantly modulated by whether eyes are open or closed

during resting-state (Patriat *et al.*, 2013; Agcaoglu *et al.*, 2020) and that task condition may impact the proportion of time spent in different network configurations (Agcaoglu *et al.*, 2020). It is therefore possible that some participants closed their eyes for all or part of the scan and may therefore have been inclined towards a less aroused state or more mind wandering than those with eyes open.

State 4, like State 2, shows an anti-correlation between DMN and cognitive controls networks, however this is absent in the left FPN, and PHG connectivity is notably weaker, which is not present in State 2. Heterogeneity within the FPN has been shown previously and it has been proposed that it is composed of two distinct subnetworks one which correlates with the dynamics of the DMN, and one which is anti-correlated (Dixon *et al.*, 2018; Murphy *et al.*, 2020). While the distinctions previously made had not been as simple as left and right as seen in state 4 here, the present results would suggest the FPN may show fractionated dynamic fluctuations in connectivity. Dynamic functional connectivity of the FPN has previously been negatively associated with working memory capacity and accuracy (Zhu *et al.*, 2021). In Chapter 3, I show that binding in working memory is significantly impaired in these acute TBI patients. The fraction time in State 4 for both patient groups does appear to be longer than controls, though there was no significant effect of group. Taken together with evidence of a dynamically fractionated network, this could suggest that abnormal coherence across the FPN disrupts working memory function.

States 3 and 4 both demonstrate a pattern of dysconnectivity in PHG bilaterally. Healthy brain function usually demonstrates strong connectivity between the DMN and the MTL subregion, which is thought to be mediated by the PHG (Ward *et al.*, 2014). In state 3 this in the context of a strong correlation across all networks except for PHG and vmPFC. The vmPFC is a key node of the DMN and is involved, alongside the PCC, in the modulation of the cognitive control networks (Uddin *et al.*, 2009). The PHG is involved in mediating the connectivity between DMN and MTL subsystem (Ward *et al.*, 2014). Lack of correlation between these nodes and other regions in the presence of high between-network connectivity may suggest a breakdown in communication required to facilitate the anti-correlation between DMN and cognitive control networks. Though not significantly so, the PTA+ group showed a tendency towards longer dwell

time in this state which would suggest it may be a sub-optimal arrangement for supporting memory function.

State 1 shows weaker and less specific network correlations and anti-correlations. This could be interpreted to represent a loss of network coherency in patients. However, TBI patients generally show intact functional networks, and this would not explain why healthy controls spent time in this state. It is therefore more likely that State 1 represents an average set of smaller states. The regions of interest chosen are regions relevant to higher order cognitive processes and State 1 is therefore likely the result of states involving other brain regions that, given their low frequency were not able to be separated out.

There were some subjects, across all groups, that did not enter certain states at all. There are several reasons this might have occurred. It is possible that due to dysfunctional communication between key nodes of networks these states of functional connectivity configurations were not available to them, though this is unlikely to explain the lack of transitions to a state in the healthy control population. An alternative possibility is that the seeds used were not sensitive to detecting sufficient signal to be recognised as a specific configuration. The ROI spheres used here were 5mm in size which leaves little room for error in between-subject variation in peaks of activity. It is therefore possible that sampling from a larger number of voxels would improve the power to detect effects at the group level, albeit sacrificing some spatial precision.

5.4.1 Limitations

The data presented in this chapter provide a promising avenue of research for understanding how functional network dynamics are affected in PTA. Nevertheless, there are several shortcomings which should be considered in the interpretation of the current results, and considerations for future work. Many of the results presented in this chapter showed a trend towards group differences and may simply be underpowered to detect an effect (see Chapter 7, section 7.2.1.1, for general discussion regarding recruitment challenges). Future work should expand on this with a larger sample size to clarify whether altered temporal dynamics in resting state fMRI are contributing to the clinical presentation seen in PTA.

A significant weakness of the experimental design presented in this chapter is the lack of cognitive data common across both the new and historical acute cohorts included in this analysis. Due to the difficulties in recruiting patients and acquiring data in an inpatient setting, the decision to combine the cohorts to improve sample size was taken. This meant however that there were no common cognitive tasks across the group, other than the clinical WPTAS. Having a rich, cognitive description of the cohort would have allowed more specific hypothesis testing regarding the relationship between cognitive deficits and temporal dynamics. This would have been especially valuable considering the previous literature suggesting the relationship between deficits in cognition and state transitions in disease groups (Douw *et al.*, 2015; van Geest *et al.*, 2018; Liang *et al.*, 2020; Nguyen *et al.*, 2017; Díez-Cirarda *et al.*, 2018). Nevertheless, a diagnosis of PTA, or the lack thereof, is in and of itself a description of cognitive ability that was available for all patients across both cohorts. By examining dynamic functional connectivity in this acute TBI cohort, the data presented in this chapter have provided novel insight into the relationship between profound mnemonic deficit and the ability to transition between different brain states.

In terms of potential confounds, the PTA+ patients were slightly older than controls, and the effect of age on dynamic functional connectivity should therefore be considered. Age has previously been related to decreases in between-network anti-correlations (Zonneveld *et al.*, 2019), suggesting that we might expect to see a weaker anti-correlation in the PTA+ group driven by an effect of age rather than diagnosis. Although no significant results are reported here with regards to the strength of the anti-correlation nor the time spent in the anti-correlation state, it should be noted that there was no relationship between age and the DMN-FPN correlation ($R=0.13$, $p=0.37$), nor the fraction time in State 2 ($R=-0.15$, $p=0.29$). I do not therefore believe that the difference in age across groups should change the interpretation of the data presented here.

As with any functional imaging study, subject movement has the potential to create spurious results. There was more movement in the raw data in both patient groups compared to controls, however the framewise displacement values used to assess this are derived from the raw data and therefore do not reflect the data subjected to the sliding window analysis. Several steps were taken during pre-processing to ensure that physiological motion artefact was accounted for during data analysis. These included regressing out 24 motion parameters from the data and

decomposing the data to eliminate components largely consisting of noise artefact. Motion should therefore not have had an impact be on the results presented in this chapter, though cautious interpretation is warranted.

5.4.2 Future Directions

An interesting future direction to expand on the work detailed in this chapter would be to use a longitudinal design to assess the prognostic value of acute dynamic functional connectivity and how this might inform cognitive outcomes. The finding presented in this chapter that state transition flexibility was associated with a more profound PTA suggests that repeated assessment of patients as they emerge from PTA may be useful prognostically. It has previously been shown in an acute mild to moderate TBI cohort that abnormalities in brain dynamics during the acute period became more marked over the proceeding months and this was associated with worse recovery (van der Horn *et al.*, 2020). Given the transient nature of PTA, an understanding of which abnormalities persist versus those that are associated with acute mnemonic impairment would clarify the contribution of dynamics between large scale brain networks in this poorly understood clinical syndrome.

Another interesting future direction would be to study the temporal dynamics of functional connectivity associated with the profound misbinding errors characterized in Chapter 3. PTA+ patients show a transient inability to integrate item and location information (Chapter 3) which is associated with a global shift towards slower oscillatory power as measured by EEG (Chapter 4). This could be achieved by asking participants to complete the precision working memory task during fMRI and applying the same sliding-window approach as utilized in this chapter to characterise functional connectivity states associated with correctly and incorrectly encoded trials. This would of course be extremely challenging in an acute clinical population but may be very fruitful from the perspectives of clinical and cognitive neuroscience. Understanding how these abnormalities are underpinned by cortical communication between large scale functional brain networks during attempts to bind information in working memory would provide a rich insight into the mechanisms supporting mnemonic function and how their failings contribute to PTA.

5.4.3 Conclusion

The data presented in this chapter has characterised four brain states associated with different configurations of connectivity between key nodes of large-scale networks. Acute TBI patients in a period of PTA show a more profound amnestic syndrome in association with abnormal transitioning between brain states. Abnormalities in specific network configurations may contribute to the mnemonic deficits seen during this period.

6

Network dysfunction in chronic TBI

In this chapter I consider how functional and structural networks are disrupted in TBI patients with enduring memory deficits in the chronic stages of recovery. I examine i) whether impairments in memory encoding are associated with abnormal brain activation in key functional networks, ii) whether changes in this brain activity predicts subsequent memory retrieval and iii) whether abnormal white matter integrity underpinning functional networks is associated with memory impairments.

6.1 INTRODUCTION

Memory impairments are among the most common and disabling consequences of traumatic brain injury (TBI; Vakil, 2005). Compared to other cognitive functions, deficits in memory are slower to recover (Lezak, 1979) though improvements during recovery are widely variable across patients (Chu *et al.*, 2007; Marsh, 2018). The degree of memory impairment can therefore vary substantially within a chronic TBI cohort (Vakil *et al.*, 2019; Chiou, Sandry & Chiaravalloti, 2015).

Functional networks underlying memory processes rely on structural connections provided by white matter microstructure that are vulnerable to traumatic damage. TBI patients show widespread abnormalities in white matter integrity (Wallace, Mathias & Ward, 2018b, 2018a) indicative of damage to structural connections. Owing to these structural disturbances arising from diffuse axonal injury (DAI), communication within and between brain networks involved in memory function is disrupted after TBI (Sharp *et al.*, 2011; Bonnelle *et al.*, 2012; Jilka *et al.*, 2014; Hayes, Bigler & Verfaellie, 2016; Yan, Feng & Wang, 2016). Reduced structural integrity of the fornix correlates with associative learning and memory performance (Kinnunen *et al.*, 2011) in both TBI patients and controls. Structural differences in white matter microstructure have also been associated with heterogeneity of episodic memory in TBI (Chiou, Genova & Chiaravalloti, 2016). Disruption to structural integrity of the white matter microstructure may thus impair functional networks required for successful encoding.

The subsequent memory (SM) paradigm, in combination with fMRI, can be used to investigate the function of the memory system. Specifically, this paradigm can offer insight into the neural activity associated with the encoding phase of memory by comparing functional activation during the encoding of events that were later remembered with those that were later forgotten. Over 100 studies have utilised this method in healthy adults (Uncapher & Wagner, 2009; Kim, 2011). Meta-analyses using the SM paradigm have identified activation of regions in the dorsal attention network (DAN), including inferior frontal junction, medial intraparietal sulcus (IPS), middle temporal area and inferior temporal cortex to indicate successful encoding (Kim, 2011, 2015). Conversely, activation of the default mode network (DMN) and regions including superior-frontal cortex, frontal pole, temporo-parietal junction, posterior cingulate cortex/precuneus, and

anterior cingulate cortex/ventromedial prefrontal cortex predict subsequently forgotten items (Kim, 2011; De Chastelaine *et al.*, 2015; Daselaar *et al.*, 2009).

Some studies have attributed episodic memory failures in TBI to be secondary to impaired attentional control, (Vakil *et al.*, 2019) which is in part supported by the functional imaging literature in this population. Changes in functional activation during encoding in TBI are relatively understudied with few studies examining whole-brain fMRI correlates of episodic encoding in this population. Those studies that have utilised a subsequent memory paradigm in a TBI population have found hyperactivation compared to healthy controls in lateral temporal lobes bilaterally, left medial temporal lobe (MTL), and left parietal lobe (Gillis & Hampstead, 2015), frontoparietal network (Arenth *et al.*, 2012) and subcortical regions (Russell *et al.*, 2011), though others have found no differences (Strangman *et al.*, 2008). These findings have been interpreted as compensatory activation drawing more heavily on other cognitive systems that support memory function (Russell *et al.*, 2011; Arenth *et al.*, 2012) however in the absence of behavioural differences between patients and controls, this is difficult to reconcile in the context of mnemonic deficits. Investigation of differences in functional activity between TBI patients with and without episodic memory impairment has not yet occurred. Assessing differences in activation patterns between TBI patient subsamples would provide a more detailed understanding of the neural basis underlying episodic memory deficits in this population.

In this experiment I therefore aimed to provide a more detailed understating of the neural basis underlying episodic memory deficits in a chronic TBI population. To do this, I investigated memory network function in chronic TBI patients with and without episodic memory impairment using a subsequent memory paradigm in conjunction with functional magnetic resonance imaging (fMRI). I examined the activation patterns during long-term memory encoding. I used diffusion tensor imaging (DTI) to investigate the white matter integrity of individual tracts and how these differed between TBI patients with and without memory impairment. I examined the structural connectome underpinning the functional networks associated with successful memory encoding,

Specifically, I test the following hypotheses: i) TBI patients with impaired SM will show altered functional activation during encoding compared to TBI patients with normal SM; ii) these

changes will be apparent within the DAN and DMN iii) DTI measures of white matter integrity will be associated with SM impairment.

6.2 METHODS

6.2.1 Patient group and clinical details

48 TBI patients were recruited into the study. Thirteen were excluded following motion analysis (see Chapter 2). Therefore 35 patients were included in the imaging analysis (9 females, mean age=43.20±11.20; range=23-65 years). All patients were in the post-acute/chronic phase after injury (mean months since injury=126.78±158.88, range=3–436 months). Injuries were secondary to road traffic accidents (54%), falls (23%), military blast (11%), assault (6%) and sports injuries (6%). Patients were recruited from specialist TBI clinics and military rehabilitation units. All patients had moderate-severe injuries according to the Mayo classification system (Malec *et al.*, 2007; see Chapter 2 section 2.3.1). Exclusion criteria and consent procedures are detailed in Chapter 2.

6.2.2 Control group

16 healthy controls (6 females, mean age=38.19±11.99 years) were included in the SM imaging analysis. An independent control group (n=28) were used for the DTI analysis (9 females, mean age=37.01±5.32 years). Controls were recruited through the National Institute for Health Research (NIHR) Imperial Clinical Research Facility, London, UK, and family members of patients. Exclusion criteria for controls were the same as for patients.

6.2.3 Neuropsychology assessment

A detailed neuropsychological battery using standardised pen and paper tests was used to assess cognitive function in all participants. Details of all cognitive assessments are given in Chapter 2.

6.2.4 Subsequent memory task

Participants viewed a series of abstract art images while in the scanner, which they were asked to commit to memory and told they would be later tested on (Figure 6.1 'Encoding'). Images were

presented for four seconds in blocks of six, with a fixation of one second between each image and 20 seconds between each block. A total of nine blocks consisting of 54 different images in total (6 unique images per block) were shown. No images were repeated. No response was required from participants during the scan. The experimental paradigm was programmed using MATLAB Psychophysics toolbox (Kleiner *et al.*, 2007) and stimuli were presented in the scanner through an IFIS-SA system. The fMRI scan was followed by further structural acquisition lasting for 15 minutes after which SM for the abstract art images was tested immediately upon exit from the scanner. Participants were shown 108 images (54 previously seen, 54 novel) and asked to indicate using a keyboard press (yes/no) whether they previously saw the image (Figure 6.1 'Recognition'). Accuracy was determined using the sensitivity index (d'), a measure taken from signal detection theory which represents the probabilities of responses being a 'true hit' rather than a 'false positive'. A higher score represents greater discrimination between previously seen (remembered) and novel items during the post-scanner recognition test, thus accounting for potential response bias.

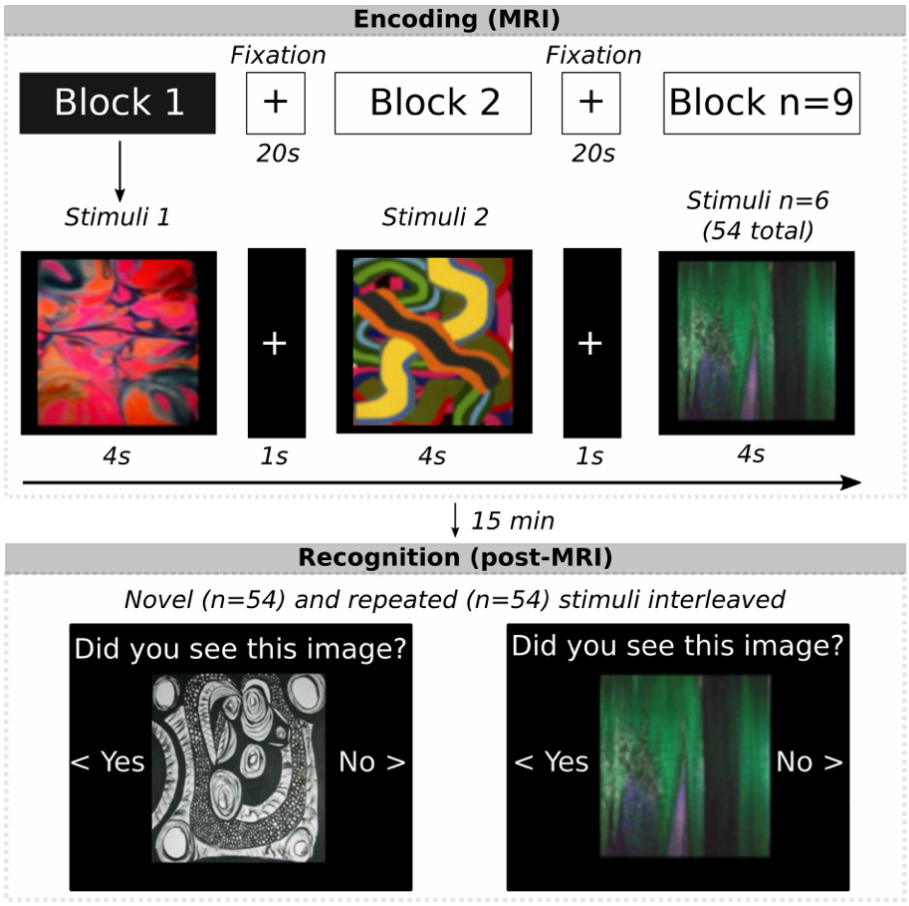

Figure 6.1 The subsequent memory task paradigm

The subsequent memory task consisted of an in-scanner encoding phase (top) and a post-scanner recognition phase (bottom). During encoding, participants viewed a 54 abstract art images which they had been asked to try and remember. In the recognition task participants were shown 108 images (54 novel) and were asked if they remembered seeing the image.

6.2.5 Imaging analysis

Details of imaging acquisition parameters and pre-processing can be found in Chapter 2. In addition to the steps taken in Chapter 2, fMRI scans were excluded if movement exceeded 3mm for any volume or if >15% of volumes exceeded an FD of 0.5 to further minimise any effect of motion on the data (De Simoni *et al.*, 2018).

6.2.5.1.1 Functional imaging analysis

fMRI data were analysed using voxel-wise time-series analysis within the framework of the general linear model. A design matrix was generated with a synthetic haemodynamic response function and its first temporal derivative to account for the time lag between stimuli presentation and the measured response. To investigate the effect of SM impairments, brain activation was compared between successful and unsuccessful encoding trials at the subject-level by subtracting forgotten trials from remembered trials. The resulting lower-level contrast images were entered into independent samples t-tests at the higher-level. These between-groups contrasts were modelled with the demeaned age of each subject as a covariate. Clusters of contiguous voxels were defined using the default threshold of $z > 2.3$ in FSL, and resulting clusters were tested for significance using a cluster extent significance threshold of $p<0.05$. A 5mm sphere was constructed around the peak of the largest significant cluster of the higher-level effects and percentage in BOLD signal change was extracted from the voxels within these spheres.

6.2.5.1.2 Diffusion imaging analysis

Non-parametric permutation testing (n=10,000) with a threshold of $p<0.05$ was applied with age as a nuisance regressor to compare the skeletonised white matter between groups. Fractional anisotropy (FA) values were extracted for each subject (i) within individual tracts as defined by the JHU White Matter Tracts atlas (Mori *et al.*, 2005) as well as (ii) the cingulum from NatBrainLab (Catani & Thiebaut De Schotten, 2008) and (iii) the mean across the whole white matter skeleton. DTI data for patients were compared to an independent group of healthy controls matched for age at the group level. The effect of group, tract and their interaction on

FA was tested using a two-way ANOVA. One-way t-tests with false-discovery rate (FDR) multiple comparison corrections were used to compare between groups across tracts.

To better understand the relationship between the functional and structural imaging results, the white matter that specifically related to the task derived functional networks was targeted to create a structural connectome of the underlying white matter architecture (Figure 6.2). White matter networks were constructed to represent the structural connectivity underlying the functional networks produced by the task. Using the IIT Human Brain Atlas (Zhang & Arfanakis, 2018) FA was extracted for each of the track density (TDI) maps. These have been defined using tractography between all possible pairs of grey matter labels in the Desikan atlas (Desikan *et al.*, 2006), thus providing a white matter atlas of connectivity between cortical and subcortical regions of the brain. A 90x90 connectivity matrix of FA between each of the grey matter nodes was produced for each subject. Functional network activation maps, derived from the Correct-Incorrect contrast for regions of increased and decreased activation during successful encoding (Figure 6.2) were binarized at a 50% probability threshold and the two resulting network masks were separately intersected with the Desikan grey matter parcellation to reveal the nodes of each network. FA values between each of the nodes were extracted from the structural connectivity matrices to inform the degree of connectivity between each node. Mean FA underlying each network was extracted and compared across groups. The influence of age on the mean connectivity values for each network was assessed by comparing linear models with and without age as an interaction term which was found to be non-significant for both encoding activation and encoding deactivation networks. Network connectivity was compared between groups on a node-by-node basis using the network-based statistic in NBS v1.2 (Zalesky, Fornito & Bullmore, 2010) implemented in MATLAB to perform 10,000 random permutations at a threshold of 3.1

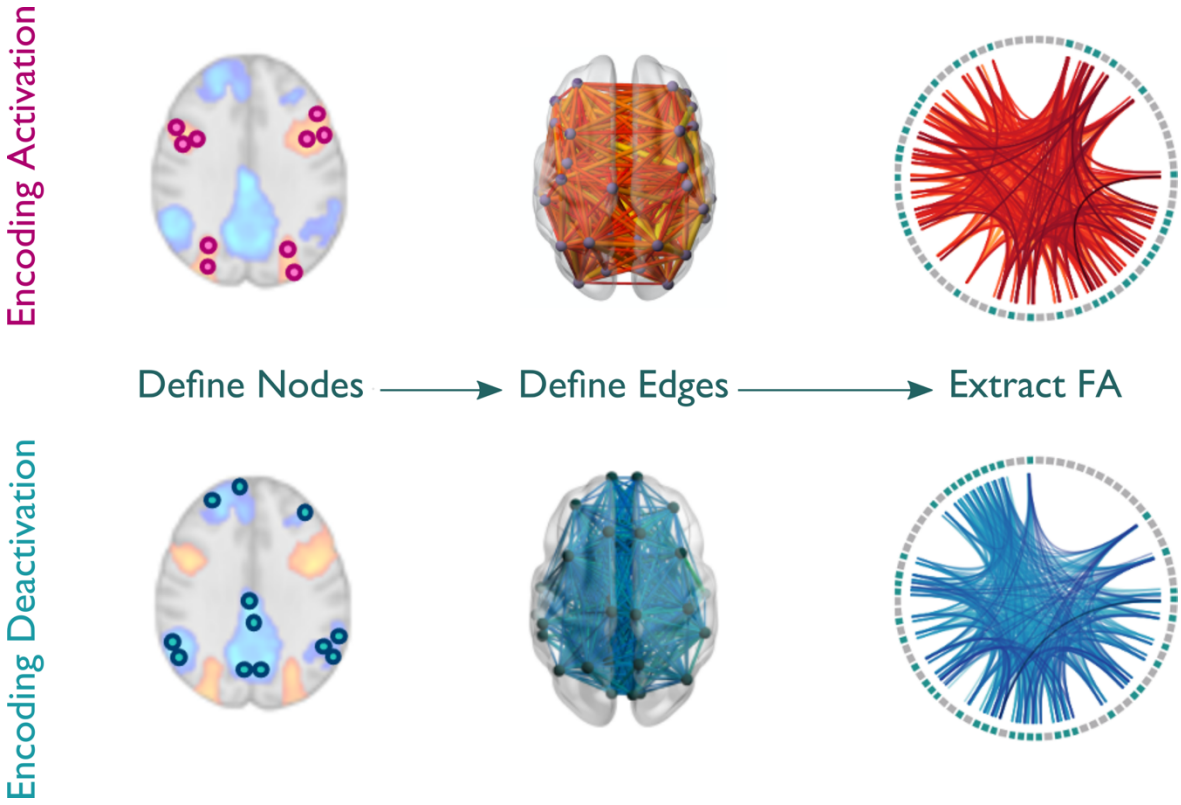

Figure 6.2 Defining the structural connectome underpinning task derived functional networks

The structural connectome underpinning the task derived functional networks during subsequent memory encoding. Grey matter nodes are defined in the regions with areas showing increased activation (top) and increased deactivation (bottom) during encoding. White matter edges are defined based on tractography connections between grey matter nodes. Fractional anisotropy (FA) is extracted from each white matter edge to form a structural network. Figure reproduced with permission from Mallas et al., *Brain*., 144 (1), 114–127 (2021).

6.2.6 Lesions

To ensure that chronic lesions were not driving results a subsidiary analysis to consider the effect of any lesions was implemented. Brain areas with focal lesions were masked using semi-automatic segmentation methods based upon an algorithm for geodesic image segmentation as described previously (Criminisi, Sharp & Blake, 2008) and implemented in IMSEG v1.8. FLAIR and T1-weighted images were co-registered and lesion maps were drawn as overlays on the T1-weighted images guided by overlapping FLAIR images to improve contrast for accuracy. Lesion overlay maps were produced to show the probability of lesions occurring at each voxel.

6.3 RESULTS

6.3.1 Patient classification and demographics

Healthy controls performed with 72.5% accuracy (± 8.8) and TBI patients with 64.9% (±10.5). Sensitivity index (d') scores were used to compare groups in order to account for response bias. TBI patients demonstrated significantly reduced SM ($t(33.1)=2.07$, $p=0.04$; mean d'=0.94±0.68) for abstract art images compared to controls (mean d'=1.33±0.59). There was high heterogeneity in memory performance (d') across the patient group (control range=27.8; TBI range=42.6). I divided patients into two groups based on a median split of d' scores. This produced two TBI groups with normal (NSM, n=18, mean accuracy=72.3%, mean d'=1.43(±0.59)) and impaired SM (ISM, n=17, mean accuracy=57.2%, mean d'=0.41(±0.26)). Compared to controls (CON), ISM patients were significantly impaired ($t(20.25)=5.66$, $p<0.001$) but NSM were not ($t(31.21)=-0.52$, $p=0.60$) in their SM performance (Figure 6.3).

Table 6.1 summarises demographic data across the three groups (CON, NSM, ISM). Detailed clinical information for each patient are included in (Supplementary Table 9.3). Groups did not differ significantly in terms of sex or age at assessment. There was a significant difference in years of education ($F(2,37)=4.95$, $p=0.01$) with the healthy control group being more educated than the ISM group ($p<0.01$). The patient groups did not differ in age at injury, years since injury, lesion volume, PTA duration or lowest recorded GCS.

Table 6.1 Demographics in the chronic TBI cohort

	CON n= 16		NSM n= 18		ISM n= 17		Statistic	*p*	Post-hoc group differences†
Sex	6F:10M		4F:14M		5F:12M		$X^2 = 0.95$	0.62	-
	Mean	*SD*	*Mean*	*SD*	*Mean*	*SD*			
Age	38.19	11.99	39.89	9.28	46.71	12.24	F = 2.72	0.08	-
Years of Education	18.21	3.87	16.08	2.84	13.77	4.15	F = 6.25	0.01	CON > ISM**
Age at Injury	-	-	33.39	11.64	31.71	14.7	t = 0.37	0.71	-
Time Since Injury (months)	-	-	80.12	104.03	176.18	192.61	t =-1.82	0.08	-
Lesion Volume (voxels)	-	-	14023	18513	24282	36578.66	t=-1.04	0.31	
PTA Duration (days)	-	-	14.6	23.87	22.69	36.89	t=-0.68	0.51	
Lowest GCS	-	-	6.15	4.91	7.22	4.35	t=-0.54	0.60	

** p < 0.01; †false discovery rate corrected for multiple comparisons; CON = Controls; ISM = impaired subsequent memory TBI patients; NSM = normal subsequent memory TBI patients

6.3.2 Neuropsychological performance

Widespread impairments of cognitive function were seen in ISM patients (Figure 6.3; Table 6.2). There were significant group effects across cognitive measures of intellectual ability ($F(2,47)=11.03$, $p<0.001$), processing speed ($F(2,47)=9.74$, $p<0.001$), executive function ($F(2,47)=6.33$,$p=0.004$), verbal memory (immediate: $F(2,26)=7.114$, $p=0.003$ and delayed: $F(2,26)=11.53$,$p<0.001$), associative memory (immediate: $F(2,47)=4.803$, $p=0.013$ and delayed: $F(2,47)=7.10$, $p=0.002$) and visuospatial memory (immediate: $F(2,26)=15.36$, $p<0.001$ and delayed: $F(2.26)=9.11$, $p=0.001$). There was no difference between groups in measures of premorbid intelligence ($F(2,26)=2.513$, $p=0.09$).

These group effects were driven primarily by impairments in the ISM group relative to controls. ISM patients showed impairments in intellectual ability ($p<0.001$), processing speed ($p<0.001$) executive function($p=0.005$), and verbal (immediate ($p=0.003$); delayed ($p=<0.001$)), associative (immediate ($p=0.017$); delayed ($p=0.004$)) and visuospatial memory (immediate ($p<0.001$); delayed ($p=0.001$)) compared to healthy controls. ISM patients were also impaired relative to NSM in intellectual ability ($p=0.005$), executive function ($p=0.011$), associative memory (immediate ($p=0.017$); delayed ($p=0.004$) and visuospatial memory (immediate ($p<0.001$); delayed ($p=0.006$). In contrast, NSM patients were impaired compared to controls only in processing speed ($p=0.003$).

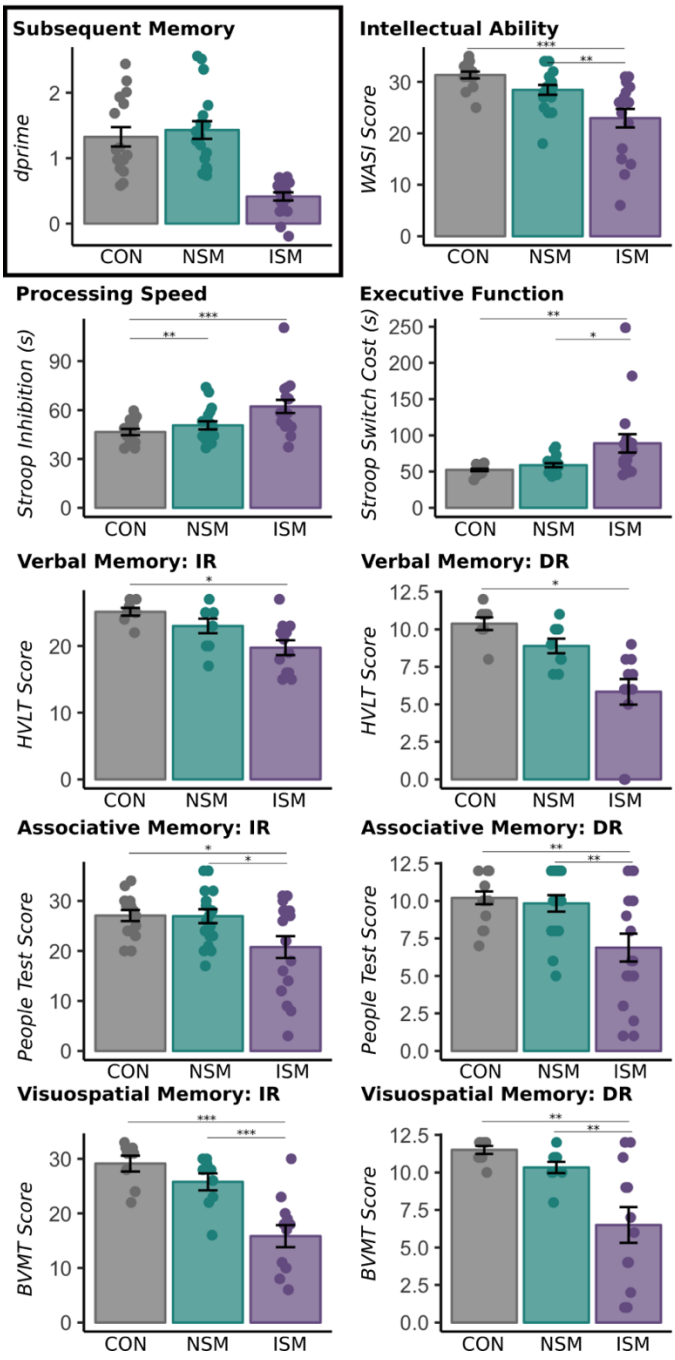

Figure 6.3 Subsequent memory and neuropsychological performance in the chronic TBI cohort

Subsequent memory performance on the post-scanner recognition task and standardized neuropsychological assessment in TBI patients split into normal subsequent memory (NSM) and impaired subsequent memory (ISM) groups, and healthy controls. *** $p < 0.001$; ** $p < 0.01$; * $p < 0.05$. Figure reproduced with permission from Mallas et al., *Brain*., 144 (1), 114–127 (2021).

Table 6.2 Neuropsychological performance in the chronic TBI cohort

Cognitive Domain	Assessment	CON Mean (± SD) *n* = 16	NSM Mean (± SD) *n* = 18	ISM Mean (± SD) *n* = 17	*F*	*p*	Post-hoc group differences†
Processing speed	Trail Making Test A (s)	20.11 (5.72)	22.51 (6.74)	38.86 (19.54)	10.99	< 0.001	ISM > CON*** ISM > NSM***
	Trail Making Test B (s)	45.47 (11.22)	55.69 (23.31)	85.02 (50.56)	6.18	0.004	ISM > CON** ISM > NSM*
	Stroop Colour Naming and Word Reading Composite Score (s)	31.65 (6.30)	40.85 (7.28)	44.01 (10.23)	9.74	< 0.001	ISM > CON*** NSM > CON**
Executive function	Trail Making Test B-A (s)	25.46 (9.18)	33.12 (20.05)	46.16 (35.96)	2.87	0.066	
	Stroop Inhibition (s)	46.52 (7.39)	50.61 (10.57)	62.19 (16.6)	7.19	0.002	ISM > CON** ISM > NSM*
	Stroop Inhibition-Switching (s)	52.34 (6.76)	58.89 (11.58)	88.91 (52.30)	6.33	0.004	ISM > CON** ISM > NSM*
	Stroop Inhibition-Switching versus Baseline Contrast (s)	25.29 (13.66)	20.18 (11.54)	46.79 (46.67)	4.04	0.024	ISM > NSM*
Intellectual ability	WTAR Scaled	112.53 (9.46)	106.44 (15.42)	100.38 (18.59)	2.51	0.092	
	WASI Matrix Reasoning	31.33 (2.55)	28.44 (4.08)	22.94 (7.43)	11.03	< 0.001	CON > ISM*** NSM > ISM**
Verbal memory	WMS-III LM Immediate Recall	48.77 (7.58)	44.35 (9.99)	37.2 (9.73)	4.48	0.012	CON > ISM*
	WMS-III LM Delayed Recall	31.23 (5.90)	28.81 (7.90)	23.50 (7.63)	3.32	0.048	CON > ISM*
	WMS-III LM Retention	89.55 (11.84)	91.68 (13.35)	84.18 (11.77)	1.13	0.335	
	WMS-III LM Recognition	28.69 (1.44)	27.06 (2.32)	24.7 (3.59)	7.32	0.002	CON > ISM** NSM >ISM*
	WMS-III LM Learning	5.00 (3.16)	3.94 (2.38)	4.80 (2.25)	0.68	0.512	
	HVLT-R Immediate Recall	25.12 (1.64)	23 (3.28)	19.75 (3.84)	7.11	0.003	CON > ISM** NSM > ISM*
	HVLT-R Delayed Recall	10.38 (1.19)	8.89 (1.45)	5.83 (2.95)	11.53	< 0.001	CON > ISM*** NSM > ISM**
	HVLT-R Recognition	10.75 (1.04)	10.67 (1.32)	9.00 (2.59)	2.79	0.080	
Associative Memory	People's Test Immediate Recall	27.07 (4.28)	26.94 (5.88)	20.76 (8.98)	4.80	0.013	NSM > ISM* CON > ISM*
	People's Test Delayed Recall	10.20 (1.66)	9.83 (2.33)	6.88 (3.82)	7.10	0.002	CON > ISM** NSM > ISM**
	People's Test Forgetting	1.53 (1.41)	1.61 (1.91)	2.71 (2.47)	1.80	0.177	
Visuospatial memory	BVMT-R Immediate Recall	29.12 (4.09)	25.78 (4.66)	15.83 (7.0)	15.36	< 0.001	CON > ISM*** NSM > ISM***
	BVMT-R Delayed Recall	11.50 (0.76)	10.33 (1.12)	6.50 (4.12)	9.11	<0.001	CON > ISM** NSM > ISM**
	BVMT-R Recognition	5.75 (0.46)	5.56 (0.88)	4.67 (1.97)	1.79	0.188	

* p < 0.05; ** p< 0.01; *** p < 0.001; † false discovery rate corrected for multiple comparisons; **BVMT-R** = Brief Visuospatial Memory Test-Revised; **CON** = controls; **HVLT-R** = Hopkins Verbal Learning Test-Revised; **ISM** = impaired subsequent memory TBI patients ; **NSM**= normal subsequent memory TBI patients; **SD** = standard deviation; **WASI** = Wechsler Abbreviated Scale for Intelligence; **WMS-III** = Wechsler Memory Scale, Third Edition; **WTAR** = Wechsler Test of Adult Reading

6.3.3 Successful encoding is associated with activation changes in the dorsal attention network and default mode network

Across all participants combined, successfully remembering items (remembered minus forgotten contrast) showed higher activation bilaterally in the inferior frontal gyrus, fusiform gyrus, superior parietal lobe, IPS, lateral occipital cortex, posterior parahippocampal gyrus (PHG) and left amygdala (shown in red-yellow in Figure 6.4A). These regions largely fall within the DAN and MTL. Decreased activation was seen during successfully remembered items in the posterior cingulate cortex, precuneus, medial prefrontal cortex, inferior parietal lobe, superior frontal gyrus, and right medial frontal gyrus (shown in blue-light blue, Figure 6.4A), regions largely falling within the DMN. These patterns of activation are also sustained in the TBI group alone (Supplementary Figure 9.2).

6.3.4 TBI patients with memory impairment show differential activation during successful encoding

When comparing activation patterns in TBI patients with and without episodic memory impairment, higher-level contrasts (*NSM>ISM* and *ISM>NSM*) revealed significant group differences during successful encoding (remembered minus forgotten). NSM showed greater activation than ISM in right precuneus, right IPS, left inferior temporal gyrus and bilaterally in the temporal-occiptial fusiform cortex, PHG and lingual gyrus (red-yellow in Figure 6.4B). All TBI patients combined did not show differential activation to controls in either direction.

In order to further explore how activation in this region related to healthy controls, and thus interpret this result in TBI patients, BOLD signal from the peak of the largest cluster (MNI:26,-80,44) of the *NSM>ISM* contrast was extracted. NSM showed a trend ($t(30.4)=-1.80$, $p=0.08$) towards greater activation than controls during successful encoding (Figure 6.4C) but did not differ during unsuccessful trials. Activation change did not differ between ISM TBI and controls during either successfully or unsuccessfully encoded trials in this region. Neither patient group demonstrated differential patterns of encoding compared to controls on a whole-brain voxel-wise level in either direction (i.e., *NSM >/< CON* and *ISM >/< CON* contrasts).

ISM patients showed significantly greater change in activation in left anterior prefrontal cortex spanning superior and middle frontal gyri compared to NSM during successful encoding (remembered minus forgotten; blue-light blue in Figure 6.4B). In the peak of this cluster (MNI:-34,52,18), ISM showed increased activation compared to controls ($t(30.5)= -2.05$, $p= 0.05$) during successfully encoded trials (Figure 6.4C). No difference was observed in these patients compared to controls in unsuccessful trials. NSM did not differ from controls in terms of BOLD activation in this cluster for either trial type. BOLD signal was not associated with motion, education, or time since injury in either the NSM > ISM or the ISM > NSM cluster.

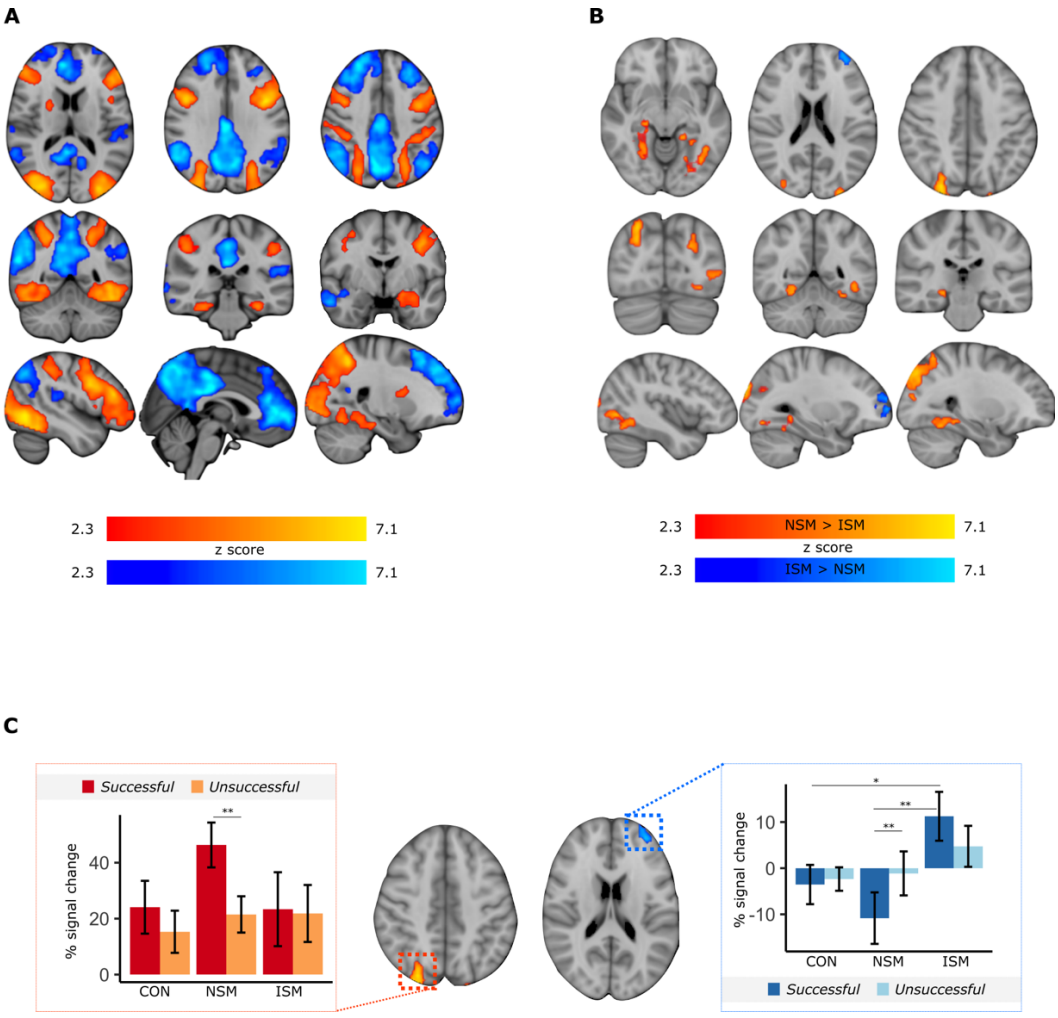

Figure 6.4 Changes in BOLD activity associated with performance on the subsequent memory task

A| All subjects. Voxels showing increased activation during successful encoding (remembered minus forgotten contrast) in red-yellow and decreased activation in blue-light blue. **B|** Contrasts between TBI patient groups. Voxels in which NSM patients showed greater increases in activation during successful encoding compared to ISM shown in red-yellow. Voxels in which ISM patients show greater decreases in activation during successful encoding compared to NSM patients shown in blue-light blue. **C|** Percentage change in BOLD signal across groups in successful and unsuccessful encoding in the peak of the NSM > ISM cluster (left) and the ISM > NSM cluster (right). All spatial results shown in standard space overlaid on MNI template with a Z-statistic threshold of 2.3. ISM = impaired subsequent memory; NSM = normal subsequent memory; CON = healthy controls. Figure reproduced with permission from Mallas et al., *Brain*., 144 (1), 114–127 (2021).

6.3.5 Patients with impaired subsequent memory show reduced white matter integrity

I then investigated whether differences in SM impairment amongst TBI patients were associated with underlying white matter abnormalities. Voxel-wise contrasts between groups on the skeletonised white matter revealed that TBI patients in the ISM group showed significantly reduced FA compared to the NSM group in tracts including the inferior fronto-occipital fasciculus, corticospinal tracts, fornix, and corpus callosum (Figure 6.5A). To provide a tract level description of the data I extracted mean FA from the body, genu, and splenium of the corpus callosum, and bilaterally from the cingulum, corticospinal tract, inferior fronto-occipital fasciculus, and inferior and superior longitudinal fasciculi (Figure 6.5B). These six white matter tracts were selected as they are large enough to allow for robust sampling and less vulnerable to partial volume effects than smaller tracts. There were significant differences in FA across group ($F(2)=120.98$, $p<0.0001$) and tract ($F(12)=179.09$, $p<0.0001$). There was no interaction effect between group and tract ($p=0.09$). Mean whole-brain FA was significantly reduced in ISM compared to NSM ($p=0.04$). Both patient groups independently demonstrated significantly reduced mean whole-brain FA compared to controls ($p=0.001$).

Next, the structural connectivity within the memory network modulated by memory encoding was investigated. In the white matter in networks derived from activated and deactivated memory networks (Encoding activation/Encoding deactivation) during successful encoding, ISM patients showed significantly reduced structural connectivity (Encoding activation: $F(1)=6.05$, $p=0.01$; Encoding deactivation: $F(1)=6.73$, $p=0.01$) on average across the whole network compared to NSM patients (Figure 6.6). The effect of age and its potential interaction with group assessed and there was no significant effect of age on FA in either network (Encoding activation($F(1)=1.61$, $p=0.21$; Encoding deactivation: $F(1)=2.51$, $p=0.12$), nor any interaction between group and age in the Encoding activation($F=0.864$, $p=0.361$) or Encoding deactivation ($F=1.25$, $p=0.272$) networks.

ISM showed reduced FA in white matter underpinning the structural connectivity between right pericalcarine cortex and left insula ($p=0.032$, $z=3.49$) derived from the Encoding activation network, compared to NSM. In the encoding deactivation network ($p=0.034$), structural connectivity was reduced between right accumbens area and right supramarginal gyrus ($z=3.11$),

left caudal middle frontal gyrus and left superior frontal gyrus (z= 3.18) and left precuneus and left rostral middle frontal gyrus (z=3.98) in ISM compared to NSM (Figure 6.6).

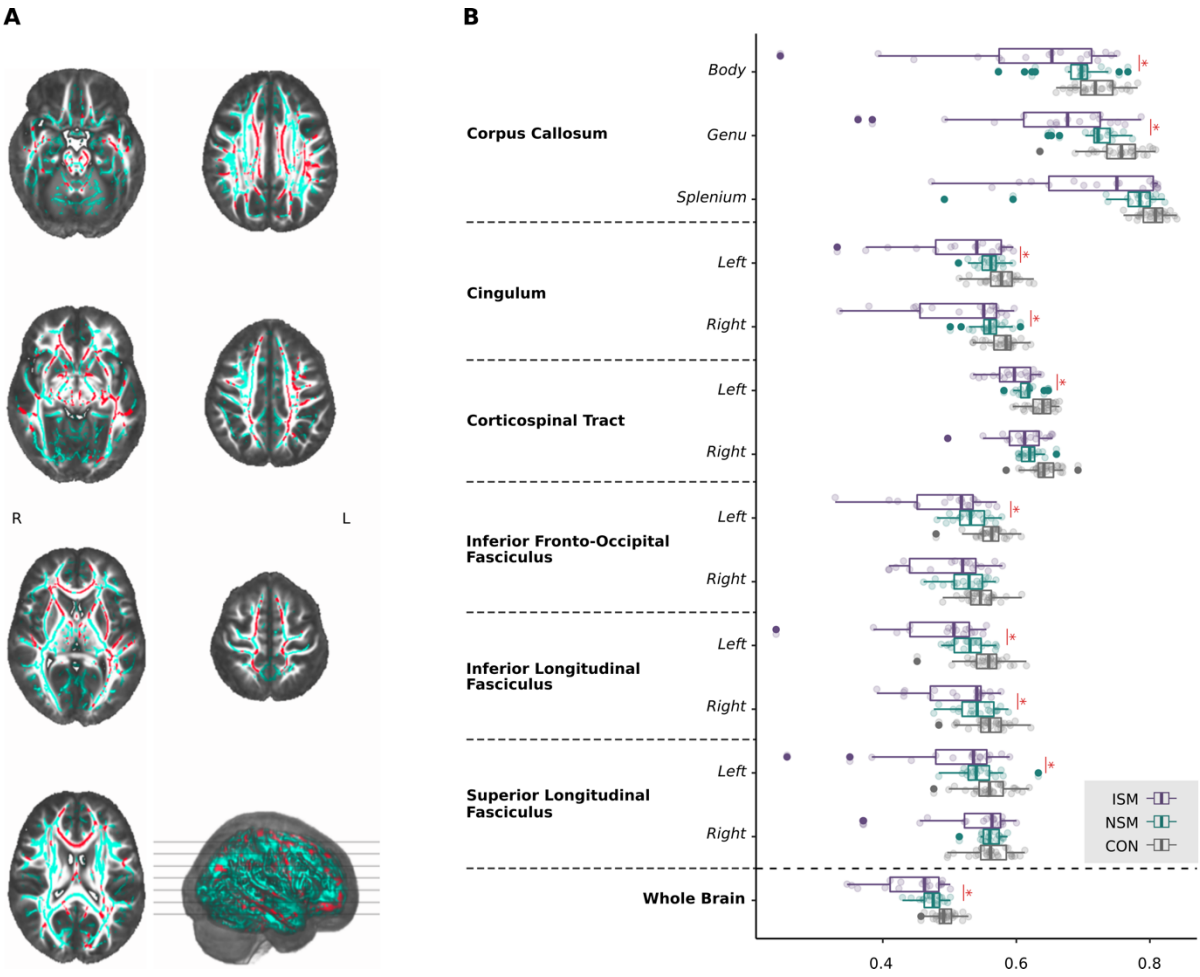

Figure 6.5 Fractional anisotropy across the whole brain in TBI patients with and without memory impairment

A| TBI patients with subsequent memory impairment showed significantly reduced FA (shown in red) compared to TBI patients with normal subsequent memory. TFCE corrected results ($p < 0.05$) shown overlaid on the mean FA skeleton (cyan). **B|** Mean FA across individual white matter tracts and whole brain for each group. ISM = impaired subsequent memory; NSM = normal subsequent memory; CON = healthy controls. Figure reproduced with permission from Mallas et al., *Brain.*, 144 (1), 114–127 (2021).

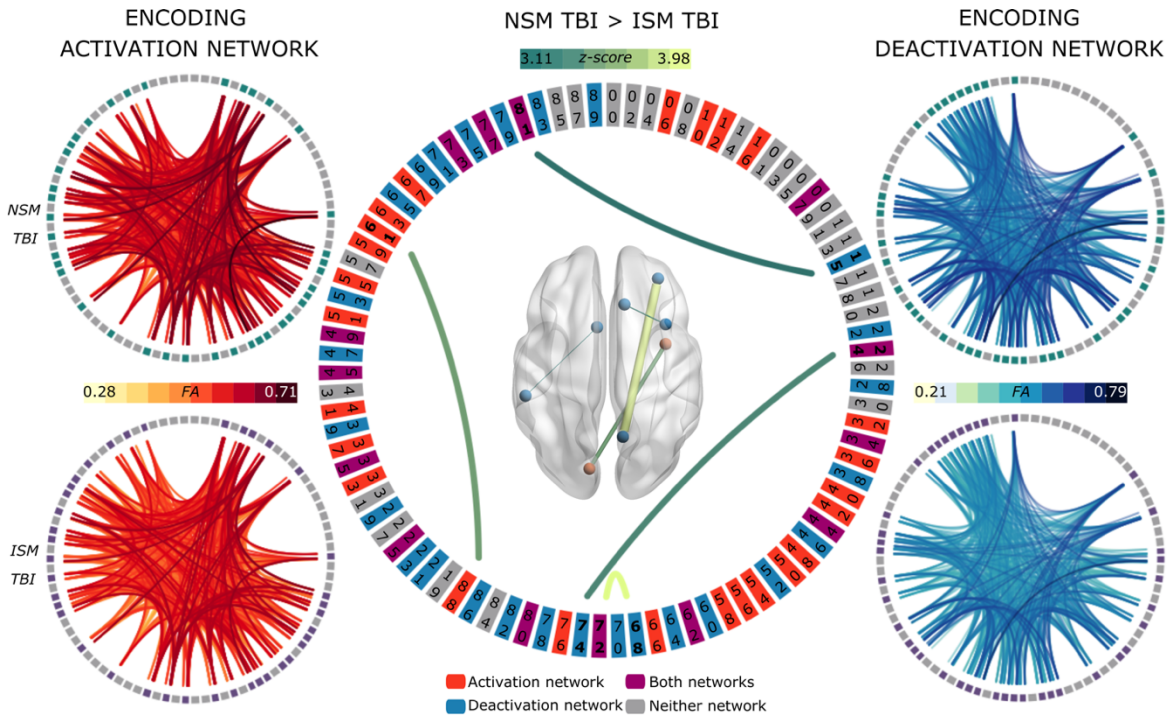

Figure 6.6 Fractional anisotropy in the structural connectome underpinning encoding networks

Structural connectome underlying the positive (red) and negative (blue) encoding networks in NSM (top row) and ISM TBI (bottom row) patients are shown in the outer circles. ISM TBI patients showed reduced structural connectivity between nodes within the positive (p=0.032) and negative (p=0.034) networks. Corresponding labels from the Deskian-Killianey grey matter parcellation scheme with significantly different connections as shown on the innermost circle are as follows: 15. Right-Accumbens-area; 24. ctx-lh-caudalmiddlefrontal; 61. ctx-rh-pericalcalcarine; 68. ctx-lh-precuneus; 72. ctx-lh-rostralmiddlefrontal; 74. ctx-lh-superiorfrontal; 81. ctx-rh-supramarginal; 88. ctx-lh-insula. ISM = impaired subsequent memory; NSM = normal subsequent memory; CON = healthy controls. Figure reproduced with permission from Mallas et al., Brain., 144 (1), 114–127 (2021).

6.3.6 Quality control analyses

Additional analyses to consider the impact of motion and lesions were carried out as quality control checks.

6.3.6.1 Motion

Motion across all participants was minimal with FD measures averaging 0.13mm across all subjects. This varied slightly across groups ($F(2,48)=3.23$, $p<0.05$) with more movement (uncorrected $p<0.05$) in the ISM group (mean=0.14, SD=0.07) compared to controls (mean=0.1, SD=0.03), however this did not survive multiple comparisons correction (FDR corrected $p=0.06$). Removal of noise components using ICA-AROMA did not differ between groups ($F(2,48)=0.77$, $p=0.47$), with 50% of resulting components being removed on average across all subjects (NSM=51%, ISM=52%, Controls=47%).

6.3.6.2 Lesions

Focal lesions were present in 10 NSM and 7 ISM patients (Figure 6.7). No lesions overlapped any significant clusters within the *NSM>ISM* contrast. The significant cluster within the *ISM>NSM* contrast overlapped with lesioned voxels in 3 ISM and 4 NSM patients. Removal of these subjects did not diminish the effect of reduced BOLD activation in the ISM compared to the NSM patients ($t(27.99)=-2.87$, $p=0.008$) during correctly encoded trials within this cluster.

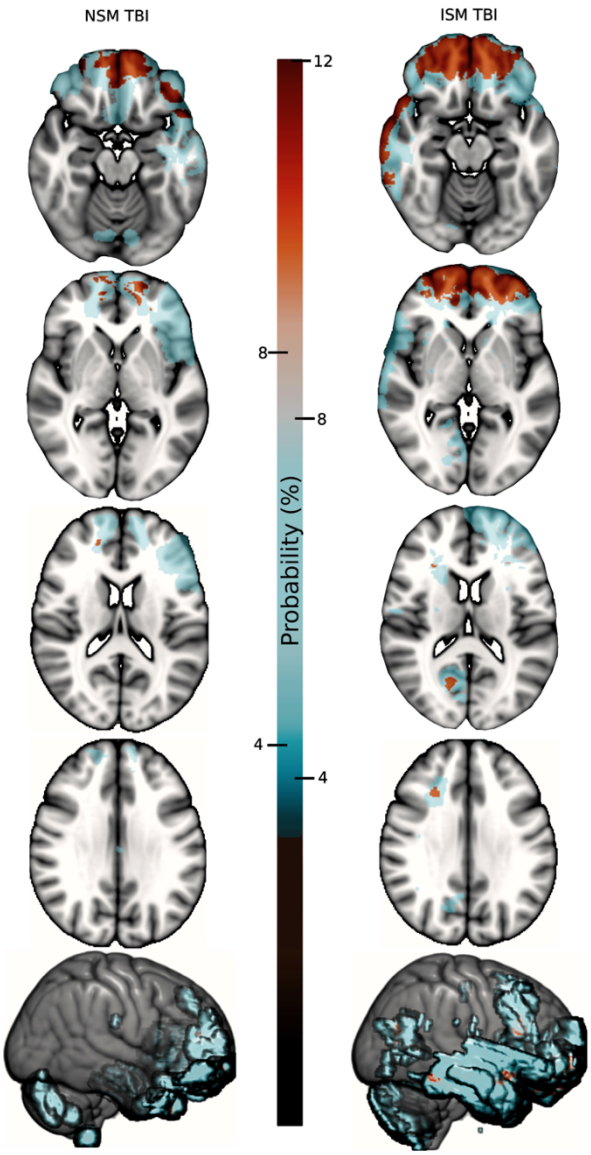

Figure 6.7 Lesion probability in TBI patients with and without memory impairment

Lesion probability maps for TBI patients with normal subsequent memory (left) and TBI patients with impaired subsequent memory (right) indicating, for every voxel, the lesion frequency within the respective patient samples. Figure reproduced with permission from Mallas et al., Brain., 144 (1), 114–127 (2021).

6.4 DISCUSSION

Episodic memory impairment is a common and enduring problem following TBI, but the neural basis for this is unclear. These results show, for the first time, that TBI patients with impaired episodic memory show abnormal activation of memory networks during successful encoding compared to patients with normal memory function. The results presented in this chapter provide novel insights into the mechanisms underlying episodic memory impairment within a chronic TBI population. Abnormal activation of key nodes within the DAN and regions regulating DMN activity during encoding are predictive of subsequent retrieval. These results demonstrate a clear relationship between functional networks activated during encoding and underlying structural abnormalities in patients with memory impairment and suggest that encoding failures in this group are likely due to failed control of attentional resources.

Successful memory encoding is normally associated with activation of a range of brain regions including extensive parts of the DAN and MTL (Kim, 2015, 2011). In contrast, subsequently forgetting is associated with greater activation in DMN regions (Kim, 2011). The results from data across all participants combined were largely in keeping with these findings and suggest that activation of the DAN and suppression of the DMN is required for successful encoding.

Activation of the DAN is thought to be crucial for stimulus directed attention (Majerus *et al.*, 2018). The right IPS, a key hub in the DAN, is particularly important because of its involvement in the mediation of goal-directed 'top-down' attention. Activation of IPS has been consistently associated with successful encoding and it has been proposed that allocating goal-directed attention during encoding increases the probability of retrieval (Uncapher & Wagner, 2009). Patients with intact memory performance showed greater activation than impaired patients in right IPS. This might be the result of compensatory recruitment of DAN regions that improves cognitive function, specifically attentional control, while ISM TBI patients are not able to utilise this mechanism. Previous work has demonstrated hyperactivation in a range of brain regions during letter encoding in TBI patients, in the absence of behavioural differences to controls (Arenth *et al.*, 2012; Russell *et al.*, 2011). Results from these studies are difficult to interpret because contrasts were between stimuli encoding conditions (e.g., picture versus word) and the

lack of behavioural deficits in the TBI group means observed increased activation cannot be associated with cognitive performance. The direct comparison of patients with and without memory impairment in the data presented here clarifies that increased activation of these regions during memory encoding is likely to be compensatory.

The data presented in this chapter also demonstrates that activation in the PHG bilaterally is decreased in TBI patients with episodic memory impairment. This region has consistently been associated with increased activation during successful encoding (Dove *et al.*, 2006; Kim, 2011). The PHG, a key node in the DMN, is thought to act as a link between the MTL memory system and the cortical nodes of the DMN (Ward *et al.*, 2014). Functional connectivity between MTL and DMN has been associated with memory encoding (Huijbers *et al.*, 2011). Previous work in the acute TBI population has shown that patients in PTA have abnormal functional connectivity between PHG and DMN (De Simoni *et al.*, 2016). The data presented here from a chronic TBI cohort provides further evidence that abnormalities of PHG function are an important determinant of memory function after TBI.

Memory impairments were associated with increased activity in the left anterior prefrontal cortex (aPFC). There are several potential reasons why aPFC activation is higher in patients with memory impairment. The region is thought to be involved in the processing of internal mental states and mind-wandering (Christoff & Gabrieli, 2000), and the transition between brain resting state and task-processing state (Peng *et al.*, 2018). One hypothesis is that activation of this region is high because patients that engaged in mind-wandering or with internally focused attention show poorer encoding of memory. The aPFC is thought to exert suppressive top-down control over the DMN to facilitate goal-directed behaviours, and procrastination or mind-wandering occurs when this control is lost (Zhang, Wang & Feng, 2016).

An alternative explanation is that the increased activity is a compensatory response to greater cognitive load during attempted memory encoding. Memory impairment associated with healthy ageing has been associated with increased PFC recruitment in older adults (Dennis, Daselaar & Cabeza, 2007). Taken with findings that show PFC-MTL connectivity is altered in ageing, it has been suggested that 'over-activation' of PFC in older adult populations could reflect functional compensation for dysfunction within the MTL system (Nyberg, 2017). The data presented in this

chapter shows increased aPFC activation in TBI patients with SM impairment which may be reflective of compensatory processes as described in the healthy ageing literature.

Consistent with this compensatory hypothesis is the direction of change in the BOLD signal extracted from the peak of the aPFC cluster (Figure 6.4C). In TBI patients with normal subsequent memory performance, the direction of signal change is the same as for controls, though exaggerated, suggesting this 'extra' suppression is required for TBI patients without overt mnemonic impairment to encode successfully. In TBI patients with impaired memory however the signal change is in the opposite direction suggesting that encoding in those with mnemonic deficits may be fundamentally altered, either through recruitment of additional resources or a functional reorganisation. Reorganisation of functional networks following brain injury can be associated with cognitive changes (Warren *et al.*, 2009; Ainsworth *et al.*, 2018). It is therefore possible that functional reorganisation within networks involved in memory function might explain the patterns of abnormal activation seen here.

Impaired SM was associated with reduced integrity of white matter microstructure. In keeping with these findings, a previous study found that successful learning was associated with higher FA values in the forceps, fronto-occipital fasciculus and thalamic radiation (Chiou, Genova & Chiaravalloti, 2016). Previous work showing the association between reduced white matter integrity in the fornix and impaired associative learning and memory is also consistent with the present findings of reduced structural connectivity and cognitive impairments (Kinnunen *et al.*, 2011). Taken together with our functional imaging findings, this suggests that normal functional activation during memory encoding is reliant on structural white matter integrity.

To explore this hypothesis further I examined the underlying white matter architecture of the functional encoding networks and showed significantly reduced connectivity in both encoding activation and encoding deactivation networks associated with memory impairment. The tracts used to define these structural networks represent tractography derived connectivity between grey matter regions, and so while these structural networks do not represent traditional anatomical tracts, they do allow a more detailed investigation of the relationship between structural and functional networks. The strongest effect was found in white matter underpinning connections between left precuneus and rostral middle frontal gyrus, core nodes within the

DMN. The precuneus, in healthy cognition, interacts with both DMN and frontoparietal networks to engage in different cognitive states (Utevsky, Smith & Huettel, 2014). Abnormal structural connections linking a key hub of the DMN with prefrontal cortex implicated in executive control, and in this case abnormal activation in impaired memory function, suggests a potential mechanism through which structural damage underpins cognitive deficits. It has previously been shown that DMN connectivity predicts variability in sustained attention impairment within a TBI population (Bonnelle *et al.*, 2011), which is consistent with the findings presented in this chapter. Furthermore, within the encoding deactivation network, all connections that showed significantly reduced integrity of the underlying white matter microstructure had connections to/from nodes that overlapped with the encoding activation network. This would suggest that communications not only within the encoding deactivation network, but also between encoding activation and deactivation networks, are associated with impaired memory in TBI. This evidence is in-keeping with memory impairment arising as the result of failure to appropriately engage and disengage functional networks modulating attentional control as a consequence of damage to the underlying white matter microstructure.

6.4.1 Limitations

An important consideration in any functional imaging study is that of subject movement. Very small amounts of motion were seen in these patients, and motion metrics did not differ between groups. It is therefore not likely that this is a factor in explaining the results presented in this chapter. Nevertheless, several steps were taken to ensure that physiological motion artefact was accounted for during data analysis including removal of subjects with larger degrees of motion and decomposing the data to eliminate components largely consisting of motion.

The patients with memory impairment were less educated than healthy controls and the potential effect that educational level could have on the behavioural results should be considered. Recent meta-analysis suggested higher educational level is associated with improved visuospatial recall and better recovery (Vakil *et al.*, 2019). However, there was no difference in educational levels between the ISM and NSM TBI groups suggesting that the interpretation of the results should therefore not be altered by this factor.

No robust measure of attention was employed during the in-scanner encoding period of the task. Caution must therefore be taken when extrapolating a failure to encode from the current paradigm. To ensure that images are attended to during the encoding phase, a simple judgement task could be utilised. The effects of not having this in place could have led to mind wandering and this could be interpreted as a failure to attend rather than a failure to encode. The deficit in these patients could therefore be representing a fundamental failure in memory, or of, as I have suggested above, a failed control of attentional resources.

In terms of lesions, the pattern of focal cortical damage observed cannot explain the functional imaging results, as the difference in BOLD activation in areas overlapped by such damage between the ISM and NSM TBI groups remained significant when patients with lesions in those areas were removed from the analysis.

Finally, the use of a separate independent control group for the structural imaging limits the ability to assess the relationship between the functional and structural encoding networks in a control population, however given the focus here was to understand underlying mechanisms of mnemonic deficits within the chronic TBI population, this did not impair the ability to explore the differences between ISM and NSM patients.

6.4.2 Future Directions

Future work should investigate longitudinal changes in brain structure and how this impacts memory performance. Brain atrophy can progress following TBI and these changes predict cognitive function (Cole, Leech & Sharp, 2015). Progressive atrophy after TBI is indicative of neurodegeneration and the relationship between this progressive process and memory function could be quantified using longitudinal assessment of brain volumes. It would be interesting to discern whether patients with enduring memory deficits are also those who show more rapid neurodegeneration.

Understanding the abnormalities of brain network function associated episodic memory failure after TBI creates opportunity for potential therapeutic intervention. Brain stimulation using transcranial direct-current stimulation (tDCS), transcranial magnetic stimulation (TMS) and

deep brain stimulation (DBS) provide opportunities to modulate brain activity and potentially improve memory function after TBI. Previous work has shown that tDCS can improve executive function, an effect that is influenced by the underlying structural connectivity of the stimulated network in healthy individuals and patients after TBI (Li *et al.*, 2019a, 2019c). The results I present in this chapter inform the choice of future stimulation studies aimed at enhancing memory function. TBI patients with intact memory performance showed greater activation than impaired patients in right IPS, perhaps due to compensatory recruitment of the DAN. This leads to the prediction right IPS stimulation during memory encoding may normalise memory impairments after TBI by increasing DAN activity. This region is accessible to non-invasive brain stimulation, which might be achieved using TDCS. However, more focal brain stimulation could be needed, achieved non-invasively with TMS or invasively through DBS, which could become an option in the future. Future work should quantify abnormalities of structural connectivity within white matter tracts connecting memory network nodes, as this is likely to influence the response to brain stimulation (Li *et al.*, 2019c).

6.4.3 Conclusion

In summary, TBI patients at the chronic stage of recovery with enduring SM impairment show dissociable functional and structural abnormalities from those with normal SM performance. The results presented in this chapter demonstrate a clear relationship between abnormal activation of functional networks during encoding and damage to the underlying structural connectivity of these networks.

7

General Discussion

In this final chapter, I first give an overview of each of the experimental chapters and highlight the novel contributions of the work in this thesis. I then interpret the main findings of the thesis and discuss how, taken together, they contribute to the understanding of post-traumatic amnesia and memory deficits following traumatic brain injury. Finally, I discuss directions for possible future research.

7.1 OVERVIEW OF EXPERIMENTAL CHAPTERS

7.1.1 Chapter Three

In the first experimental chapter, I began by examining the cognitive profile of acute traumatic brain injury (TBI) patients with and without current post-traumatic amnesia (PTA). Consistent with recent work (Hennessy, Delle Baite & Marshman, 2021), I found that patients in PTA are not globally more impaired than patients without PTA, but rather they exhibit deficits primarily related to tasks requiring attention and working memory processes. I then used a precision visual working memory task to assess the point at which working memory failures were occurring. Patients in PTA demonstrated a significant impairment in binding object and location information. I used a novel measure of entropy ratio to examine the distribution of responses at the individual patient level and found that patients in PTA showed greater affinity towards the non-target location. These results suggest that PTA patients have intact memory for object identity and location independently, but they fail to integrate, or bind them, into a coherent representation.

I found that this binding deficit was transient and specific to the acute period of PTA. At 6-month follow-up, patients that had previously been in PTA no longer demonstrated impairments in object-location binding and their distribution of responses was no longer discernible from TBI patients without PTA. These results offer support for a deficit in working memory binding being a sensitive cognitive biomarker of PTA.

7.1.2 Chapter Four

In Chapter 4, I investigated the electrophysiological effects of PTA and extended the work of the previous chapter to examine the neural basis of the misbinding failure. I found that there was a shift towards dominant lower frequency power in PTA patients. The global delta to alpha power ratio (DAR) was significantly higher in patients in PTA compared to acute TBI patients no longer in PTA and healthy controls. At 6-month follow-up DAR normalised suggesting that pathological slowing is a transient abnormality in PTA patients.

I extended the work of the previous chapter by showing that the pathological slowing was associated with object-location binding ability across all TBI patients. Global DAR positively correlated with the entropy ratio of the distribution of responses in the precision working memory task but showed no relationship to markers of injury severity. I further highlighted this point by presenting a series of individual patient case studies showing the transient nature of the binding impairment and shift towards slow wave power against conventional diagnostic imaging and suggest these measures may be more sensitive to the PTA period.

I also found that acute TBI patients showed hyperconnectivity between frontal-parietal and frontal-temporal channels in the theta frequency band, but this was irrespective of whether they were currently experiencing a period of PTA. Increases in theta coherence between these regions is normally associated with working memory and executive function (Fell & Axmacher, 2011) and I therefore expected to see a relationship with binding ability. Instead, increases in theta phase synchronisation showed a trend towards an association with PTA duration and may reflect a restorative process reflecting neuroplastic recovery following TBI.

7.1.3 Chapter Five

In Chapter 5, I examined the functional connectivity within and between core resting state networks involved in cognition. I did not replicate previous findings of reduced connectivity between the default mode network (DMN) and the medial temporal lobe (MTL) subsystem (De Simoni *et al.*, 2016) using seed based static approaches. Using a sliding window dynamic functional connectivity approach to examine fluctuating patters of connectivity between 20 regions of interest I found four independent brain states. These demonstrated dynamic changes in network configurations across time, including striking anti-correlations between key nodes of large-scale networks. I explored the temporal characteristics of these states including how long was spent in each state and how frequently that state was accessed across groups though found no significant differences.

Within the PTA+ patients, there was a tendency to spend more time in fewer states associated with poorer cognitive abilities. PTA+ patients in a more profound state of PTA, showed the least flexible transitioning between states, with a more even distribution of state transitions associated

with higher WPTAS scores. This finding is consistent with previous literature in psychiatric and neurological disease groups supporting the relationship between impaired cognition and less flexible brain dynamics (Douw *et al.*, 2015; Liang *et al.*, 2020; Nguyen *et al.*, 2017). Taken together this may suggest that abnormalities in specific network configurations may contribute to the cognitive deficits associated with a period of PTA. Emergence of more flexible transitioning between states may be an indicator of emergence from PTA.

7.1.4 Chapter Six

In the final experimental chapter, I investigated how functional and structural connectivity is differentially impaired in chronic TBI patients with and without enduring memory impairment. First, I assessed which brain regions were associated with successful encoding during a subsequent memory task. In keeping with previous meta-analyses (Kim, 2011, 2015) when averaged across all TBI patients and healthy controls together, successful encoding was associated with activation changes in the dorsal attention network (DAN) and DMN. TBI patients with memory impairment showed differential activation during successful encoding: activation was increased in regions of the DAN and MTL and decreased in prefrontal cortex (PFC) compared to TBI patients with intact normal memory function. Furthermore, compared to healthy controls, TBI patients showed a pattern of exaggerated signal change whereas for patients with memory impairment the direction was reversed, suggesting TBI patients with memory impairment were failing to suppress prefrontal activity during encoding.

I found that there was substantial white matter damage in TBI patients with memory impairment. White matter integrity was reduced in several large tracts in impaired TBI patients compared to TBI patients without memory impairment and healthy controls. I directly tested whether the white matter damage was related to the abnormalities in functional activation during encoding by constructing a structural connectome of white matter underpinning the task derived encoding networks. TBI patients with memory impairment had more damage to white matter microstructure underpinning both the encoding networks than TBI patients with normal memory function.

Taken together, these results suggest that chronic TBI patients with enduring memory impairments show dissociable functional and structural abnormalities from those with normal memory function. There is a clear relationship between abnormal activation of functional networks during encoding and damage to the underlying structural connectivity of these networks.

7.2 NOVEL CONTRIBUTIONS

7.2.1 A novel acute cohort

Chapters 3, 4, and 5 present data in a highly novel cohort of patients. While there is a wealth of literature studying moderate-severe TBI patients in the chronic stages of recovery, the majority of acute TBI research in conscious patients required to actively participate in cognitive assessments and imaging protocols is in those less severely injured and discharged from hospital. This is likely due to the challenges associated with recruitment of an acute moderate-severe TBI cohort. I have stated several limitations throughout the experimental chapters of the thesis, and one common thread surrounds recruitment issues. I recruited all the patients in the acute clinical cohort for the purpose of this thesis. All these patients were recruited as in-patients on the major trauma ward and were within the first 2 weeks of injury. This brought with it many challenges which I shall briefly outline in the following section.

7.2.1.1 Recruitment challenges in an acute cohort

Firstly, it should be highlighted that the patients assessed here were acutely unwell and had sustained serious traumatic injuries. Asking people to give their time and energy during this period should not be overlooked. The nature of head injury means that patients are often combative, un-cooperative, confused, aggressive, anxious, upset and fatigued. Many patients simply do not want to, or feel unable to, undergo additional testing during this time.

Most patients acquired their injuries through accidents that involved injuries that were not isolated to the head. In addition to their brain injury, many poly-trauma patients also had damage to other organs or orthopaedic injuries resulting in problems such as limited mobility and pain management requirements. This can make adopting positions required for the research tasks difficult (e.g., being seated at computer, lying flat for a scan). Additionally, orthopaedic patients may have metal plates inserted during surgical intervention that within the acute period is not compatible with MRI. Similarly, neurosurgical intervention in TBI patients may mean that EEG

assessment is not appropriate due to missing bone flaps following craniotomy or healing wounds. These factors can exclude many trauma patients from being able to take part in research.

The widespread nature of injuries associated with poly-trauma often means that patients need to be seen by a large multi-disciplinary team. Patients may also be reluctant to be away from the ward during visiting hours with family members. In practice this means that patients are often not available for long periods of time and co-ordinating patient availability to undergo MRI scans, EEG and cognitive assessments within a narrow time frame is an added challenge to the recruitment process. Similarly, scanning equipment in an acute clinical care facility may need to be re-allocated to respond to clinical emergencies. There is therefore a logistical challenge to carrying out acute clinical research in this patient cohort.

Perhaps the most challenging aspect of recruitment is also that which makes the dataset the most novel and valuable. PTA patients are usually very confused and disorientated which makes it challenging to ensure appropriate engagement with cognitive tasks and study protocols. Extreme care and time were taken to help patients understand the requirements of each element of the study, nevertheless for some patients in PTA it was deemed that they would not be able to engage appropriately and thus were not included.

As I highlighted in Chapter 1, most of the literature in PTA is concerned with recovery both in terms of recovery of cognitive domains as well as long term functional outcomes. This has been important work in aiding understanding of presentation and prognosis, but little progress had been made in terms of mechanistic understanding. Despite many of the practical, logistical, and clinical challenges associated with recruiting an acute TBI cohort into the experiments presented in this thesis the data has made novel contributions to the mechanistic understanding of PTA.

7.2.2 Cognitive heterogeneity in TBI

Studying patient groups in a way that characterises them by their degree of cognitive impairment rather than type of injury has enabled novel findings regarding the neural underpinnings of memory deficits in TBI.

In the acute cohorts, patients were separated by their PTA status, and this revealed that some abnormalities were specific to a transient period of PTA, while others were more generally associated with a diagnosis of TBI. In Chapter 3 this was highlighted using an extensive cognitive battery in combination with a precision spatial working memory task. I showed for the first time that PTA patients were not anymore globally impaired than acute TBI patients without PTA but rather they had a specific deficit in binding ability. I extended this work in Chapter 4 and again for the first time showed that some of the abnormalities in this cohort were specific to PTA (increased delta to alpha power ratio) and underpinned this working memory failure, but others were non-specific to memory impairments in acute TBI (theta power hyperconnectivity). These findings not only provide mechanistic insight into the neural underpinnings of PTA, but also contribute to the understanding of brain systems involved in specific cognitive processes.

In Chapter 6 I showed for the first time that patients with impaired episodic memory show abnormal activation of key nodes in large-scale resting state networks during encoding. Successful encoding was associated with an opposite direction of signal change between patients with and without memory impairment. TBI patients, especially in the chronic stages of recovery from injury are frequently grouped based on injury severity, mechanism of injury or patterns of injury rather than by the cognitive domains affected by the injury. By acknowledging the cognitive heterogeneity in this population, I have shown that that memory encoding mechanisms may be fundamentally altered in a subset of TBI patients with memory impairment.

7.3 INTERPRETATION

7.3.1 Are patients with more severe memory impairments more severely injured?

PTA duration is considered as a marker of injury severity (Malec *et al.*, 2007; Walker *et al.*, 2018). Patients with a longer duration of PTA are therefore considered to be more severely injured than those who do not experience a period of PTA or spend less time in this period. It could therefore be argued that patients in PTA, who by definition have more severe cognitive impairments during the acute period are simply more severely injured than acute TBI patients not in TBI. Can the presence of PTA then, be explained by injury severity?

When describing injury severity in the context of TBI, there are several levels at which this can be quantified. PTA occurs in the absence of focal injury. In Chapter 4 I presented four individual case studies of acute TBI patients. In these patients there is no discernible pattern of CT abnormalities specifically associated with PTA, or a relationship between the imaging evidence and the distribution of responses towards the non-target object in the precision spatial working memory task (Chapter 3). This data would thus refute the notion that PTA+ are more severely injured as far as focal lesions and other visible injury on conventional imaging is concerned.

However, injury severity may also be conceptualized as functional disruption. I showed that the delta to alpha power ratio (DAR) was significantly higher in PTA+ patients than PTA- patients or healthy controls. At the individual level, the the striking distribution of responses illustrating the misbinding occurring in PTA patients at baseline, that is absent in TBI patients without PTA, is underpinned by abnormal DAR that normalizes at follow-up. These results could therefore be interpreted to suggest that the delta to alpha ratio is a more sensitive measure of injury severity. Oscillatory slowing is associated with disease (May *et al.*, 2014; de Waal *et al.*, 2013; Stoffers *et al.*, 2007). In this context, PTA patients could be considered to be more severely injured than the TBI patients without PTA, as reflected by an increased DAR. Consistent with this is the finding in Chapter 5 that patients in a more profound state of PTA spend more time in fewer brain states. The ability to flexible transition between brain states is needed for cognitive function and impairments are associated with disease (Douw *et al.*, 2015; van Geest *et al.*, 2018; Liang *et al.*, 2020; Nguyen *et al.*, 2017; Díez-Cirarda *et al.*, 2018). Taken together, these findings would

suggest that PTA is associated with a period of disruption to communication. The data in the acute cohorts would therefore suggest that PTA+ are more severely injured in the context of more severe disruption to brain function, though this is not necessarily reflected in larger bleeds or more extensive structural damage.

Taken together, the data I present in the acute chapters of this thesis would suggest that a period of PTA is not simply reflective of patients with more severe injuries. There are multiple dimensions of injury and some of these are applicable to the memory deficits that hallmark PTA, such as disruption to cortical communication and altered large-scale network dynamics. Others such as the theta hyperconnectivity I demonstrated in Chapter 4 and the more conventional markers of injury severity such as visible focal lesions and acute haemorrhages are less specific to PTA.

7.3.2 What are the mechanisms of memory impairment in TBI?

PTA is classically conceptualised as a discrete period of anterograde amnesia during which patients are unable to encode or form new memories. The results I present in Chapter 3 suggests that this view needs updating. PTA patients showed a significant deficit in the binding of object and location features to form a coherent associative representation, but they did show that they were able to encode, and retain, single item information. Episodic memory formation requires contextual binding to associate the 'what', 'where' and 'when'. This absent binding ability would suggest that learning of single item information is taking place without episodic memory processes that are required for the 'real world' memory formation on which PTA is assessed. The binding of object and location features is process thought to rely on independent projections from prefrontal cortex being integrated in the hippocampus (Ranganath, 2010). This would support the hypothesis that PTA is reflective of a transient dysconnectivity between hippocampal regions to the rest of the brain and would be consistent with the findings from De Simoni *et al.*, (2016), but not with the static functional connectivity results I present in Chapter 5. The data I present in this thesis supports a more global disruption to cortical communication, which may in turn disrupt the communications critical for binding.

The data I have presented in this thesis and discussed above supports the notion that others have previously argued: that PTA is likely a network level dysfunction (Bigler, 2016; De Simoni *et al.*, 2016). The disruption to cortical communication I have demonstrated in PTA may be due to diffuse axonal injury (DAI) producing disruption between grey matter regions (Sharp, Scott & Leech, 2014; Figure 1.1). De Simoni *et al.,* (2016) previously found widespread damage to white matter which was especially marked in the white matter underpinning MTL to DMN connections in a PTA cohort. This has not been directly tested in the acute cohorts presented in this thesis and therefore is speculative.

As I demonstrated in Chapter 6, cognitive deficits, especially those pertaining to memory function, endure for many years after injury even in cases of otherwise good functional recovery. From a cognitive perspective then, PTA may be seen as a more extreme form of memory impairment present in the acute period. These chronic patients do not however meet the criteria for PTA and are able to form continuous episodic memories. The mechanism of memory impairment in chronic TBI is more established. In Chapter 6 I showed that memory impairment is associated with disruption to functional networks that are required for memory processes and attentional control, as well as damage to the white matter microstructure directly underpinning these networks. Mechanistically, this is consistent with previous studies that have found structural damage to be associated with functional network disruption and injury severity following TBI (De Simoni *et al.*, 2018; Palacios *et al.*, 2012; Sharp *et al.*, 2011; Tang *et al.*, 2012; Spitz *et al.*, 2013). As I suggested in Chapter 6, failure in episodic memory encoding in this chronic population is likely due to failed control of attentional resources. This would suggest that memory deficits in a chronic cohort may be due to a different mechanism, at least from a cognitive perspective, than in an acute TBI cohort.

Whether the underlying mechanisms between memory impairment in the acute and chronic cohorts are distinguishable cannot be readily answered from data I have presented. It is possible that there are differences in mechanisms underpinning memory failure in acute and chronic patients due to chronic TBI patients having had longer for functional reorganisation to take place. This could be reflected by compensatory activity in the form of hyperconnectivity or alternative activation that has not had sufficient time to develop in acute TBI. This is highly

speculative and close temporal longitudinal tracking of both cognitive and imaging measures would be required to confirm or refute this idea.

7.3.3 Is PTA an extension of a period of reduced consciousness?

PTA is the period immediately following the regaining of consciousness after head injury (McMillan, 2015). For at least some of the period of PTA it may be considered as a period of reduced awareness. Indeed, the duration of PTA also includes the time spent in coma or state of reduced consciousness when applicable. From a conceptual perspective then, is this period of PTA a continuum of emergence from a state of reduced consciousness?

This view is not supported from a behavioural perspective. The PTA patients that I assessed were generally alert and able to engage in their environment. In Chapter 3 I demonstrated that PTA patients do not show global cognitive impairments compared to acute TBI patients without PTA, but rather they are selectively impaired in the binding or integration of separate features. This selective impairment supports the view that PTA patients are not in a state of reduced consciousness, but rather that disruption to cortical communication as evidenced in Chapters 4 and 5, produces specific mnemonic deficits. However, it should be considered that the PTA patients that underwent cognitive assessment were able to do so precisely *because* they were sufficiently alert. PTA patients in significantly reduced states of awareness were not assessed as part of this research.

In Chapter 4 I found that PTA was associated with a global shift towards slow-wave power as indexed by an increased DAR. Pathological oscillatory slowing is well documented in the literature and is associated with depression of the central nervous system and reduced levels of consciousness (Howells *et al.*, 2018). From this perspective, the increased DAR in PTA+ patients could be interpreted to suggest that these patients are experiencing a form of reduced consciousness. This view is consistent with the association between a more profound state of PTA and increased time spent in less brain states in the dynamic functional connectivity analysis presented in Chapter 5. Animal studies have shown that as anaesthesia deepens there are fewer transitions between states (Hutchison *et al.*, 2014; Ma, Hamilton & Zhang, 2017). Taken

together these findings could be interpreted to suggest that PTA patients show attenuated brain changes consistent with emergence from a period of reduced consciousness.

PTA could therefore represent a period of global cortical disruption as the reorganisation required for higher order cognition occurs. It is possible that the network dynamics that support normal communication and are disrupted following head injury are producing a spectrum of impairment. At the severe end of this spectrum is loss of consciousness. At the milder end, this may be reflected in the binding impairments I have demonstrated in PTA patients. Close temporal monitoring of brain dynamics in acute TBI patients emerging from periods of reduced consciousness and into a period of PTA could provide insight as to whether these mechanisms are discernible.

7.4 FUTURE DIRECTIONS

Development of a cognitive battery to, reliably and sensitively, detect specific cognitive abnormalities during the acute period should be a priority. This will aid in the updating of PTA as a concept. It will also enable a better understanding of how patients can best benefit from rehabilitation. During my PhD I have also been involved in a project that has developed a cognitive battery sensitive to detecting cognitive deficits in a sub-acute and chronic TBI population. These tasks are fast to deliver and can be deployed on handheld tablet devices thus making them appropriate and convenient for an inpatient setting. This work should be extended to develop a battery sensitive to PTA and include repeatable measures to aid in tracking emergence that can be used routinely in place of current standard assessments.

Alongside cognitive monitoring of emergence from PTA, EEG should be carried out at close intervals during this period. I have shown that increased DAR may be useful as a potential biomarker for a period of PTA characterised behaviourally by an inability to integrate information. Understanding the resolution of the increased DAR and how this corresponds to improvement in cognitive abilities may provide further mechanistic insight into the memory disturbances in PTA.

In the discussion section of Chapter 6 I highlighted the opportunity to use understanding of the abnormalities of brain network function in memory failure to explore potential therapeutic interventions such as brain stimulation. In a stable, chronic population this could be used to aid in the appropriate recruitment of networks required for encoding. This is potentially more problematic to apply into an acute population for several reasons. Firstly, the disruption that is specific to the memory deficits in PTA appears to be more diffuse and therefore there is no obvious target for stimulation. Based on the specific cognitive deficit of binding failures which rely on prefrontal to hippocampal projections, stimulation of the hippocampus could be hypothesised to improve this function. This could be achieved using temporal interference stimulation with the aim of modulating oscillatory activity to facilitate binding ability. Temporal interference produces neural stimulation through interference between multiple electric fields (Mirzakhalili *et al.*, 2020) allowing for sub-cortical regions such as hippocampal regions to be targeted. This method also has the advantage of allowing concurrent EEG monitoring which

could be mechanistically informative. This has recently been shown to be beneficial for modifying behaviour in the context of essential tremor (Schreglmann *et al.*, 2021) and shows promise for ameliorating cognitive deficits. It should however be considered that PTA may be serving a restorative function, and this may not therefore be a desirable direction.

Finally, an interesting future direction to expand on the work detailed in this thesis as a whole would be to estimate the relative contributions of fMRI, diffusion MRI and lesion location to individual variability in memory performance. This could be achieved using a multivariate pattern recognition approach such as the Pattern Recognition for Neuroimaging Toolbox (PRoNTo; Schrouff *et al.*, 2013). PRoNTo is a widely available toolbox that uses statistical learning models to identify properties of multi-modal imaging data that can be used to discriminate between conditions or continuous measures. This approach could inform whether PTA is associated with specific lesion locations, damage to specific white matter tracts or interruption to communication between specific grey matter regions. This would also allow a better understanding of the patterns of injury most at risk of longer durations of PTA to inform early prognostic ability. This would be useful from a clinical perspective in the context of resource allocation and family communications. This approach could also be useful in answering questions regarding the respective mechanisms of memory impairment in acute and chronic cohorts and understanding how abnormalities in different modalities contribute to memory impairments.

8 REFERENCES

Agcaoglu, O., Wilson, T.W., Wang, Y.P., Stephen, J.M., et al. (2020) Dynamic Resting-State Connectivity Differences in Eyes Open Versus Eyes Closed Conditions. *Brain Connectivity*. [Online] 10 (9), 504–519. Available from: doi:10.1089/brain.2020.0768.

Aggarwal, C.C., Hinneburg, A. & Keim, D.A. (2001) On the surprising behavior of distance metrics in high dimensional space. In: *Lecture Notes in Computer Science (including subseries Lecture Notes in Artificial Intelligence and Lecture Notes in Bioinformatics)*. [Online]. 2001 Springer Verlag. pp. 420–434. Available from: doi:10.1007/3-540-44503-x_27.

Ahmed, S., Bierley, R., Sheikh, J.I. & Date, E.S. (2000) Post-traumatic amnesia after closed head injury: a review of the literature and some suggestions for further research. *Brain injury*. 14 (9), 765–780.

Ainsworth, M., Browncross, H., Mitchell, D.J., Mitchell, A.S., et al. (2018) Functional reorganisation and recovery following cortical lesions: A preliminary study in macaque monkeys. *Neuropsychologia*. [Online] 119, 382–391. Available from: doi:10.1016/j.neuropsychologia.2018.08.024.

Alekseichuk, I., Turi, Z., Amador de Lara, G., Antal, A., et al. (2016) Spatial Working Memory in Humans Depends on Theta and High Gamma Synchronization in the Prefrontal Cortex. *Current Biology*. [Online] 26 (12), 1513–1521. Available from: doi:10.1016/j.cub.2016.04.035.

Allen, E.A., Damaraju, E., Plis, S.M., Erhardt, E.B., et al. (2014) Tracking whole-brain connectivity dynamics in the resting state. *Cerebral Cortex*. [Online] 24 (3), 663–676. Available from: doi:10.1093/cercor/bhs352.

Amaro, E. & Barker, G.J. (2006) Study design in fMRI: Basic principles. In: *Brain and Cognition*. [Online]. 1 April 2006 Academic Press. pp. 220–232. Available from: doi:10.1016/j.bandc.2005.11.009.

Andreasen, S.H., Andersen, K.W., Conde, V., Dyrby, T.B., et al. (2020) Two Coarse Spatial Patterns of Altered Brain Microstructure Predict Post-traumatic Amnesia in the Subacute Stage of Severe Traumatic Brain Injury. *Frontiers in Neurology*. [Online] 11, 800. Available from: doi:10.3389/fneur.2020.00800.

Andrews-Hanna, J.R., Reidler, J.S., Sepulcre, J., Poulin, R., et al. (2010) Functional-Anatomic Fractionation of the Brain's Default Network. *Neuron*. [Online] 65 (4), 550–562. Available

from: doi:10.1016/j.neuron.2010.02.005.

Andrews-Hanna, J.R., Smallwood, J. & Spreng, R.N. (2014) The default network and self-generated thought: Component processes, dynamic control, and clinical relevance. *Annals of the New York Academy of Sciences*. [Online] 1316 (1), 29–52. Available from: doi:10.1111/nyas.12360.

Andrews-Hanna, J.R., Snyder, A.Z., Vincent, J.L., Lustig, C., et al. (2007) Disruption of Large-Scale Brain Systems in Advanced Aging. *Neuron*. [Online] 56 (5), 924–935. Available from: doi:10.1016/j.neuron.2007.10.038.

Andriessen, T.M.J.C.J.C., De Jong, B., Jacobs, B., van der Werf, S.P., et al. (2009) Sensitivity and specificity of the 3-item memory test in the assessment of post traumatic amnesia. *Brain Injury*. [Online] 23 (4), 345–352. Available from: doi:10.1080/02699050902791414.

Anticevic, A., Cole, M.W., Murray, J.D., Corlett, P.R., et al. (2012) The role of default network deactivation in cognition and disease. *Trends in Cognitive Sciences*. [Online]. 16 (12) pp.584–592. Available from: doi:10.1016/j.tics.2012.10.008.

Antonakakis, M., Dimitriadis, S.I., Zervakis, M., Micheloyannis, S., et al. (2016) Altered cross-frequency coupling in resting-state MEG after mild traumatic brain injury. *International Journal of Psychophysiology*. [Online] 102, 1–11. Available from: doi:10.1016/j.ijpsycho.2016.02.002.

Arenth, P.M., Russell, K.C., Scanlon, J.M., Kessler, L.J., et al. (2012) Encoding and recognition after traumatic brain injury: neuropsychological and functional magnetic resonance imaging findings. *Journal of clinical and experimental neuropsychology*. [Online] 34 (4), 333–344. Available from: doi:10.1080/13803395.2011.633896.

Van Asselen, M., Kessels, R.P.C., Wester, A.J. & Postma, A. (2005) Spatial working memory and contextual cueing in patients with Korsakoff amnesia. *Journal of Clinical and Experimental Neuropsychology*. [Online] 27 (6), 645–655. Available from: doi:10.1081/13803390490919281.

Axmacher, N., Henseler, M.M., Jensen, O., Weinreich, I., et al. (2010) Cross-frequency coupling supports multi-item working memory in the human hippocampus. *Proceedings of the National Academy of Sciences of the United States of America*. [Online] 107 (7), 3228–3233. Available from: doi:10.1073/pnas.0911531107.

Azouvi, P., Arnould, A., Dromer, E. & Vallat-Azouvi, C. (2017) Neuropsychology of traumatic brain injury: An expert overview. *Revue Neurologique*. [Online]. 173 (7–8) pp.461–472.

Available from: doi:10.1016/j.neurol.2017.07.006.

Azouvi, P., Vallat-Azouvi, C., Joseph, P.A., Meulemans, T., et al. (2016) Executive functions deficits after severe traumatic brain injury: The GREFEX study. *Journal of Head Trauma Rehabilitation*. [Online] 31 (3), E10–E20. Available from: doi:10.1097/HTR.0000000000000169.

Baddeley, A. (2000a) The episodic buffer: A new component of working memory? *Trends in Cognitive Sciences*. [Online]. 4 (11) pp.417–423. Available from: doi:10.1016/S1364-6613(00)01538-2.

Baddeley, A.D. (2000b) Short-Term and Working Memory. In: *The Oxford Handbook of Memory*. [Online]. Oxford, Oxford University Press. p. Available from: doi:10.1093/brain/awf064.

Baddeley, A.D., Allen, R.J. & Hitch, G.J. (2011) Binding in visual working memory: The role of the episodic buffer. *Neuropsychologia*. [Online] 49 (6), 1393–1400. Available from: doi:10.1016/j.neuropsychologia.2010.12.042.

Baddeley, A.D., Emslie, H. & Nimmo-Smith, I. (1994) Doors and People: A Test of Visual and Verbal Recall and Recognition, Thames Valley Test Company, Bury St. *Edmunds, UK*.

Baddeley, A.D. & Hitch, G. (1974) Working memory. *Psychology of Learning and Motivation - Advances in Research and Theory*. [Online] 8 (C), 47–89. Available from: doi:10.1016/S0079-7421(08)60452-1.

Bailey, N.W., Rogasch, N.C., Hoy, K.E., Maller, J.J., et al. (2017) Increased gamma connectivity during working memory retention following traumatic brain injury. *Brain Injury*. [Online] 00 (00), 1–11. Available from: doi:10.1080/02699052.2016.1239273.

Baird, A., Papadopoulou, K., Greenwood, R. & Cipolotti, L. (2005) Memory function after resolution of post-traumatic amnesia. *Brain injury*. [Online] 19 (10), 811–817. Available from: doi:10.1080/02699050500149213.

Beckmann, C.F., DeLuca, M., Devlin, J.T. & Smith, S.M. (2005) Investigations into resting-state connectivity using independent component analysis. *Philosophical Transactions of the Royal Society B: Biological Sciences*. [Online] 360 (1457), 1001–1013. Available from: doi:10.1098/rstb.2005.1634.

Benedict, R.H.B., Groninger, L., Schretlen, D., Dobraski, M., et al. (1996) Revision of the brief visuospatial memory test: Studies of normal performance, reliability, and, validity. *Psychological Assessment*. [Online] 8 (2), 145–153. Available from: doi:10.1037/1040-3590.8.2.145.

Beniczky, S. & Schomer, D.L. (2020) Electroencephalography: basic biophysical and technological aspects important for clinical applications. *Epileptic Disorders*. [Online] 22 (6), 697–715. Available from: doi:10.1684/epd.2020.1217.

Benwell, C.S.Y., Davila-Pérez, P., Fried, P.J., Jones, R.N., et al. (2020) EEG spectral power abnormalities and their relationship with cognitive dysfunction in patients with Alzheimer's disease and type 2 diabetes. *Neurobiology of Aging*. [Online] 85, 83–95. Available from: doi:10.1016/j.neurobiolaging.2019.10.004.

Berry, C., Ley, E.J., Tillou, A., Cryer, G., et al. (2009) The effect of gender on patients with moderate to severe head injuries. *Journal of Trauma - Injury, Infection and Critical Care*. [Online] 67 (5), 950–953. Available from: doi:10.1097/TA.0b013e3181ba3354.

Bigler, E.D. (2007) Anterior and Middle Cranial Fossa in Traumatic Brain Injury: Relevant Neuroanatomy and Neuropathology in the Study of Neuropsychological Outcome. *Neuropsychology*. [Online] 21 (5), 515–531. Available from: doi:10.1037/0894-4105.21.5.515.

Bigler, E.D. (2016) Default mode network, connectivity, traumatic brain injury and post-traumatic amnesia. *Brain*. [Online] 139 (12), 3054–3057. Available from: doi:10.1093/brain/aww277.

Bigler, E.D. (2013) Neuroinflammation and the dynamic lesion in traumatic brain injury. *Brain*. [Online] 136 (1), 9–11. Available from: doi:10.1093/brain/aws342.

Bird, C.M. & Burgess, N. (2008) The hippocampus and memory: insights from spatial processing. *Nature Reviews Neuroscience*. [Online] 9 (3), 182–194. Available from: doi:10.1038/nrn2335.

Bishara, S.N., Partridge, F.M., Godfrey, H.P.D. & Knight, R.G. (1992) Post-traumatic amnesia and glasgow coma scale related to outcome in survivors in a consecutive series of patients with severe closed-head injury. *Brain Injury*. [Online] 6 (4), 373–380. Available from: doi:10.3109/02699059209034952.

Bonkhoff, A.K., Espinoza, F.A., Gazula, H., Vergara, V.M., et al. (2020) Acute ischaemic stroke alters the brain's preference for distinct dynamic connectivity states. *Brain*. [Online] 143 (5), 1525–1540. Available from: doi:10.1093/brain/awaa101.

Bonnelle, V., Ham, T.E., Leech, R., Kinnunen, K.M., et al. (2012) Salience network integrity predicts default mode network function after traumatic brain injury. *Proceedings of the National Academy of Sciences*. [Online] 109 (12), 4690–4695. Available from:

doi:10.1073/pnas.1113455109.

Bonnelle, V., Leech, R., Kinnunen, K.M., Ham, T.E., et al. (2011) Default Mode Network Connectivity Predicts Sustained Attention Deficits after Traumatic Brain Injury. *Journal of Neuroscience*. [Online] 31 (38), 13442–13451. Available from: doi:10.1523/JNEUROSCI.1163-11.2011.

Boord, P., Madhyastha, T.M., Askren, M.K. & Grabowski, T.J. (2017) Executive attention networks show altered relationship with default mode network in PD. *NeuroImage: Clinical*. [Online] 13, 1–8. Available from: doi:10.1016/j.nicl.2016.11.004.

Bramlett, H.M. & Dietrich, W.D. (2015) Long-Term Consequences of Traumatic Brain Injury: Current Status of Potential Mechanisms of Injury and Neurological Outcomes. *Journal of Neurotrauma*. [Online] 32 (23), 1834–1848. Available from: doi:10.1089/neu.2014.3352.

Brezova, V., Moen, K.G., Skandsen, T., Vik, A., et al. (2014) Prospective longitudinal MRI study of brain volumes and diffusion changes during the first year after moderate to severe traumatic brain injury. *NeuroImage: Clinical*. [Online] 5, 128–140. Available from: doi:10.1016/J.NICL.2014.03.012.

Buckner, R.L., Andrews-Hanna, J.R. & Schacter, D.L. (2008) The brain's default network: Anatomy, function, and relevance to disease. *Annals of the New York Academy of Sciences*. [Online] 1124 (1), 1–38. Available from: doi:10.1196/annals.1440.011.

Burke, J.F., Zaghlou, K.A., Jacobs, J., Williams, R.B., et al. (2013) Synchronous and asynchronous theta and gamma activity during episodic memory formation. *Journal of Neuroscience*. [Online] 33 (1), 292–304. Available from: doi:10.1523/JNEUROSCI.2057-12.2013.

Cao, C. & Slobounov, S. (2010) Alteration of cortical functional connectivity as a result of traumatic brain injury revealed by graph theory, ICA, and sLORETA analyses of EEG signals. *IEEE Transactions on Neural Systems and Rehabilitation Engineering*. [Online] 18 (1), 11–19. Available from: doi:10.1109/TNSRE.2009.2027704.

Capizzi, A., Woo, J. & Verduzco-Gutierrez, M. (2020) Traumatic Brain Injury: An Overview of Epidemiology, Pathophysiology, and Medical Management. *Medical Clinics of North America*. [Online]. 104 (2) pp.213–238. Available from: doi:10.1016/j.mcna.2019.11.001.

Castellanos, N.P., Paúl, N., Ordóñez, V.E., Demuynck, O., et al. (2010) Reorganization of functional connectivity as a correlate of cognitive recovery in acquired brain injury. *Brain : a journal of neurology*. [Online] 133 (Pt 8), 2365–2381. Available from:

doi:10.1093/brain/awq174.

Catani, M. & Thiebaut De Schotten, M. (2008) A diffusion tensor imaging tractography atlas for virtual in vivo dissections. *Cortex*. [Online] 44 (8), 1105–1132. Available from: doi:10.1016/j.cortex.2008.05.004.

Cecchini, M.A., Yassuda, M.S., Bahia, V.S., de Souza, L.C., et al. (2017) Recalling feature bindings differentiates Alzheimer's disease from frontotemporal dementia. *Journal of Neurology*. [Online] 264 (10), 2162–2169. Available from: doi:10.1007/s00415-017-8614-9.

Chai, W.J., Abd Hamid, A.I. & Abdullah, J.M. (2018) Working memory from the psychological and neurosciences perspectives: A review. *Frontiers in Psychology*. [Online]. 9 (MAR) p.401. Available from: doi:10.3389/fpsyg.2018.00401.

Chang, C. & Glover, G.H. (2010) Time-frequency dynamics of resting-state brain connectivity measured with fMRI. *NeuroImage*. [Online] 50 (1), 81–98. Available from: doi:10.1016/j.neuroimage.2009.12.011.

De Chastelaine, M., Mattson, J.T., Wang, T.H., Donley, B.E., et al. (2015) Sensitivity of negative subsequent memory and task-negative effects to age and associative memory performance. *Brain Research*. [Online]. 1612 pp.16–29. Available from: doi:10.1016/j.brainres.2014.09.045.

Chatterjee, R., Datta, A. & Sanyal, D.K. (2019) Ensemble Learning Approach to Motor Imagery EEG Signal Classification. In: *Machine Learning in Bio-Signal Analysis and Diagnostic Imaging*. [Online]. Elsevier. pp. 183–208. Available from: doi:10.1016/b978-0-12-816086-2.00008-4.

Chiou, K.S., Genova, H.M. & Chiaravalloti, N.D. (2016) Structural white matter differences underlying heterogeneous learning abilities after TBI. *Brain Imaging and Behavior*. [Online] 10 (4), 1274–1279. Available from: doi:10.1007/s11682-015-9497-y.

Chiou, K.S., Sandry, J. & Chiaravalloti, N.D. (2015) Cognitive contributions to differences in learning after moderate to severe traumatic brain injury. *Journal of clinical and experimental neuropsychology*. [Online] 37 (10), 1074–1085. Available from: doi:10.1080/13803395.2015.1078293.

Cho, M.J. & Jang, S.H. (2021) Relationship between post-traumatic amnesia and white matter integrity in traumatic brain injury using tract-based spatial statistics. *Scientific Reports*. [Online] 11 (1), 6898. Available from: doi:10.1038/s41598-021-86439-0.

Christodoulou, C., DeLuca, J., Ricker, J.H., Madigan, N.K., et al. (2001) Functional magnetic

resonance imaging of working memory impairment after traumatic brain injury. *Journal of Neurology Neurosurgery and Psychiatry*. [Online] 71 (2), 161–168. Available from: doi:10.1136/jnnp.71.2.161.

Christoff, K. & Gabrieli, J.D.E. (2000) The frontopolar cortex and human cognition: Evidence for a rostrocaudal hierarchical organization within the human prefrontal cortex. *Psychobiology*. [Online] 28 (2), 168–186. Available from: doi:10.3758/BF03331976.

Chu, B.C., Millis, S., Arango-Lasprilla, J.C., Hanks, R., et al. (2007) Measuring recovery in new learning and memory following traumatic brain injury: A mixed-effects modeling approach. *Journal of Clinical and Experimental Neuropsychology*. [Online] 29 (6), 617–625. Available from: doi:10.1080/13803390600878893.

Claassen, J., Hirsch, L.J., Kreiter, K.T., Du, E.Y., et al. (2004) Quantitative continuous EEG for detecting delayed cerebral ischemia in patients with poor-grade subarachnoid hemorrhage. *Clinical Neurophysiology*. [Online] 115 (12), 2699–2710. Available from: doi:10.1016/j.clinph.2004.06.017.

Cohen, X.M. (2014) *Analyzing Neural Time Series Data*. [Online]. Available from: doi:10.1007/s13398-014-0173-7.2.

Cole, D.M., Smith, S.M. & Beckmann, C.F. (2010) Advances and pitfalls in the analysis and interpretation of resting-state FMRI data. *Frontiers in Systems Neuroscience*. [Online]. 4. Available from: doi:10.3389/fnsys.2010.00008.

Cole, J.H., Leech, R. & Sharp, D.J. (2015) Prediction of brain age suggests accelerated atrophy after traumatic brain injury. *Annals of Neurology*. [Online] 77 (4), 571–581. Available from: doi:10.1002/ana.24367.

Collins, P., Roberts, A.C., Dias, R., Everitt, B.J., et al. (1998) Perseveration and strategy in a novel spatial self-ordered sequencing task for nonhuman primates: Effects of excitotoxic lesions and dopamine depletions of the prefrontal cortex. *Journal of Cognitive Neuroscience*. [Online] 10 (3), 332–354. Available from: doi:10.1162/089892998562771.

Cooper, R.A. & Ritchey, M. (2020) Progression from feature-specific brain activity to hippocampal binding during episodic encoding. *Journal of Neuroscience*. [Online] 40 (8), 1701–1709. Available from: doi:10.1523/JNEUROSCI.1971-19.2019.

Corporation, T.P. (1999) *Manual for the Wechsler Abbreviated Scale of Intelligence*.

Corrigan, J.D., Mysiw, W.J., Gribble, M.W. & Chock, S.K. (1992) Agitation, cognition and attention during post-traumatic amnesia. *Brain injury*. 6 (2), 155–160.

Corrigan, J.D., Whiteneck, G. & Mellick, D. (2004) Perceived needs following traumatic brain injury. *Journal of Head Trauma Rehabilitation*. [Online]. 19 (3) pp.205–216. Available from: doi:10.1097/00001199-200405000-00002.

Corsi, P.M. (1973) *Human memory and the medial region of the brain*. McGill Univeristy.

Cowan, N. (2005) *Working Memory Capacity*. [Online]. Psychology Press. Available from: doi:10.4324/9780203342398.

Criminisi, A., Sharp, T. & Blake, A. (2008) GeoS: Geodesic Image Segmentation. In: David Forsyth, Philip Torr, & Andrew Zisserman (eds.). *Computer Vision – ECCV 2008*. 2008 Berlin, Heidelberg, Springer Berlin Heidelberg. pp. 99–112.

D'Esposito, M. & Postle, B.R. (2015) The cognitive neuroscience of working memory. *Annual review of psychology*. [Online] 66, 115–142. Available from: doi:10.1146/annurev-psych-010814-015031.

Damoiseaux, J.S., Rombouts, S.A.R.B., Barkhof, F., Scheltens, P., et al. (2006) Consistent resting-state networks across healthy subjects. *Proceedings of the National Academy of Sciences of the United States of America*. [Online] 103 (37), 13848–13853. Available from: doi:10.1073/pnas.0601417103.

Darling, S., Sala, S. Della, Logie, R.H. & Cantagallo, A. (2006) Neuropsychological evidence for separating components of visuo-spatial working memory. *J Neurol*. [Online] 253, 176–180. Available from: doi:10.1007/s00415-005-0944-3.

Daselaar, S.M., Prince, S.E., Dennis, N.A., Hayes, S.M., et al. (2009) Posterior midline and ventral parietal activity is associated with retrieval success and encoding failure. *Frontiers in Human Neuroscience*. [Online] 3 (JUL). Available from: doi:10.3389/neuro.09.013.2009.

Daume, J., Gruber, T., Engel, A.K. & Friese, U. (2017) Phase-amplitude coupling and long-range phase synchronization reveal frontotemporal interactions during visual working memory. *Journal of Neuroscience*. [Online] 37 (2), 313–322. Available from: doi:10.1523/JNEUROSCI.2130-16.2016.

Davachi, L. (2006) Item, context and relational episodic encoding in humans. *Current Opinion in Neurobiology*. [Online]. 16 (6) pp.693–700. Available from: doi:10.1016/j.conb.2006.10.012.

Davachi, L. & Wagner, A.D. (2002) Hippocampal contributions to episodic encoding: Insights from relational and item-based learning. *Journal of Neurophysiology*. [Online] 88 (2), 982–990. Available from: doi:10.1152/jn.2002.88.2.982.

Delis, D.C., Kaplan, E. & Kramer, J.H. (2001) *Delis-Kaplan executive function system (D-KEFS)*. Psychological Corporation.

Dennis, N.A., Daselaar, S. & Cabeza, R. (2007) Effects of aging on transient and sustained successful memory encoding activity. *Neurobiology of aging*. [Online] 28 (11), 1749–1758. Available from: doi:10.1016/j.neurobiolaging.2006.07.006.

Desikan, R.S., Ségonne, F., Fischl, B., Quinn, B.T., et al. (2006) An automated labeling system for subdividing the human cerebral cortex on MRI scans into gyral based regions of interest. *NeuroImage*. [Online] 31 (3), 968–980. Available from: doi:10.1016/j.neuroimage.2006.01.021.

Di, X. & Biswal, B.B. (2014) Modulatory interactions between the default mode network and task positive networks in resting-state. *PeerJ*. [Online] 2014 (1). Available from: doi:10.7717/peerj.367.

Díez-Cirarda, M., Strafella, A.P., Kim, J., Peña, J., et al. (2018) Dynamic functional connectivity in Parkinson's disease patients with mild cognitive impairment and normal cognition. *NeuroImage: Clinical*. [Online] 17, 847–855. Available from: doi:10.1016/j.nicl.2017.12.013.

Dixon, M.L., De La Vega, A., Mills, C., Andrews-Hanna, J., et al. (2018) Heterogeneity within the frontoparietal control network and its relationship to the default and dorsal attention networks. *Proceedings of the National Academy of Sciences of the United States of America*. [Online] 115 (7), E1598–E1607. Available from: doi:10.1073/pnas.1715766115.

Douw, L., Leveroni, C.L., Tanaka, N., Emerton, B.C., et al. (2015) Loss of resting-state posterior cingulate flexibility is associated with memory disturbance in left temporal lobe epilepsy. *PLoS ONE*. [Online] 10 (6). Available from: doi:10.1371/journal.pone.0131209.

Dove, A., Brett, M., Cusack, R. & Owen, A.M. (2006) Dissociable contributions of the mid-ventrolateral frontal cortex and the medial temporal lobe system to human memory. *NeuroImage*. [Online] 31 (4), 1790–1801. Available from: doi:10.1016/j.neuroimage.2006.02.035.

Du, Y., Fu, Z. & Calhoun, V.D. (2018) Classification and prediction of brain disorders using functional connectivity: Promising but challenging. *Frontiers in Neuroscience*. [Online]. 12 (AUG) p.525. Available from: doi:10.3389/fnins.2018.00525.

Dudai, Y. (2004) The Neurobiology of Consolidations, Or, How Stable is the Engram? *Annual Review of Psychology*. [Online] 55 (1), 51–86. Available from:

doi:10.1146/annurev.psych.55.090902.142050.

Dunkley, B.T., Da Costa, L., Bethune, A., Jetly, R., et al. (2015) Low-frequency connectivity is associated with mild traumatic brain injury. *NeuroImage: Clinical*. [Online] 7, 611–621. Available from: doi:10.1016/j.nicl.2015.02.020.

Dunn, C.J., Duffy, S.L., Hickie, I.B., Lagopoulos, J., et al. (2014) Deficits in episodic memory retrieval reveal impaired default mode network connectivity in amnestic mild cognitive impairment. *NeuroImage: Clinical*. [Online] 4, 473–480. Available from: doi:10.1016/j.nicl.2014.02.010.

Eastvold, A.D., Walker, W.C., Curtiss, G., Schwab, K., et al. (2013) The differential contributions of posttraumatic amnesia duration and time since injury in prediction of functional outcomes following moderate-to-severe traumatic brain injury. *The Journal of head trauma rehabilitation*. [Online] 28 (1), 48–58. Available from: doi:10.1097/HTR.0b013e31823c9317.

Ebner, A., Sciarretta, G., Epstein, C.M. & Nuwer, M. (1999) Chapter 1.2 EEG instrumentation. *Recommendations for the practice of clinical neurophysiology*.

Ellenberg, J.H., Levin, H.S. & Saydjari, C. (1996) Posttraumatic Amnesia as a predictor of outcome after severe closed head injury. Prospective assessment. *Archives of neurology*. 53 (8), 782–791.

Ewert, J., Levin, H.S., Watson, M.G. & Kalisky, Z. (1989) Procedural Memory During Posttraumatic Amnesia in Survivors of Severe Closed Head Injury. *Archives of Neurology*. [Online] 46 (8), 911. Available from: doi:10.1001/archneur.1989.00520440105027.

Fagerholm, E.D., Hellyer, P.J., Scott, G., Leech, R., et al. (2015) Disconnection of network hubs and cognitive impairment after traumatic brain injury. *Brain*. [Online] 138 (6), 1696–1709. Available from: doi:10.1093/brain/awv075.

Fell, J. & Axmacher, N. (2011) The role of phase synchronization in memory processes. *Nature Reviews Neuroscience*. [Online] 12 (2), 105–118. Available from: doi:10.1038/nrn2979.

Finnigan, S., Wong, A. & Read, S. (2016) Defining abnormal slow EEG activity in acute ischaemic stroke: Delta/alpha ratio as an optimal QEEG index. *Clinical Neurophysiology*. [Online] 127 (2), 1452–1459. Available from: doi:10.1016/j.clinph.2015.07.014.

Fleminger, S. & Ponsford, J. (2005) Long term outcome after traumatic brain injury. *British Medical Journal*. [Online]. 331 (7530) pp.1419–1420. Available from: doi:10.1136/bmj.331.7530.1419.

Fox, M.D., Snyder, A.Z., Vincent, J.L., Corbetta, M., et al. (2005) The human brain is intrinsically organized into dynamic, anticorrelated functional networks. *Proceedings of the National Academy of Sciences of the United States of America*. [Online] 102 (27), 9673–9678. Available from: doi:10.1073/pnas.0504136102.

Friedland, D. & Swash, M. (2016) Post-traumatic amnesia and confusional state: hazards of retrospective assessment. *Journal of neurology, neurosurgery, and psychiatry*. [Online] 87 (10), 1068–1074. Available from: doi:10.1136/jnnp-2015-312193.

Friese, U., Köster, M., Hassler, U., Martens, U., et al. (2013) Successful memory encoding is associated with increased cross-frequency coupling between frontal theta and posterior gamma oscillations in human scalp-recorded EEG. *NeuroImage*. [Online] 66, 642–647. Available from: doi:10.1016/j.neuroimage.2012.11.002.

Friston, K.J. (2011) Functional and Effective Connectivity: A Review. *Brain Connectivity*. [Online] 1 (1), 13–36. Available from: doi:10.1089/brain.2011.0008.

Gabard-Durnam, L.J., Mendez Leal, A.S., Wilkinson, C.L. & Levin, A.R. (2018) The Harvard Automated Processing Pipeline for Electroencephalography (HAPPE): Standardized Processing Software for Developmental and High-Artifact Data . *Frontiers in Neuroscience* .12 p.97.

Gasquoine, P.G. (1991) Learning in post-traumatic amnesia following extremely severe closed head injury. *Brain Injury*. [Online] 5 (2), 169–175. Available from: doi:10.3109/02699059109008087.

van Geest, Q., Hulst, H.E., Meijer, K.A., Hoyng, L., et al. (2018) The importance of hippocampal dynamic connectivity in explaining memory function in multiple sclerosis. *Brain and Behavior*. [Online] 8 (5). Available from: doi:10.1002/brb3.954.

Geffen, G.M., Encel, J.S. & Forrester, G.M. (1991) Stages of recovery during post-traumatic amnesia and subsequent everyday memory deficits. *Neuroreport*. [Online] 2 (2), 105–108. Available from: doi:10.1097/00001756-199102000-00010.

Van Geldorp, B., Bergmann, H.C., Robertson, J., Wester, A.J., et al. (2012) The interaction of working memory performance and episodic memory formation in patients with Korsakoff's amnesia. *Brain Research*. [Online] 1433, 98–103. Available from: doi:10.1016/j.brainres.2011.11.036.

Gentry, L.R., Godersky, J.C. & Thompson, B. (1988) MR imaging of head trauma: Review of the distribution and radiopathologic features of traumatic lesions. *American Journal of*

Roentgenology. [Online] 150 (3), 663–672. Available from: doi:10.2214/ajr.150.3.663.

Gilbert, N., Bernier, R.A., Calhoun, V.D., Brenner, E., et al. (2018) Diminished neural network dynamics after moderate and severe traumatic brain injury. *PLoS ONE*. [Online] 13 (6). Available from: doi:10.1371/journal.pone.0197419.

Gillis, M.M. & Hampstead, B.M. (2015) A two-part preliminary investigation of encoding-related activation changes after moderate to severe traumatic brain injury: hyperactivation, repetition suppression, and the role of the prefrontal cortex. *Brain Imaging and Behavior*. [Online] 9 (4), 801–820. Available from: doi:10.1007/s11682-014-9337-5.

Glisky, E.L. & Delaney, S.M. (1996) Implicit memory and new semantic learning in posttraumatic amnesia. *J Head Trauma Rehabil*. 11 (2), 31–42.

Gloor, P., Ball, G. & Schaul, N. (1977) Brain lesions that produce delta waves in the EEG. *Neurology*. [Online] 27 (4), 326–333. Available from: doi:10.1212/wnl.27.4.326.

Gorgoraptis, N., Zaw-Linn, J., Feeney, C., Tenorio-Jimenez, C., et al. (2019) Cognitive impairment and health-related quality of life following traumatic brain injury. *NeuroRehabilitation*. [Online] 44 (3), 321–331. Available from: doi:10.3233/NRE-182618.

Gosselin, N., Lassonde, M., Petit, D., Leclerc, S., et al. (2009) Sleep following sport-related concussions. *Sleep Medicine*. [Online] 10 (1), 35–46. Available from: doi:10.1016/j.sleep.2007.11.023.

Gould, R.L., Brown, R.G., Owen, A.M., Bullmore, E.T., et al. (2005) Functional neuroanatomy of successful paired associate learning in Alzheimer's disease. *American Journal of Psychiatry*. [Online] 162 (11), 2049–2060. Available from: doi:10.1176/appi.ajp.162.11.2049.

Goulden, N., Khusnulina, A., Davis, N.J., Bracewell, R.M., et al. (2014) The salience network is responsible for switching between the default mode network and the central executive network: Replication from DCM. *NeuroImage*. [Online] 99, 180–190. Available from: doi:10.1016/j.neuroimage.2014.05.052.

Graham, D.I., McIntosh, T.K., Maxwell, W.L. & Nicoll, J.A.R. (2000) Recent Advances in Neurotrauma. *Journal of Neuropathology & Experimental Neurology*. [Online] 59 (8), 641–651. Available from: doi:10.1093/jnen/59.8.641.

Graham, N.S.N., Jolly, A., Zimmerman, K., Bourke, N.J., et al. (2020) Diffuse axonal injury predicts neurodegeneration after moderate-severe traumatic brain injury. *Brain*. [Online] 143 (12), 3685–3698. Available from: doi:10.1093/brain/awaa316.

Griffanti, L., Douaud, G., Bijsterbosch, J., Evangelisti, S., et al. (2017) Hand classification of

fMRI ICA noise components. *NeuroImage*. [Online] 154, 188–205. Available from: doi:10.1016/J.NEUROIMAGE.2016.12.036.

Grogan, J.P., Husain, M., Manohar, S.G., Fallon, S.J., et al. (2020) A new toolbox to distinguish the sources of spatial memory error. *Journal of Vision*. [Online] 20 (13), 1–19. Available from: doi:10.1167/jov.20.13.6.

Gurin, L., Rabinowitz, L. & Blum, S. (2016) Predictors of Recovery From Posttraumatic Amnesia. *The Journal of Neuropsychiatry and Clinical Neurosciences*. [Online] 28 (1), 32–37. Available from: doi:10.1176/appi.neuropsych.15040081.

Hacker, C.D., Snyder, A.Z., Pahwa, M., Corbetta, M., et al. (2017) Frequency-specific electrophysiologic correlates of resting state fMRI networks. *NeuroImage*. [Online] 149, 446–457. Available from: doi:10.1016/j.neuroimage.2017.01.054.

Hampshire, A., Highfield, R.R., Parkin, B.L. & Owen, A.M. (2012) Fractionating Human Intelligence. *Neuron*. [Online] 76 (6), 1225–1237. Available from: doi:10.1016/j.neuron.2012.06.022.

Hampson, M., Driesen, N.R., Skudlarski, P., Gore, J.C., et al. (2006) Brain connectivity related to working memory performance. *Journal of Neuroscience*. [Online] 26 (51), 13338–13343. Available from: doi:10.1523/JNEUROSCI.3408-06.2006.

Han, Y., Wang, K., Jia, J. & Wu, W. (2017) *Changes of EEG Spectra and Functional Connectivity during an Object-Location Memory Task in Alzheimer's Disease*. [Online] Available from: doi:10.3389/fnbeh.2017.00107.

Haveman, M.E., Van Putten, M.J.A.M., Hom, H.W., Eertman-Meyer, C.J., et al. (2019) Predicting outcome in patients with moderate to severe traumatic brain injury using electroencephalography. *Critical Care*. [Online] 23 (1), 401. Available from: doi:10.1186/s13054-019-2656-6.

Hayes, J.P., Bigler, E.D. & Verfaellie, M. (2016) Traumatic brain injury as a disorder of brain connectivity. *Journal of the International Neuropsychological Society*. [Online] 22 (2), 120–137. Available from: doi:10.1017/S1355617715000740.

Hayes, S.M., Salat, D.H. & Verfaellie, M. (2012) Default network connectivity in medial temporal lobe amnesia. *Journal of Neuroscience*. [Online] 32 (42), 14622–14630. Available from: doi:10.1523/JNEUROSCI.0700-12.2012.

Hebb, D. 0 (2005) *The Organization of Behavior A NEUROPSYCHOLOGICAL THEORY*.

Hennessy, M.J., Delle Baite, L. & Marshman, L.A.G. (2021) More than amnesia: prospective

cohort study of an integrated novel assessment of the cognitive and behavioural features of PTA. *Brain Impairment*. [Online] 1–18. Available from: doi:10.1017/BrImp.2021.2.

Hennessy, M.J., Marshman, L.A.G., delle Baite, L. & McLellan, J. (2020) Optimizing and simplifying post-traumatic amnesia testing after moderate-severe traumatic brain injury despite common confounders in routine practice. *Journal of Clinical Neuroscience*. [Online] 81, 37–42. Available from: doi:10.1016/j.jocn.2020.09.030.

Herweg, N.A., Solomon, E.A. & Kahana, M.J. (2020) Theta Oscillations in Human Memory. *Trends in Cognitive Sciences*. [Online]. Available from: doi:10.1016/j.tics.2019.12.006.

Heusser, A.C., Poeppel, D., Ezzyat, Y. & Davachi, L. (2016) Episodic sequence memory is supported by a theta-gamma phase code. *Nature Neuroscience*. [Online] Available from: doi:10.1038/nn.4374.

High, W.M., Levin, H.S. & Gary, H.E. (1990) Recovery of orientation following closed-head injury. *Journal of Clinical and Experimental Neuropsychology*. [Online] 12 (5), 703–714. Available from: doi:10.1080/01688639008401013.

Hillary, F.G., Slocomb, J., Hills, E.C., Fitzpatrick, N.M., et al. (2011) Changes in resting connectivity during recovery from severe traumatic brain injury. *International Journal of Psychophysiology*. [Online] 82 (1), 115–123. Available from: doi:10.1016/j.ijpsycho.2011.03.011.

van der Horn, H.J., Vergara, V.M., Espinoza, F.A., Calhoun, V.D., et al. (2020) Functional outcome is tied to dynamic brain states after mild to moderate traumatic brain injury. *Human Brain Mapping*. [Online] 41 (3), 617–631. Available from: doi:10.1002/hbm.24827.

Hosomi, S., Ohnishi, M., Ogura, H. & Shimazu, T. (2020) Traumatic brain injury-related inflammatory projection: beyond local inflammatory responses. *Acute Medicine & Surgery*. [Online] 7 (1), e520. Available from: doi:10.1002/ams2.520.

Hou, W., Sours Rhodes, C., Jiang, L., Roys, S., et al. (2019) Dynamic Functional Network Analysis in Mild Traumatic Brain Injury. *Brain Connectivity*. [Online] 9 (6), 475–487. Available from: doi:10.1089/brain.2018.0629.

Howells, F.M., Temmingh, H.S., Hsieh, J.H., Van Dijen, A. V., et al. (2018) Electroencephalographic delta/alpha frequency activity differentiates psychotic disorders: A study of schizophrenia, bipolar disorder and methamphetamine-induced psychotic disorder. *Translational Psychiatry*. [Online]. 8 (1) p.75. Available from: doi:10.1038/s41398-018-0105-y.

Huang, M.X., Nichols, S., Baker, D.G., Robb, A., et al. (2014) Single-subject-based whole-brain MEG slow-wave imaging approach for detecting abnormality in patients with mild traumatic brain injury. *NeuroImage: Clinical*. [Online] 5 (109), 109–119. Available from: doi:10.1016/j.nicl.2014.06.004.

Huang, M.X., Theilmann, R.J., Robb, A., Angeles, A., et al. (2009) Integrated imaging approach with MEG and DTI to detect mild traumatic brain injury in military and civilian patients. *Journal of Neurotrauma*. [Online] 26 (8), 1213–1226. Available from: doi:10.1089/neu.2008.0672.

Huang, Z., Tarnal, V., Vlisides, P.E., Janke, E.L., et al. (2021) Anterior insula regulates brain network transitions that gate conscious access. *Cell Reports*. [Online] 35 (5), 109081. Available from: doi:10.1016/j.celrep.2021.109081.

Huijbers, W., Pennartz, C.M.A., Cabeza, R. & Daselaar, S.M. (2011) The Hippocampus Is Coupled with the Default Network during Memory Retrieval but Not during Memory Encoding Georges Chapouthier (ed.). *PLoS ONE*. [Online] 6 (4), e17463. Available from: doi:10.1371/journal.pone.0017463.

Hur, J.-W., Kim, T., Cho, K.I.K. & Kwon, J.S. (2021) Attenuated Resting-State Functional Anticorrelation between Attention and Executive Control Networks in Schizotypal Personality Disorder. *Journal of Clinical Medicine*. [Online] 10 (2), 312. Available from: doi:10.3390/jcm10020312.

Hutchison, R.M., Hutchison, M., Manning, K.Y., Menon, R.S., et al. (2014) Isoflurane induces dose-dependent alterations in the cortical connectivity profiles and dynamic properties of the brain's functional architecture. *Human Brain Mapping*. [Online] 35 (12), 5754–5775. Available from: doi:10.1002/hbm.22583.

Inoue, S. & Matsuzawa, T. (2007) Working memory of numerals in chimpanzees. *Current Biology*. [Online]. 17 (23) pp.R1004–R1005. Available from: doi:10.1016/j.cub.2007.10.027.

Jackson, A.F. & Bolger, D.J. (2014) *The neurophysiological bases of EEG and EEG measurement: A review for the rest of us*. [Online] Available from: doi:10.1111/psyp.12283.

Jaiswal, S., Tsai, S.-Y., Juan, C.-H., Muggleton, N.G., et al. (2019) Low delta and high alpha power are associated with better conflict control and working memory in high mindfulness, low anxiety individuals. *Social cognitive and affective neuroscience*. [Online] 14 (6), 645–655. Available from: doi:10.1093/scan/nsz038.

James, S.L., Bannick, M.S., Montjoy-Venning, W.C., Lucchesi, L.R., et al. (2019) Global,

regional, and national burden of traumatic brain injury and spinal cord injury, 1990-2016: A systematic analysis for the Global Burden of Disease Study 2016. *The Lancet Neurology*. [Online] 18 (1), 56–87. Available from: doi:10.1016/S1474-4422(18)30415-0.

Jann, K., Kottlow, M., Dierks, T., Boesch, C., et al. (2010) Topographic electrophysiological signatures of fMRI resting state networks. *PLoS ONE*. [Online] 5 (9), 1–10. Available from: doi:10.1371/journal.pone.0012945.

Jasper, H.H. (1958) Report of the committee on methods of clinical examination in electroencephalography. In: *Electroencephalography and Clinical Neurophysiology*. [Online]. 1958 pp. 370–375. Available from: doi:10.1016/0013-4694(58)90053-1.

Jenkinson, M., Bannister, P., Brady, M. & Smith, S. (2002) Improved optimization for the robust and accurate linear registration and motion correction of brain images. *NeuroImage*. 17 (2), 825–841.

Jilka, S.R., Scott, G., Ham, T., Pickering, A., et al. (2014) Damage to the Salience Network and Interactions with the Default Mode Network. *Journal of Neuroscience*. [Online] 34 (33), 10798–10807. Available from: doi:10.1523/JNEUROSCI.0518-14.2014.

Johnson, V.E., Stewart, W. & Smith, D.H. (2013) Axonal pathology in traumatic brain injury. *Experimental Neurology*. [Online]. 246 pp.35–43. Available from: doi:10.1016/j.expneurol.2012.01.013.

Jolly, A.E., Scott, G.T., Sharp, D.J. & Hampshire, A.H. (2020) Distinct patterns of structural damage underlie working memory and reasoning deficits after traumatic brain injury. *Brain*. [Online] 143 (3), 1158–1176. Available from: doi:10.1093/brain/awaa067.

Jones, K.T., Johnson, E.L. & Berryhill, M.E. (2020) Frontoparietal theta-gamma interactions track working memory enhancement with training and tDCS. *NeuroImage*. [Online] 211, 116615. Available from: doi:10.1016/j.neuroimage.2020.116615.

Jourdan, C., Azouvi, P., Genêt, F., Selly, N., et al. (2018) Disability and Health Consequences of Traumatic Brain Injury: National Prevalence. *American Journal of Physical Medicine and Rehabilitation*. [Online] 97 (5), 323–331. Available from: doi:10.1097/PHM.0000000000000848.

Jung, R. & Berger, W. (1979) Hans Bergers Entdeckung des Elektrenkephalogramms und seine ersten Befunde 1924-1931. *Archiv für Psychiatrie und Nervenkrankheiten*. [Online] 227 (4), 279–300. Available from: doi:10.1007/BF00344814.

Kalmar, K., Novack, T.A., Nakase-Richardson, R., Sherer, M., et al. (2008) Feasibility of a Brief

Neuropsychologic Test Battery During Acute Inpatient Rehabilitation After Traumatic Brain Injury. *Archives of Physical Medicine and Rehabilitation*. [Online] 89 (5), 942–949. Available from: doi:10.1016/j.apmr.2008.01.008.

Karlsen, P.J., Allen, R.J., Baddeley, A.D. & Hitch, G.J. (2010) Binding across space and time in visual working memory. *Memory and Cognition*. [Online] 38 (3), 292–303. Available from: doi:10.3758/MC.38.3.292.

Katz, D.I. & Alexander, M.P. (1994) Traumatic brain injury. Predicting course of recovery and outcome for patients admitted to rehabilitation. *Archives of neurology*. 51 (7), 661–670.

Keelan, R.E., Mahoney, E.J., Sherer, M., Hart, T., et al. (2019) Neuropsychological characteristics of the confusional state following traumatic brain injury. *Journal of the International Neuropsychological Society*. [Online] 25 (3), 302–313. Available from: doi:10.1017/S1355617718001157.

Keerativittayayut, R., Aoki, R., Sarabi, M.T., Jimura, K., et al. (2018) Large-scale network integration in the human brain tracks temporal fluctuations in memory encoding performance. *eLife*. [Online] 7. Available from: doi:10.7554/eLife.32696.

Kelly, A.M.C., Uddin, L.Q., Biswal, B.B., Castellanos, F.X., et al. (2008) Competition between functional brain networks mediates behavioral variability. *NeuroImage*. [Online] 39 (1), 527–537. Available from: doi:10.1016/j.neuroimage.2007.08.008.

Kim, H. (2015) Encoding and retrieval along the long axis of the hippocampus and their relationships with dorsal attention and default mode networks: The HERNET model. *Hippocampus*. [Online] 25 (4), 500–510. Available from: doi:10.1002/hipo.22387.

Kim, H. (2011) Neural activity that predicts subsequent memory and forgetting: A meta-analysis of 74 fMRI studies. *NeuroImage*. [Online] 54 (3), 2446–2461. Available from: doi:10.1016/j.neuroimage.2010.09.045.

Kim, J. & Kang, E. (2018) Strength of resting-state functional connectivity associated with performance-adjustment ability. *Behavioural Brain Research*. [Online] 347, 377–384. Available from: doi:10.1016/j.bbr.2018.02.024.

Kim, Seo, Lee, Lee, et al. (2019) Altered White Matter Integrity after Mild to Moderate Traumatic Brain Injury. *Journal of Clinical Medicine*. [Online] 8 (9), 1318. Available from: doi:10.3390/jcm8091318.

Kinnunen, K.M., Greenwood, R., Powell, J.H., Leech, R., et al. (2011) White matter damage and cognitive impairment after traumatic brain injury. *Brain : a journal of neurology*. [Online] 134

(Pt 2), 449–463. Available from: doi:10.1093/brain/awq347.

Kiviniemi, V., Vire, T., Remes, J., Elseoud, A.A., et al. (2011) A Sliding Time-Window ICA Reveals Spatial Variability of the Default Mode Network in Time. *Brain Connectivity*. [Online] 1 (4), 339–347. Available from: doi:10.1089/brain.2011.0036.

Kleiner, M., Brainard, D.H., Pelli, D.G., Broussard, C., et al. (2007) What's new in Psychtoolbox-3? A free cross-platform toolkit for psychophysiscs with Matlab and GNU/Octave. *Cognitive and Computational Psychophysics*.36.

Königs, M., De Kieviet, J.F. & Oosterlaan, J. (2012) Post-traumatic amnesia predicts intelligence impairment following traumatic brain injury: a meta-analysis. *Journal of neurology, neurosurgery, and psychiatry*. [Online] 83 (11), 1048–1055. Available from: doi:10.1136/jnnp-2012-302635.

Konstantinou, N., Pettemeridou, E., Stamatakis, E.A., Seimenis, I., et al. (2018) Altered resting functional connectivity is related to cognitive outcome in males with moderate-severe traumatic brain injury. *Frontiers in Neurology*. [Online] 9, 1163. Available from: doi:10.3389/fneur.2018.01163.

Kontaxopoulou, D., Beratis, I.N., Fragkiadaki, S., Pavlou, D., et al. (2017) Incidental and Intentional Memory: Their Relation with Attention and Executive Functions. *Archives of Clinical Neuropsychology*. [Online] 32 (5), 519–532. Available from: doi:10.1093/arclin/acx027.

Köster, M., Finger, H., Graetz, S., Kater, M., et al. (2018) Theta-gamma coupling binds visual perceptual features in an associative memory task. *Scientific Reports*. [Online] 8 (1). Available from: doi:10.1038/s41598-018-35812-7.

Kumar, S., Rao, S.L., Chandramouli, B.A. & Pillai, S. V. (2009) Reduction of functional brain connectivity in mild traumatic brain injury during working memory. *Journal of neurotrauma*. [Online] 26 (5), 665–675. Available from: doi:10.1089/neu.2008.0644.

Kunz, A., Dirnagl, U. & Mergenthaler, P. (2010) Acute pathophysiological processes after ischaemic and traumatic brain injury. *Best Practice and Research: Clinical Anaesthesiology*. [Online]. 24 (4) pp.495–509. Available from: doi:10.1016/j.bpa.2010.10.001.

Lakatos, P., Shah, A.S., Knuth, K.H., Ulbert, I., et al. (2005) An oscillatory hierarchy controlling neuronal excitability and stimulus processing in the auditory cortex. *Journal of Neurophysiology*. [Online] 94 (3), 1904–1911. Available from: doi:10.1152/jn.00263.2005.

Lara, A.H. & Wallis, J.D. (2015) The role of prefrontal cortex in working memory: A mini

review. *Frontiers in Systems Neuroscience*. [Online]. 9 (DEC) p.173. Available from: doi:10.3389/fnsys.2015.00173.

Lasry, O., Liu, E.Y., Powell, G.A., Ruel-Laliberté, J., et al. (2017) Epidemiology of recurrent traumatic brain injury in the general population: A systematic review. *Neurology*. [Online]. 89 (21) pp.2198–2209. Available from: doi:10.1212/WNL.0000000000004671.

Lawrence, T., Helmy, A., Bouamra, O., Woodford, M., et al. (2016) Traumatic brain injury in England and Wales: prospective audit of epidemiology, complications and standardised mortality. *BMJ open*. [Online] 6 (11), e012197. Available from: doi:10.1136/bmjopen-2016-012197.

Leach, K., Kinsella, G., Jackson, M. & Matyas, T. (2006) Recovery of components of memory in post-traumatic amnesia. *Brain injury : [BI]*. 20 (November), 1241–1249.

Leech, R., Kamourieh, S., Beckmann, C.F. & Sharp, D.J. (2011) Fractionating the Default Mode Network: Distinct Contributions of the Ventral and Dorsal Posterior Cingulate Cortex to Cognitive Control. *Journal of Neuroscience*. [Online] 31 (9). Available from: doi:10.1523/JNEUROSCI.5626-10.2011.

Leech, R. & Sharp, D.J. (2014) The role of the posterior cingulate cortex in cognition and disease. *Brain*. [Online] 137 (1), 12–32. Available from: doi:10.1093/brain/awt162.

Lega, B., Burke, J., Jacobs, J. & Kahana, M.J. (2016) Slow-Theta-to-Gamma Phase-Amplitude Coupling in Human Hippocampus Supports the Formation of New Episodic Memories. *Cerebral cortex (New York, N.Y. : 1991)*. [Online] 26 (1), 268–278. Available from: doi:10.1093/cercor/bhu232.

Leon-Carrion, J., Martin-Rodriguez, J.F., Damas-Lopez, J., Barroso y Martin, J.M., et al. (2009) Delta-alpha ratio correlates with level of recovery after neurorehabilitation in patients with acquired brain injury. *Clinical Neurophysiology*. [Online] 120 (6), 1039–1045. Available from: doi:10.1016/j.clinph.2009.01.021.

Levin, H.S., High, W.M. & Eisenberg, H.M. (1988) Learning and forgetting during posttraumatic amnesia in head injured patients. *Journal of neurology, neurosurgery, and psychiatry*. [Online] 51 (1), 14–20. Available from: doi:10.1136/JNNP.51.1.14.

Levin, H.S., O'Donnell, V.M. & Grossman, R.G. (1979) The Galveston Orientation and Amnesia Test. A practical scale to assess cognition after head injury. *The Journal of nervous and mental disease*. 167 (11), 675–684.

Lewine, J.D., Davis, J.T., Bigler, E.D., Thoma, R., et al. (2007) Objective documentation of

traumatic brain injury subsequent to mild head trauma: Multimodal brain imaging with MEG, SPECT, and MRI. *Journal of Head Trauma Rehabilitation*. [Online] 22 (3), 141–155. Available from: doi:10.1097/01.HTR.0000271115.29954.27.

Lezak, M.D. (1979) Recovery of Memory and Learning Functions Following Traumatic Brain Injury. *Cortex*. [Online] Available from: doi:10.1016/S0010-9452(79)80007-6.

Li, L.M., Violante, I.R., Leech, R., Hampshire, A., et al. (2019a) Cognitive enhancement with Salience Network electrical stimulation is influenced by network structural connectivity. *NeuroImage*. [Online] 185, 425–433. Available from: doi:10.1016/j.neuroimage.2018.10.069.

Li, L.M., Violante, I.R., Leech, R., Ross, E., et al. (2019b) Brain state and polarity dependent modulation of brain networks by transcranial direct current stimulation. *Human Brain Mapping*. [Online] 40 (3), 904–915. Available from: doi:10.1002/hbm.24420.

Li, L.M., Violante, I.R., Zimmerman, K., Leech, R., et al. (2019c) Traumatic axonal injury influences the cognitive effect of non-invasive brain stimulation. *Brain*. [Online] 142 (10), 3280–3293. Available from: doi:10.1093/brain/awz252.

Liang, Y., Jiang, X., Zhu, W., Shen, Y., et al. (2020) Disturbances of Dynamic Function in Patients With Bipolar Disorder I and Its Relationship With Executive-Function Deficit. *Frontiers in Psychiatry*. [Online] 11, 1010. Available from: doi:10.3389/fpsyt.2020.537981.

Liang, Y., Pertzov, Y., Nicholas, J.M., Henley, S.M.D., et al. (2016) *Visual short-term memory binding deficit in familial Alzheimer's disease ScienceDirect*. [Online] Available from: doi:10.1016/j.cortex.2016.01.015.

Libby, L.A., Hannula, D.E. & Ranganath, C. (2014) Medial temporal lobe coding of item and spatial information during relational binding in working memory. *Journal of Neuroscience*. [Online] 34 (43), 14233–14242. Available from: doi:10.1523/JNEUROSCI.0655-14.2014.

Liégeois, R., Laumann, T.O., Snyder, A.Z., Zhou, J., et al. (2017) Interpreting temporal fluctuations in resting-state functional connectivity MRI. *NeuroImage*. [Online]. 163 pp.437–455. Available from: doi:10.1016/j.neuroimage.2017.09.012.

Lisman, J.E. & Jensen, O. (2013) The Theta-Gamma Neural Code. *Neuron*. [Online]. Available from: doi:10.1016/j.neuron.2013.03.007.

Lloyd, S.P. (1982) Least Squares Quantization in PCM. *IEEE Transactions on Information Theory*. [Online] 28 (2), 129–137. Available from: doi:10.1109/TIT.1982.1056489.

Louis, E.K. St., Frey, L.C., Britton, J.W., Frey, L.C., et al. (2016) *Electroencephalography (EEG):*

An Introductory Text and Atlas of Normal and Abnormal Findings in Adults, Children, and Infants. Chicago, American Epilepsy Society.

De Luca, M., Beckmann, C.F., De Stefano, N., Matthews, P.M., et al. (2006) fMRI resting state networks define distinct modes of long-distance interactions in the human brain. *NeuroImage*. [Online] 29 (4), 1359–1367. Available from: doi:10.1016/j.neuroimage.2005.08.035.

Luo, W. & Guan, J.-S. (2018) Do Brain Oscillations Orchestrate Memory? *Brain Science Advances*. [Online] 4 (1), 16–33. Available from: doi:10.26599/bsa.2018.9050008.

Ma, Y., Hamilton, C. & Zhang, N. (2017) Dynamic Connectivity Patterns in Conscious and Unconscious Brain. *Brain Connectivity*. [Online] 7 (1), 1–12. Available from: doi:10.1089/brain.2016.0464.

Majerus, S., Péters, F., Bouffier, M., Cowan, N., et al. (2018) The dorsal attention network reflects both encoding load and top-down control during working memory. *Journal of Cognitive Neuroscience*. [Online] 30 (2), 144–159. Available from: doi:10.1162/jocn_a_01195.

Malec, J.F., Brown, A.W., Leibson, C.L., Flaada, J.T., et al. (2007) The Mayo Classification System for Traumatic Brain Injury Severity. *Journal of Neurotrauma*. [Online] 24 (9), 1417–1424. Available from: doi:10.1089/neu.2006.0245.

Mallas, E.-J., De Simoni, S., Scott, G., Jolly, A.E., et al. (2021) Abnormal dorsal attention network activation in memory impairment after traumatic brain injury. *Brain*. [Online] 144 (1), 114–127. Available from: doi:10.1093/brain/awaa380.

Mandleberg, I.A. (1975) Cognitive recovery after severe head injury. 2. Wechsler Adult Intelligence Scale during post-traumatic amnesia. *Journal of Neurology, Neurosurgery & Psychiatry*. [Online] 38 (11), 1127–1132. Available from: doi:10.1136/jnnp.38.11.1127.

Maris, E. & Oostenveld, R. (2007) Nonparametric statistical testing of EEG- and MEG-data. *Journal of Neuroscience Methods*. [Online] 164 (1), 177–190. Available from: doi:10.1016/j.jneumeth.2007.03.024.

Marosszeky, N.E.V., Ryan, L., Shores, E.A., Batchelor, J., et al. (2009) *The PTA Protocol: Guidelines for using the Westmead Post-Traumatic Amnesia (PTA) Scale*. Sydney, Wild & Wooley.

Marsh, N. V. (2018) Cognitive functioning following traumatic brain injury: The first 5 years. *NeuroRehabilitation*. [Online] 43 (4), 377–386. Available from: doi:10.3233/NRE-182457.

Marshman, L.A.G.G., Jakabek, D., Hennessy, M., Quirk, F., et al. (2013) Post-traumatic amnesia.

Journal of Clinical Neuroscience. [Online] 20 (11), 1475–1481. Available from: doi:10.1016/j.jocn.2012.11.022.

May, E.S., Butz, M., Kahlbrock, N., Brenner, M., et al. (2014) Hepatic encephalopathy is associated with slowed and delayed stimulus-associated somatosensory alpha activity. *Clinical Neurophysiology*. [Online] 125 (12), 2427–2435. Available from: doi:10.1016/j.clinph.2014.03.018.

Mazwi, N.L., Izzy, S., Tan, C.O., Martinez, S., et al. (2019) Traumatic Microbleeds in the Hippocampus and Corpus Callosum Predict Duration of Posttraumatic Amnesia. *Journal of Head Trauma Rehabilitation*. [Online] 34 (6), E10–E18. Available from: doi:10.1097/HTR.0000000000000479.

Mcdowell, S., Whyte, J. & D'Esposito, M. (1997) Working memory impairments in traumatic brain injury: Evidence from a dual-task paradigm. *Neuropsychologia*. [Online] 35 (10), 1341–1353. Available from: doi:10.1016/S0028-3932(97)00082-1.

McFarland, K., Jackson, L. & Geffe, G. (2001) Post-Traumatic amnesia: consistency-of-recovery and duration-to-recovery following traumatic brain impairment. *The Clinical neuropsychologist*. [Online] 15 (1), 59–68. Available from: doi:10.1076/clin.15.1.59.1916.

McKay, A., Love, J., Trevena-Peters, J., Gracey, J., et al. (2020) The relationship between agitation and impairments of orientation and memory during the PTA period after traumatic brain injury. *Neuropsychological Rehabilitation*. [Online] 30 (4), 579–590. Available from: doi:10.1080/09602011.2018.1479276.

Mckee, A.C. & Daneshvar, D.H. (2015) The neuropathology of traumatic brain injury. In: *Handbook of Clinical Neurology*. [Online]. Elsevier B.V. pp. 45–66. Available from: doi:10.1016/B978-0-444-52892-6.00004-0.

McMillan, T.M. (2015) *Post Traumatic Amnesia*. Second Edi. [Online]. Elsevier. Available from: doi:10.1016/B978-0-08-097086-8.51053-8.

Menon, D.K., Schwab, K., Wright, D.W. & Maas, A.I. (2010) Position statement: Definition of traumatic brain injury. *Archives of Physical Medicine and Rehabilitation*. [Online]. 91 (11) pp.1637–1640. Available from: doi:10.1016/j.apmr.2010.05.017.

Miller, E.K. (2000) The prefontral cortex and cognitive control. *Nature Reviews Neuroscience*. [Online] 1 (1), 59–65. Available from: doi:10.1038/35036228.

Mirzakhalili, E., Barra, B., Capogrosso, M. & Lempka, S.F. (2020) Biophysics of Temporal Interference Stimulation. *Cell Systems*. [Online] 11 (6), 557-572.e5. Available from:

doi:10.1016/j.cels.2020.10.004.

Modarres, M.H., Kuzma, N.N., Kretzmer, T., Pack, A.I., et al. (2017) EEG slow waves in traumatic brain injury: Convergent findings in mouse and man. *Neurobiology of Sleep and Circadian Rhythms*. [Online] 2, 59–70. Available from: doi:10.1016/j.nbscr.2016.06.001.

De Monte, V.E., Malke Geffen, G., Bronwyn, &, Massavelli, M., et al. (2006) The effects of post-traumatic amnesia on information processing following mild traumatic brain injury. *Brain Injury*. [Online] 20 (13–14), 13–14. Available from: doi:10.1080/02699050601082073.

Mori, S., Wakana, S., Nagae-Poetscher, L.M. & van Zijl, P.C.M. (2005) *MRI Atlas of Human White Matter*. 1st edition. Amsterdam, Elsevier.

Mullen T (2012) *NITRC: CleanLine: Tool/Resource Info*. 2012. NITRC: CleanLine: Tool/Resource Info.

Müller, G.E. & Pilzecker, A. (1900) *Müller: Experimentelle beiträge zur lehre vom gedächtniss - Google Scholar*. Vol. 1. Leipzig, J. A. Barth.

Murphy, A.C., Bertolero, M.A., Papadopoulos, L., Lydon-Staley, D.M., et al. (2020) Multimodal network dynamics underpinning working memory. *Nature Communications*. [Online] 11 (1), 1–13. Available from: doi:10.1038/s41467-020-15541-0.

Nakase-Richardson, R., Sherer, M., Seel, R.T., Hart, T., et al. (2011) Utility of post-traumatic amnesia in predicting 1-year productivity following traumatic brain injury: comparison of the Russell and Mississippi PTA classification intervals. *Journal of neurology, neurosurgery, and psychiatry*. [Online] 82 (5), 494–499. Available from: doi:10.1136/jnnp.2010.222489.

Nguyen, T.T., Kovacevic, S., Dev, S.I., Lu, K., et al. (2017) Dynamic functional connectivity in bipolar disorder is associated with executive function and processing speed: A preliminary study. *Neuropsychology*. [Online] 31 (1), 73–83. Available from: doi:10.1037/neu0000317.

Nickerson, L.D., Smith, S.M., Öngür, D. & Beckmann, C.F. (2017) Using dual regression to investigate network shape and amplitude in functional connectivity analyses. *Frontiers in Neuroscience*. [Online] 11 (MAR), 115. Available from: doi:10.3389/fnins.2017.00115.

von Nicolai, C., Engler, G., Sharott, A., Engel, A.K., et al. (2014) Corticostriatal coordination through coherent phase-amplitude coupling. *Journal of Neuroscience*. [Online] Available from: doi:10.1523/JNEUROSCI.5007-13.2014.

Nott, M.T., Chapparo, C. & Heard, R. (2008) Effective occupational therapy intervention with adults demonstrating agitation during post-traumatic amnesia. *Brain Injury*. [Online] 22 (9), 669–683. Available from: doi:10.1080/02699050802227170.

Nyberg, L. (2017) Functional brain imaging of episodic memory decline in ageing. *Journal of Internal Medicine*. [Online] 281 (1), 65–74. Available from: doi:10.1111/joim.12533.

Olson, I.R., Page, K., Moore, K.S., Chatterjee, A., et al. (2006) Working memory for conjunctions relies on the medial temporal lobe. *Journal of Neuroscience*. [Online] 26 (17), 4596–4601. Available from: doi:10.1523/JNEUROSCI.1923-05.2006.

Oostenveld, R., Fries, P., Maris, E. & Schoffelen, J.M. (2011) FieldTrip: Open source software for advanced analysis of MEG, EEG, and invasive electrophysiological data. *Computational Intelligence and Neuroscience*. [Online] Available from: doi:10.1155/2011/156869.

Palacios, E.M., Sala-Llonch, R., Junque, C., Roig, T., et al. (2013) Resting-State Functional Magnetic Resonance Imaging Activity and Connectivity and Cognitive Outcome in Traumatic Brain Injury. *JAMA Neurology*. [Online] 70 (7), 845. Available from: doi:10.1001/jamaneurol.2013.38.

Palacios, E.M., Sala-Llonch, R., Junque, C., Roig, T., et al. (2012) White matter integrity related to functional working memory networks in traumatic brain injury. *Neurology*. [Online] 78 (12), 852–860. Available from: doi:10.1212/WNL.0b013e31824c465a.

Parra, M.A., Abrahams, S., Logie, R.H., Méndez, L.G., et al. (2010) Visual short-term memory binding deficits in familial Alzheimer's disease. *Brain*. [Online] 133 (9), 2702–2713. Available from: doi:10.1093/brain/awq148.

Patriat, R., Molloy, E.K., Meier, T.B., Kirk, G.R., et al. (2013) The effect of resting condition on resting-state fMRI reliability and consistency: A comparison between resting with eyes open, closed, and fixated. *NeuroImage*. [Online] 78, 463–473. Available from: doi:10.1016/j.neuroimage.2013.04.013.

Pavlovic, D., Pekic, S., Stojanovic, M. & Popovic, V. (2019) Traumatic brain injury: neuropathological, neurocognitive and neurobehavioral sequelae. *Pituitary*. [Online] 22 (3), 270–282. Available from: doi:10.1007/s11102-019-00957-9.

Pearn, M.L., Niesman, I.R., Egawa, J., Sawada, A., et al. (2017) Pathophysiology Associated with Traumatic Brain Injury: Current Treatments and Potential Novel Therapeutics. *Cellular and Molecular Neurobiology*. [Online]. 37 (4) pp.571–585. Available from: doi:10.1007/s10571-016-0400-1.

Peng, K., Steele, S.C., Becerra, L. & Borsook, D. (2018) Brodmann area 10: Collating, integrating and high level processing of nociception and pain. *Progress in neurobiology*. [Online] 161, 1–22. Available from: doi:10.1016/j.pneurobio.2017.11.004.

Pertzov, Y., Dong, M.Y., Peich, M.C. & Husain, M. (2012) Forgetting What Was Where: The Fragility of Object-Location Binding. *PLoS ONE*. [Online] 7 (10). Available from: doi:10.1371/journal.pone.0048214.

Pertzov, Y., Heider, M., Liang, Y. & Husain, M. (2015) Effects of Healthy Ageing on Precision and Binding of Object Location in Visual Short Term Memory. *Psychol Aging*. 30 (1), 26–35.

Piekema, C., Fernández, G., Postma, A., Hendriks, M.P.H., et al. (2007) Spatial and non-spatial contextual working memory in patients with diencephalic or hippocampal dysfunction. *Brain Research*. [Online] 1172 (1), 103–109. Available from: doi:10.1016/j.brainres.2007.07.066.

Ponsford, J., Sloan, S. & Snow, P. (2012) *Traumatic Brain Injury: Rehabilitation for Everyday Adaptive Living*. East Sussex, UK, Psychology Press.

Ponsford, J., Spitz, G. & McKenzie, D. (2015) Using Post-Traumatic Amnesia To Predict Outcome after Traumatic Brain Injury. *J neurotrauma*. [Online] Epub ahead, 1–8. Available from: doi:10.1089/neu.2015.4025.

Postma, A. & De Haan, E.H.F. (1996) What Was Where? Memory for Object Locations. *The Quarterly Journal of Experimental Psychology Section A*. [Online] 49 (1), 178–199. Available from: doi:10.1080/713755605.

Power, J.D., Barnes, K.A., Snyder, A.Z., Schlaggar, B.L., et al. (2012) Spurious but systematic correlations in functional connectivity MRI networks arise from subject motion. *NeuroImage*. [Online] 59 (3), 2142–2154. Available from: doi:10.1016/j.neuroimage.2011.10.018.

Preston, A.R. & Eichenbaum, H. (2013) Interplay of hippocampus and prefrontal cortex in memory. *Current biology : CB*. [Online] 23 (17), R764-73. Available from: doi:10.1016/j.cub.2013.05.041.

Pruim, R.H.R., Mennes, M., van Rooij, D., Llera, A., et al. (2015) ICA-AROMA: A robust ICA-based strategy for removing motion artifacts from fMRI data. *NeuroImage*. [Online] 112, 267–277. Available from: doi:10.1016/j.neuroimage.2015.02.064.

Quinette, P., Guillery-Girard, B., Noël, A., de la Sayette, V., et al. (2006) The relationship between working memory and episodic memory disorders in transient global amnesia. *Neuropsychologia*. [Online] 44 (12), 2508–2519. Available from: doi:10.1016/j.neuropsychologia.2006.03.031.

Raichle, M.E., MacLeod, A.M., Snyder, A.Z., Powers, W.J., et al. (2001) A default mode of brain function. *Proceedings of the National Academy of Sciences of the United States of America*. [Online] 98 (2), 676–682. Available from: doi:10.1073/pnas.98.2.676.

Ranganath, C. (2010) Binding items and contexts: The cognitive neuroscience of episodic memory. *Current Directions in Psychological Science*. [Online] 19 (3), 131–137. Available from: doi:10.1177/0963721410368805.

Reinhart, R.M.G. & Nguyen, J.A. (2019) Working memory revived in older adults by synchronizing rhythmic brain circuits. *Nature Neuroscience*. [Online] 22 (5), 820–827. Available from: doi:10.1038/s41593-019-0371-x.

Reitan, R.M. (1958) Validity of the Trail Making Test as an indicator of organic brain damage. *Perceptual and motor skills*. 8 (3), 271–276.

Roach, B.J. & Mathalon, D.H. (2008) Event-Related EEG Time-Frequency Analysis: An Overview of Measures and An Analysis of Early Gamma Band Phase Locking in Schizophrenia. *Schizophrenia Bulletin*. [Online] 34 (5), 907–926. Available from: doi:10.1093/schbul/sbn093.

Robb Swan, A., Nichols, S., Drake, A., Angeles, A.M., et al. (2015) Magnetoencephalography slow-wave detection in patients with mild traumatic brain injury and ongoing symptoms correlated with long-term neuropsychological outcome. *Journal of Neurotrauma*. [Online] 32 (19), 1510–1521. Available from: doi:10.1089/neu.2014.3654.

Roberts, C.M., Spitz, G. & Ponsford, J.L. (2015) Retrospective analysis of the recovery of orientation and memory during posttraumatic amnesia. *Neuropsychology*. [Online] 29 (4), 522–529. Available from: doi:10.1037/neu0000178.

Russell, K.C., Arenth, P.M., Scanlon, J.M., Kessler, L.J., et al. (2011) A functional magnetic resonance imaging investigation of episodic memory after traumatic brain injury. *Journal of clinical and experimental neuropsychology*. [Online] 33 (5), 538–547. Available from: doi:10.1080/13803395.2010.537253.

Russell, W.R. (1935) AMNESIA FOLLOWING HEAD INJURIES. *The Lancet*. [Online] 226 (5849), 762–763. Available from: doi:10.1016/S0140-6736(00)47843-8.

Russell, W.R. & Nathan, P.W. (1946) Traumatic amnesia. *Brain*. [Online] 69 (4), 280–300. Available from: doi:10.1093/brain/69.4.280.

Della Sala, S., Parra, M.A., Fabi, K., Luzzi, S., et al. (2012) Short-term memory binding is impaired in AD but not in non-AD dementias. *Neuropsychologia*. [Online] 50 (5), 833–840.

Available from: doi:10.1016/j.neuropsychologia.2012.01.018.

Sanchez-Carrion, R., Fernandez-Espejo, D., Junque, C., Falcon, C., et al. (2008) A longitudinal fMRI study of working memory in severe TBI patients with diffuse axonal injury. *NeuroImage*. [Online] 43 (3), 421–429. Available from: doi:10.1016/j.neuroimage.2008.08.003.

Sarnthein, J., Petsche, H., Rappelsberger, P., Shaw, G.L., et al. (1998) Synchronization between prefrontal and posterior association cortex during human working memory. *Proceedings of the National Academy of Sciences*. [Online] 95 (12), 7092–7096. Available from: doi:10.1073/pnas.95.12.7092.

Sauseng, P., Klimesch, W., Schabus, M. & Doppelmayr, M. (2005) Fronto-parietal EEG coherence in theta and upper alpha reflect central executive functions of working memory. *International Journal of Psychophysiology*. [Online] 57 (2), 97–103. Available from: doi:10.1016/j.ijpsycho.2005.03.018.

Schleiger, E., Sheikh, N., Rowland, T., Wong, A., et al. (2014) Frontal EEG delta/alpha ratio and screening for post-stroke cognitive deficits: The power of four electrodes. *International Journal of Psychophysiology*. [Online] 94 (1), 19–24. Available from: doi:10.1016/j.ijpsycho.2014.06.012.

Schneegans, S. & Bays, P.M. (2018) *New perspectives on binding in visual working memory*. [Online] 1–38. Available from: doi:10.1111/bjop.12345.

Schreglmann, S.R., Wang, D., Peach, R.L., Li, J., et al. (2021) Non-invasive suppression of essential tremor via phase-locked disruption of its temporal coherence. *Nature Communications*. [Online] 12 (1), 1–15. Available from: doi:10.1038/s41467-020-20581-7.

Schrouff, J., Rosa, M.J., Rondina, J.M., Marquand, A.F., et al. (2013) PRoNTo: Pattern recognition for neuroimaging toolbox. *Neuroinformatics*. [Online] 11 (3), 319–337. Available from: doi:10.1007/s12021-013-9178-1.

Sharp, D.J., Beckmann, C.F., Greenwood, R., Kinnunen, K.M., et al. (2011) Default mode network functional and structural connectivity after traumatic brain injury. *Brain*. [Online] 134 (8), 2233–2247. Available from: doi:10.1093/brain/awr175.

Sharp, D.J., Scott, G. & Leech, R. (2014) Network dysfunction after traumatic brain injury. *Nature Reviews Neurology*. [Online] 10 (3), 156–166. Available from: doi:10.1038/nrneurol.2014.15.

Sherer, M., Struchen, M.A., Yablon, S.A., Wang, Y., et al. (2008) Comparison of indices of

traumatic brain injury severity: Glasgow Coma Scale, length of coma and post-traumatic amnesia. *Journal of neurology, neurosurgery, and psychiatry*. [Online] 79 (6), 678–685. Available from: doi:10.1136/jnnp.2006.111187.

Shores, E.A., Marosszeky, J.E., Sandanam, J. & Batchelor, J. (1986) Preliminary validation of a clinical scale for measuring the duration of post-traumatic amnesia. *The Medical journal of Australia*. 144 (11), 569–572.

De Simoni, S., Grover, P.J., Jenkins, P.O., Honeyfield, L., et al. (2016) Disconnection between the default mode network and medial temporal lobes in post-traumatic amnesia. *Brain*. [Online] 1–14. Available from: doi:10.1093/brain/aww241.

De Simoni, S., Jenkins, P.O., Bourke, N.J., Fleminger, J.J., et al. (2018) Altered caudate connectivity is associated with executive dysfunction after traumatic brain injury. *Brain*. [Online] 141 (1), 148–164. Available from: doi:10.1093/brain/awx309.

Smith, S.M. (2002) Fast robust automated brain extraction. *Human Brain Mapping*. [Online] 17 (3), 143–155. Available from: doi:10.1002/hbm.10062.

Smith, S.M., Fox, P.T., Miller, K.L., Glahn, D.C., et al. (2009) Correspondence of the brain's functional architecture during activation and rest. *Proceedings of the National Academy of Sciences of the United States of America*. [Online] 106 (31), 13040–13045. Available from: doi:10.1073/pnas.0905267106.

Smith, S.M., Jenkinson, M., Johansen-Berg, H., Rueckert, D., et al. (2006) Tract-based spatial statistics: Voxelwise analysis of multi-subject diffusion data. *NeuroImage*. [Online] 31 (4), 1487–1505. Available from: doi:10.1016/j.neuroimage.2006.02.024.

Smith, S.M., Jenkinson, M., Woolrich, M.W., Beckmann, C.F., et al. (2004) Advances in functional and structural MR image analysis and implementation as FSL. *NeuroImage*. [Online] 23, S208–S219. Available from: doi:10.1016/j.neuroimage.2004.07.051.

Solomon, E.A., Kragel, J.E., Sperling, M.R., Sharan, A., et al. (2017) Widespread theta synchrony and high-frequency desynchronization underlies enhanced cognition. *Nature Communications*. [Online] 8 (1). Available from: doi:10.1038/s41467-017-01763-2.

Solomon, E.A., Stein, J.M., Das, S., Gorniak, R., et al. (2019) Dynamic Theta Networks in the Human Medial Temporal Lobe Support Episodic Memory. *Current Biology*. [Online] 29 (7), 1100-1111.e4. Available from: doi:10.1016/j.cub.2019.02.020.

Spiteri, C.J., Ponsford, J.L., Roberts, C.M. & McKay, A. (2021) Aspects of Cognitive Impairment Associated with Agitated Behaviour during Post-traumatic Amnesia. *Journal of the*

International Neuropsychological Society. [Online] 1–9. Available from: doi:10.1017/s1355617721000588.

Spitz, G., Maller, J.J., O'Sullivan, R. & Ponsford, J.L. (2013) White matter integrity following traumatic brain injury: The association with severity of injury and cognitive functioning. *Brain Topography*. [Online] 26 (4), 648–660. Available from: doi:10.1007/s10548-013-0283-0.

Sponheim, S.R., McGuire, K.A., Kang, S.S., Davenport, N.D., et al. (2011) Evidence of disrupted functional connectivity in the brain after combat-related blast injury. *NeuroImage*. [Online] 54 (SUPPL. 1), S21–S29. Available from: doi:10.1016/j.neuroimage.2010.09.007.

Spreng, R.N., Stevens, W.D., Chamberlain, J.P., Gilmore, A.W., et al. (2010) Default network activity, coupled with the frontoparietal control network, supports goal-directed cognition. *NeuroImage*. [Online] 53 (1), 303–317. Available from: doi:10.1016/j.neuroimage.2010.06.016.

Sprott, J.C. (1996) Strange attractor symmetric icons. *Comput. & Graphics*. 20, 325–332.

Sridharan, D., Levitin, D.J. & Menon, V. (2008) A critical role for the right fronto-insular cortex in switching between central-executive and default-mode networks. *Proceedings of the National Academy of Sciences of the United States of America*. [Online] 105 (34), 12569–12574. Available from: doi:10.1073/pnas.0800005105.

Staffaroni, A.M., Brown, J.A., Casaletto, K.B., Elahi, F.M., et al. (2018) The longitudinal trajectory of default mode network connectivity in healthy older adults varies as a function of age and is associated with changes in episodic memory and processing speed. *Journal of Neuroscience*. [Online] 38 (11), 2809–2817. Available from: doi:10.1523/JNEUROSCI.3067-17.2018.

Stam, C.J., Nolte, G. & Daffertshofer, A. (2007) Phase lag index: Assessment of functional connectivity from multi channel EEG and MEG with diminished bias from common sources. *Human Brain Mapping*. [Online] Available from: doi:10.1002/hbm.20346.

Stoffers, D., Bosboom, J.L.W., Deijen, J.B., Wolters, E.C., et al. (2007) Slowing of oscillatory brain activity is a stable characteristic of Parkinson's disease without dementia. *Brain*. [Online] 130 (7), 1847–1860. Available from: doi:10.1093/brain/awm034.

Strangman, G.E., Goldstein, R., O'Neil-Pirozzi, T.M., Kelkar, K., et al. (2008) Neurophysiological Alterations During Strategy-Based Verbal Learning in Traumatic Brain Injury. *Neurorehabilitation and Neural Repair*. [Online] 23 (3), 226–236. Available from:

doi:10.1177/1545968308324225.

Stuss, D.T., Binns, M.A., Carruth, F.G., Levine, B., et al. (1999) The acute period of recovery from traumatic brain injury: posttraumatic amnesia or posttraumatic confusional state? *Journal of Neurosurgery*. [Online] 90 (4), 635–643. Available from: doi:10.3171/jns.1999.90.4.0635.

Symonds, C.P. (1937) Mental Disorder Following Head Injury. *Proceedings of the Royal Society of Medicine*. [Online] XXX (1081), 33–46. Available from: doi:10.1016/S0140-6736(00)94008-X.

Symonds, C.P. & Ritchie Russell, W. (1943) ACCIDENTAL HEAD INJURIES. PROGNOSIS IN SERVICE PATIENTS. *The Lancet*. [Online] 241 (6227), 7–10. Available from: doi:10.1016/S0140-6736(00)70687-8.

Tang, C.Y., Eaves, E., Dams-O'Connor, K., Ho, L., et al. (2012) Diffuse disconnectivity in Traumatic Brain Injury: A resting state fMRI and DTI study. *Translational Neuroscience*. [Online] 3 (1), 9–14. Available from: doi:10.2478/s13380-012-0003-3.

Tate, R.L. & Pfaff, A. (2000) Problems and Pitfalls in the Assessment of Posttraumatic Amnesia. *Brain Impairment*. [Online] 1 (2), 116–129. Available from: doi:10.1375/brim.1.2.116.

Tate, R.L., Pfaff, A., Baguley, I.J., Marosszeky, J.E., et al. (2006) A multicentre, randomised trial examining the effect of test procedures measuring emergence from post-traumatic amnesia. *Journal of neurology, neurosurgery, and psychiatry*. [Online] 77 (7), 841–849. Available from: doi:10.1136/jnnp.2005.074989.

Tate, R.L., Pfaff, A. & Jurjevic, L. (2000) Resolution of disorientation and amnesia during post-traumatic amnesia. *Journal of neurology, neurosurgery, and psychiatry*. [Online] 68 (2), 178–185. Available from: doi:10.1136/JNNP.68.2.178.

Thatcher, R.W., North, D.M., Curtin, R.T., Walker, R.A., et al. (2001) An EEG Severity Index of Traumatic Brain Injury. *The Journal of Neuropsychiatry and Clinical Neurosciences*. [Online] 13 (1), 77–87. Available from: doi:10.1176/jnp.13.1.77.

Thatcher, R.W., Walker, R.A., Gerson, I. & Geisler, F.H. (1989) EEG discriminant analyses of mild head trauma. *Electroencephalography and Clinical Neurophysiology*. [Online] 73 (2), 94–106. Available from: doi:10.1016/0013-4694(89)90188-0.

Threlkeld, Z.D., Bodien, Y.G., Rosenthal, E.S., Giacino, J.T., et al. (2018) Functional networks reemerge during recovery of consciousness after acute severe traumatic brain injury. *Cortex*. [Online] 106, 299–308. Available from: doi:10.1016/j.cortex.2018.05.004.

Tittle, A. & Burgess, G.H. (2011) Relative contribution of attention and memory toward disorientation or post-traumatic amnesia in an acute brain injury sample. *Brain Injury*. [Online] 25 (10), 933–942. Available from: doi:10.3109/02699052.2011.597042.

Tort, A.B.L., Komorowski, R., Eichenbaum, H. & Kopell, N. (2010) Measuring phase-amplitude coupling between neuronal oscillations of different frequencies. *Journal of Neurophysiology*. [Online] 104 (2), 1195–1210. Available from: doi:10.1152/jn.00106.2010.

Tort, A.B.L., Komorowski, R.W., Manns, J.R., Kopell, N.J., et al. (2009) Theta-gamma coupling increases during the learning of item-context associations. *Proceedings of the National Academy of Sciences of the United States of America*. [Online] 106 (49), 20942–20947. Available from: doi:10.1073/pnas.0911331106.

Treisman, A. (1986) Features and Objects in Visual Processing. *Scientific American*. [Online] 255 (5), 114–125. Available from: doi:10.1038/scientificamerican1186-114b.

Treisman, A.M. & Gelade, G. (1980) A feature-integration theory of attention. *Cognitive Psychology*. [Online] 12 (1), 97–136. Available from: doi:10.1016/0010-0285(80)90005-5.

Tulving, E. (2002) Episodic Memory: From Mind to Brain. *Annual Review of Psychology*. [Online] 53 (1), 1–25. Available from: doi:10.1146/annurev.psych.53.100901.135114.

Turner, E. (1969) Hippocampus and memory. *The Lancet*. [Online] 294 (7630), 1123–1126. Available from: doi:10.1016/S0140-6736(69)90718-1.

Uddin, L.Q., Kelly, A.M.C., Biswal, B.B., Castellanos, F.X., et al. (2009) Functional Connectivity of Default Mode Network Components: Correlation, Anticorrelation, and Causality. *Human Brain Mapping*. [Online] 30 (2), 625–637. Available from: doi:10.1002/hbm.20531.

Ulam, F., Shelton, C., Richards, L., Davis, L., et al. (2015) Cumulative effects of transcranial direct current stimulation on EEG oscillations and attention/working memory during subacute neurorehabilitation of traumatic brain injury. *Clinical Neurophysiology*. [Online] 126 (3), 486–496. Available from: doi:10.1016/j.clinph.2014.05.015.

Uncapher, M.R. & Wagner, A.D. (2009) Neurobiology of Learning and Memory Posterior parietal cortex and episodic encoding : Insights from fMRI subsequent memory effects and dual-attention theory. *Neurobiology of Learning and Memory*. [Online] 91 (2), 139–154. Available from: doi:10.1016/j.nlm.2008.10.011.

Utevsky, A. V, Smith, D. V & Huettel, S.A. (2014) Precuneus is a functional core of the default-mode network. *The Journal of neuroscience : the official journal of the Society for Neuroscience*. [Online] 34 (3), 932–940. Available from: doi:10.1523/JNEUROSCI.4227-13.2014.

Vakil, E. (2005) The Effect of Moderate to Severe Traumatic Brain Injury (TBI) on Different Aspects of Memory: A Selective Review Memory Impairment in Patients with Traumatic Brain Injury E. Vakil. *Journal of Clinical and Experimental Neuropsychology*. [Online] 27 (08), 0–0. Available from: doi:10.1080/13803390490919245.

Vakil, E., Greenstein, Y., Weiss, I. & Shtein, S. (2019) The Effects of Moderate-to-Severe Traumatic Brain Injury on Episodic Memory: a Meta-Analysis. *Neuropsychology Review*. [Online] 29 (3), 270–287. Available from: doi:10.1007/s11065-019-09413-8.

Vanderploeg, R.D., Donnell, A.J., Belanger, H.G. & Curtiss, G. (2014) Consolidation deficits in traumatic brain injury: The core and residual verbal memory defect. *Journal of Clinical and Experimental Neuropsychology*. [Online] 36 (1), 58–73. Available from: doi:10.1080/13803395.2013.864600.

Vidaurre, D., Smith, S.M. & Woolrich, M.W. (2017) Brain network dynamics are hierarchically organized in time. *Proceedings of the National Academy of Sciences of the United States of America*. [Online] 114 (48), 12827–12832. Available from: doi:10.1073/pnas.1705120114.

Vinck, M., Oostenveld, R., Van Wingerden, M., Battaglia, F., et al. (2011) An improved index of phase-synchronization for electrophysiological data in the presence of volume-conduction, noise and sample-size bias. *NeuroImage*. [Online] Available from: doi:10.1016/j.neuroimage.2011.01.055.

Vlahou, E.L., Thurm, F., Kolassa, I.T. & Schlee, W. (2014) Resting-state slow wave power, healthy aging and cognitive performance. *Scientific Reports*. [Online] 4 (1), 1–6. Available from: doi:10.1038/srep05101.

de Waal, H., Stam, C.J., de Haan, W., van Straaten, E.C.W., et al. (2013) Alzheimer's disease patients not carrying the apolipoprotein E ε4 allele show more severe slowing of oscillatory brain activity. *Neurobiology of Aging*. [Online] 34 (9), 2158–2163. Available from: doi:10.1016/j.neurobiolaging.2013.03.007.

Walker, W.C., Ketchum, J.M., Marwitz, J.H., Chen, T., et al. (2010) A multicentre study on the clinical utility of post-traumatic amnesia duration in predicting global outcome after moderate-severe traumatic brain injury. *Journal of neurology, neurosurgery, and psychiatry*. [Online] 81 (1), 87–89. Available from: doi:10.1136/jnnp.2008.161570.

Walker, W.C., Stromberg, K.A., Marwitz, J.H., Sima, A.P., et al. (2018) Predicting Long-Term Global Outcome after Traumatic Brain Injury: Development of a Practical Prognostic Tool Using the Traumatic Brain Injury Model Systems National Database. *Journal of*

Neurotrauma. [Online] 35 (14), 1587–1595. Available from: doi:10.1089/neu.2017.5359.

Wallace, E.J., Mathias, J.L. & Ward, L. (2018a) Diffusion tensor imaging changes following mild, moderate and severe adult traumatic brain injury: a meta-analysis. *Brain imaging and behavior*. [Online] 12 (6), 1607–1621. Available from: doi:10.1007/s11682-018-9823-2.

Wallace, E.J., Mathias, J.L. & Ward, L. (2018b) The relationship between diffusion tensor imaging findings and cognitive outcomes following adult traumatic brain injury: A meta-analysis. *Neuroscience and biobehavioral reviews*. [Online] 92, 93–103. Available from: doi:10.1016/j.neubiorev.2018.05.023.

Wang, C., Costanzo, M.E., Rapp, P.E., Darmon, D., et al. (2017) Disrupted gamma synchrony after mild traumatic brain injury and its correlation with white matter abnormality. *Frontiers in Neurology*. [Online] 8 (OCT), 571. Available from: doi:10.3389/fneur.2017.00571.

Wang, L., Zang, Y., He, Y., Liang, M., et al. (2006) Changes in hippocampal connectivity in the early stages of Alzheimer's disease: Evidence from resting state fMRI. *NeuroImage*. [Online] 31 (2), 496–504. Available from: doi:10.1016/j.neuroimage.2005.12.033.

Ward, A.M., Schultz, A.P., Huijbers, W., Van Dijk, K.R.A., et al. (2014) The parahippocampal gyrus links the default-mode cortical network with the medial temporal lobe memory system. *Human Brain Mapping*. [Online] 35 (3), 1061–1073. Available from: doi:10.1002/hbm.22234.

Warren, J.E., Crinion, J.T., Lambon Ralph, M.A. & Wise, R.J.S. (2009) Anterior temporal lobe connectivity correlates with functional outcome after aphasic stroke. *Brain*. [Online] 132 (12), 3428–3442. Available from: doi:10.1093/brain/awp270.

Wechsler, D. (1997) *Wechsler memory scale (WMS-III)*. Psychological corporation San Antonio, TX.

Wechsler, D. (2001) *Wechsler Test of Adult Reading: WTAR*. San Antonio, TX, Psychological Corporation.

Weiler, M., Machado de Campos, B., Vieira de Ligo Teixeira, C., Casseb, R.F., et al. (2017) Intranetwork and internetwork connectivity in patients with Alzheimer disease and the association with cerebrospinal fluid biomarker levels. *Journal of Psychiatry and Neuroscience*. [Online] 42 (6), 366–377. Available from: doi:10.1503/jpn.160190.

Werner, C. & Engelhard, K. (2007) Pathophysiology of traumatic brain injury. *British Journal of Anaesthesia*. [Online]. 99 (1) pp.4–9. Available from: doi:10.1093/bja/aem131.

Whitman, S., Coonley-Hoganson, R. & Desai, B.T. (1984) Comparative head trauma

experiences in two socioeconomically different chicago-area communities: A population study. *American Journal of Epidemiology*. [Online] 119 (4), 570–580. Available from: doi:10.1093/oxfordjournals.aje.a113774.

Whitnall, L., McMillan, T.M., Murray, G.D. & Teasdale, G.M. (2006) Disability in young people and adults after head injury: 5-7 year follow up of a prospective cohort study. *Journal of neurology, neurosurgery, and psychiatry*. [Online] 77 (5), 640–645. Available from: doi:10.1136/jnnp.2005.078246.

Wilde, E.A., Bigler, E.D., Pedroza, C. & Ryser, D.K. (2006) Post-traumatic amnesia predicts long-term cerebral atrophy in traumatic brain injury. *Brain Injury*. [Online] 20 (7), 695–699. Available from: doi:10.1080/02699050600744079.

Wilson, B.A., Baddeley, A., Shiel, A. & Patton, G. (1992) How does post-traumatic amnesia differ from the amnesic syndrome and from chronic memory impairment? *Neuropsychological Rehabilitation*. [Online] 2 (3), 231–243. Available from: doi:10.1080/09602019208401410.

Wilson, B.A., Evans, J.J., Emslie, H., Balleny, H., et al. (1999) Measuring recovery from post traumatic amnesia. *Brain injury*. 13 (7), 505–520.

Winkler, I., Haufe, S. & Tangermann, M. (2011) Automatic Classification of Artifactual ICA-Components for Artifact Removal in EEG Signals. *Behavioral and Brain Functions*. [Online] 7 (1), 30. Available from: doi:10.1186/1744-9081-7-30.

Wood, R.L. & Rutterford, N.A. (2006) Demographic and cognitive predictors of long-term psychosocial outcome following traumatic brain injury. *Journal of the International Neuropsychological Society : JINS*. 12 (3), 350–358.

Xin, F. & Lei, X. (2014) Competition between frontoparietal control and default networks supports social working memory and empathy. *Social Cognitive and Affective Neuroscience*. [Online] 10 (8), 1144–1152. Available from: doi:10.1093/scan/nsu160.

Yan, H., Feng, Y. & Wang, Q. (2016) Altered Effective Connectivity of Hippocampus-Dependent Episodic Memory Network in mTBI Survivors. *Neural plasticity*. [Online] 2016, 6353845. Available from: doi:10.1155/2016/6353845.

Yates, P.J., Williams, W.H., Harris, A., Round, A., et al. (2006) An epidemiological study of head injuries in a UK population attending an emergency department. *Journal of Neurology, Neurosurgery and Psychiatry*. [Online] 77 (5), 699–701. Available from: doi:10.1136/jnnp.2005.081901.

Yonelinas, A.P., Ranganath, C., Ekstrom, A.D. & Wiltgen, B.J. (2019) A contextual binding theory of episodic memory: systems consolidation reconsidered. *Nature Reviews Neuroscience*. [Online]. 20 (6) pp.364–375. Available from: doi:10.1038/s41583-019-0150-4.

Yuan, H., Zotev, V., Phillips, R., Drevets, W.C., et al. (2012) Spatiotemporal dynamics of the brain at rest - Exploring EEG microstates as electrophysiological signatures of BOLD resting state networks. *NeuroImage*. [Online] 60 (4), 2062–2072. Available from: doi:10.1016/j.neuroimage.2012.02.031.

Zalesky, A., Fornito, A. & Bullmore, E.T. (2010) Network-based statistic: Identifying differences in brain networks. *NeuroImage*. [Online] 53 (4), 1197–1207. Available from: doi:10.1016/j.neuroimage.2010.06.041.

Zanto, T.P., Clapp, W.C., Rubens, M.T., Karlsson, J., et al. (2016) Expectations of Task Demands Dissociate Working Memory and Long-Term Memory Systems. *Cerebral Cortex*. [Online] 26 (3), 1176–1186. Available from: doi:10.1093/cercor/bhu307.

Zhang, H., Yushkevich, P.A., Alexander, D.C. & Gee, J.C. (2006) Deformable registration of diffusion tensor MR images with explicit orientation optimization. *Medical Image Analysis*. [Online] 10 (5), 764–785. Available from: doi:10.1016/j.media.2006.06.004.

Zhang, J., Tian, L., Zhang, L., Cheng, R., et al. (2019) Relationship between white matter integrity and post-traumatic cognitive deficits: A systematic review and meta-analysis. *Journal of Neurology, Neurosurgery and Psychiatry*. [Online]. 90 (1) pp.98–107. Available from: doi:10.1136/jnnp-2017-317691.

Zhang, S. & Arfanakis, K. (2018) Evaluation of standardized and study-specific diffusion tensor imaging templates of the adult human brain: Template characteristics, spatial normalization accuracy, and detection of small inter-group FA differences. *NeuroImage*. [Online] 172, 40–50. Available from: doi:10.1016/j.neuroimage.2018.01.046.

Zhang, W., Wang, X. & Feng, T. (2016) Identifying the Neural Substrates of Procrastination: a Resting-State fMRI Study OPEN. *Nature Publishing Group*. [Online] Available from: doi:10.1038/srep33203.

Zhang, Y., Brady, M. & Smith, S. (2001) Segmentation of brain MR images through a hidden Markov random field model and the expectation-maximization algorithm. *IEEE Transactions on Medical Imaging*. [Online] 20 (1), 45–57. Available from: doi:10.1109/42.906424.

Zhou, Y., Dougherty, J.H., Hubner, K.F., Bai, B., et al. (2008) Abnormal connectivity in the

posterior cingulate and hippocampus in early Alzheimer's disease and mild cognitive impairment. *Alzheimer's and Dementia*. [Online] 4 (4), 265–270. Available from: doi:10.1016/j.jalz.2008.04.006.

Zhu, J., Li, Y., Fang, Q., Shen, Y., et al. (2021) Dynamic functional connectome predicts individual working memory performance across diagnostic categories. *NeuroImage: Clinical*. [Online] 30, 102593. Available from: doi:10.1016/j.nicl.2021.102593.

Zokaei, N., Burnett Heyes, S., Gorgoraptis, N., Budhdeo, S., et al. (2015) Working memory recall precision is a more sensitive index than span. *Journal of Neuropsychology*. [Online] 9 (2), 319–329. Available from: doi:10.1111/jnp.12052.

Zonneveld, H.I., Pruim, R.H., Bos, D., Vrooman, H.A., et al. (2019) Patterns of functional connectivity in an aging population: The Rotterdam Study. *NeuroImage*. [Online] 189, 432–444. Available from: doi:10.1016/j.neuroimage.2019.01.041.

9 APPENDIX

The following section contains supplementary materials.

Supplementary Table 9.1 Demographics and clinical characteristics of patients in the new acute cohort

PTA Status	Ch 3	Ch 4	Ch 5	Age	Sex	Time since injury (days)	Cause of Injury	PTA Duration (days)	Lowest GCS	Length of Hospital Admission (days)	Clinical Imaging Report	Medications
PTA-	Yes	No	No	41	M	11	Assault	10	13	11	SAH; anterior temporal lobe contusion; parietal and occipital skull fracture; thrombosed venous sinus	Ondanestron 4mg; Lactulose 14ml; Levetiracetam 1g; Paracetamol 1g; Senna 15mg; Morphine 10mg
PTA+	Yes	No	No	17	F	7	Sports injury: Football	2	3	8	Negative	Nil recorded
PTA+	Yes	No	No	46	M	6	RTA: Cyclist	2	15	6	SAH	Nil recorded
PTA+	Yes	No	No	22	M	21	Fall from height	22	8	21	SDH; SAH; ME; MS;	Nil recorded
PTA+	Yes	No	No	37	M	6	RTA: Ped vs Car	23	3	23	SDH; EAH	Nil recorded
PTA-	Yes	No	No	32	M	3	Assault	0	14	5	SAH	Ciprofloxacin; Dihydrocodeine; Morphine; Ondanestron; Senna Paracetamol 1g; Tinzaparin; Lansoprazole 30mg; Ibuprofen 400mg; Ondanestron 4mg; Levetiracetam 1g; Dihydrocodeine 30mg; Paracetamol 1g;
PTA-	Yes	No	No	23	M	26	Assault	28	3	26	EDH; ME; MS; SDH; SAH	
PTA-	Yes	No	No	63	M	2	Fall from standing	2	14	2	SDH; SAH	
PTA-	Yes	No	No	40	M	2	Fall from height	0	8	2	SAH	Dihydrocodeine 30mg; Paracetamol 1g
PTA+	Yes	No	No	51	M	5	RTA: Cyclist	6	14	6	SAH	Senna, Dihydrocodeine, Macrogal, morphine, levetiracetam, ondanestron
PTA+	Yes	No	No	49	M	32	Assault	30	10	30	SDH; SAH	Haloperidol 1mg; Lansoprazole 30mg; Lorazepam 0.5mg; Morphine 2.5mg; Paracetamol 1g; Zopiclone 7.5mg
PTA-	Yes	No	No	60	F	3	Fall from height	0	8	2	Small temporal contusion + SAH; SDH (bifrontal)	citalopram
PTA+	Yes	No	No	42	M	16	RTA: Motorcyclist	20	3	30	SAH; DAI	Nil recorded
PTA-	Yes	Yes	Yes	33	M	5	RTA: Ped vs Car	0	14	21	DAI	Nil recorded
PTA+	Yes	Yes	Yes	43	M	1	Fall from height	5	3	5	SAH; inferior frontal intraparenchymal haemorrhage	Chlordiazepoxide (10mg); Polyethylene glycol with electrolytes
PTA+	Yes	Yes	Yes	62	F	3	RTA: Ped vs Bus	5	15	5	SAH; SDH; occipital skull fracture; left frontal contusion	Morphine sulphate 20mg; ondansetron 4mh; dihydrocodeine 60mg; paracetamol 1g; phenytoin 300mg; chloraphenamine 4mg; lactulose 15ml; senna 15mg
PTA+	Yes	Yes	Yes	58	M	16	Assault	23	6	23	SAH	Haliperidol 2mg; Oxycodon 5mg; Docusate 200mg; Senna 10mg; Paracetamol 1g; Salbutamol 2.5mg; Chlorphenamine 4mg;

PTA+	Yes	Yes	Yes	45	M	8	Fall from standing	12	14	12	SDH; SAH; bifrontal contusions; midline shift	Lansoprazole 30mg; Nicotine 1 patch; Nystatin 100000 units; Morphine sulphate 20mg; cyclizine 50mg; dihydrocodeine 60mg; paracetamol 1g; carbimazole 5mg; ondansetron 8mg; metformin 500mg; lactulose 10ml; levetiracetam 500mg;
PTA+	Yes	Yes	Yes	26	M	20	RTA: Ped vs Car	25	3	30	SDH	Dihydrocodeine 30mg; ondansetron 4mg; haloperidol 3mg; docusate 200mg; paracetamol 1g; flucloxacillin 1g; chlordiazepoxide 20mg; senna 7.5mg; Enoxaparin 40mg
PTA-	No	Yes	Yes	41	F	3	RTA: Cyclist	0	14	6	SAH; parenchymal contusions	Nil recorded
PTA+	Yes	Yes	Yes	26	M	24	RTA: Cyclist	38	7	37	DAI	Docusate 200mg; Senna 10ml; Enoxaparin 40mg; Flucloxacillin 1g; Haloperidol 2.5mg; Paracetamol 1mg; Ciprofloxacin 400mg; Levetiracetam 1000mg
PTA+	Yes	Yes	Yes	19	M	7	Fall from height	24	7	9	Left temporal contusion; pneumocephalus; skull fracture	Ondansetron 4mg; Noradrenaline 50ml; Docusate 200mg; Haloperidol 2.5mg; Paracetamol 1g; Co-amoxiclav 625mg; Levetiracetam 1g; Senna 15mg; Sodium chloride nebulised 5ml;
PTA+	Yes	Yes	Yes	67	M	5	RTA: Cyclist	7	13	28	SDH; left temporal contusions; EDH; skull base fractures; pneumocephalus	Lactulose 10ml; levetiracetam 1g; paracetamol 1g; senna 15mg; cyclizine 50mg; morphine sulphate 2mg; naloxone 100 micrograms; ondansetron 4mg; gabapentin 600mg; beclomethasone 1 puff; enoxaparin 40mg; ferrous fumarate 210 mg;
PTA+	Yes	Yes	Yes	52	M	2	Sports injury: Ice skating	3	13	3	SDH; SAH; midline shift; right frontal contusion; right temporal contusion; skull fracture	Cyclizine 50mg; paracetamol 1g; levetiracetam 1g; ondansetron 4mg; dihydrocodeine 16mg
PTA+	Yes	Yes	No	33	M	8	Fall from height	7	13	9	EDH; SDH	Nil recorded
PTA-	Yes	Yes	No	73	F	3	Fall from standing	0	15	3	SDH	Nil recorded
PTA-	Yes	Yes	No	47	M	4	Fall from standing	0	14	4	Contusions in left frontal lobe and right temporal lobe compatible with contrecoup injury; SAH	Dihydrocodeine 30mg; Ondansetron 4mg; Paracetamol 1g; Senna 15mg; Prochlorperazine 10mg
PTA-	Yes	Yes	No	24	M	18	Assault	8	8	9	Bilateral extra-axial haemorrhages in temporal lobes, SAH, left temporal bone fracture.	Nil recorded
PTA-	Yes	Yes	No	22	M	19	RTA: Cyclist	2	14	2	DAI	Dihydrocodeine 30mg
PTA-	Yes	Yes	No	28	M	14	RTA: Motorcyclist	5	14	14	SDH	Paracetamol 1g

M = male; F = female; RTA = road traffic accident; Ped = pedestrian; SAH = subarachnoid haemorrhage; SDH = subdural haemorrhage; ME = mass effect; MS = midline shift; EDH = extradural haemorrhage; EAH = extra-axial haematoma; DAI = diffuse axonal injury

Supplementary Table 9.2 Entropy ratio statistics across varying bin widths

No of bins	ANOVA
2	F=6.1128, p=0.004171
3	F=3.1176, p=0.0528 [×]
4	F=12.546, p=0.00003707
5	F = 11.053, p=0.0001028
6	F=9.9287, p=0.0002281
7	F=10.264, p=0.0001795
8	F=9.081, p=0.0004233
9	F=9.3073, p=0.0003582
10	**F=9.3267, p=0.0003532 [+]**
11	F=10.085, p=0.000204
12	F=9.8891, p=0.002348
13	F=9.7897, p=0.002522
14	F=9.8909, p=0.002344
15	F=8.5717, p=0.0006176
16	F=8.3049, p=0.0007547
17	F=8.9557, p=0.0004641
18	F=8.4928, p=0.0006552
19	F=7.5655, p=0.001327
20	F=8.0751, p=0.0008981
21	F=7.6965, p=0.001199
22	F=8.887, p=0.0004883
23	F=9.3287, p=0.0003527
24	F=8.2399, p=0.0007927
25	F=0.80764, p=0.008973
26	F=7.7744, p=0.00113
27	F=7.7997, p=0.001108
28	F=8.1494, p=0.0008489
29	F=8.2276, p=0.0008001
30	F=7.6389, p=0.001254

[×] = not significant. [+] = bin width 10 was used in analysis

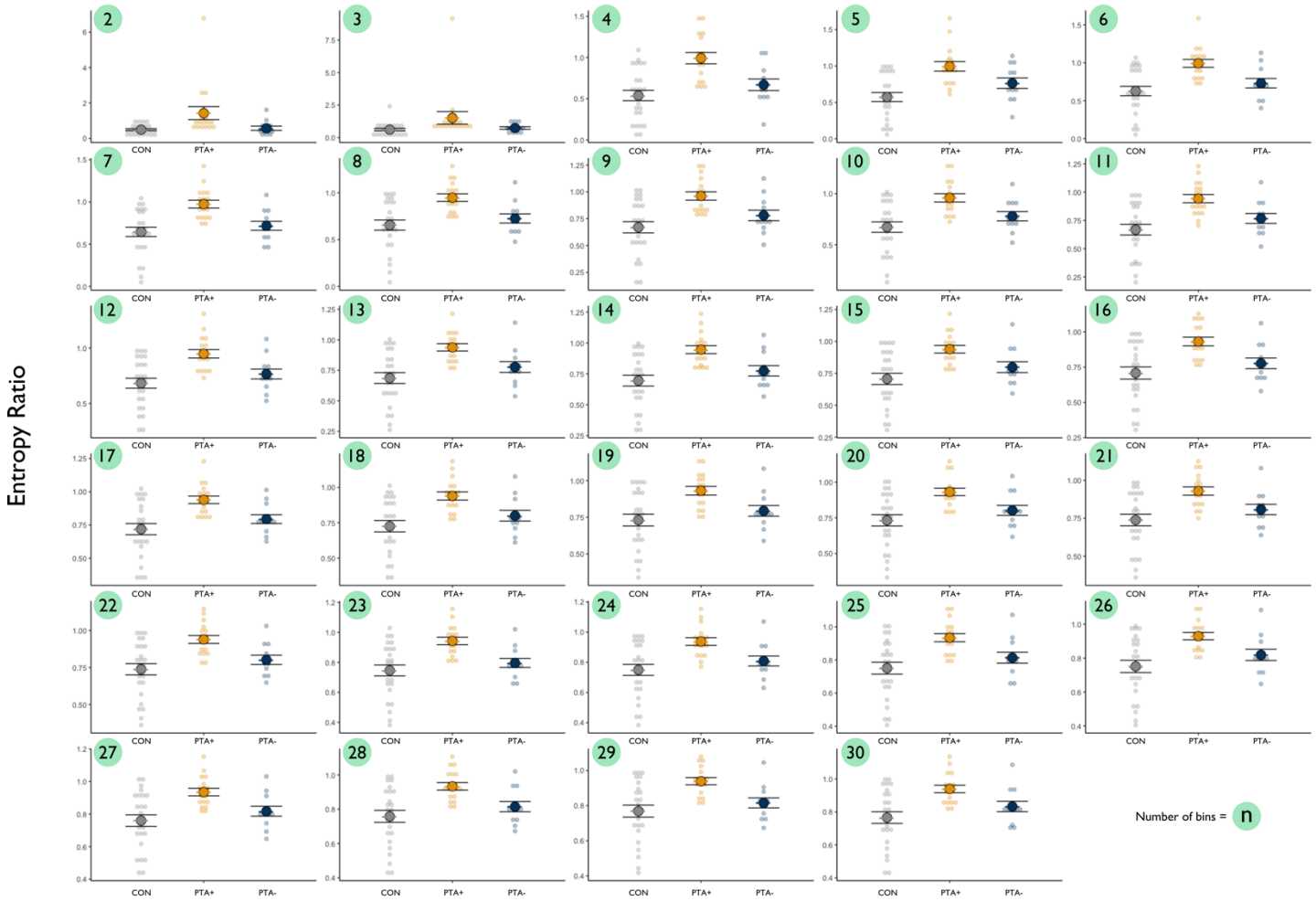

Supplementary Figure 9.1 Entropy ratio at different bin widths

Supplementary Table 9.3 Demographics and clinical characteristics of the TBI patients in Chapter 6

Group	Age	Sex	Time since injury (months)	Cause of Injury	PTA Duration (days)	Lowest GCS	LOC	MRI	Medications
NSM TBI	41	Male	84	Blast	Unknown	3	Yes	Tiny cortical gliotic scar in the right frontal lobe underlying the site of a burr hole relating to previous pressure bolt.	Nil
NSM TBI	35	Male	58	Blast	14	3	Yes	Indented skull vault overlying left frontal and temporal loves. Mature gliotic damage affecting the frontal and temporal cortex.	Nil
ISM TBI	31	Male	52	Blast	Unknown	Unknown	No	Mild generalised volume loss (subjective)	Nil
NSM TBI	32	Male	82	Blast	Unknown	3	Yes	Nil	Pregabalin 300mg BD, Fluoxetine 40mg, Docusate, Amitriptyline 50mg, Fentanyl 50mg, Sevredol PRN, Zomorph 30mg BD, Testosterone & GH
NSM TBI	38	Male	10	Fall	2	4	Yes	Left frontal and left occipital microbleeds	Vitamin D supp. OD
NSM TBI	42	Male	152	RTA	0	15	No	Nil	GH 0.2mg OD, Modafinil 300mg OD, citalopram 20mg OD, Omeprazol 40mg Nebido 1g, Viagra PRN
NSM TBI	37	Male	12	RTA	4	Unknown	Yes	Left inferior frontal and opercular contusion	Omeprazol 40mg OD, Gabapentin 900mg OD, Vitamin D supp. OD
ISM TBI	34	Male	6	Fall	1	Unknown	Yes	Nil	Nil
ISM TBI	59	Male	3	RTA	7	8	Yes	Microbleeds in parafalcine distribution	Nil
ISM TBI	39	Male	7	RTA	0	14	No	Microbleeds in parafalcine distribution, medial temporal lobes and right thalamus	Nil
NSM TBI	48	Female	3	Fall	2	Unknown	Yes	Mature gliotic damage in right temporal pole and inferior temporal gyri. Right frontal gliotic damage.	Ibuprofen
NSM TBI	44	Male	20	RTA	6	12	Yes	Contusions overlying both orbits. Right parietal and left perisylvian cortex microbleeds	Hydrocellulose 10mg, Lansoprazole 30mg
NSM TBI	30	Male	67	Assault	90	Unknown	Yes	Left temporal contusion, gliosis superior vermis	Nil
NSM TBI	23	Female	11	Fall	2	Unknown	Yes	Frontal and temporal pole gliosis	COCP OD
ISM TBI	59	Male	15	RTA	7	3	Yes	Left and right frontal contusions left temporal contusions	Simvastatin 40mg OD, Omeprazole 20mg OD
NSM TBI	61	Male	10.19	RTA	2	Unknown	Yes	Sub-frontal and left frontal pole contusions	Nil
ISM TBI	26	Male	17	RTA	3	14	Yes	Bifrontal and right temporal contusions	Nil
ISM TBI	53	Male	13	Fall	Unknown	8		Bifrontal and bitemporal pole contusions	Lamotrigine 50mg BD
NSM TBI	53	Male	19	Fall	7	10	Yes	Left temporal contusion	Vitamin D supp. OD
NSM TBI	38	Male	41	Assault	3	3	Yes	Left frontal and temporal contusions; left temporal volume loss	Nil
ISM TBI	58	Male	6	RTA	7	7	Yes	Bifrontal and right temporal pole contusions	Nil
NSM TBI	40	Male	134	RTA	42	3	Yes	Bifrontal contusions	Nil
NSM TBI	42	Female	48	RTA	3	Unknown	Unknow	Left frontal contusion and diffuse microbleeds	Nil

ISM TBI	40	Female	50	Sports injury	3	Unknown	Yes	Superficial siderosis and right frontal contusion	Nil
ISM TBI	31	Male	42	Sports injury	1	Unknown	Yes	Possible temporal lobe contusion	Nil
NSM TBI	25	Male	15	RTA	14	3	Yes	Microbleeds in parafalcine distribution	Nil
ISM TBI	44	Female	436	RTA	Unknown	Unknown	Unknown	Left temporal and sub-frontal contusions.	Nil
ISM TBI	44	Male	353	RTA	42	3	Yes	Marked volume loss of body and splenium of corpus callosum	Nil
ISM TBI	61	Female	426	RTA	120	5	Yes	Mature gliotic frontal damage. Bilateral frontal microbleeds	Citalopram 10mg OD
ISM TBI	40	Female	370	RTA	Unknown	Unknown	Yes	Bifrontal contusions. Mature gliotic damage in right parietal cortex. Extensive damage extending left temporal pole and posterior frontal lobe.	Carbamazepine 100mg, propanalol 40mg, contraceptive implant
ISM TBI	65	Male	372	Fall	14	Unknown	Yes	Mature cortical infarcts in right medial occipital lobe. Mature damage in left cerebellar	Amlodipine 5mg, Simvastatin 40mg, Ramipril 2.5mg
ISM TBI	54	Male	412	RTA	10	Unknown	Yes	Right frontal, temporal, occipital and parietal contusions. Widespread microbleeds	Tegretol 200mg BD, Cocodamol PRN, Amytriptyline 100mg, Naproxen PRN
ISM TBI	56	Female	415	RTA	80	3	Yes	Mature gliotic damage in the right frontal lobe. Marked loss of volume in the corpus callosum	Statins, Ventolin, Seretide (dosages unknown)
NSM TBI	43	Male	300	RTA	Unknown	3	Yes	Frontal contusions, left temporal pole contusions	Pregabalin 75mg BD, Ventolin, Cetirizine, Omeprazole, Lamotrigine 50mg BD, Paracetamol PRN, Ibuprofen PRN, Codydramol 30:500 PRN
NSM TBI	46	Female	376	Fall	28	3	Yes	Left superior frontal and left middle frontal gyrus contusions. Small amount of cortical damage in right inferior frontal gyrus. Cerebellar atrophy.	Penicillin (dosage unknown)

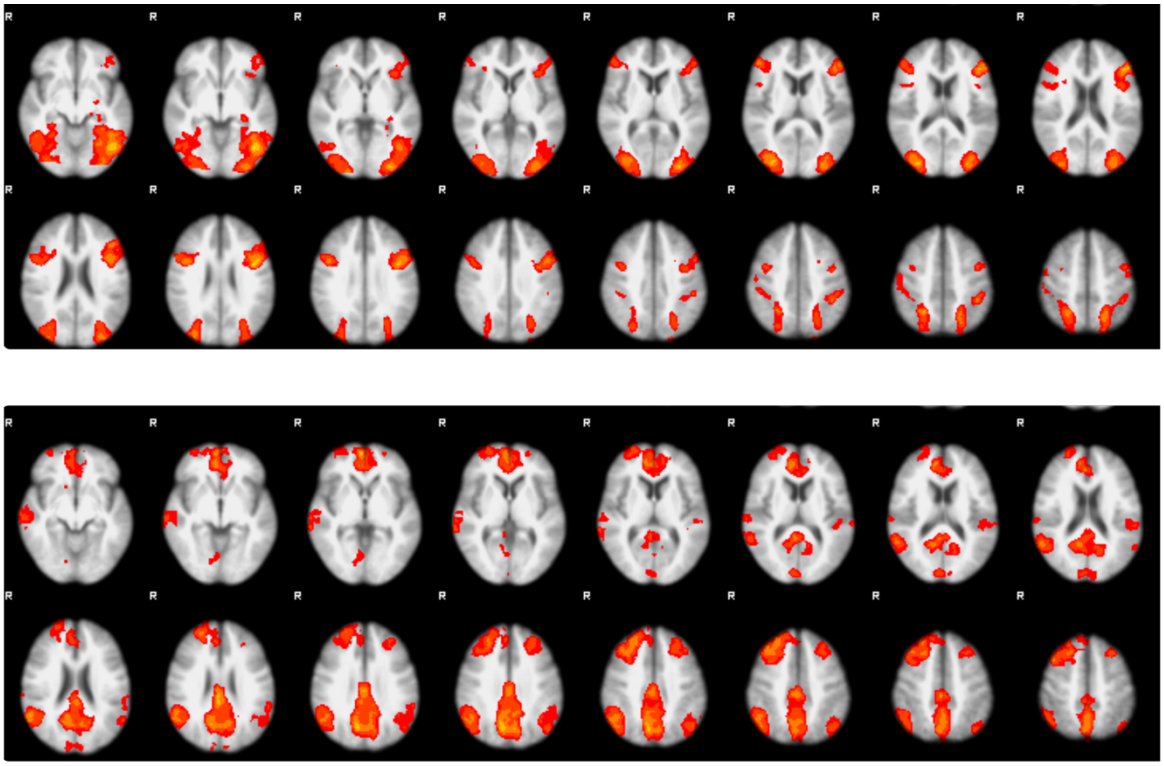

Supplementary Figure 9.2 Alterations in BOLD activity associated with performance on the memory encoding task for TBI patients alone.

Alterations in BOLD activity associated with performance on the memory encoding task presented in Chapter 6 for TBI patients alone. All spatial results shown in standard space overlaid on MNI template with a Z-statistic threshold of 2.3. Successful encoding (remembered minus forgotten contrast) is shown for **Top panel:** increased activation during successful encoding and **Bottom panel:** decreased activation during successful encoding in TBI patients

Supplementary Table 9.4 Permission to reuse figures

Figure	Publication	Licence Number
Figure 1.1 Axonal injury and the consequences for large-scale network disruption	Sharp, Scott & Leech, *Nature Reviews Neurology* (2014)	5087081213817
Figure 2.6 Frequency bands in EEG		5054760514487
Figure 2.8 The haemodynamic response function	Amaro & Barker, *Brain and Cognition* (2006)	5097111216265
Figure 2.9 Fractional anisotropy in the axon membrane	Hayes, Bigler & Verfaellie, *Journal of the International Neuropsychological Society* (2016)	Licence not required: "Permission is granted at no cost for use of content in a Master's Thesis and/or Doctoral Dissertation."
Figure 6.1 The subsequent memory task paradigm	Mallas et al., *Brain* (2021)	5094710414959
Figure 6.3 Subsequent memory and neuropsychological performance	Mallas et al., *Brain* (2021)	5094710414959
Figure 6.4 Changes in BOLD activity associated with performance on the subsequent memory task	Mallas et al., *Brain* (2021)	5094710414959
Figure 6.5 Fractional anisotropy across the whole brain	Mallas et al., *Brain* (2021)	5094710414959
Figure 6.6 Fractional anisotropy in the structural connectome	Mallas et al., *Brain* (2021)	5094710414959
Figure 6.7 Lesion probability in TBI patients	Mallas et al., *Brain* (2021)	5094710414959